Title
Structural and functional characterization of Hsp90 mediated Raf Kinase Regulation

Author
Jaime-Garza, Maru

Publication Date
2023

Peer reviewed|Thesis/dissertation

Structural and functional characterization of Hsp90 mediated Raf Kinase Regulation

by
Maria Eugenia Jaime Garza

DISSERTATION
Submitted in partial satisfaction of the requirements for degree of
DOCTOR OF PHILOSOPHY

in

Biophysics

in the

GRADUATE DIVISION
of the
UNIVERSITY OF CALIFORNIA, SAN FRANCISCO

Approved:

DocuSigned by:
David A. Agard
D6BB224E0EB04B9...

David A. Agard
Chair

DocuSigned by:
Tanja Kortemme
D4BB1D7E9402...

Tanja Kortemme

DocuSigned by:
Jason Gestwicki
4909848DBB404E5...

Jason Gestwicki

Committee Members

I dedicate this work to *my family*,

for their unconditional support and motivation.

I could not have asked for a better team through this PhD.

Acknowledgements

There are so many people to thank, and so many moments to be thankful for as I reach the end of my PhD. I could write a whole thesis on what I have learned from the incredible people I have been surrounded by these past five years, but a summary will have to do. I have not been able to capture every interaction that has made me feel supported or grateful, as there are more people and moments than I can count.

Throughout my PhD, I was constantly inspired by the passion and love David has for discovery. I hope to carry that with me throughout my life, asking many questions and seeking answers with curiosity. I admire David's line of questioning. He is fully present in every Lab Meeting, and every fact presented (new or old) receives fresh exploration. Hearing the same Hsp90 introduction slides was not a formality, but instead something that he could question and seek to understand more deeply. I admire the determination and fearlessness with which he approaches new problems, "Every project is possible, it just might take longer". David trained me to answer questions, to think critically, and to be brave enough to seek understanding. In the Agard Lab I learned to take responsibility of my work and my future. I am also grateful for the people David brought into my life. Thank you, David, for having me in your lab.

Since the start of my rotation, Tanja has been an incredible mentor and advisor. She has invited me to her lab's journal clubs and motivated my scientific exploration. I could always count on Tanja's support and encouragement as I worked through each part of my PhD. She was the first person I wanted to talk to upon hearing bad science news, and she allowed me to be very honest about how I was doing. When talking about science, Tanja reminded me to step outside my experiments and ask if I am asking the right questions. Tanja celebrated my scientific progress in a way that allowed me to recognize how much work it had taken me to get to where I

was. She helped remind me that I should be proud of my work. Thank you Tanja, I feel very lucky to have shared my PhD experience with you.

I am extremely grateful for Jason Gestwicki's affirmations through my qualifying exam, and my many thesis meetings. He helped give me the strength to speak my mind and steered me when I wasn't sure I knew in what direction I was going.

None of these thesis meetings, exciting Research In Progress talks, retreats or recruiting events could have been possible without Nicole Flowers. Nicole was there for every question, and every uncertainty we biophysics students faced. She made us biophysics students feel loved.

I would like to thank the biophysics and bioinformatics graduate students who joined me in this journey and helped me become a better person. Christina Stephen's strength, determination, and baking (best tres leches cake to date!), Wren Saylor's imagination, love, and understanding, Elissa Fink's coffee walks with Ella and her encouragement chats, Calla Martin's ability to talk about life and our PhD process objectively, Matt Johnsons's warmth, and Aji Palar's commiseration through our after-lab night climbing sessions.

A key factor in my decision to join the Agard Lab was the support I felt from the lab's graduate students. I would like to thank Chari Noddings for her exciting science conversations, and for teaching me that proteins can, and do, follow logic when it was hard for me to see in the beginning. Thank you, Chari, for your objective perspective that always reminded me to step back and simplify. I would like to thank Carlos Nowotny for his positivity, his new perspectives, the teamwork we shared with kinases, and his fabulously themed cards. Carlos, thank you for walking me through my first western blot, and for teaching me how to work with mammalian cells. I would like to thank Melissa Mendez and Simon Sanders for their company, having you all as my lab neighbors made my lab days so much happier.

I am so grateful to have shared so much time with Eliza Nieweglowska, and to have learned through her that there is an important place for emotion in science. Her scientific support (even on the microscope at 3am, or Friday nights) was invaluable to my experience in the Lab, but her friendship was essential for my graduation. Late night ice cream runs, possible future job discussion calls, plant shopping, and craft nights allowed me to air all my grievances and show up in lab happier than I had left it. Eliza, you have felt like part of my family, and I cannot thank you enough for that!

Mariano Tabios was the soul of the lab, and on hard days, the reason I would come into lab. He was always happy to talk about science, lab dynamics, his family, our weekends, anything. He would entertain my whining just the right amount; and remind me when it was my fault when I needed to hear it. He shared farmers market fruits, and Ginger's delicious desserts. I admire his ability to call people out for their mess while being loving and responsible. I admire Mariano's parenting, and how he would step up to help make Ginger's career dreams possible. Mariano texted me when he knew I needed it, and celebrated with me when he thought I should be celebrating. Thank you, Mariano, for having my back and helping me be a better person through my PhD.

I am also grateful for the incredible scientists and postdocs in the Agard Lab. Daniel Coutandin taught me about important systems of organization, and how to be a stronger independent scientist. Feng Wang worked with me, grid after grid and microscope time after microscope time as we optimized freezing conditions and samples. I enjoyed Feng's updates and questions throughout my PhD. Evita Tsiolaki took on the FCS with me, and helped remind me how lucky we all were to have access to incredible instruments and cool science. Tristan Owen's humor and helpful biochemistry tricks helped keep the Covid lab days friendly. Michelle Mortiz

was always happy to help and commiserate on the process of learning EM. Ray Wang and Yanxin Liu were excellent scientific role models. While not in the Agard lab, I am extremely grateful for Joana's constant company in the lab. She made me laugh often, shared her life with me and always reminded me to respect myself in every hard lab situation. Each and every scientist in the Agard Lab (And Stroud Lab) contributed to making the lab feel like my home, and for that I am very grateful.

None of the cryoEM work done through my PhD would have been possible without the help of David Bulkley, Glenn Gilbert, or Zanlin Yu, who at various points helped me find the lost beam, align the microscope, load grids, figure out where my data went and much much more.

UCSF is home to researchers who crave to know more, and love science with passion and determination. Every P.I. has science and life knowledge to share, and I have been very lucky to receive their inspiration, their tidbits of knowledge and their pushes of strength. Brian Shoichet demonstrated to me the importance of asking questions and showed me that a moderator can create the environment required for people of all backgrounds to feel safe asking questions. When I approached Dan Southworth for science advice, he perceived my need for a moral boost and gave me this essential perspective: It is a great privilege to work with the microscopes we do, to be able to see these tiny molecular machines come to life. Matt Jacobsen reminded me that biophysics exists in every problem in science if we know how to look for it. Sophie Dumont and Carol Gross gave me the strength to drive the direction of my own project. Carol connected me with the right people and reminded me that I hold the reins of the science I am driving. Klim Verba listened and exchanged ideas with me, and provided quick hallway answers to random questions that arose in lab. For them, and so many other faculty of UCSF, I am forever grateful.

I am so so grateful for my previous education at Johns Hopkins as an undergraduate student. I am grateful of every single incredible professor who welcomed me to talk about a random paper I had seen in Science, or about random experiments I wanted to try in their classes. I never lacked the scientific resources to explore, and I never lacked the mentors required to assist me as I made my every decision. I am so grateful for Van Moudrianakis, who sat with me, offered me tea, and discussed with me the philosophy of science. He and his wife Penny felt like my family away from home, and there was always fun science to discuss in their presence. Thank you, Van, for reminding me how incredible the world around me is, and how important dedication is when projects are hard. I would also like to thank Bertrand Garcia-Moreno, who wasn't afraid to tell me "I told you so" when I returned to Hopkins, hungry for knowledge and growth. "Dr. Bertrand" welcomed me in his lab, and alongside Aaron Robinson taught me the importance of daily coffee side chats, and how to create a clear and concise presentation. Thank you Hopkins for creating a world of opportunities for me.

I would like to thank the many talented women who cheered for me and guided me as I considered my career path and made career decisions. Cherié Butts pushed me to be more confident in who I am as a scientist. Cherié made me laugh and feel understood. She reminded me that differences are strengths to be proud of and act upon. Natasha Aziz, Eva Harris, Eva Nogales, Sherry LaPorte, Liz Campbell, and many other women are shining examples of the never ending adventures, and the amazing feats that can be accomplished with dedication and a love of science.

Finally, I want to thank all the people in my life, outside of science, who kept me going through the moments of self-doubt and career fear. My partner Matt Muir saw the strength in me when I couldn't find it myself. He was in lab with me on late nights, and on weekends. He read

my work and listened to my presentations. Matt pushed me to be braver, stronger and more adventurous throughout my PhD. There's a whole wonderful world out there, and I'm so excited to explore it with you Matt. My parents have supported me through every good and bad decision I have made, always with love and pride. My Dad has given me the strength and passion to steer my future and speak my mind. My mom has given me the heart to remember that people are what really matters. My brother can always make me laugh, no matter how much crying my calls start with. Through our adventures, he has showed me how to be competitive, and how to not fall prey to my fears. Cristy's unwavering strength inspires me to get out and get involved, even as I figure things out as I go. From Lucy, I have learned the power of connection and the importance of persistence. I am grateful for my grandmothers, who in their own way taught me to be a stronger woman. My grandma Catalina crafted her opinions expertly through reading and thought, always looking for knowledge. Even today, my grandma Sylvia looks for adventure anywhere she can find it. Thank you for paving the way for my scientific thought.

Prefijas, thank you for inspiring me to be who I am in a world where people may not be like us. Strong, confident, passionate women are created through friends like you. Battling through big law might not seem too similar to a PhD, but Natalia commiserated and reminded me to crush the hard things we chose to pursue. Bibis inspired me to dream about a life after my PhD. Fer and I talked through facetime each in our respective labs (she in Houston, me in SF) past midnight as we waited for our experiments to fail (or on lucky days work). Dani reminded me to laugh deeply, Ani how to persevere and make beautiful things, Gaby and Isa taught me the power of perspective and the outcome of hard work, and Paola taught me to communicate clearly and live fully. I am so lucky to have you all.

While lab experiments tend not to work for long periods of time, climbing gave me challenging puzzles that I could solve using my brain and body. More than climbing though, the people who forced me out of lab and saw me as a person outside of science, reminded me who I was week after week. Thank you Kiara, Van, Sammy, and Arthur for making me get out there and take on bigger challenges. When I said “watch me close, I might fall”, they always told me I wouldn’t fall and they had me if I did.

Thank you all for helping me grow throughout my PhD. You have made these five years of my life an incredible journey, and you have prepared me to go out into the world with scientific rigor, integrity, and humility.

Acknowledgement of Previously Published Work

Chapter 4 of this thesis was published under the following citation:

Jaime-Garza, M., Nowotny, C. A., Coutandin, D., Wang, F., Tabios, M., & Agard, D. A. (2023). Hsp90 provides a platform for kinase dephosphorylation by PP5. Nature Communications, 14(1), 2197. https://doi.org/10.1038/s41467-023-37659-7

All we have to decide is what to do with the time that is given us.

- J.R.R. Tolkien

Structural and functional characterization of Hsp90 mediated Raf Kinase Regulation

Maru Jaime-Garza

Abstract

The molecular chaperone Hsp90 collaborates with the phosphorylated Cdc37 cochaperone for the folding and activation of its many client kinases. Reconstitution of kinase loading onto Hsp90 has proven challenging. In this work we describe our efforts towards isolating a complex that captures kinase loading onto Hsp90, and we study the constituents involved in initial Hsp90-Kinase interactions. Kinases are highly regulated by chaperones like Hsp90, but also through phosphorylation at specific regulatory sites. In the second half of this work, we explore how the cochaperone phosphatase PP5 dephosphorylates the kinase CRaf and the Hsp90 cochaperone Cdc37 in an Hsp90-dependent manner. Although dephosphorylating Cdc37 has been proposed as a mechanism for releasing Hsp90-bound kinases, here we show that Cdc37 dephosphorylation does not occur if a kinase is simultaneously bound to Hsp90. Our cryoEM structure of PP5 in complex with Hsp90:Cdc37:CRaf reveals how Hsp90 both activates PP5 and scaffolds its dephosphorylation of the bound CRaf phosphorylation sites. From this work we begin to get insight into the structure of an Hsp90:Cdc37 complex, and how PP5 might dephosphorylate Cdc37's key kinase-recruiting phosphorylation site.

Table of Contents

CHAPTER 1 ..... **1**

INTRODUCTION 1

Hsp90 ..... *2*

Cdc37 ..... *4*

Protein Phosphatase 5 ..... *8*

CRaf (Raf1) Kinase *10*

Hsp90-Kinase Interactions *12*

The Hsp90 Client Loading Complex *15*

Thesis Project Objective *17*

CHAPTER 2 ..... **30**

THE ELUSIVE HSP90 "KINASE LOADING COMPLEX" 30

Preface *30*

Summary *31*

Results *32*

References *46*

CHAPTER 3 ..... **49**

PP5 ACTIVITY AND COMPLEX OPTIMIZATION 49

Preface *49*

Summary *50*

Results *51*

References *74*

CHAPTER 4 ..... **79**

HSP90 PROVIDES A PLATFORM FOR KINASE DEPHOSPHORYLATION BY PP5 79

Abstract *79*

Introduction *80*

Results *83*

Discussion *96*

Methods *99*

Data Availability *108*

Acknowledgements *109*

Author Contributions Statement *110*

Inclusion & Ethics Statement *110*

Supplementary Figures *111*

References *121*

CHAPTER 5 ..... **131**

FUTURE DIRECTIONS 131

Hsp90 kinase loading *131*

Hsp90-Cdc37 Interactions *133*

The role of Cdc37 phosphorylation in Kinase chaperoning *135*

Mechanism of PP5 substrate dephosphorylation – Kinase, GR and beyond *135*

References *139*

APPENDIX **141**

METHODS 141

Buffers *141*

Individual protein expression *145*

Individual protein purification *145*

Protein complex expression *146*

Protein complex purification *147*

Dephosphorylation Assays *148*

EM Sample Preparation *150*

FCS assays *151*

PLASMID LIBRARY 152
Cdc37 ..... *152*
sBRaf *154*
Hsp90B *158*
Protein Phosphatase 5 ..... *161*
Hsp90:Cdc37:CRaf$^{336-618}$ – yeast expressed *164*
Hsp90:Cdc37:CRaf – mammalian cell expressed *169*

List of Figures

Fig. 1.1 Hsp90 is a dynamic protein that works in concert with its cochaperone helpers. 3

Fig. 1.2. Hsp90 interacts with Cdc37 in two very distinct ways. 6

Fig. 1.3. PP5 structures show TPR-occluded active site and catalytic domain interaction with substrate. 9

Fig. 1.4. Hsp90:Cdc37:Cdk4 complex shows Kinase stretched apart into N and C-lobes. 14

Fig. 1.5. Hypothesis of Kinase Loading Complex born from existing Hsp90-Glucocorticoid interactions. 16

Fig. 2.1 The Kinase Loading Complex may comigrate on Size Exclusion Chromatography. 34

Fig. 2.2. Crosslinked "Kinase Loading Complex" appears similar in size to Hsp90:Cdc37:sBRaf complex. 36

Fig. 2.3. "Kinase Loading Complex" not stable on Cu or Gold Quantifoil functionalized grids. 37

Fig. 2.4. Hydrodynamic radius measured by FCS allows for testing of Kinase Loading Complex conditions. 39

Fig. 2.5. Pulldown experiments may show coelution of Hsc70 and Hop with Hsp90:Cdc37:sBRaf complex. 41

Fig. 2.6 Fluorescently labelled sBRaf aggregation and solubility can be visualized using FCS. 44

Fig. 3.1. Mn buffer leads to faster dephosphorylation and decreased coelution of PP5 complex. 52

Fig. 3.2. SDS gel shift assay provides readout of PP5 dephosphorylation of Cdc37. 56

Fig. 3.3. Hsp90:Cdc37:PP5 complex crosslinks heterogeneously. 57

Fig. 3.4. The Hsp90:Cdc37 complex likely resembles a semi-open Hsp90 state. 59

Fig. 3.5. Mammalian Hsp90:Cdc37:CRaf$^{304-648}$ complex ideal for biochemical studies. 63

Fig. 3.6. Hsp90:Cdc37:CRaf^{ExtD} complex forms larger complex upon initial purification. 64

Fig. 3.7. PP5 dephosphorylates CRaf^{pS338} in cells and in vitro. 66

Fig. 3.8. Mammalian and yeast Hsp90:Cdc37:CRaf:PP5 complex can be crosslinked. 68

Fig. 3.9. Elevated temperatures contribute to Hsp90:Cdc37:Kinase complex dissociation. 70

Fig. 3.10. PP5 does not dephosphorylate CK2 phosphorylated Hsp90. 73

Fig. 4.1. Kinase sterically blocks Cdc37 dephosphorylation. 85

Fig. 4.2. Hsp90 activates PP5, acting as a phosphatase scaffold. 88

Fig. 4.3. Distinct TPR a7 helix – Hsp90 C-terminal domain interaction mode. 90

Fig. 4.4. Heterogeneous PP5 catalytic domain in position for CRaf^{pS621} dephosphorylation. 91

Fig. 4.5. Deletion of PP5's aJ helix increases rate of dephosphorylation. 94

Fig. 4.6. Model of PP5's role in kinase and Cdc37 dephosphorylation. 96

Chapter 1

Introduction

Eukaryotic cells are tightly regulated through the endless phosphorylation and dephosphorylation of key protein targets. Through phosphorylation, kinases can activate or inhibit their substrates, recruit new binding partners, impede binding interactions, and even conformationally modify their substrates. These modifications are often tied to key cellular decisions such as cellular division, growth or autophagy and must therefore be carefully regulated to ensure cellular health. Human kinases are multi-domain proteins that may exhibit poor folding stability, and therefore often require the help of molecular chaperones for their folding and activation. Specifically, the molecular chaperone Heat-shock protein 90 (Hsp90) has been implicated in interacting with over 60% of human kinases (Taipale et al., 2010; Taipale et al., 2012). Through this work we will examine the role of Hsp90, the kinase specific Hsp90-"adaptor" cochaperone Cdc37, and the Hsp90-cochaperone phosphatase Protein Phosphatase 5 (PP5) in the regulation of CRaf kinase.

Hsp90

Hsp90 (heat shock protein, 90kDa) is a highly conserved and abundant molecular chaperone known to assist in the folding and activation of a significant portion of the human proteome (Taipale et al., 2012). The proteins which require Hsp90 for function are called Hsp90 "clients", and these clients are enriched in signaling and regulatory proteins. Examples of these clients include steroid hormone receptors, approximately 60% of human kinases, heat shock factor 1 (HSF1), p53 and many more. Most eukaryotes contain compartment specific Hsp90 proteins as well as two cytosolic Hsp90 homologs, the constitutively expressed Hsp90B and the stress expressed Hsp90A (Johnson, 2012; Taipale et al., 2010).

Hsp90 predominantly exists as a homodimer (Fig. 1.1a); each protomer contains a highly conserved N-terminal ATPase domain, a client binding Middle domain, and a C-terminal dimerization and cochaperone binding domain (Schopf et al., 2017). The Hsp90 dimer can undergo an ATP-dependent and highly dynamic conformational cycle (Fig. 1.1b). Client activation has been shown to require Hsp90 hydrolysis, although it is still unclear to what degree ATP hydrolysis is deterministic of Hsp90 closing (Panaretou, 1998). Differing Hsp90 assisting proteins called cochaperones can bind distinct Hsp90 conformational states and help stabilize or guide specific states in the Hsp90 conformational cycle (Fig. 1.1c) (Schopf et al., 2017; Taipale et al., 2010).

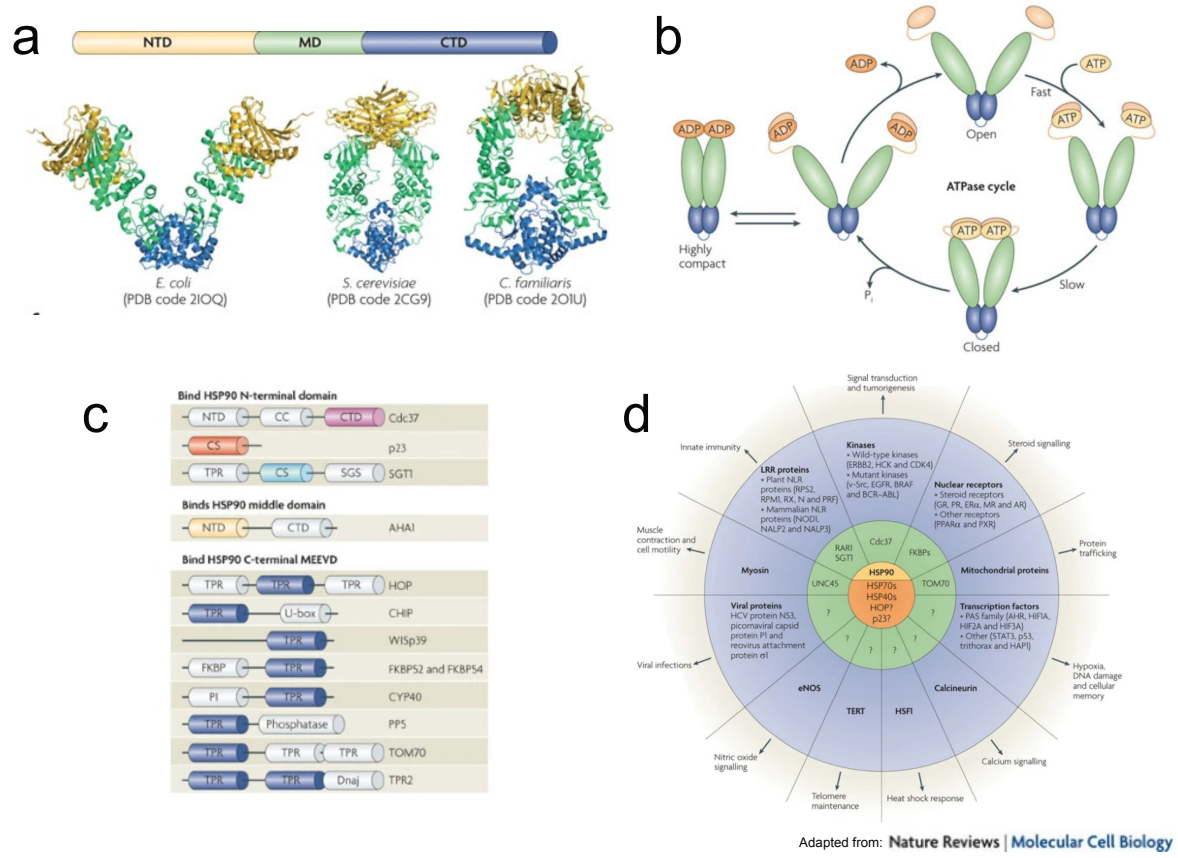

Adapted from: Nature Reviews | Molecular Cell Biology

Fig. 1.1 Hsp90 is a dynamic protein that works in concert with its cochaperone helpers.

a Hsp90 is a dimer composed of a monomer with an N-terminal domain, a Middle domain, and a C-terminal domain. Structural characterization of these domains has shown the large degree of conformational flexibility the Hsp90 dimer is capable of. **b** Hsp90 undergoes an ATP dependent cycle which leads to large Hsp90 rearrangements. **c** Hsp90 cochaperones help guide this conformational cycle, and give Hsp90 additional tool to modify its protein clients. A lot of these cochaperones contain TPR binding domains, known to bind the Hsp90 C-terminal tail. **d** Distinct Hsp90 clients require the help of different cochaperones to work as adaptors or key players in the Hsp90-client interaction.

The folding, activation and modification of Hsp90's protein clients requires the help of these Hsp90 cochaperones (Boysen et al., 2019; Dahiya et al., 2019; Kirschke et al., 2014; Tsuboyama et al., 2018). Functioning as modular components of the Hsp90 machinery, these cochaperones enable Hsp90 to participate in a wide berth of functions (Taipale et al., 2010). Certain cochaperones function as adaptors for specific classes of proteins (e.g. Cdc37) (Fig.

1.1d) (Grammatikakis et al., 1999; Taipale et al., 2012), while others have functional domains attached to Hsp90 binding domains (e.g. TPR domain containing proteins) (Das, 1998; Taipale et al., 2010).

Amongst these cochaperones, a specific class of cochaperone proteins contain an Hsp90-binding tetratricopeptide (TPR) domain (D'Andrea & Regan, 2003). The TPR motif is made up of a degenerative set of 34-amino acid repeats that form two anti-parallel alpha helices connected by a turn. Differing numbers of TPR motifs create TPR domains, known to bind have a basic pocket which binds the "MEEVD" sequenced C-terminal tail of Hsp90 (Chen et al., 1998). These TPR domains have also been shown to make additional stabilizing contacts with the Hsp90 C-terminal groove, as has been seen with the cochaperone FKBP51(Lee et al., 2021; Noddings et al., 2023). TPR domains are often accompanied by diversely functioning domains such as the phosphatase domain in Protein Phosphatase 5 (PP5), or the peptidyl prolyl isomerase domains in FKBP51 and FKBP52.

While much is known about the importance of Hsp90, its many clients, its ubiquity of action, and the large number of cochaperone proteins driving its activity, there are many aspects of Hsp90 yet to be uncovered. In this work we set out to understand how Hsp90 might be modifying and stabilizing kinase clients. This would be impossible to do without talking about Hsp90's kinase "adaptor" Cdc37.

Cdc37

First identified as a cell division cycle gene in yeast studies p50 (Reed, 1980), now known as Cdc37, is an Hsp90 cochaperone known to assist in Hsp90:kinase regulation. Conserved from yeast to humans, Cdc37 has been shown to interact with most of the Hsp90

kinase clients (Johnson & Brown, 2009; Taipale et al., 2012). Initial biochemical studies showed Cdc37's function as a molecular "bridge" between kinases and Hsp90 (Silverstein et al., 1998), and further studies showed that Cdc37 slowed the rate of ATPase activity in Hsp90 (Siligardi et al., 2002). While the most highly conserved region of Cdc37, its N-terminus, has been shown to be essential for kinase binding and specificity (Cutforth & Rubin, 1994; Polier et al., 2013), the middle domain (Cutforth & Rubin, 1994; Terasawa et al., 2005) and the C terminal domain (Eckl et al., 2016; Shao, Irwin, et al., 2003) have also been implicated in kinase interactions.

NMR studies further explained the nature of Cdc37-kinase interactions (Keramisanou et al., 2016). Work by the Gelis lab showed that the Cdc37 N-terminal domain interacts loosely and transiently with both "client" and "non-client" kinases, while the Cdc37 C-terminal domain interacts only with client kinases. Furthermore, Cdc37 binding to a BRaf model client showed destabilization upon Cdc37 binding. Limited proteolysis shows that the client destabilization takes place not only at the N-lobe - C-lobe interface, but throughout the kinase domain. This led to Cdc37 being labelled a "scanning" factor for Hsp90-kinase interactions, with the N terminus of Cdc37 interacting with all kinases and scanning for the "unstable" clients, and the C-terminal domain interacting only with client kinases.

Other structural efforts have been undertaken to visualize two modes of interactions between Hsp90 and Cdc37. The first used crystallography efforts to visualize interactions between a truncated C-terminal Cdc37 domain and a truncated N-terminal Hsp90 domain (NTD) (Fig. 1.2b)(Roe et al., 2004). In this structure, the Hsp90 nucleotide binding domain appears bound to the C-terminal domain of Cdc37, keeping the N-terminal Hsp90 lid from being able to close over the ATP binding site. This interaction supports the decreased ATPase rate of Hsp90 when in complex with Cdc37 (Siligardi et al., 2002).

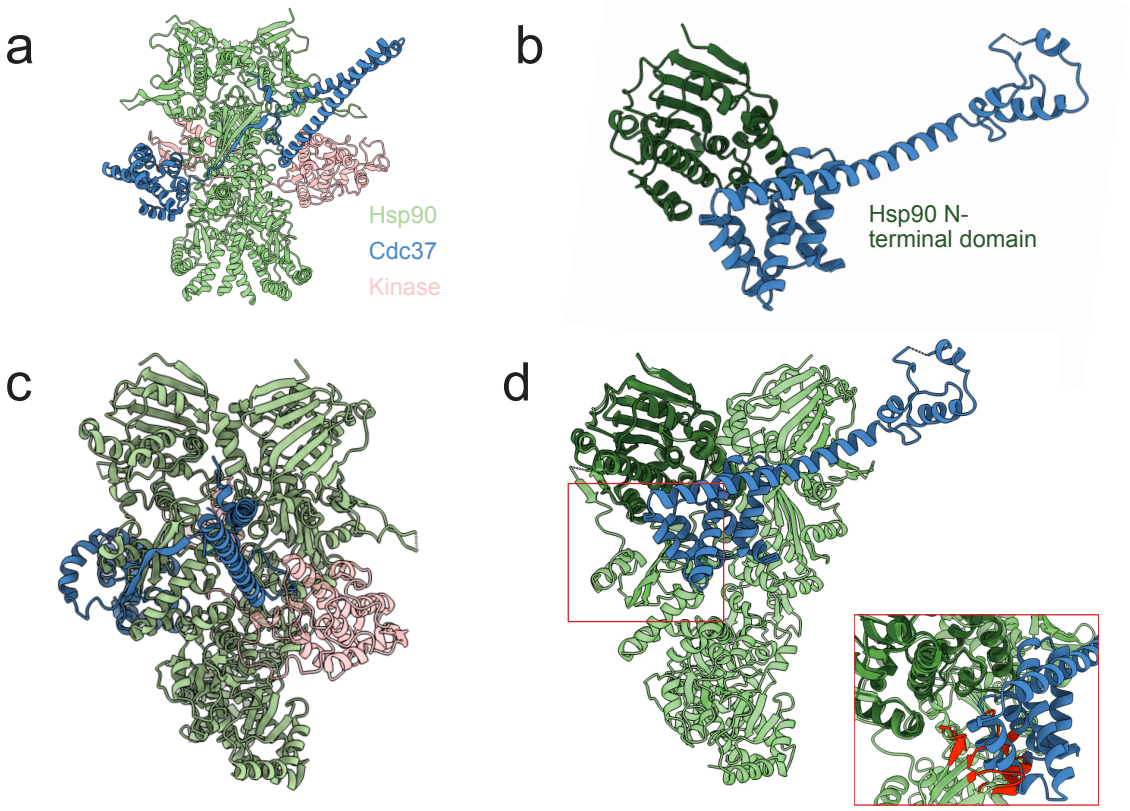

Fig. 1.2. Hsp90 interacts with Cdc37 in two very distinct ways.

a A cryoEM structure shows the N-terminal domain of Cdc37 wrapped around the Hsp90:Kinase complex while the Cdc37 Middle domain rests near the kinase N-lobe (PDB: 5fwl). **b** A crystal structure of the Hsp90 N-terminal domain and the Cdc37 C-terminal domain shows a radically different binding mode (PDB: 1us7). **c,d** Similar Hsp90 conformations show the differences between Cdc37 binding to Hsp90. d The N-terminal crystal structure was aligned to a closed Hsp90 complex. This alignment leads to a large clash (2Å overlap in red) with the Hsp90 middle domain, which suggests that this binding conformation may need to happen when Hsp90 is in an "open" conformation.

Years later, cryo-EM enable the visualization of the larger Hsp90:Cdc37:Cdk4 complex (Vaughan et al., 2006; Verba et al., 2016). In this complex, and various other complexes that came after it (García-Alonso et al., 2022; Oberoi et al., 2022), Cdc37 could be seen making completely different interactions (Fig. 1.2a,c). In these full length Hsp90 and Cdc37 structures, the NTDs of Hsp90 appears in a closed position and the NTD of Cdc37 makes minimal

interactions with the inter-NTD interface of the two Hsp90 monomers. In this structure, Cdc37 wraps around the Hsp90 middle domain, and a small portion of the Cdc37 CTD alpha helical bundle can be visualized. These two distinct structures hint at the large conformational changes that Cdc37 may be able to reaccommodate to enable complex kinase-Hsp90 interactions (Fig. 1.2d).

Essential to the Cdc37 role in bridging Hsp90-Kinase interactions, is a conserved CK2 phosphorylation site at Cdc37's N-terminal S13 (Miyata & Nishida, 2004; Shao, Irwin, et al., 2003). Cdc37 S13 phosphorylation has been shown to be essential in its ability to recruit kinases to Hsp90. Kinase pulldowns in lysates with Cdc37 mutations S13A, S13D, or S13E lead to a decrease in both Cdc37 and Hsp90 interactions with the kinases (Miyata & Nishida, 2007; Shao, Prince, et al., 2003).

Further biochemical work by Vaughan et al showed that Cdc37 was phosphorylated at the S13 position in both insect cell purified Cdc37:Cdk4 complexes and Hsp90:Cdc37:Cdk4 complexes (Vaughan et al., 2008). The group found that while Cdc37^{pS13} could become dephosphorylated by a non-specific phosphatase (lambda PP) in Cdc37:Cdk4 complexes, dephosphorylation was not efficient in Hsp90:Cdc37:Cdk4 complexes. They suggested Cdc37 was "protected" from dephosphorylation while in complex with Hsp90, but noted that the complex could be more readily dephosphorylated after incubation with a TPR containing phosphatase called Protein Phosphatase 5 (PP5). The dephosphorylation of Cdc37^{pS13} in the Hsp90:Cdc37:Cdk4 complex was competed by a TPR binding ligand, and excess Hsp90 addition, which showed that PP5 dephosphorylation happened within the same complex and not in trans. Further work showed that AMPPNP slowed down PP5 dephosphorylation of Cdc37.

Protein Phosphatase 5

Initially discovered as an unimpressively inactive phosphatase, Protein phosphatase 5 (PP5) was later found to contain an autoinhibitory domain that limited its phosphatase activity (Becker et al., 1994; Chen et al., 1994). PP5 belongs to the PPP family of serine/threonine protein phosphatases that is highly conserved in eukaryotes. The PP5 catalytic domain shares 35-45% sequence identity with other PPP phosphatases, but unlike other phosphatases which require binding cofactors or regulatory subunits, PP5 includes the regulatory subunit in its primary sequence (Sacco et al., 2012). Like its family members, PP5 can be inhibited through the binding of okadaic acid, microcystin, cantharidin and others but unlike other PPP family phosphatases, it can be activated by binding polyunsaturated fatty acids like arachidonic acid (Chen et al., 1994; Ramsey & Chinkers, 2002).

Initial cleavage and mutagenesis experiments were able to show an increased rate of PP5 dephosphorylation upon truncation of its N-terminal domain, or truncation of its last 13 residues (Chen et al., 1994; Kang et al., 2001; Sinclair et al., 1999). The crystallographic structure of the PP5 TPR domain then enabled further mutagenesis studies (Das, 1998). Soon after, the C-terminal domain of Hsp90 was also found to activate PP5 activity through TPR interactions to the carboxyl end of Hsp90, and through interaction of PP5 with acidic residues in the Hsp90 CTD. Following structural work leading from these studies have since elucidated a potential mechanism for the autoinhibition of PP5.

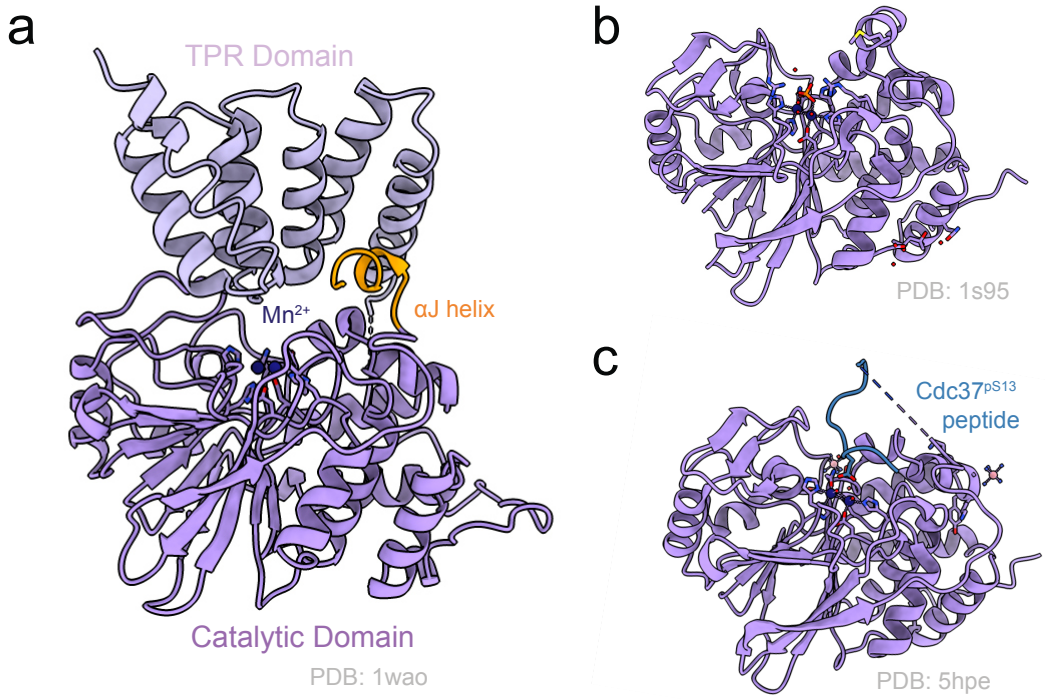

Fig. 1.3. PP5 structures show TPR-occluded active site and catalytic domain interaction with substrate.

a PP5 TPR domain sits atop the Mn bound active site, as the aJ helix helps stabilize inhibitory interactions between the two domains. **b** A proposed mechanism of PP5 dephosphorylation was worked out without the presence of the TPR domain. **c** Shows a crystal structure of chimeric protein composed of a Cdc37 peptide bound to the PP5 catalytic domain.

A crystal structure of the PP5 catalytic domain began unearthing the structural reasons for the autoinhibition caused by the TPR domain and the C-terminal αJ helix (Fig. 1.2b) (Swingle et al., 2004). These reasons were later confirmed by a full length PP5 crystal structure which shows the PP5 active site sandwiched between the TPR domain and the catalytic domain of PP5 (Fig. 1.2a)(Yang et al., 2005). The loops between the alpha helices of the TPR domain make mostly nonpolar interactions with the catalytic domain and its αJ helix. A couple of important hydrogen bonds interaction can be seen between E76 in the TPR domain and two catalytic site residues R275 and Y451. Isothermal calorimetry studies confirmed the binding of

the Hsp90 C-terminal MEEVD peptide to the PP5 TPR domain, but further activation was seen when PP5 was incubated with full length Hsp90. This suggests that further interactions between Hsp90 and PP5 exist that strengthen the activation of the phosphatase activity of PP5 (Yang et al., 2005).

Phosphorylation and dephosphorylation are key yin and yang in cellular division and regulation. PP5 is involved in a wide range of signaling pathways ranging from kinase and glucocorticoid regulation to heat shock factor 1 regulation (Conde et al., 2005; Zuo et al., 1999). PP5 function has been thought to impact proliferation, migration, differentiation, apoptosis, and DNA damage repair amongst others (Golden et al., 2008). Because of its promiscuous activity in so many pathways, extent of PP5's role in specific pathways is mostly still unclear, but PP5 has been shown to dephosphorylate Raf (von Kriegsheim et al., 2006), and ASK1 kinases in the MAPK pathway (Morita et al., 2001), as well as checkpoint kinases like ATM (ataxia telangiectasia mutated) and ATR (ATM and Rad3 related) in the DNA-damage repair and cell cycle arrest pathways (Ali et al., 2004; Zhang et al., 2005).

CRaf (Raf1) Kinase

CRaf Kinase is part of the MAPK pathway, frequently implicated in cellular proliferation and differentiation (Chong et al., 2003; Lavoie & Therrien, 2015; Wellbrock et al., 2004). Mutation of this pathway is often known to lead to oncogenic outcomes, as the closely controlled balance of protein signaling breaks down (Maurer et al., 2011; Tsai et al., 2008). Large efforts have been undertaken to understand this pathway in attempts to find molecular targets capable of inhibiting oncogenic potential. While targets such as the Raf kinases have been successfully targeted, the complexity of the pathway has been shown to lead to paradoxical pathway

activation (Cox & Der, 2010; Lavoie et al., 2013). Further studying the MAPK pathway allows for a better understanding of the complexities around cellular proliferation and differentiation, and it introduces new molecular players which may allow for the ideation of improved therapeutics against human disease.

While further studies are ongoing, the currently mapped out ERK pathway starts with the binding of an extracellular signal such as epidermal growth factor or tumor necrosis factor to a receptor tyrosine kinase at the surface of the cell. This leads the receptor to bind the "connector" protein growth factor receptor-binding protein 2 (Grb2), which activates Son of sevenless (SOS) and the translocates the cytoplasmic SOS to the membrane. The high concentration of SOS near Ras promotes the conversion of Ras-GDP to Ras-GTP, which leads to the initiation of the Ras driven MAPK pathway.

After Ras binding, Raf kinases can be phosphorylated and activated in a series of complex steps (Wellbrock et al., 2004). The Raf kinase family consists of three kinase subtypes: A-Raf, B-Raf, and C-Raf (Raf-1). We will focus our attention on CRaf through this work. Activation requires that Raf kinases translocate to the membrane to interact with Ras and dimerize with another member of the Raf family (Lavoie et al., 2014). This dimerization allows for a highly coordinated sequence of phosphorylation and dephosphorylation steps, which allows for Raf phosphorylation of MEK and finally MEK phosphorylation of ERK. ERK can then amplify the MAPK signal further by regulating transcription factors and phosphorylating other downstream effectors.

Raf kinases consist of three conserved regions (CR), CRaf residue numbering will be used to further describe Raf kinase activation (Wellbrock et al., 2004). The CR1 includes the Ras-binding domain required for membrane recruitment and the Cysteine-rich domain. CR2

consists of a Serine/Threonine-rich domain or the N-terminal acidic region whose phosphorylated state is essential for activation. The CR3 consists of the kinase domain, a domain known to interact with Hsp90. In its inactive state, CRaf is autoinhibited through interactions between their N-terminal region and their catalytic domain, stabilized by 14-3-3 chaperones which bind to two key phosphorylation sites S259 and S621. When activated, pS259 in the CR1 is dephosphorylated and S338/Y341 in the CR2 is phosphorylated. This allows an open conformation of CRaf, where CRaf can dimerize with its kinase partners and become phosphorylated at its activation loop and phosphorylate its downstream effector MEK.

Inactivation of the Raf kinases requires the dephosphorylation of activating phosphorylation sites such as those in the CRaf activation loop, and those in the N-terminal acidic region (Chong et al., 2001; Chong et al., 2003). While inactivation pathways have yet to be clearly outlined, work by A. von Kriegsheim et al. identified PP5 as a key CRaf inactivator through its dephosphorylation of the pS338 phosphorylation site (von Kriegsheim et al., 2006). PP5 dephosphorylation at this location was correlated with a decrease in MEK phosphorylation. Mutation of the PP5 TPR domain described earlier could inhibit the phosphorylation interaction, leading to the hypothesis that Hsp90 might be involved in the CRaf inactivation process.

Hsp90-Kinase Interactions

Early studies of CRaf activation found that CRaf coeluted with Cdc37 and Hsp90 (Silverstein et al., 1998; Stancato et al., 1993), and required these components to in vitro phosphorylate MEK (Grammatikakis et al., 1999; Wartmann & Davis, 1994). Previous examples of Hsp90 coprecipitating with kinases such as v-src, CK2 and eIF-2 alpha had already been shown (Miyata & Yahara, 1992; Rose et al., 1987; Stepanova et al., 1996; Whitesell et al., 1994),

and increasing accounts of kinase interactions with Hsp90 eventually led to the systemic study of Hsp90 interactions with various of its client kinases.

Over 60% of human kinases have been shown to interact with Hsp90, yet no structural motif has been found to explain all Hsp90 interactors (Taipale et al., 2012). Kinase Hsp90 requirement is not necessarily kinase-family specific, instead appearing to scatter throughout the kinome. Not only this but kinases bind Hsp90 at a continuum from "strong" to "weak", varying not only in strength of interactions but also in the stage of kinase life at which they will associate with Hsp90. Closely related kinases such as ErbB1 and ErbB2 or ARaf and BRaf might have completely different Hsp90 requirements, and thorough efforts to distinguish Hsp90-binders to non-binders have been unable to find unifying principles other than a potential correlation between Hsp90 requirement with kinase stability (Bunney et al., 2018; Citri et al., 2006; Taipale et al., 2012; Xu et al., 2005).

Several years ago, the first cryoEM structures of Hsp90 bound to a kinase (Cdk4) and Cdc37 showed an unexpected kinase binding conformation, with the kinase domain N and C lobes stretched apart and the kinase held in the Hsp90 lumen by its ß5 strand (Fig. 1.4) (Verba et al., 2016). Following structures composed of distinct kinases (CRaf, Her2, BRaf) bound to Cdc37 and Hsp90 have shown comparable binding modes (García-Alonso et al., 2022; Oberoi et al., 2022). While this complex conformation might be stabilized upon ATP hydrolysis and

molybdate active site binding, there may be more complex conformations that have yet to be visualized.

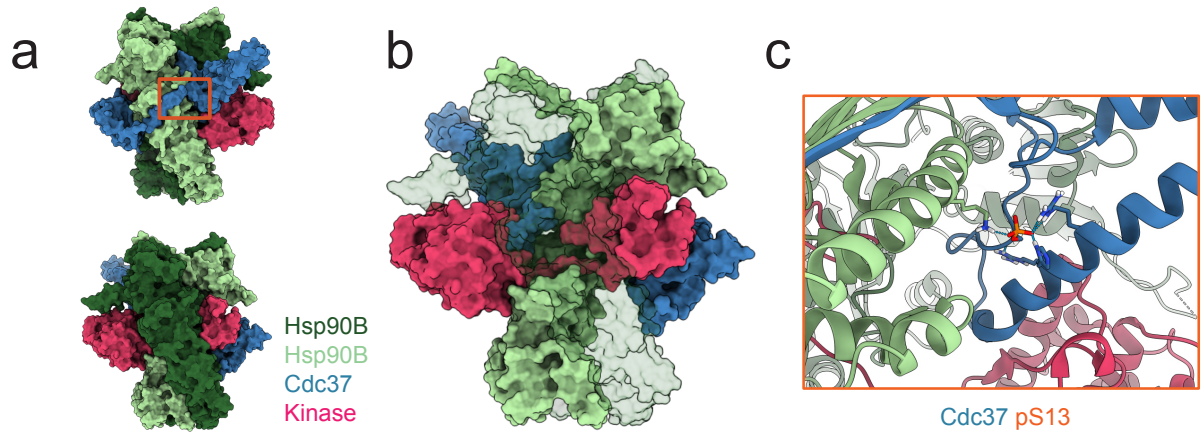

Fig. 1.4. Hsp90:Cdc37:Cdk4 complex shows Kinase stretched apart into N and C-lobes.

a Front and back of Hsp90:Cdc37:Cdk4 complex. **b** Transparent Hsp90B shows Kinase threaded through Hsp90 lumen, with the two kinase lobes on opposite side of Hsp90. **c** Essential Cdc37 pS13 phosphorylation (shown in orange box in **a**) makes key interactions stabilizing Cdc37 and Hsp90 interactions.

Hsp90 appears to play a large breadth of functions on its kinase clients. While some Hsp90 clients require Hsp90 co-translationally, others require Hsp90 throughout their lifespans. Hsp90 has been shown to participate in folding, ligand binding, protein translocation, post translational modification and even degradation decision-making. Inhibiting Hsp90 may lead to protein client degradation, signaling malfunction and eventual toxicity. While the importance of Hsp90 is indisputable, a generalizable mechanism of kinase recruitment, release, or modification while on Hsp90 has yet to be worked out. This work will continue the work of many in an effort to understand Hsp90-kinase interactions.

The Hsp90 Client Loading Complex

Steroid hormone receptors are amidst the numerous signaling Hsp90 clients, and thorough work has been done to understand how the Glucocorticoid Receptor (GR) is chaperoned by Hsp90 (Kirschke et al., 2014; Morishima et al., 2000; Picard et al., 1990; Pratt & Toft, 1997). From this work, a series of complex steps outline how Hsp90 binds the GR, and the number of other chaperones and cochaperones required to go through this process. In this model (Fig. 1.5a), Hsp70 and its corresponding J-protein (Hsp70 nucleotide exchange factor) bind the GR and lead to the partial unfolding of the GR and to the release of ligand bound deep within a GR hydrophobic pocket. Once inhibited by Hsp70, the Hsp Organizing Protein (Hop) bridges Hsp70 and Hsp90 and hands off the GR to from one chaperone to the other for further modification. In this interaction Hsp70 leads Hsp90 to hydrolyze ATP in one of its monomers as the "Client loading complex" becomes disassembled (Johnson et al., 1998). Hsp70 and Hop are ejecting from the Hsp90 complex, and the Hsp90:GR complex binds p23, which allows for Hsp90 closure and leads to ligand rebinding by the GR. Finally, GR is released in a functional ligand-bound state. CryoEM atomic depiction of this elaborate cycle has yielded valuable insights into Hsp90-chaperone interactions (Noddings et al., 2022; Wang et al., 2022).

Efforts to understand if this chaperone cycle is conserved between other Hsp90 clients have found that a conserved mechanism utilizing similar chaperones and co-chaperones (Hsp90, Hsp70, J protein, and Hop) increases client refolding in a wide range of substrates. These clients include other androgen receptors, the p53 tumor suppressor protein, and an argonaute protein (Boysen et al., 2019; Tsuboyama et al., 2018). Work from the Toft and Karnitz labs found that kinases may follow this paradigm as well, however, Hsp90:kinase reconstitution requires an additional recruiter protein, Cdc37 (Arlander et al., 2006; Felts et al., 2007). Arlander et al, used

Chk1 kinase as a model kinase, expressing the kinase through a cell-free system and attaching the nascent protein to agarose beads. This was done in the presence of rabbit reticulocyte, previously known to chaperone kinases. In this work, Cdc25C phosphorylation was used as a kinase activity read-out. Upon Hsp90 inhibition of the system, Chk1 phosphorylation of Cdc25C was noticeably reduced. They next expressed Chk1 in E. Coli, and they reconstituted the kinase chaperone reaction by adding different chaperones. By testing out the importance of various components, the group was able to conclude that Hsp70, Cdc37, Ydj1 (J-protein), Hsp90, CK2, and Hop were required to chaperone Chk1. These components appear similar to those required for the GR chaperone cycle, and so became a focus of our initial studies.

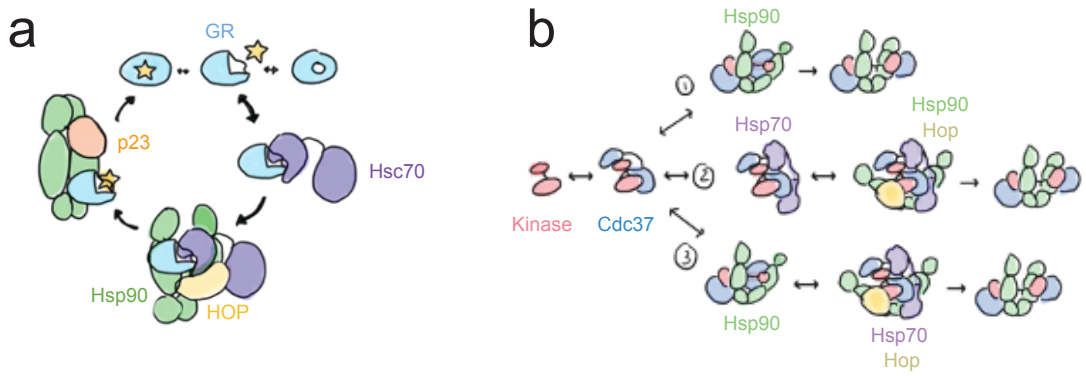

Fig. 1.5. Hypothesis of Kinase Loading Complex born from existing Hsp90-Glucocorticoid interactions.

a The steps of the Glucocorticoid Receptor (GR) chaperone cycle are as follows: GR is unfolded and held by Hsp70 until it can be transferred to Hsp90 with the help of the Hop cochaperone. Once on Hsp90, Hsp90 closes and p23 helps refold GR into its ligand-bound state. Ligand bound GR can now be translocated into the nucleus, or the cycle can begin once again. b Kinases have an addition cochaperone Cdc37 known to loosen the kinase fold to allow for Hsp90 binding. We began with three different hypotheses for kinase loading onto Hsp90. The first considers Cdc37 enough to load the kinase onto Hsp90. The second requires Hsp70 to interact with Cdc37 and the Kinase, to then become loaded onto Hsp90. This model resembles the Hsp90-GR chaperone cycle. Finally, the third model leads to Hsp90:Cdc37:Kinase complex creation, with the need of Hsp70 and Hop for further kinase rearrangement.

Thesis Project Objective

The aim of this thesis project was to further understand how Hsp90 interacts with and modifies CRaf kinase, to work towards a generalizable principle of Hsp90-kinase regulation. My initial work focused on understanding kinase recruitment onto Hsp90, using purified recombinant proteins to reconstitute kinase loading onto Hsp90. The importance of kinase phosphorylation state led to the second half of my project, aimed towards understanding how Hsp90 is involved in the posttranslational modification of its kinase clients. This work involved purification of Hsp90-kinase complexes, and the reconstitution of PP5 dependent dephosphorylation. After biochemical characterization, structural efforts yielded a better understanding of kinase dephosphorylation bound to an Hsp90 complex.

References

Ali, A., Zhang, J., Bao, S., Liu, I., Otterness, D., Dean, N. M., Abraham, R. T., & Wang, X.-F. (2004). Requirement of protein phosphatase 5 in DNA-damage-induced ATM activation. *Genes & Development*, *18*(3), 249-254. https://doi.org/10.1101/gad.1176004

Arlander, S. J. H., Felts, S. J., Wagner, J. M., Stensgard, B., Toft, D. O., & Karnitz, L. M. (2006). Chaperoning Checkpoint Kinase 1 (Chk1), an Hsp90 Client, with Purified Chaperones. *Journal of Biological Chemistry*, *281*(5), 2989-2998. https://doi.org/10.1074/jbc.M508687200

Becker, W., Kentrup, H., Klumpp, S., Schultz, J. E., & Joost, H. G. (1994). Molecular cloning of a protein serine/threonine phosphatase containing a putative regulatory tetratricopeptide repeat domain. *Journal of Biological Chemistry*, *269*(36), 22586-22592. https://doi.org/10.1016/S0021-9258(17)31686-1

Boysen, M., Kityk, R., & Mayer, M. P. (2019). Hsp70- and Hsp90-Mediated Regulation of the Conformation of p53 DNA Binding Domain and p53 Cancer Variants. *Molecular Cell*, *74*(4), 831-843.e834. https://doi.org/10.1016/j.molcel.2019.03.032

Bunney, T. D., Inglis, A. J., Sanfelice, D., Farrell, B., Kerr, C. J., Thompson, G. S., Masson, G. R., Thiyagarajan, N., Svergun, D. I., & Williams, R. L. (2018). Disease variants of FGFR3 reveal molecular basis for the recognition and additional roles for Cdc37 in Hsp90 chaperone system. *Structure*, *26*(3), 446-458. e448.

Chen, M. X., McPartlin, A. E., Brown, L., Chen, Y. H., Barker, H. M., & Cohen, P. T. (1994). A novel human protein serine/threonine phosphatase, which possesses four tetratricopeptide repeat motifs and localizes to the nucleus. *The EMBO Journal*, *13*(18), 4278-4290. https://doi.org/10.1002/j.1460-2075.1994.tb06748.x

Chen, S., Sullivan, W. P., Toft, D. O., & Smith, D. F. (1998). Differential interactions of p23 and the TPR-containing proteins Hop, Cyp40, FKBP52 and FKBP51 with Hsp90 mutants. *Cell Stress Chaperones*, *3*(2), 118-129. https://doi.org/10.1379/1466-1268(1998)003<0118:diopat>2.3.co;2

Chong, H., Lee, J., & Guan, K.-L. (2001). Positive and negative regulation of Raf kinase activity and function by phosphorylation. *The EMBO Journal*, *20*(14), 3716-3727.

Chong, H., Vikis, H. G., & Guan, K.-L. (2003). Mechanisms of regulating the Raf kinase family. *Cellular Signalling*, *15*(5), 463-469. https://doi.org/10.1016/S0898-6568(02)00139-0

Citri, A., Harari, D., Shohat, G., Ramakrishnan, P., Gan, J., Lavi, S., Eisenstein, M., Kimchi, A., Wallach, D., & Pietrokovski, S. (2006). Hsp90 recognizes a common surface on client kinases. *Journal of Biological Chemistry*, *281*(20), 14361-14369.

Conde, R., Xavier, J., McLoughlin, C., Chinkers, M., & Ovsenek, N. (2005). Protein Phosphatase 5 Is a Negative Modulator of Heat Shock Factor 1. *Journal of Biological Chemistry*, *280*(32), 28989-28996. https://doi.org/10.1074/jbc.M503594200

Cox, A. D., & Der, C. J. (2010). The Raf Inhibitor Paradox: Unexpected Consequences of Targeted Drugs. *Cancer Cell*, *17*(3), 221-223. https://doi.org/https://doi.org/10.1016/j.ccr.2010.02.029

Cutforth, T., & Rubin, G. M. (1994). Mutations in Hsp83 and cdc37 impair signaling by the sevenless receptor tyrosine kinase in Drosophila. *Cell*, *77*(7), 1027-1036.

D'Andrea, L. D., & Regan, L. (2003). TPR proteins: the versatile helix. *Trends in Biochemical Sciences*, *28*(12), 655-662. https://doi.org/https://doi.org/10.1016/j.tibs.2003.10.007

Dahiya, V., Agam, G., Lawatscheck, J., Rutz, D. A., Lamb, D. C., & Buchner, J. (2019). Coordinated Conformational Processing of the Tumor Suppressor Protein p53 by the

Hsp70 and Hsp90 Chaperone Machineries. *Molecular Cell*, *74*(4), 816-830.e817. https://doi.org/10.1016/j.molcel.2019.03.026

Das, A. K. (1998). The structure of the tetratricopeptide repeats of protein phosphatase 5: implications for TPR-mediated protein-protein interactions. *The EMBO Journal*, *17*(5), 1192-1199. https://doi.org/10.1093/emboj/17.5.1192

Eckl, J. M., Daake, M., Schwartz, S., & Richter, K. (2016). Nucleotide-Free sB-Raf is Preferentially Bound by Hsp90 and Cdc37 In Vitro. *Journal of Molecular Biology*, *428*(20), 4185-4196. https://doi.org/10.1016/j.jmb.2016.09.002

Felts, S. J., Karnitz, L. M., & Toft, D. O. (2007). Functioning of the Hsp90 machine in chaperoning checkpoint kinase 1 (Chk1) and the progesterone receptor (PR). *Cell Stress & Chaperones*, *12*(4), 353. https://doi.org/10.1379/CSC-299.1

García-Alonso, S., Mesa, P., Ovejero, L. d. l. P., Aizpurua, G., Lechuga, C. G., Zarzuela, E., Santiveri, C. M., Sanclemente, M., Muñoz, J., Musteanu, M., Campos-Olivas, R., Martínez-Torrecuadrada, J., Barbacid, M., & Montoya, G. (2022). Structure of the RAF1-HSP90-CDC37 complex reveals the basis of RAF1 regulation. *Molecular Cell*, *82*(18), 3438-3452.e3438. https://doi.org/10.1016/j.molcel.2022.08.012

Golden, T., Swingle, M., & Honkanen, R. E. (2008). The role of serine/threonine protein phosphatase type 5 (PP5) in the regulation of stress-induced signaling networks and cancer. *Cancer and Metastasis Reviews*, *27*(2), 169-178. https://doi.org/10.1007/s10555-008-9125-z

Grammatikakis, N., Lin, J.-H., Grammatikakis, A., Tsichlis, P. N., & Cochran, B. H. (1999). p50 ^{cdc37} Acting in Concert with Hsp90 Is Required for Raf-1

Function. *Molecular and Cellular Biology*, *19*(3), 1661-1672. https://doi.org/10.1128/MCB.19.3.1661

Johnson, B. D., Schumacher, R. J., Ross, E. D., & Toft, D. O. (1998). Hop Modulates hsp70/hsp90 Interactions in Protein Folding. *Journal of Biological Chemistry*, *273*(6), 3679-3686. https://doi.org/10.1074/jbc.273.6.3679

Johnson, J. L. (2012). Evolution and function of diverse Hsp90 homologs and cochaperone proteins. *Biochimica et Biophysica Acta (BBA) - Molecular Cell Research*, *1823*(3), 607-613. https://doi.org/https://doi.org/10.1016/j.bbamcr.2011.09.020

Johnson, J. L., & Brown, C. (2009). Plasticity of the Hsp90 chaperone machine in divergent eukaryotic organisms. *Cell Stress and Chaperones*, *14*(1), 83-94. https://doi.org/10.1007/s12192-008-0058-9

Kang, H., Sayner, S. L., Gross, K. L., Russell, L. C., & Chinkers, M. (2001). Identification of Amino Acids in the Tetratricopeptide Repeat and C-Terminal Domains of Protein Phosphatase 5 Involved in Autoinhibition and Lipid Activation. *Biochemistry*, *40*(35), 10485-10490. https://doi.org/10.1021/bi010999i

Keramisanou, D., Aboalroub, A., Zhang, Z., Liu, W., Marshall, D., Diviney, A., Larsen, Randy W., Landgraf, R., & Gelis, I. (2016). Molecular Mechanism of Protein Kinase Recognition and Sorting by the Hsp90 Kinome-Specific Cochaperone Cdc37. *Molecular Cell*, *62*(2), 260-271. https://doi.org/10.1016/j.molcel.2016.04.005

Kirschke, E., Goswami, D., Southworth, D., Griffin, Patrick R., & Agard, David A. (2014). Glucocorticoid Receptor Function Regulated by Coordinated Action of the Hsp90 and Hsp70 Chaperone Cycles. *Cell*, *157*(7), 1685-1697. https://doi.org/10.1016/j.cell.2014.04.038

Lavoie, H., Li, J. J., Thevakumaran, N., Therrien, M., & Sicheri, F. (2014). Dimerization-induced allostery in protein kinase regulation. *Trends in Biochemical Sciences*, *39*(10), 475-486. https://doi.org/10.1016/j.tibs.2014.08.004

Lavoie, H., & Therrien, M. (2015). Regulation of RAF protein kinases in ERK signalling. *Nature Reviews Molecular Cell Biology*, *16*(5), 281-298. https://doi.org/10.1038/nrm3979

Lavoie, H., Thevakumaran, N., Gavory, G., Li, J. J., Padeganeh, A., Guiral, S., Duchaine, J., Mao, D. Y. L., Bouvier, M., Sicheri, F., & Therrien, M. (2013). Inhibitors that stabilize a closed RAF kinase domain conformation induce dimerization. *Nature Chemical Biology*, *9*(7), 428-436. https://doi.org/10.1038/nchembio.1257

Lee, K., Thwin, A. C., Nadel, C. M., Tse, E., Gates, S. N., Gestwicki, J. E., & Southworth, D. R. (2021). The structure of an Hsp90-immunophilin complex reveals cochaperone recognition of the client maturation state. *Molecular Cell*, *81*(17), 3496-3508.e3495. https://doi.org/10.1016/j.molcel.2021.07.023

Maurer, G., Tarkowski, B., & Baccarini, M. (2011). Raf kinases in cancer–roles and therapeutic opportunities. *Oncogene*, *30*(32), 3477-3488. https://doi.org/10.1038/onc.2011.160

Miyata, Y., & Nishida, E. (2004). CK2 Controls Multiple Protein Kinases by Phosphorylating a Kinase-Targeting Molecular Chaperone, Cdc37. *Molecular and Cellular Biology*, *24*(9), 4065-4074. https://doi.org/10.1128/MCB.24.9.4065-4074.2004

Miyata, Y., & Nishida, E. (2007). Analysis of the CK2-dependent phosphorylation of serine 13 in Cdc37 using a phospho-specific antibody and phospho-affinity gel electrophoresis: Cdc37 phosphorylation by CK2 and signaling kinases. *FEBS Journal*, *274*(21), 5690-5703. https://doi.org/10.1111/j.1742-4658.2007.06090.x

Miyata, Y., & Yahara, I. (1992). The 90-kDa heat shock protein, HSP90, binds and protects casein kinase II from self-aggregation and enhances its kinase activity. *Journal of Biological Chemistry*, *267*(10), 7042-7047.

Morishima, Y., Murphy, P. J., Li, D.-P., Sanchez, E. R., & Pratt, W. B. (2000). Stepwise assembly of a glucocorticoid receptor· hsp90 heterocomplex resolves two sequential ATP-dependent events involving first hsp70 and then hsp90 in opening of the steroid binding pocket. *Journal of Biological Chemistry*, *275*(24), 18054-18060.

Morita, K., Saitoh, M., Tobiume, K., Matsuura, H., Enomoto, S., Nishitoh, H., & Ichijo, H. (2001). Negative feedback regulation of ASK1 by protein phosphatase 5 (PP5) in response to oxidative stress. *The EMBO Journal*, *20*(21), 6028-6036. https://doi.org/10.1093/emboj/20.21.6028

Noddings, C. M., Johnson, J. L., & Agard, D. A. (2023). *Cryo-EM reveals how Hsp90 and FKBP immunophilins co-regulate the Glucocorticoid Receptor* [preprint]. http://biorxiv.org/lookup/doi/10.1101/2023.01.10.523504

Noddings, C. M., Wang, R. Y.-R., Johnson, J. L., & Agard, D. A. (2022). Structure of Hsp90–p23–GR reveals the Hsp90 client-remodelling mechanism. *Nature*, *601*(7893), 465-469. https://doi.org/10.1038/s41586-021-04236-1

Oberoi, J., Aran-Guiu, X., Outwin, E. A., Schellenberger, P., Roumeliotis, T. I., Choudhary, J. S., & Pearl, L. H. (2022). *HSP90-CDC37-PP5 forms a structural platform for kinase dephosphorylation* [preprint]. http://biorxiv.org/lookup/doi/10.1101/2022.05.03.490524

Panaretou, B. (1998). ATP binding and hydrolysis are essential to the function of the Hsp90 molecular chaperone invivo. *The EMBO Journal*, *17*(16), 4829-4836. https://doi.org/10.1093/emboj/17.16.4829

Picard, D., Khursheed, B., Garabedian, M. J., Fortin, M. G., Lindquist, S., & Yamamoto, K. R. (1990). Reduced levels of hsp90 compromise steroid receptor action in vivo. *Nature*, *348*(6297), 166-168.

Polier, S., Samant, R. S., Clarke, P. A., Workman, P., Prodromou, C., & Pearl, L. H. (2013). ATP-competitive inhibitors block protein kinase recruitment to the Hsp90-Cdc37 system. *Nature Chemical Biology*, *9*(5), 307-312. https://doi.org/10.1038/nchembio.1212

Pratt, W. B., & Toft, D. O. (1997). Steroid receptor interactions with heat shock protein and immunophilin chaperones. *Endocrine reviews*, *18*(3), 306-360.

Ramsey, A. J., & Chinkers, M. (2002). Identification of Potential Physiological Activators of Protein Phosphatase 5. *Biochemistry*, *41*(17), 5625-5632. https://doi.org/10.1021/bi016090h

Reed, S. I. (1980). THE SELECTION OF S. CEREVISIAE MUTANTS DEFECTIVE IN THE START EVENT OF CELL DIVISION. *Genetics*, *95*(3), 561-577. https://doi.org/10.1093/genetics/95.3.561

Roe, S. M., Ali, M. M. U., Meyer, P., Vaughan, C. K., Panaretou, B., Piper, P. W., Prodromou, C., & Pearl, L. H. (2004). The Mechanism of Hsp90 Regulation by the Protein Kinase-Specific Cochaperone p50cdc37. *Cell*, *116*(1), 87-98. https://doi.org/https://doi.org/10.1016/S0092-8674(03)01027-4

Rose, D. W., Wettenhall, R. E., Kudlicki, W., Kramer, G., & Hardesty, B. (1987). The 90-kilodalton peptide of the heme-regulated eIF-2. alpha. kinase has sequence homology with the 90-kilodalton heat shock protein. *Biochemistry*, *26*(21), 6583-6587.

Sacco, F., Perfetto, L., Castagnoli, L., & Cesareni, G. (2012). The human phosphatase interactome: An intricate family portrait. *FEBS Letters*, *586*(17), 2732-2739. https://doi.org/10.1016/j.febslet.2012.05.008

Schopf, F. H., Biebl, M. M., & Buchner, J. (2017). The HSP90 chaperone machinery. *Nature Reviews Molecular Cell Biology*, *18*(6), 345-360. https://doi.org/10.1038/nrm.2017.20

Shao, J., Irwin, A., Hartson, S. D., & Matts, R. L. (2003). Functional Dissection of Cdc37: Characterization of Domain Structure and Amino Acid Residues Critical for Protein Kinase Binding. *Biochemistry*, *42*(43), 12577-12588. https://doi.org/10.1021/bi035138j

Shao, J., Prince, T., Hartson, S. D., & Matts, R. L. (2003). Phosphorylation of Serine 13 Is Required for the Proper Function of the Hsp90 Co-chaperone, Cdc37. *Journal of Biological Chemistry*, *278*(40), 38117-38120. https://doi.org/10.1074/jbc.C300330200

Siligardi, G., Panaretou, B., Meyer, P., Singh, S., Woolfson, D. N., Piper, P. W., Pearl, L. H., & Prodromou, C. (2002). Regulation of Hsp90 ATPase Activity by the Co-chaperone Cdc37p/p50cdc37 *. *Journal of Biological Chemistry*, *277*(23), 20151-20159. https://doi.org/https://doi.org/10.1074/jbc.M201287200

Silverstein, A. M., Grammatikakis, N., Cochran, B. H., Chinkers, M., & Pratt, W. B. (1998). p50cdc37 Binds Directly to the Catalytic Domain of Raf as Well as to a Site on hsp90 That Is Topologically Adjacent to the Tetratricopeptide Repeat Binding Site*. *Journal of Biological Chemistry*, *273*(32), 20090-20095. https://doi.org/https://doi.org/10.1074/jbc.273.32.20090

Sinclair, C., Borchers, C., Parker, C., Tomer, K., Charbonneau, H., & Rossie, S. (1999). The Tetratricopeptide Repeat Domain and a C-terminal Region Control the Activity of

Ser/Thr Protein Phosphatase 5*. *Journal of Biological Chemistry*, *274*(33), 23666-23672. https://doi.org/https://doi.org/10.1074/jbc.274.33.23666

Stancato, L. F., Chow, Y. H., Hutchison, K. A., Perdew, G. H., Jove, R., & Pratt, W. B. (1993). Raf exists in a native heterocomplex with hsp90 and p50 that can be reconstituted in a cell-free system. *Journal of Biological Chemistry*, *268*(29), 21711-21716. https://doi.org/10.1016/S0021-9258(20)80600-0

Stepanova, L., Leng, X., Parker, S. B., & Harper, J. W. (1996). Mammalian p50Cdc37 is a protein kinase-targeting subunit of Hsp90 that binds and stabilizes Cdk4. *Genes & Development*, *10*(12), 1491-1502. https://doi.org/10.1101/gad.10.12.1491

Swingle, M. R., Honkanen, R. E., & Ciszak, E. M. (2004). Structural Basis for the Catalytic Activity of Human Serine/Threonine Protein Phosphatase-5. *Journal of Biological Chemistry*, *279*(32), 33992-33999. https://doi.org/10.1074/jbc.M402855200

Taipale, M., Jarosz, D. F., & Lindquist, S. (2010). HSP90 at the hub of protein homeostasis: emerging mechanistic insights. *Nature Reviews Molecular Cell Biology*, *11*(7), 515-528. https://doi.org/10.1038/nrm2918

Taipale, M., Krykbaeva, I., Koeva, M., Kayatekin, C., Westover, Kenneth D., Karras, Georgios I., & Lindquist, S. (2012). Quantitative Analysis of Hsp90-Client Interactions Reveals Principles of Substrate Recognition. *Cell*, *150*(5), 987-1001. https://doi.org/10.1016/j.cell.2012.06.047

Terasawa, K., Minami, M., & Minami, Y. (2005). Constantly Updated Knowledge of Hsp90. *The Journal of Biochemistry*, *137*(4), 443-447. https://doi.org/10.1093/jb/mvi056

Tsai, J., Lee, J. T., Wang, W., Zhang, J., Cho, H., Mamo, S., Bremer, R., Gillette, S., Kong, J., Haass, N. K., Sproesser, K., Li, L., Smalley, K. S. M., Fong, D., Zhu, Y.-L., Marimuthu,

A., Nguyen, H., Lam, B., Liu, J., . . . Bollag, G. (2008). Discovery of a selective inhibitor of oncogenic B-Raf kinase with potent antimelanoma activity. *Proceedings of the National Academy of Sciences*, *105*(8), 3041-3046. https://doi.org/10.1073/pnas.0711741105

Tsuboyama, K., Tadakuma, H., & Tomari, Y. (2018). Conformational Activation of Argonaute by Distinct yet Coordinated Actions of the Hsp70 and Hsp90 Chaperone Systems. *Molecular Cell*, *70*(4), 722-729.e724. https://doi.org/10.1016/j.molcel.2018.04.010

Vaughan, C. K., Gohlke, U., Sobott, F., Good, V. M., Ali, M. M. U., Prodromou, C., Robinson, C. V., Saibil, H. R., & Pearl, L. H. (2006). Structure of an Hsp90-Cdc37-Cdk4 Complex. *Molecular Cell*, *23*(5), 697-707. https://doi.org/https://doi.org/10.1016/j.molcel.2006.07.016

Vaughan, C. K., Mollapour, M., Smith, J. R., Truman, A., Hu, B., Good, V. M., Panaretou, B., Neckers, L., Clarke, P. A., Workman, P., Piper, P. W., Prodromou, C., & Pearl, L. H. (2008). Hsp90-Dependent Activation of Protein Kinases Is Regulated by Chaperone-Targeted Dephosphorylation of Cdc37. *Molecular Cell*, *31*(6), 886-895. https://doi.org/10.1016/j.molcel.2008.07.021

Verba, K. A., Wang, R. Y.-R., Arakawa, A., Liu, Y., Shirouzu, M., Yokoyama, S., & Agard, D. A. (2016). Atomic structure of Hsp90-Cdc37-Cdk4 reveals that Hsp90 traps and stabilizes an unfolded kinase. *Science*, *352*(6293), 1542-1547. https://doi.org/10.1126/science.aaf5023

von Kriegsheim, A., Pitt, A., Grindlay, G. J., Kolch, W., & Dhillon, A. S. (2006). Regulation of the Raf–MEK–ERK pathway by protein phosphatase 5. *Nature Cell Biology*, *8*(9), 1011-1016. https://doi.org/10.1038/ncb1465

Wang, R. Y.-R., Noddings, C. M., Kirschke, E., Myasnikov, A. G., Johnson, J. L., & Agard, D. A. (2022). Structure of Hsp90–Hsp70–Hop–GR reveals the Hsp90 client-loading mechanism. *Nature*, *601*(7893), 460-464. https://doi.org/10.1038/s41586-021-04252-1

Wartmann, M., & Davis, R. J. (1994). The native structure of the activated Raf protein kinase is a membrane-bound multi-subunit complex. *The Journal of Biological Chemistry*, *269*(9), 6695-6701. http://www.ncbi.nlm.nih.gov/pubmed/8120027

Wellbrock, C., Karasarides, M., & Marais, R. (2004). The RAF proteins take centre stage. *Nature Reviews Molecular Cell Biology*, *5*(11), 875-885. https://doi.org/10.1038/nrm1498

Whitesell, L., Mimnaugh, E. G., De Costa, B., Myers, C. E., & Neckers, L. M. (1994). Inhibition of heat shock protein HSP90-pp60v-src heteroprotein complex formation by benzoquinone ansamycins: essential role for stress proteins in oncogenic transformation. *Proceedings of the National Academy of Sciences*, *91*(18), 8324-8328. https://doi.org/10.1073/pnas.91.18.8324

Xu, W., Yuan, X., Xiang, Z., Mimnaugh, E., Marcu, M., & Neckers, L. (2005). Surface charge and hydrophobicity determine ErbB2 binding to the Hsp90 chaperone complex. *Nature Structural & Molecular Biology*, *12*(2), 120-126.

Yang, J., Roe, S. M., Cliff, M. J., Williams, M. A., Ladbury, J. E., Cohen, P. T. W., & Barford, D. (2005). Molecular basis for TPR domain-mediated regulation of protein phosphatase 5. *The EMBO Journal*, *24*(1), 1-10. https://doi.org/10.1038/sj.emboj.7600496

Zhang, J., Bao, S., Furumai, R., Kucera, K. S., Ali, A., Dean, N. M., & Wang, X.-F. (2005). Protein Phosphatase 5 Is Required for ATR-Mediated Checkpoint Activation. *Molecular*

and Cellular Biology, *25*(22), 9910-9919. https://doi.org/10.1128/MCB.25.22.9910-9919.2005

Zuo, Z., Urban, G., Scammell, J. G., Dean, N. M., McLean, T. K., Aragon, I., & Honkanen, R. E. (1999). Ser/Thr Protein Phosphatase Type 5 (PP5) Is a Negative Regulator of Glucocorticoid Receptor-Mediated Growth Arrest. *Biochemistry*, *38*(28), 8849-8857. https://doi.org/10.1021/bi990842e

Chapter 2

The Elusive Hsp90 "Kinase Loading Complex"

Preface

Biochemical and structural work on the interaction between Hsp90 and the Glucocorticoid Receptor (GR) demonstrated a vital series of steps required for the unfolding and loading of the GR onto Hsp90 (Kirschke et al., 2014; Morishima et al., 2000; Noddings et al., 2022; Picard et al., 1990; Pratt & Toft, 1997; Wang et al., 2022). Further work on a kinase system showed that similar chaperones and cochaperones are required to aid Chk1 kinase loading onto Hsp90 (Arlander et al., 2006; Felts et al., 2007). Given Hsp90's interaction with a wide number of kinases, understanding the mechanism behind Kinase binding of Hsp90 would enable in-vitro work on Hsp90-Kinase interactions (Taipale et al., 2012), and make possible the pharmaceutical inhibition of key interactions between Hsp90 and oncogenic kinases (Trepel et al., 2010).

Kinases are essential signaling molecules and they therefore require careful regulation to ensure proper cellular function. One of the many ways to regulate kinases, is to modulate these labile protein's folding stability and build in a dependence for the use of molecular chaperones that can in turn be regulated. In fact, oncogenic cells have been known to overexpress molecular chaperones and in doing so allow unstable and overactive kinase variants to thrive and continue their oncogenic process. For this reason, we included an oncogenic kinase in our initial attempts to isolate a Kinase Loading Complex. With one key mutation (V600E) BRaf kinase can turn from a relatively Hsp90 independent kinase, to a highly dependent Hsp90 kinase (Polier et al., 2013). This mutation not only makes BRaf "addicted" to Hsp90, but it also shifts BRaf towards an active conformation and leads to Ras-independent MAPK signaling. This variant has been shown to be present in over 50% of melanoma cases, and it is also prevalent in colorectal, ovarian, and thyroid cancers (Davies et al., 2002).

Medical interest in BRaf kinase has led to its thorough biochemical characterization and the discovery of key solubilizing mutations on the BRaf kinase domain. The combination of the solubilizing mutations with the activating V600E mutation allows BRaf to be a "friendlier" protein to work with biochemically, while still preserving the Hsp90-kinase interactions of interest(Polier et al., 2013; Tsai et al., 2008). For these reasons, we set out to isolate the "Kinase Loading Complex" using BRaf kinase as a model protein. This mutated form of BRaf will be called sBRaf for the remainder of this chapter.

Summary

A Glucocorticoid Receptor (GR) Hsp90 loading complex has been isolated and characterized through cryoEM, giving the Hsp90 field a better understanding of GR recruitment

onto Hsp90. Efforts to isolate a similar "Kinase Loading Complex" have previously been undertaken by D. Coutandin and K. Verba, but the Kinase Loading Complex has remained elusive. The use of sBRaf kinase allows for further biochemical characterization of kinase interactions with various chaperones, but the immediate binding of sBRaf to Hsp90 and Cdc37 was not seen for Her2 kinase domain, leading to distrust of the highly mutated sBRaf kinase as an Hsp90 substrate. D. Coutandin's efforts to isolate a Kinase Loading Complex led to the coelution of various chaperones and cochaperones with sBRaf kinase through Size Exclusion Chromatography. These initial experiments allowed for the optimization of Fluorescence Correlation Spectroscopy (FCS) conditions that could visualize larger complexes by studying the sBRaf-bound Kinase Loading Complex's hydrodynamic radius. Visualized through FCS, the reconstituted complexes appeared heterogeneous in size. Pulldowns of the Kinase Loading Complex were inconclusive and have yet to be optimized. Efforts to visualize the reconstituted complexes on cryoEM grids led to aggregated, dark, or non-existent particles on the micrographs. The lack of homogeneity in the complexes seen through FCS, Size Exclusion, pulldowns and cryoEM suggests there is still much work to do to understand the formation of a Kinase Loading Complex.

Results

Isolating a Kinase Loading Complex through size exclusion

Previous work has demonstrated that sBRaf will bind phosphorylated Cdc37 and Hsp90 without the need for a full Kinase Loading Complex (Polier et al., 2013). The kinase domain of sBRaf, full length Cdc37 and full length Hsp90 were expressed and purified in E. coli BL21 cells. Cdc37 was subsequently in-vitro phosphorylated by CK2 and purified, ensuring the

presence of the essential Cdc37^{pS13} phosphorylation. These proteins were mixed on ice for 30 min, ran through an Superose6 size exclusion column, and the fractions were analyzed using an SDS gel. We were able to reproduce the previously mentioned results (Polier et al., 2013), noting the importance of Cdc37 for sBRaf – Hsp90 interactions (Fig. 2.1a). Similar efforts to purify the HER2 kinase domain and incubate with Cdc37 and Hsp90 did not yield a similar complex, showing the Hsp90:Cdc37 complex eluting first, before seeing the HER2 kinase elute on its own.

We hypothesized that if the Kinase Loading Complex could be reconstituted with sBRaf, similar conditions would apply to HER2 kinase. This allowed a further test condition to validate the Kinase Loading Complex formation. D. Coutandin began to optimize for the Kinase Loading complex through minimal addition of the protein components previously found to be essential for Chk1 kinase. Protein components, protein component concentrations, temperature, buffer composition, nucleotide addition, Hsp90 inhibition, complex assembly time. After many optimizing iterations the following conditions found were as follows: 5 µM sBRaf, 5 µM DNAJB1, 20 µM Hsc70, 5µM Cdc37^{pS13}, 5 µM Hop, 5 µM Hsp90B$^{dimer\ inhibited}$ and 2.5mM ATP or AMPPNP. Hsc70 and Hsp90B were both used instead of Hsp70 and Hsp90A because unlike the latter, they are constitutively expressed in cells. Hsp90B was also shown to interact with kinases in previously published work (Taipale et al., 2012). Following the work of Wang et al. (Wang et al., 2022), the client loading cycle was stalled to allow complex accumulation by either Hsp90 covalent inhibitor AC50 binding (Cuesta et al., 2020), or the use of the Hsp90^{D88N} hydrolysis incompetent mutant (Fig. 2.1b).

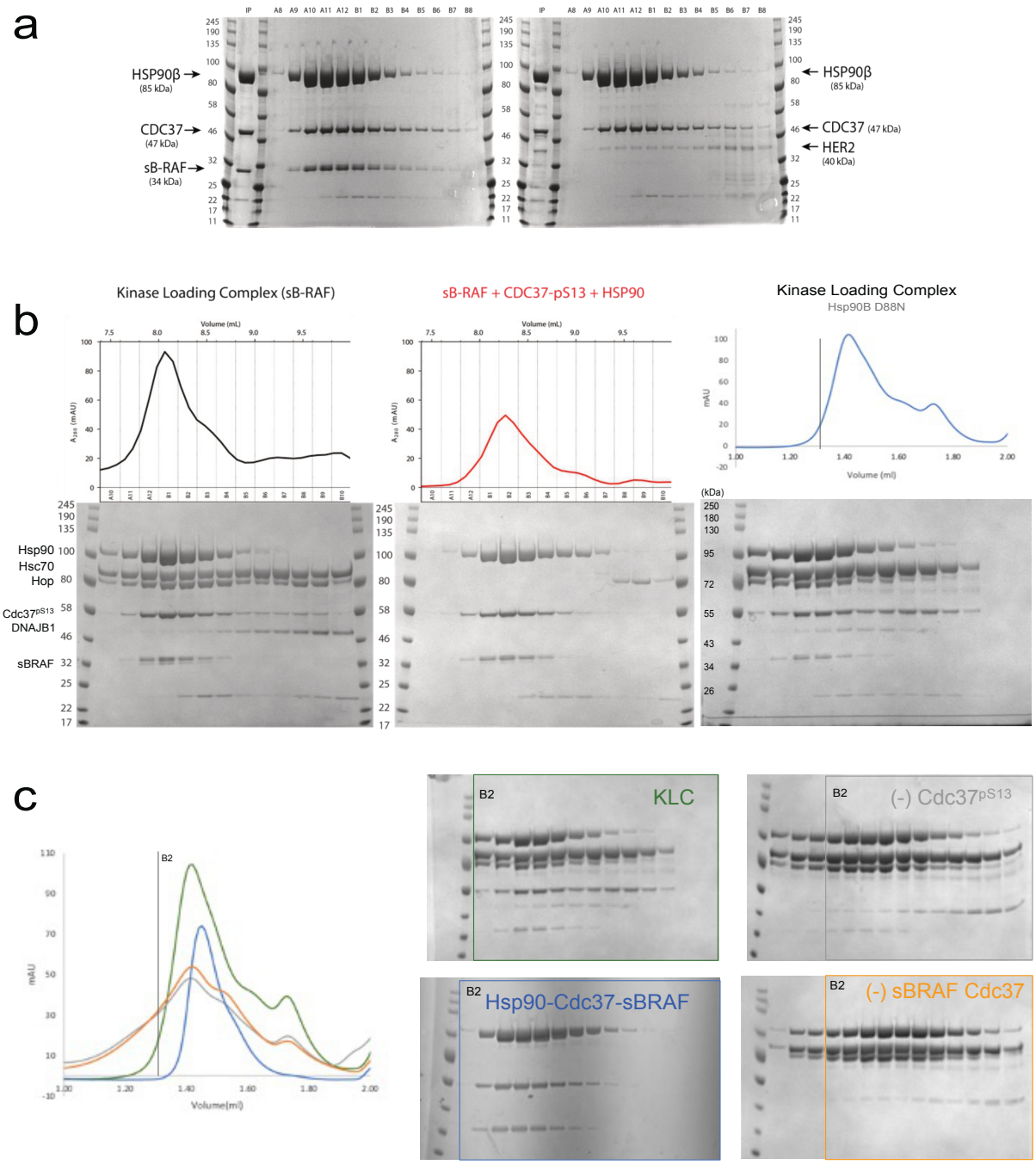

Fig. 2.1 The Kinase Loading Complex may comigrate on Size Exclusion Chromatography.

a sBRaf kinase is readily incorporated into an Hsp90:Cdc37:sBRaf complex, while HER2 lags behind most of the Hsp90:Cdc37 complex. Work done by D. Coutandin. **b** A peak larger than the Hsp90:Cdc37:sBRaf complex elutes off of the Sup6 column after Kinase Loading Conditions were optimized. The Hsp90 inhibitor AC50 or the Hsp90 mutant Hsp90^{D88N} were used to lead to the accumulation of this complex. **c** Control traces of differing complexes

show elution of proteins starting at the same B2 well. Similar traces led to the conclusion that more sensitive method needed to be explored.

Although the "Kinase Loading Complex" conditions led to the formation of a large peak, the large concentrations of proteins used and the possible heterogeneity of the complexes present, made it essential for the right controls to be run. After running sizing traces with complexes from which Cdc37, sBRaf and Cdc37, and the Hsp70 components were left out, very similar SDS traces could be visualized. Hsp70 is known to oligomerize and bind Hop, leading to the elution of these proteins at high molecular weights potentially confusable with the Kinase Loading Complex peak (Fig. 2.1c).

Crosslinking experiments were then carried out to compare the size of Kinase Loading Complex and Hsp90:Cdc37:sBRaf crosslinked complexes. The Kinase Loading Complex experiment was expected to yield a larger SDS band than the Hsp90:Cdc37:sBRaf band. The Kinase Loading Complex was crosslinked with glutaraldehyde before or after Size Exclusion Chromatography, and run on an SDS gel. Different well samples were looked at with mass photometry to see a large variability in complex sizes. Comparison of these large complexes with

a crosslinked Hsp90:Cdc37:sBRaf or an Hsc70:DNAJB1 crosslinked complex showed similar sizes (Fig.2.2).

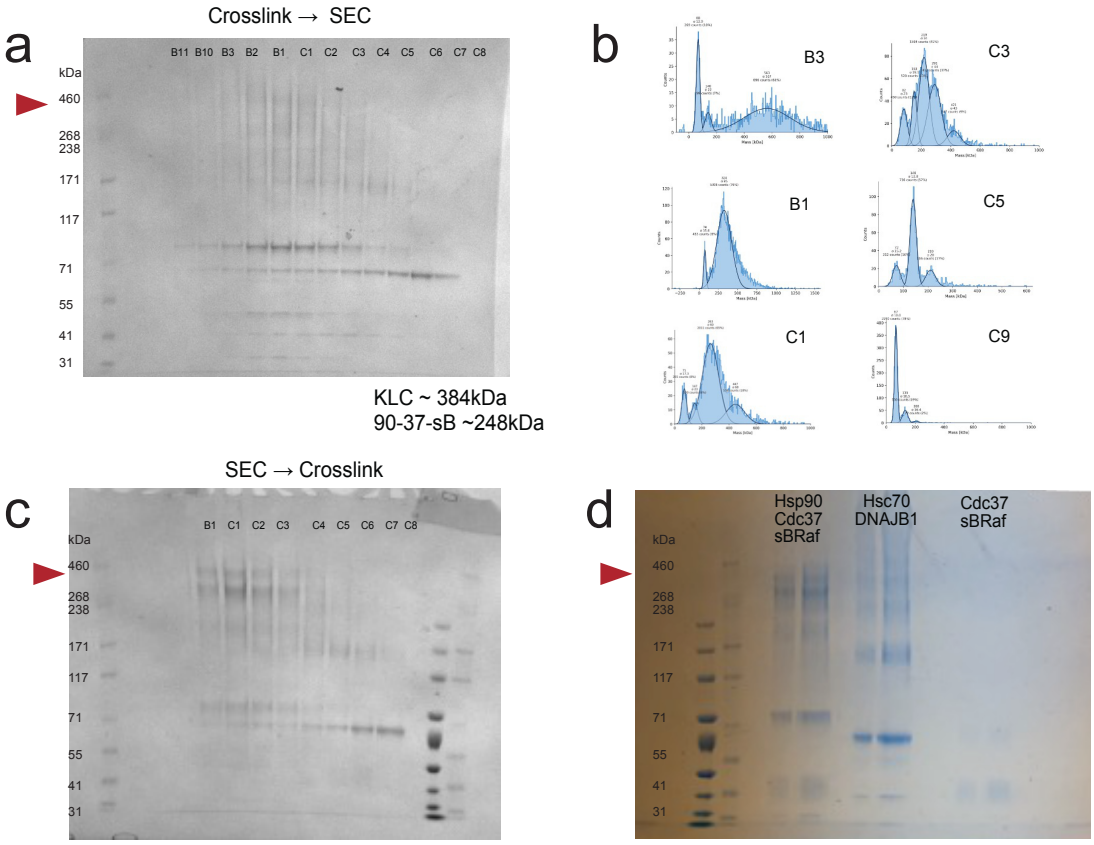

Fig. 2.2. Crosslinked "Kinase Loading Complex" appears similar in size to Hsp90:Cdc37:sBRaf complex.

a, c The optimized Kinase Loading Complex was crosslinked and run through size exclusion, or run through size exclusion and then crosslink. SDS gel traces of these runs show a large molecular weight band (red triangle) around the right molecular weight. **b** Mass photometry traces of each of the size exclusion wells shows heterogeneous complexes, with some peaks around 440kDa and 320kDa. d Control crosslinking of the Hsp90:Cdc37:sBRaf complex, and the Hsc70:DNAJB1 complex shows large molecular weight bands possibly indistinguishable from the Kinase Loading Complex bands in previous experiments.

Nevertheless, the potential Kinase Loading Complex was placed on quantifoil copper grids, and gold graphene oxide amino functionalized grids. The micrographs from these samples

yielded no clear particles, showing dark, small or aggregated particles (Fig. 2.3). Various rounds of screening led to the conclusion that more needed to be done to stabilize the complex. We turned to finer measuring methods in which the reconstitution conditions could be further tested.

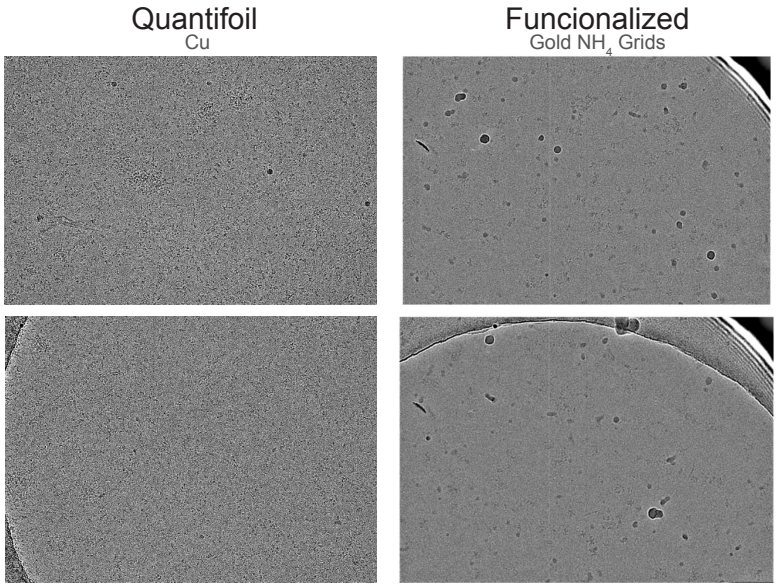

Fig. 2.3. "Kinase Loading Complex" not stable on Cu or Gold Quantifoil functionalized grids.

Several freezing conditions, and detergents were tested, but none yielded clear particles. Aggregates, dark particles, or no particles at all were visible in most screening conditions.

Fluorescence anisotropy of BRaf inhibitor fused with BODIPY shows nonspecific binding

H. Mikula from the Weissleder Lab at the Center for Systems Biology, Massachusetts General Hospital synthesized a Vemurafenib analog which contained fluorescent BODIPY (Mikula et al., 2017). This lyophilized molecule was reconstituted in 100% DMSO. Dilution of the complex into buffer (10% DMSO) allowed the reading of an ~50 mP fluorescence anisotropy reading when excited at 485 nm, and with the emission measured at 512 nm with a cutoff at 515 nm. Lowering the DMSO percentage even further led to an increase in fluorescence anisotropy to

~150 mP after 1h recordings, potentially due to the crashing out of the molecule. 50 nM concentrations allowed for a somewhat stable fluorescent anisotropy baseline, lowering to 5 nM led to a steady increase of fluorescence anisotropy. Different DMSO percentages and addition of 0.2% Tween did not change these observations. Using 50 nM fluorescent inhibitor in fluorescence anisotropy experiments led to nonspecific binding to Hsp70 and Hsp90 in experiments. Fluorescence Correlation spectroscopy mirrored the results seen in the Fluorescent Anisotropy experiments. These experiments were discontinued after this point but may still be optimizable.

Fluorescence correlation spectroscopy allows sBRaf labeling

While size exclusion chromatography allowed for discovery of potentially favorable reconstitution conditions, Fluorescence Correlation Spectroscopy (FCS) measures the hydrodynamic radius (R_{hyd}) of fluorescent complexes amidst a large number of "dark proteins" (Fig 2.4a). When using a large excess of chaperones and cochaperones, the labelled protein complex would be the complex visualized. We decided to label BRaf kinase using sub-stoichiometric amounts of malemide linked Alexa488, and stabilized the kinase by using AMPPNP. HullRad (Fleming & Fleming, 2018) was used to estimate radii of hydration of different expected complexes, and to compare with experimental results (Fig. 2.4b). Forty 4 second traces were collected and averaged, with approximately 5 molecules flowing through the observed volume (~10-15 nM labelled particles).

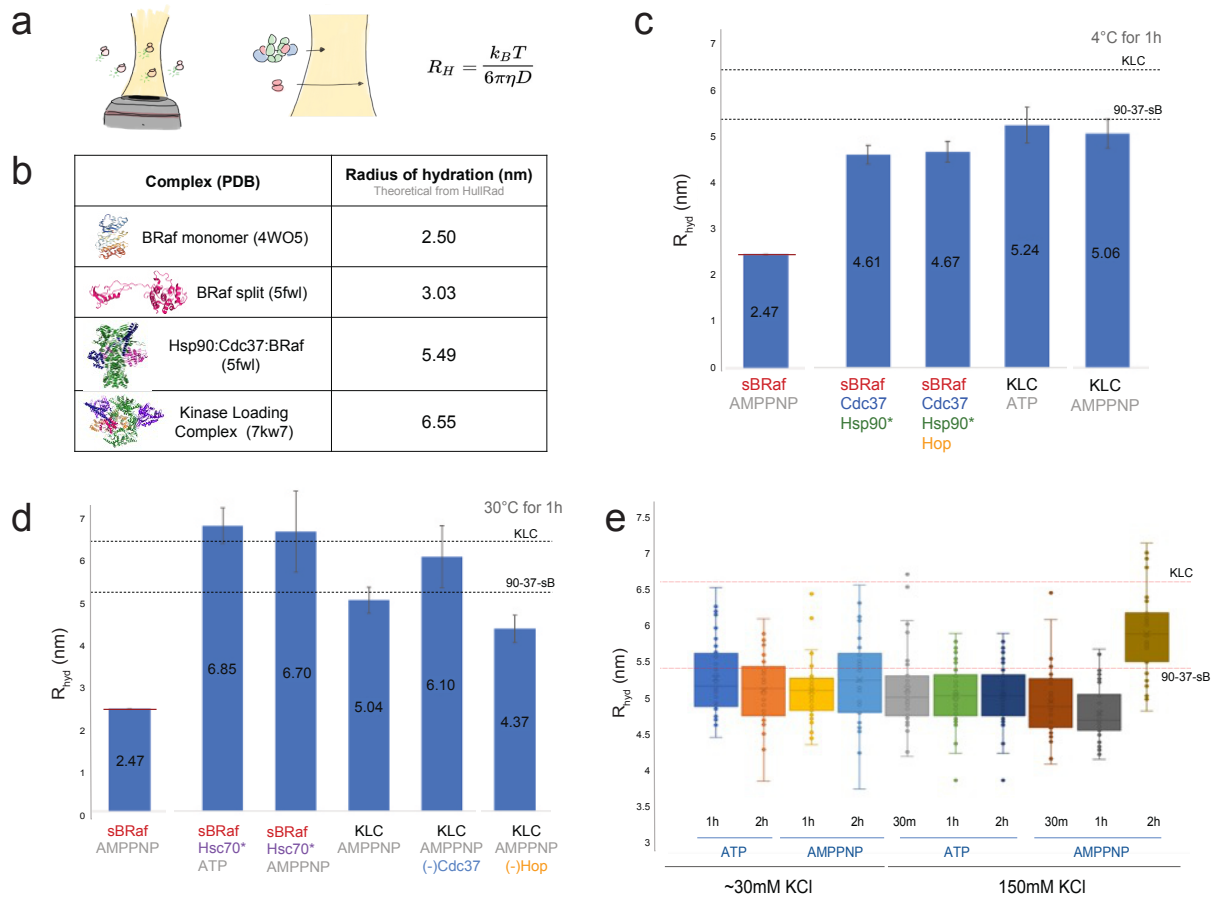

Fig. 2.4. Hydrodynamic radius measured by FCS allows for testing of Kinase Loading Complex conditions.

a Diagram of how fluorescence correlation spectroscopy measures the hydrodynamic radius of its labelled components. Larger complexes diffuse through the FCS volume slower than smaller complexes. **b** The HullRad software was used to estimate approximate the hydrodynamic radii of translation of various PDB's that resemble complexes of interest. **c** The R_{hyd} of sBRaf stabilized by AMPPNP closely matches the expected R_{hyd} of the kinase, but larger expected complex R_{hyd} don't meet the estimated R_{hyd} at 4°C. **d** Testing of different complexes incubated for 1h at 30°C show sBRaf interaction with the Hsc70 chaperone system (including DNAJB1). Further experiments are required to tease apart the visualized complexes. e Kinase Loading conditions were tested using FCS. All complexes measured had highly variable and smaller R_{hyd} than expected. The ideal conditions appeared to include long incubations at 150mM KCl with AMPPNP. Further optimization and repetitions are required.

The labelled sBRaf gave a R_{hyd} consistent with BRaf kinase crystal structures bound to inhibitors (Fig. 2.4c). Cdc37 and Hsp90:Cdc37 binding of sBRaf could be easily visualized as an

increase in R_{hyd} of the labelled kinase, but Hsp90:Cdc37:sBRaf complexes appeared smaller than the R_{hyd} expected for an Hsp90:Cdc37:Kinase complex (PDB: 5fwl). This smaller R_{hyd} could be due free dye if present, so labelled sBRaf was run through a desalting column and a subsequent SEC column to ensure no free dye remained in the sample. Shorter traces (1s each) were then taken to visualize less molecules at a time and potentially distinguish between smaller and larger particles without averaging. All traces remained close to the 2.5 nm R_{hyd} expected.

Addition of Hop to the sBRaf:Cdc37:Hsp90 complex did not lead to an increase in R_{hyd}, but addition of all of the components required for the Kinase Loading Complex did lead to a slightly larger R_{hyd} (Fig. 2.4d). The cryoEM GR Loading Complex (PDB: 7kw7) was used to model the expected R_{hyd} of a Kinase Loading Complex, but the value seen in our FCS experiments did not approach this size of complex. This could be due to heterogeneity of complexes, or the inability of sBRaf to engage with the full chaperone machinery. We hypothesized that destabilizing sBRaf might lead to further engagement with the Hsp70 chaperone system, and increased the temperature of the kinase complex mixture to 30°C. This led to a moderate increase in R_{hyd} , possibly due to the binding of Hsp70. Increasing the temperature of the experiment without Hsp70 present, led R_{hyd} larger than expected for a single particle, likely meaning that sBRaf would aggregate at these higher temperatures. Interestingly, Hsp70 allowed the sBRaf R_{hyd} to remain relatively constant at a R_{hyd} of around 6.7-6.8 nm regardless of ATP or AMPPNP nucleotide state (Fig. 2.4e). The addition of Hop and Cdc37 to the Hsp70 stabilized sBRaf once again led to a decrease in R_{hyd} value, suggesting that the signal may be a combination between the Hsp90:Cdc37:sBRaf complex and the sBRaf:Hsc70 complex. Removal of Cdc37 from the sample led to a slightly larger R_{hyd}. We hypothesized that Cdc37 may be competing with Hsp70 for the binding of sBRaf, but further experiments would be

required to show this is true. To see complex components in more resolution, we moved towards pulldowns.

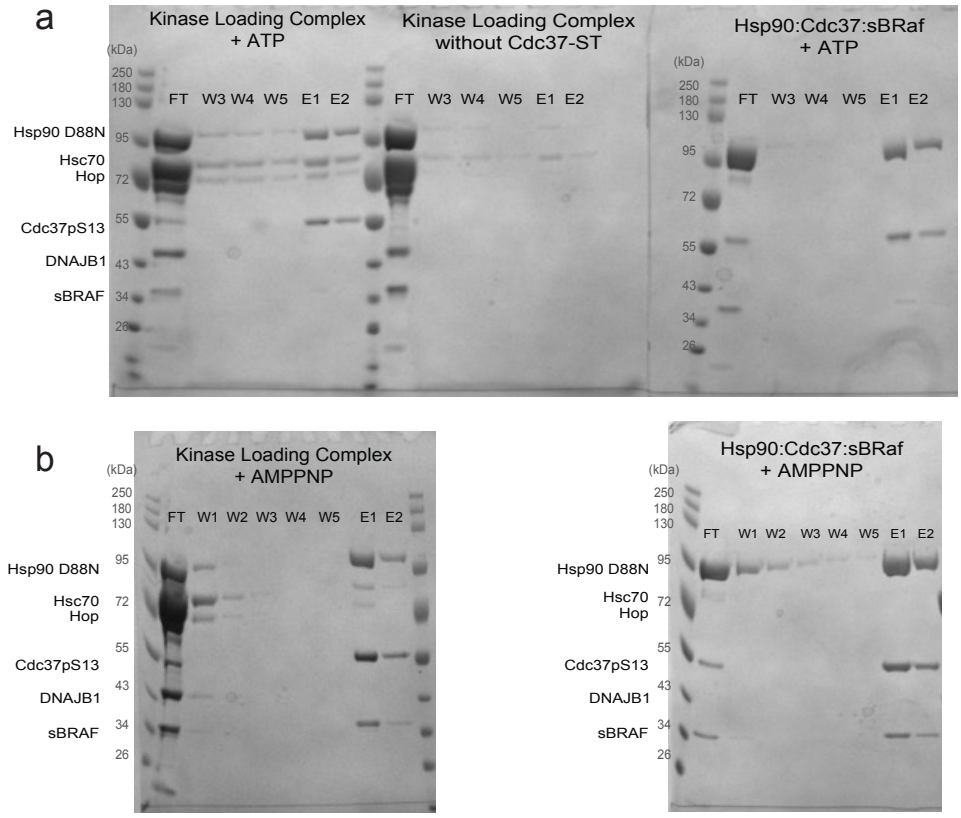

Fig. 2.5. Pulldown experiments may show coelution of Hsc70 and Hop with Hsp90:Cdc37:sBRaf complex.

Strep-Tag affinity beads were used to perform pulldowns by pulling on Cdc37-StrepTag II. **a** Previously identified Kinase Loading Complex conditions with ATP as the nucleotide present shows co-elution of Hsp90, Hsc70, Hop and sBRaf with Cdc37-ST. Leaving Cdc37-ST out leads to slight nonspecific binding of Hsp90 and Hsc70 even after 5 washes, but the bands present seem fainter than those seen in the first pulldown. The pulldown of an Hsp90:Cdc37:sBRaf complex was included for comparison. **b** Similar experiments were repeated with AMPPNP instead of ATP, and stronger coelution of sBRaf can be seen. These results need to be repeated.

Kinase Loading Complex Pulldown preliminary results

A double Streptag II construct was cloned into the Cdc37 plasmid, expressed, and phosphorylated with CK2. The Kinase Loading Complex conditions that resulted in a larger

complex through FCS (150mM KCl, 2h incubation, 5 µM sBRaf, 5 µM DNAJB1, 20 µM Hsc70, 5µM Cdc37^{pS13}, 5 µM Hop, 5 µM Hsp90B$^{dimer\ inhibited}$ and 2.5mM nucleotide) were used in these pulldown experiments, with both ATP and AMPPNP nucleotides tested (Fig. 2.5). Both Kinase Loading Complex conditions pulled down Hsp90, Hsc70, Hop with Cdc37-StrepTag. sBRaf is present in the AMPPNP pulldown, yet faint in the ATP sample. The control experiment, a pulldown with StrepTag beads but without Cdc37, still bound slight levels of Hsc70 and Hsp90 even after thorough washing. While non-specific binding might be responsible for some of the Hsp70 and Hsp90 in the pulldown elution, the bands appear to be thicker when Cdc37-ST is present and suggest there may be some degree of binding. Interestingly, both AMPPNP samples lead to a higher amount of sBRaf eluting with the complexes, but this might simply be due to the stabilization of sBRaf which is prone to aggregate. These pulldown results would need to be repeated, and optimized if this were to be carried forward into crosslinking optimization and cryoEM.

While the proteins expected in a Kinase Loading Complex appear to be interacting, it is hard to rule many heterogeneous interactions happening at once. Even in the case of the Glucocorticoid Receptor Loading Complex, a lot of particles and computational efforts were required to tease apart the minimal set of particles from the whole dataset that recreate this complex. To this effect, optimizing this complex for cryoEM might be the best path forward. Alternatively, showing not just coelution or complex formation but also a rescue in kinase activity as has been seen previously, might be an ideal way to optimize for the Kinase Loading Complex.

E. coli purified Chk1 aggregates upon purification

Chk1 was used previously as a test kinase activity and chaperone activity recovery. While this has yet to be repeated with any other kinases, purifying Chk1 and reproducing the experiments done by Arlander et al. might be the best start towards isolating a Kinase Loading Complex (Arlander et al., 2006). Arlander et al. purified Chk1 from E. coli and noted faint activity before incubation with chaperones. Our initial attempts to purify Chk1 led to milky white lysates with aggregated protein. Expression testing with different E. coli strains led to the realization that a large percentage of the Chk1 protein appears insoluble upon expression. Attempts at refolding aggregated Chk1 with Guanidine Hydrochloride, or Urea in columns or in solution did not yield stable protein. The addition of a stabilizing tag might aid purification in the future, and more work would be required to get this system up and running.

sBRaf aggregation appears mitigated by chaperone presence

While searching for the Kinase Loading Complex, Alexa488 labelled sBRaf showed different levels of aggregation as measured by larger and larger hydrodynamic radii of the particles in the microscope. Harnessing the single molecule capabilities of FCS, the recorded traces were shortened to 1 second, and the number or recorded traces were increased. This allowed for the visualization of more unaveraged sBRaf kinase “events”. Leaving sBRaf out at room temperature for 1-2 h showed different aggregation propensities depending on salt and temperature conditions (Fig. 2.5a). Box plots show the average and spread of events visualized, with “folded” sBRaf R_{hyd} being around 2.5 nm as shown previously (Fig. 2.5c). Aggregates of sBRaf quickly become large conglomerates of protein.

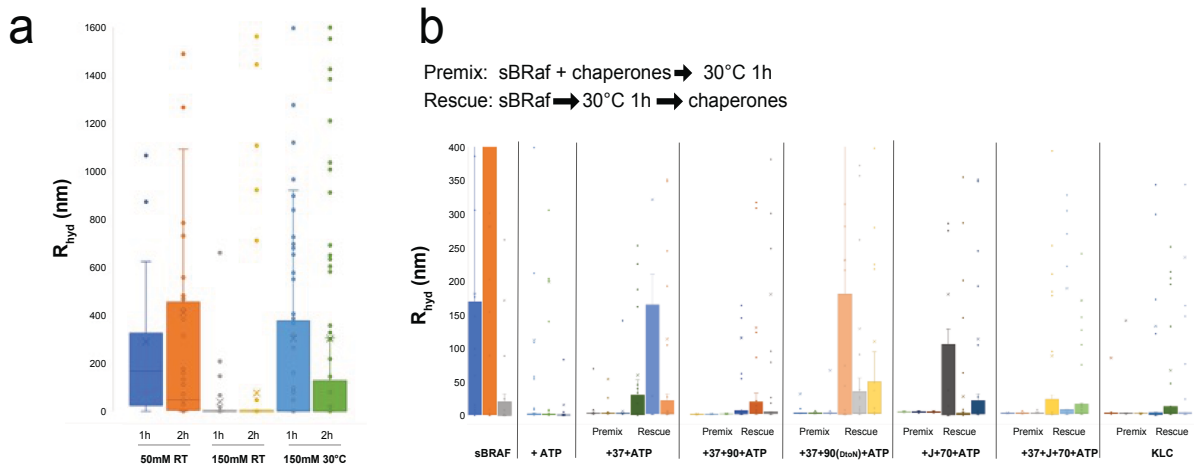

Fig. 2.6 Fluorescently labelled sBRaf aggregation and solubility can be visualized using FCS.

a sBRaf aggregation can be visualized by studying the R_{hyd} measured by FCS. Incubation for an hour at different buffer conditions (50mM KCl or 150mM KCl) and different temperatures (RT or 30°C) show different amounts of aggregation. Less aggregation is seen at higher KCl concentration and lower temperatures. **b** sBRaf is either Premixed with chaperones for 1-3 hours or allowed to aggregate for an hour and then supplemented with chaperones for 1-3 hours. sBRaf stability increases when bound to ATP. Premixed conditions keep sBRaf aggregation at bay in the conditions tested, while little rescue is seen in the rescue conditions tested.

Arlander et al. demonstrated the ability of certain chaperones to refold and activate Chk1 kinase. We hypothesized that these same chaperone interactions might rescue an aggregates sBRaf. Two different conditions were tested, (1) a premixed sBRaf and chaperone condition measured at 1, 2, and 3 hours after incubation at 30°C, and (2) a sample in which sBRaf would be allowed to aggregate for an hour at 30°C, after which the corresponding chaperones would be added and the sBRaf aggregation conditions measured for 1, 2 or 3 hours afterwards. Interestingly, premixed chaperones kept sBRaf in a seemingly folded soluble state, while the later addition of chaperones could not rescue sBRaf kinase completely. These experiments were exploratory, and further results would be required to reach any conclusions. The combination of

this aggregation system with and activity assay for kinase recovery would be very useful to study different kinds of chaperone activity.

References

Arlander, S. J. H., Felts, S. J., Wagner, J. M., Stensgard, B., Toft, D. O., & Karnitz, L. M. (2006). Chaperoning Checkpoint Kinase 1 (Chk1), an Hsp90 Client, with Purified Chaperones. *Journal of Biological Chemistry*, *281*(5), 2989-2998. https://doi.org/10.1074/jbc.M508687200

Cuesta, A., Wan, X., Burlingame, A. L., & Taunton, J. (2020). Ligand Conformational Bias Drives Enantioselective Modification of a Surface-Exposed Lysine on Hsp90. *Journal of the American Chemical Society*, *142*(7), 3392-3400. https://doi.org/10.1021/jacs.9b09684

Davies, H., Bignell, G. R., Cox, C., Stephens, P., Edkins, S., Clegg, S., Teague, J., Woffendin, H., Garnett, M. J., Bottomley, W., Davis, N., Dicks, E., Ewing, R., Floyd, Y., Gray, K., Hall, S., Hawes, R., Hughes, J., Kosmidou, V., . . . Futreal, P. A. (2002). Mutations of the BRAF gene in human cancer. *Nature*, *417*(6892), 949-954. https://doi.org/10.1038/nature00766

Felts, S. J., Karnitz, L. M., & Toft, D. O. (2007). Functioning of the Hsp90 machine in chaperoning checkpoint kinase 1 (Chk1) and the progesterone receptor (PR). *Cell Stress & Chaperones*, *12*(4), 353. https://doi.org/10.1379/CSC-299.1

Fleming, P. J., & Fleming, K. G. (2018). HullRad: Fast calculations of folded and disordered protein and nucleic acid hydrodynamic properties. *Biophysical journal*, *114*(4), 856-869.

Kirschke, E., Goswami, D., Southworth, D., Griffin, Patrick R., & Agard, David A. (2014). Glucocorticoid Receptor Function Regulated by Coordinated Action of the Hsp90 and Hsp70 Chaperone Cycles. *Cell*, *157*(7), 1685-1697. https://doi.org/10.1016/j.cell.2014.04.038

Mikula, H., Stapleton, S., Kohler, R. H., Vinegoni, C., & Weissleder, R. (2017). Design and Development of Fluorescent Vemurafenib Analogs for In Vivo Imaging. *Theranostics*, *7*(5), 1257-1265. https://doi.org/10.7150/thno.18238

Morishima, Y., Murphy, P. J., Li, D.-P., Sanchez, E. R., & Pratt, W. B. (2000). Stepwise assembly of a glucocorticoid receptor· hsp90 heterocomplex resolves two sequential ATP-dependent events involving first hsp70 and then hsp90 in opening of the steroid binding pocket. *Journal of Biological Chemistry*, *275*(24), 18054-18060.

Noddings, C. M., Wang, R. Y.-R., Johnson, J. L., & Agard, D. A. (2022). Structure of Hsp90–p23–GR reveals the Hsp90 client-remodelling mechanism. *Nature*, *601*(7893), 465-469. https://doi.org/10.1038/s41586-021-04236-1

Picard, D., Khursheed, B., Garabedian, M. J., Fortin, M. G., Lindquist, S., & Yamamoto, K. R. (1990). Reduced levels of hsp90 compromise steroid receptor action in vivo. *Nature*, *348*(6297), 166-168.

Polier, S., Samant, R. S., Clarke, P. A., Workman, P., Prodromou, C., & Pearl, L. H. (2013). ATP-competitive inhibitors block protein kinase recruitment to the Hsp90-Cdc37 system. *Nature Chemical Biology*, *9*(5), 307-312. https://doi.org/10.1038/nchembio.1212

Pratt, W. B., & Toft, D. O. (1997). Steroid receptor interactions with heat shock protein and immunophilin chaperones. *Endocrine reviews*, *18*(3), 306-360.

Taipale, M., Krykbaeva, I., Koeva, M., Kayatekin, C., Westover, Kenneth D., Karras, Georgios I., & Lindquist, S. (2012). Quantitative Analysis of Hsp90-Client Interactions Reveals Principles of Substrate Recognition. *Cell*, *150*(5), 987-1001. https://doi.org/10.1016/j.cell.2012.06.047

Trepel, J., Mollapour, M., Giaccone, G., & Neckers, L. (2010). Targeting the dynamic HSP90 complex in cancer. *Nature Reviews Cancer*, *10*(8), 537-549. https://doi.org/10.1038/nrc2887

Tsai, J., Lee, J. T., Wang, W., Zhang, J., Cho, H., Mamo, S., Bremer, R., Gillette, S., Kong, J., Haass, N. K., Sproesser, K., Li, L., Smalley, K. S. M., Fong, D., Zhu, Y.-L., Marimuthu, A., Nguyen, H., Lam, B., Liu, J., . . . Bollag, G. (2008). Discovery of a selective inhibitor of oncogenic B-Raf kinase with potent antimelanoma activity. *Proceedings of the National Academy of Sciences*, *105*(8), 3041-3046. https://doi.org/10.1073/pnas.0711741105

Wang, R. Y.-R., Noddings, C. M., Kirschke, E., Myasnikov, A. G., Johnson, J. L., & Agard, D. A. (2022). Structure of Hsp90–Hsp70–Hop–GR reveals the Hsp90 client-loading mechanism. *Nature*, *601*(7893), 460-464. https://doi.org/10.1038/s41586-021-04252-1

Chapter 3

PP5 Activity and Complex Optimization

Preface

Phosphorylation is essential for protein kinase regulation. Through these posttranslational modifications, all essential cellular processes such as cell-cycle progression, differentiation, transcription, cellular movement, and many others can be fine-tuned and modulated. With over 60% of kinases interacting with Hsp90, it would be no surprise to learn that regulation through phosphorylation impacts the way Hsp90 interacts with kinases. Kinases bind Hsp90 on a spectrum from weak to strong binders. The weak kinase binders may require Hsp90 in their early folding moments as they are being translated, while the stronger binders require Hsp90 assistance throughout their lifespan. While cryoEM structures of Hsp90:Cdc37:Kinase complexes show the kinase in an unfolded, ATP binding-incompetent state, other unseen and more transient Hsp90-Kinase interactions may also exist. As phosphorylation is an essential mechanism of kinase regulation, the kinase phosphorylation state may signal the need for Hsp90 interaction. The search for the elusive Kinase Loading Complex led us to believe that the

purification of such a complex might require the understanding of kinase phosphorylation patterns before being able to understand Hsp90-Kinase loading.

Hsp90 is a modular molecular machine which requires the assistance of cochaperones to enable its many functions (Schopf et al., 2017; Taipale et al., 2010). Many of these cochaperones have TPR domains, known to bind the Hsp90 C-terminal tail MEEVD sequence motif (Chen et al., 1998; Lee et al., 2021; Noddings et al., 2023; Ramsey et al., 2000). One of these cochaperones is Protein Phosphatase 5 (PP5), a protein split into two functional domains: a TPR domain, and a catalytically active phosphatase domain (Chen et al., 1994; Yang et al., 2005). PP5 presented an ideal way to study the dephosphorylation of Hsp90-bound substrates. Based on work by A. von Kriegsheim et al and CK Vaughan et al. (Vaughan et al., 2008; von Kriegsheim et al., 2006), we set out to understand how PP5 uses Hsp90 to dephosphorylate two of its substrates: Cdc37 and CRaf. Initial PP5 optimization experiments (Fig. 3.1 and 3.2) were explored with the help of D. Coutandin.

Summary

Conditions for E. coli purified PP5 dephosphorylation were initially optimized, finding low salt, Manganese samples to dephosphorylate PP5 substrates more readily. Various dephosphorylation readouts were established to probe PP5 function towards different phosphorylated substrates. Amongst these, a gel shift assay, a phosphorylation gel stain, and phosphorylation specific western blots were optimized to test PP5 dephosphorylation. PP5 was found to dephosphorylate Cdc37 in an Hsp90:Cdc37:PP5 complex, and this complex was further studied using negative stain. Preliminary results show a semi-open Hsp90 complex binds to Cdc37. Next, the phosphorylation state of CRaf kinase purified in different Hsp90:Cdc37:CRaf

complex constructs and expression methods was tested. This led to phosphorylation site specific testing of PP5 dephosphorylation, and set the stage for the more in-depth Chapter 4 work, where we delve deeper into the use of Hsp90 as a scaffold for PP5 dephosphorylation.

Results

PP5 dephosphorylates more efficiently when bound to Manganese (Mn)

The PPP family of phosphatases is highly conserved, yet the physiological metal ions used by these proteins are not fully known. While PP2B is believed to use Fe^{2+} and Zn^{2+} ions, PP5 crystallography experiments noticed two metal binding sites, which alongside X-ray fluorescence helped identify the presence of Mn^{2+}, Fe^{2+} and Zn^{2+} ions within the active site (Swingle et al., 2004). Further work by A.J. Ramsey and M. Chinkers identified that Mn and Mg could both activate the PP5 dephosphorylation of a small molecule substrate (Ramsey & Chinkers, 2002). In their work they found lower concentrations of Mn to bind and activate PP5 activity, while at higher concentrations Mg had a higher overall turnover rate.

We purified PP5 in E. coli using adding Mg, or Mn and Mg in the lysis steps of purification and through ion exchange chromatography. PP5 was then buffer exchanged into the "storage" buffer using size exclusion chromatography. The storage buffer contained either 1mM Mn and 10mM Mg, or 10mM Mg without Mn. PP5 under these two different buffer conditions tested for activity by a small molecule colorimetric assay in which p-nitrophenylphosphate becomes dephosphorylated into the colorful p-nitrophenol. Through this system, we noticed faster dephosphorylation of PP5 purified and stored in Mn containing buffer (Fig. 3.1a). We next tested the ability of PP5 to dephosphorylate a protein substrate, Cdc37, while in the presence of Hsp90. A band shift assay (described in Fig. 3.2) showed that PP5 dephosphorylates Cdc37 most

efficiently when Mn is present, and more efficiently in conditions of lower salt (20mM KCl) than in conditions of high salt (150mM KCl) (Fig. 3.1b). The increase in activity at low salt might be due to the stabilization of protein-protein interactions required to activate PP5, and not necessarily due to an increase in PP5 catalytic rate.

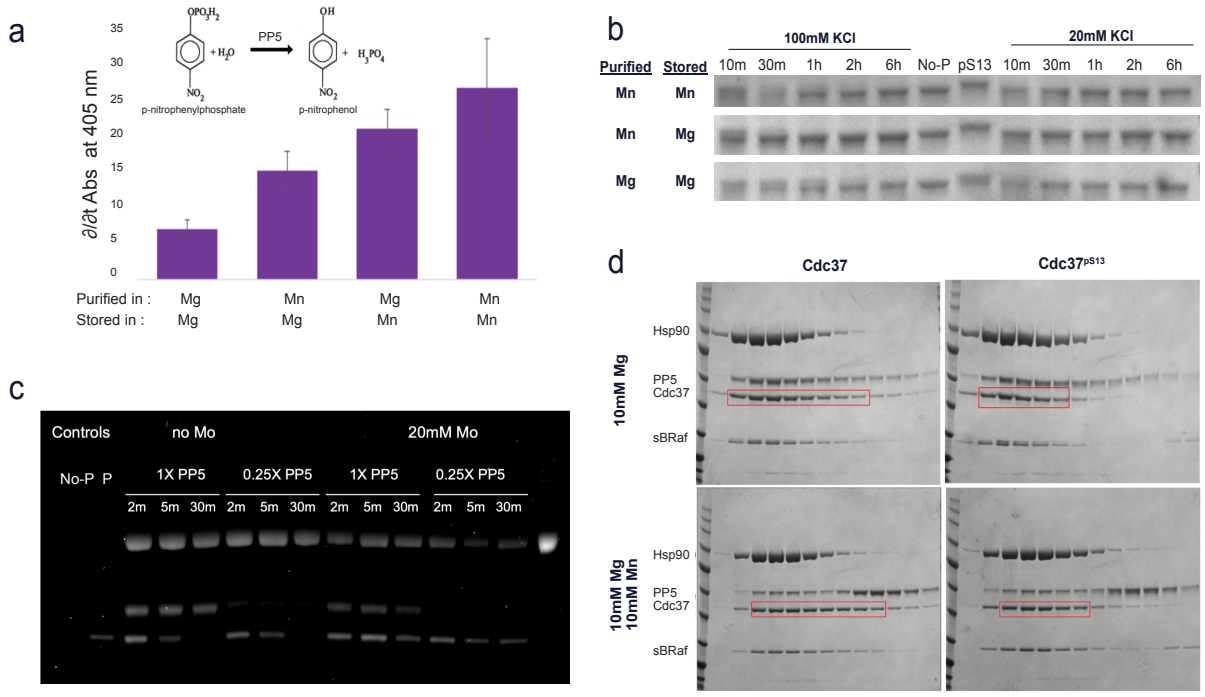

Fig. 3.1. Mn buffer leads to faster dephosphorylation and decreased coelution of PP5 complex.

PP5 dephosphorylates a pNPP substrate, leading to a colorimetric change measured at 405 nm. PP5 was purified in the presence of either Mn (1mM) or Mg (10mM), and buffer exchanged as the last step of purification in to a buffer containing either Mn (1mM) or Mg (10mM). PP5 dephosphorylates pNPP (**a**) and Cdc37 (**b**) best when Mn is present throughout purification and storage. **b** Cdc37 dephosphorylation can be visualized using a SDS gel shift assay, which shows that low salt conditions and an increase in Mn concentrations lead to faster PP5 dephosphorylation. **c** Molybdate leads to PP5 inhibition as has been shown previously for other phosphatases. **d** Hsp90:Cdc37:sBRaf complex was incubated with PP5 and coelution of PP5 was tested depending on buffer conditions. Increased Mn in the buffer during size exclusion chromatography leads to a decrease in PP5 coelution, as seen by an SDS gel of the collected fractions.

Often present in phosphatase inhibitors, Molybdate salt has been shown to be useful tool for the isolation of closed Hsp90 complexes. To study PP5 activity on substrates bound to Hsp90 would require the isolation of Molybdate purified complexes, so understanding the effects of Molybdate (20mM, used in Hsp90 experiments in the lab) on PP5 was of the utmost importance. A Pro-Q Diamond phosphorylation gel stain (ThermoFischer) was used to measure the dephosphorylation of the PP5 substrate Cdc37 while in the presence of Molybdate. Molybdate was found to inhibit PP5 activity, so buffer exchange of Hsp90 complexes would be required to prevent PP5 inhibition while testing dephosphorylation conditions (Fig. 3.1c).

Our interest in PP5 dephosphorylation includes both activity and structure. While excess Mn in our experiments might improve PP5 activity, we also require a higher PP5 residence time on its substrate to be able to visualize PP5 in action and learn more about its dephosphorylation mechanism. This led us to test the ability of PP5 to coelute with distinct complexes in Mn free and Mn containing buffer systems. Hsp90, Cdc37 or Cdc37^{pS13}, sBRaf and PP5 were mixed at 4°C for 30 min and then ran through a Superose6 column in buffer with or without Mn present. The fractions eluted off the column were then ran on an SDS gel, with the larger fraction loaded on the left side of the gel (Fig. 3.1d). PP5 was seen to coelute less in complexes moving through Mn buffer than Mg buffer. This suggested the importance of having trace Mn for PP5 activity, but ideally having less Mn present while attempting to visualize PP5 in action.

Shift in SDS gel shows PP5 dephosphorylation activity

Experiments by C.K. Vaughan et al. suggested that PP5 could dephosphorylate Cdc37 while in complex with Hsp90 and Cdk4 kinase (Vaughan et al., 2008). Yeast expression and preparation of Hsp90:Cdc37:CRaf Kinase domain, and Hsp90:Cdc37:Her2 Kinase domain

complexes had been recently established in the lab through work by K. Verba, D. Coutandin, and C.A. Nowotny. Both human and yeast Cdc37 phosphorylation has been shown to be essential for the recruitment of human kinases to Hsp90(Miyata & Nishida, 2004, 2007; Shao, Irwin, et al., 2003; Shao, Prince, et al., 2003). Structural work in the Agard Lab has shown this state of Cdc37 phosphorylation is essential for the maintenance of key interactions between Hsp90 and Cdc37 as they chaperone kinases (Verba et al., 2016). For this reason, Cdc37 in Hsp90:Cdc37:Kinase complexes seemed like the ideal substrate to test PP5 dephosphorylation.

A readout would be required for Cdc37 dephosphorylation, so Cdc37 was expressed and purified in E. coli cells, and half of the purified Cdc37 was phosphorylated by CK2 as had been shown previously (Miyata & Nishida, 2004, 2007). Following the repurification of phosphorylated Cdc37, Cdc37 and Cdc37^{pS13} were both ran on SDS gels to attempt to visualize if the extra phosphate would lead to a shift in band size. Tris-Acetate gels, which exhibit wide separation at around the 45kDa molecular weight were used, and the samples were allowed to run through to the very end of the gel to improve the resolution in the molecular weight of interest (Fig. 3.2a). Cdc37 and Cdc37^{pS13} could be identified as two separate bands in the gel, providing a low resource readout of Cdc37 phosphorylation. PP5 was added to Hsp90:Cdc37^{pS13}:Her2 samples but no dephosphorylation of Cdc37 was visible. Different cochaperones were added to the Hsp90:Cdc37^{pS13}:Her2 complex with no change in Cdc37 dephosphorylation (Abbas-Terki et al., 2002; Harst et al., 2005; Skarra et al., 2011).

Through observation of the Hsp90:Cdc37:Kinase structures available, we hypothesized that the Cdc37 phosphorylation might not be sterically accessible to PP5. We hypothesized that an “open” Hsp90 complex might lead to a change in Cdc37 conformation that would allow PP5 to dephosphorylate its substrate. Previous Kinase Loading Complex work (See Chapter 2)

ensured that Hsp90, Cdc37 and sBRaf coelute as a complex, so PP5 was added to this open complex and Cdc37 dephosphorylation was measured through the SDS shift assay. Dephosphorylation of Cdc37 was then visible, and seemed more pronounced when sBRaf was not present in solution (Fig. 3.2b,c).

Open Hsp90 complexes have proven difficult for the field to visualize because of the Hsp90 conformational heterogeneity, so potentially stabilizing cochaperones were added to the PP5 reaction. Cochaperones that allowed or accelerated PP5 dephosphorylation of Cdc37, yet stabilized Hsp90 in a more limited conformation would allow for improved cryoEM characterization. AHA1, Hop and FKBP51 were all tested as potential Hsp90-Cdc37 stabilizers which would allow PP5 dephosphorylation. FKBP51 competed against PP5, but AHA1 and Hop seemed to allow for PP5 activity (Fig. 3.2d). Size Exclusion chromatography of these complexes showed that neither Hop nor AHA1 stabilized PP5 interactions with an Hsp90:Cdc37:sBRaf complex. PP5 dephosphorylation of Cdc37 could be readily seen in Hsp90:Cdc37 complexes without other tested cochaperones or kinases, so efforts began to structurally characterize the potentially flexible Hsp90:Cdc37:PP5 complex.

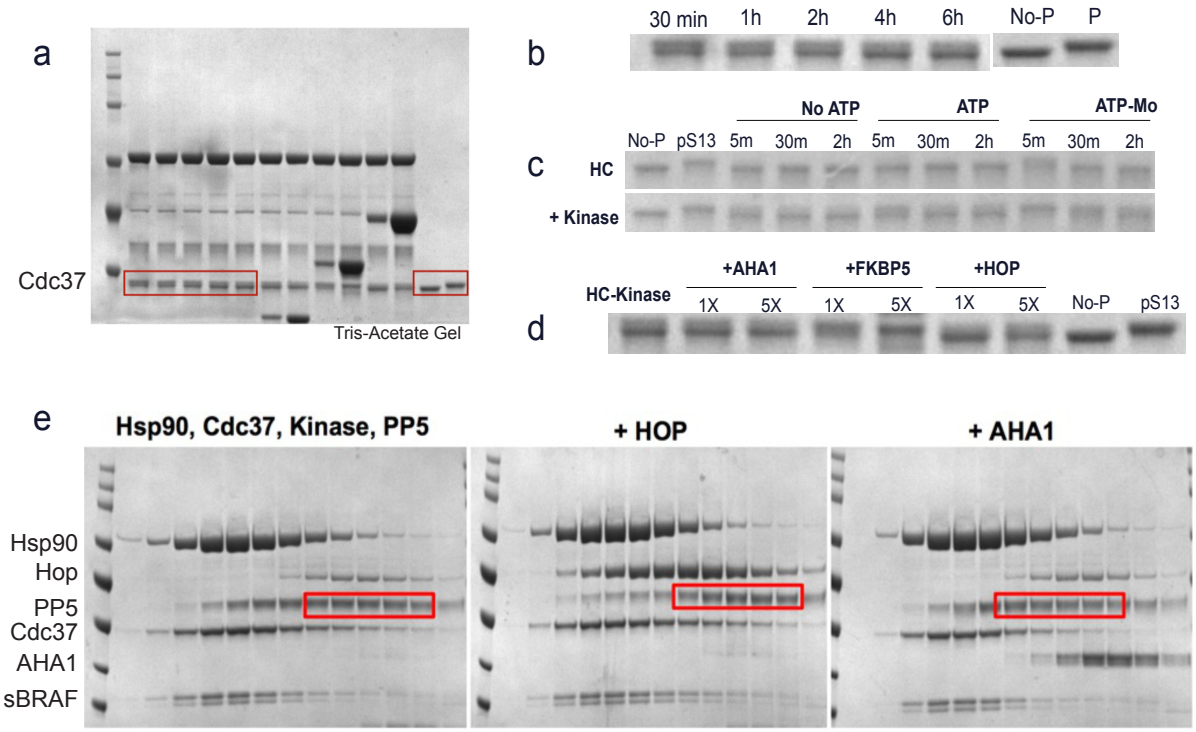

Fig. 3.2. SDS gel shift assay provides readout of PP5 dephosphorylation of Cdc37.

a Running a Tris-Acetate Gel until the bands of interest are near the bottom of the gel allows for improved separation of Cdc37 species: a phosphorylated, and a dephosphorylated band are visible. **b** Cdc37 is dephosphorylated when bound to Hsp90, as is seen by a gel shift. **c** sBRaf addition to the Hsp90:Cdc37 complex leads to a decreased rate of Cdc37 dephosphorylation. d While the AHA1 and Hop cochaperones don't appear to affect the ability of PP5 to dephosphorylate, FKBP51 seems to decrease PP5 dephosphorylation. **e** Neither Hop not AHA1 appear to considerably stabilize PP5 binding to Hsp90:Cdc37:sBRaf complex.

Optimizing crosslinking of the highly heterogeneous Hsp90:Cdc37:PP5 sample

Open Hsp90 complexes have been notoriously hard to visualize structurally. To date, two open full length Hsp90 structures have been seen, (1) the cochaperone stabilized Glucocorticoid Receptor Loading Complex (Wang et al., 2022), and (2) the conformationally simpler E. coli Hsp90 homolog HtpG (Shiau et al., 2006). This observation, alongside the tendency of Hsp90 to move towards the air-water interface when frozen in cryoEM grids (observed repeatedly in lab),

led to the optimization of crosslinking as the best way to stabilize an open Hsp90:Cdc37:PP5 complex (Fig. 3.3).

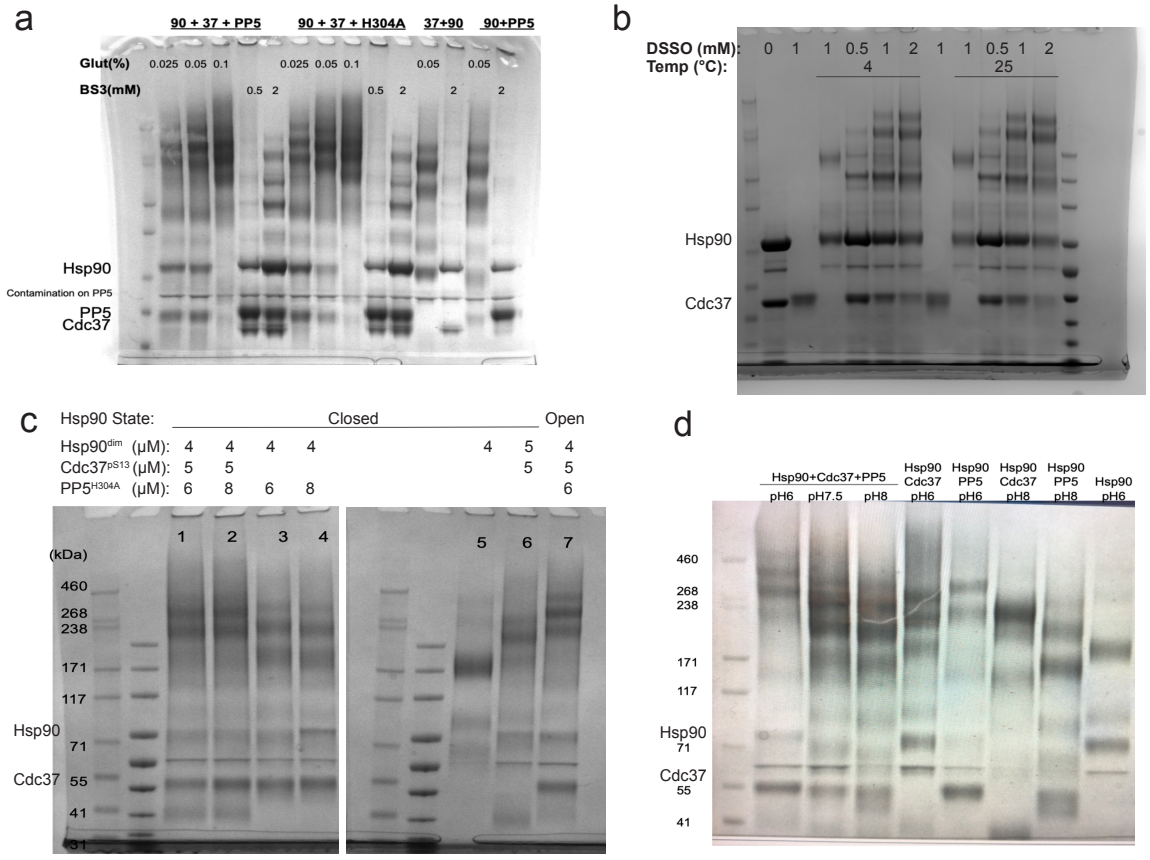

Fig. 3.3. Hsp90:Cdc37:PP5 complex crosslinks heterogeneously.

a Crosslinking conditions with Glutaraldehyde and BS3 were tested for the Hsp90:Cdc37:PP5 complex, showing more efficient crosslinking for the Glutaraldehyde sample. **b** Crosslinking conditions of the Hsp90:Cdc37 complex show similar crosslinking with DSSO as seen with Glutaraldehyde. Glutaraldehyde crosslinks more efficiently and was therefore kept for the next steps of optimization. **c** Concentrations of complex components were varied slightly to search for most productive crosslinking concentration ranges, and open vs molybdate closed Hsp90 was tested for Cdc37 and PP5 crosslinking capacity. Open Hsp90 seemed ideal for crosslinking of Hsp90:Cdc37:PP5 complex. **d** Buffer pH conditions vary crosslinking ability of complexes, with more acidic pH being ideal for crosslinking the Hsp90:Cdc37:PP5 complex.

The Hsp90:Cdc37:PP5 complex crosslinked similarly with $PP5^{WT}$ or the catalytically dead $PP5^{H304A}$ (Fig. 3.3a). Different crosslinking conditions were tested with different

crosslinker concentrations, temperatures, and protein concentrations. The crosslinked products were run on SDS gels. As seen by the large number of bands present on the SDS gels, there are many different interactions between the separate components of the Hsp90:Cdc37:PP5 complex. To tease apart each band, separate components were crosslinked and run separately. BS3 seemed to be the least active crosslinker at the conditions tested, followed by DSSO and the most active Glutaraldehyde (Fig. 3.3a,b). Glutaraldehyde was optimized further, where different concentrations of the individual components were varied slightly (Fig 3.3c), and different buffer pH's were tested (Fig. 3.3d). The crosslinking effects seemed to vary slightly, with the Hsp90:Cdc37:PP5 complex seeming to create the most stable large complex at pH 6, but the Hsp90:Cdc37 complex was most stable at pH 8.

The crosslinked Hsp90:Cdc37:PP5^{H304A} sample was run over a sizing column and a wide peak eluted, demonstrating the large conformational and/or component heterogeneity in the sample (Fig. 3.4a,b). This sample was then placed on negative stain and cryoEM grids, and screened (Fig. 3.c,d), yielding well dispersed particles. A small collection on cryoEM Quantifoil grids, followed by data processing yielded the 2D classes shown in Figure 3.4d but further efforts to 2D and 3D classify did not allow for refinement to lower resolution. Comparison between the negative stain (Fig. 3.4c) and cryoEM classes (Fig. 3.4d) suggest that the higher contrast of negative stain allows the averaging and visualization of a wide range of Hsp90 conformations.

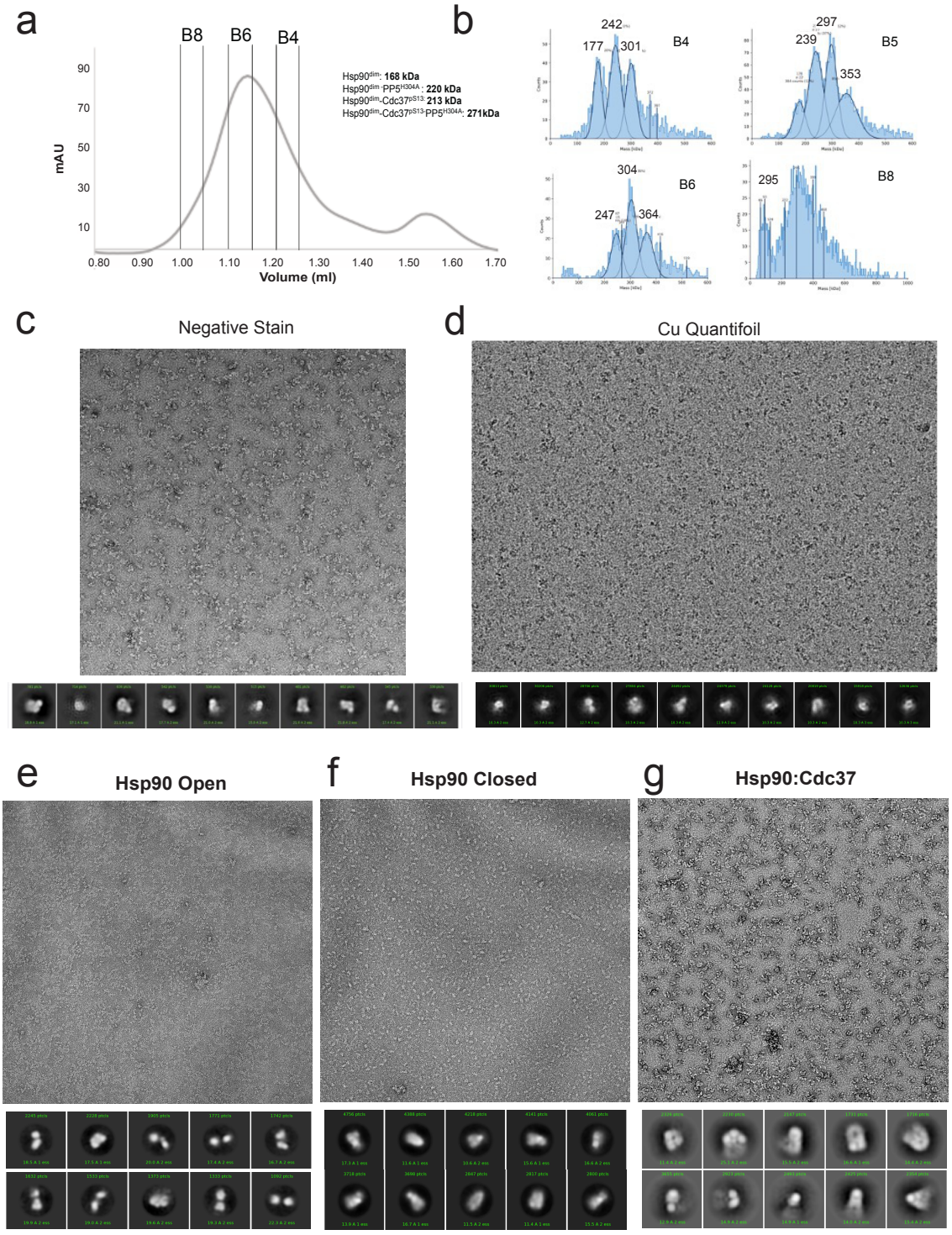

Fig. 3.4. The Hsp90:Cdc37 complex likely resembles a semi-open Hsp90 state.

a Sizing run of a 15 min 0.05% glutaraldehyde crosslinked Hsp90:Cdc37:PP5 complex shows a wide peak. **b** Differently sized species are visible in different fractions of the wide peak. These particles were placed on negative

stain (**c**) or cryoEM (**d**) grids and showed well-dispersed particles. While the negative stain particles gave clean 2D classes, cryoEM requires a larger number of particles to show the high contrast 2D classes of conformationally heterogeneous Hsp90 arms. **e,f** Negative stain micrographs of open and closed Hsp90 show examples of 2D classes from these Hsp90 states, and comparison of these with the Hsp90:Cdc37:PP5 classes allows the hypothesis that HSp90:Cdc37:PP5 complexes are neither fully closed nor fully open. **g** The crosslinked Hsp90:Cdc37 complex shows similar 2D classes to the Hsp90:Cdc37:PP5 complex, also showing a semi-closed conformation.

The negative stain 2D classes show a seemingly semi-open Hsp90 complex. To compare between an open Hsp90 and closed Hsp90 complex, negative stain grids were prepared, imaged and processed to compare with the Hsp90:Cdc37:PP5 complex (Fig. 3.4e,f). The open Hsp90 complex 2D classes show two separate Hsp90 monomers whose C-terminal domains point towards each other. Alternatively, the closed Hsp90 sample shows a neat micrograph and almond shaped Hsp90 dimer complexes. The Hsp90:Cdc37:PP5 complex 2D classes resemble the closed Hsp90 complex more than the open. Efforts were undertaken to use models from the negative stain data to bring out the signal in cryoEM data, but more thorough continuation of this work is necessary.

Realizing the large amount of heterogeneity in the sample might be limiting to cryoEM studies, we decided to screen for a simpler complex. Through understanding the structure of an Hsp90:Cdc37 complex, it might become easier to visualize the new Cdc37 conformation that allows PP5 dephosphorylation of Cdc37. Achieving a higher resolution structure of the simpler two component complex would then allow for the building of an improved model to help improve the alignment of the Hsp90:Cdc37:PP5 complex. The Hsp90:Cdc37 sample was crosslinked, run through size exclusion chromatography, and imaged through negative stain. The 2D classes from these micrographs were similar to those obtained for the Hsp90:Cdc37:PP5 complex, showing more detail within the Hsp90 monomer claws.

The Hsp90:Cdc37 sample was also frozen on Quantifoil grids and is ready for cryoEM collection. This project would be a great start for any rotation students in the lab. The initial 3D volumes obtained through negative stain might allow for improved data processing, and the large improvement in the data collection capacities of UCSF's microscopes would allow the collection of enough particles to bring this complex to higher resolution.

While the Open Hsp90:Cdc37:PP5 complex is structurally demanding, there is still much left to attempt and a lot left to learn from this complex. The Hsp90:Cdc37 complex might be the best place to start towards the open Hsp90 complex goal. Alternatively, cell biology work done by von Kriegsheim et al. recognized that PP5 can specifically dephosphorylate CRaf (von Kriegsheim et al., 2006). This interaction seemed to be coordinated by Hsp90, and there was a possibility that PP5 would dephosphorylate CRaf while bound to a closed Hsp90:Cdc37:CRaf complex.

Different Hsp90:Cdc37:CRaf constructs show different phosphorylation

Von Kriegsheim et al. showed that CRaf could get dephosphorylated by PP5 in a TPR domain dependent manner. Mutation of a PP5 TPR residue key to MEEVD binding led to no dephosphorylation of CRaf, which suggested the involvement of Hsp90 in CRaf dephosphorylation by PP5. The yeast purified Hsp90:Cdc37:CRaf$^{336\text{-}618}$ complex had been previously purified by D. Coutandin, and incubation of this complex with PP5 led to complex formation over size exclusion, and very efficient crosslinking using glutaraldehyde. This inspired the study of the relationship between PP5 and Hsp90:Cdc37:Kinase complexes.

While the yeast purified Hsp90:Cdc37:CRaf$^{336\text{-}618}$ and E. coli PP5 complex could be efficiently crosslinked and visualized using cryoEM, the yeast purified Hsp90:Cdc37:CRaf$^{336\text{-}618}$ complex showed little to no phosphorylation signal when observed through a phosphorylation stained gel. To test the PP5 dephosphorylation of CRaf at its S338 position as had been shown previously by von Kriegsheim et al., CRaf would need to be phosphorylated in a more mammalian-like physiological manner. This, in combination with the suboptimal yeast prep yield and slow growth, led to the optimization of the transient expression of Hsp90:Cdc37:CRaf in mammalian Expi HEK293 cells.

Using a similar P2A readthrough system, and the co-expression of all three protein components, Hsp90:Cdc37:CRaf complexes were purified from mammalian cells using a Strep Tag to pull on CRaf kinase. CRaf kinase was pulled down with Hsp90 and Cdc37, and subsequent size exclusion chromatography ensured complex purity. Three different CRaf construct lengths were expressed in this way (Sup. Fig. 2). The full-length construct was purified at a lower yield, than the Extended Domain and Kinase Domain constructs (Fig. 3.5a), but all complexes included the three main components. “Open” and molybdate trapped “closed” complexes were purified. The Molybdate trapped complexes were buffer exchanged to remove any unbound molybdate in the buffer and ensure that PP5 activity would not be inhibited.

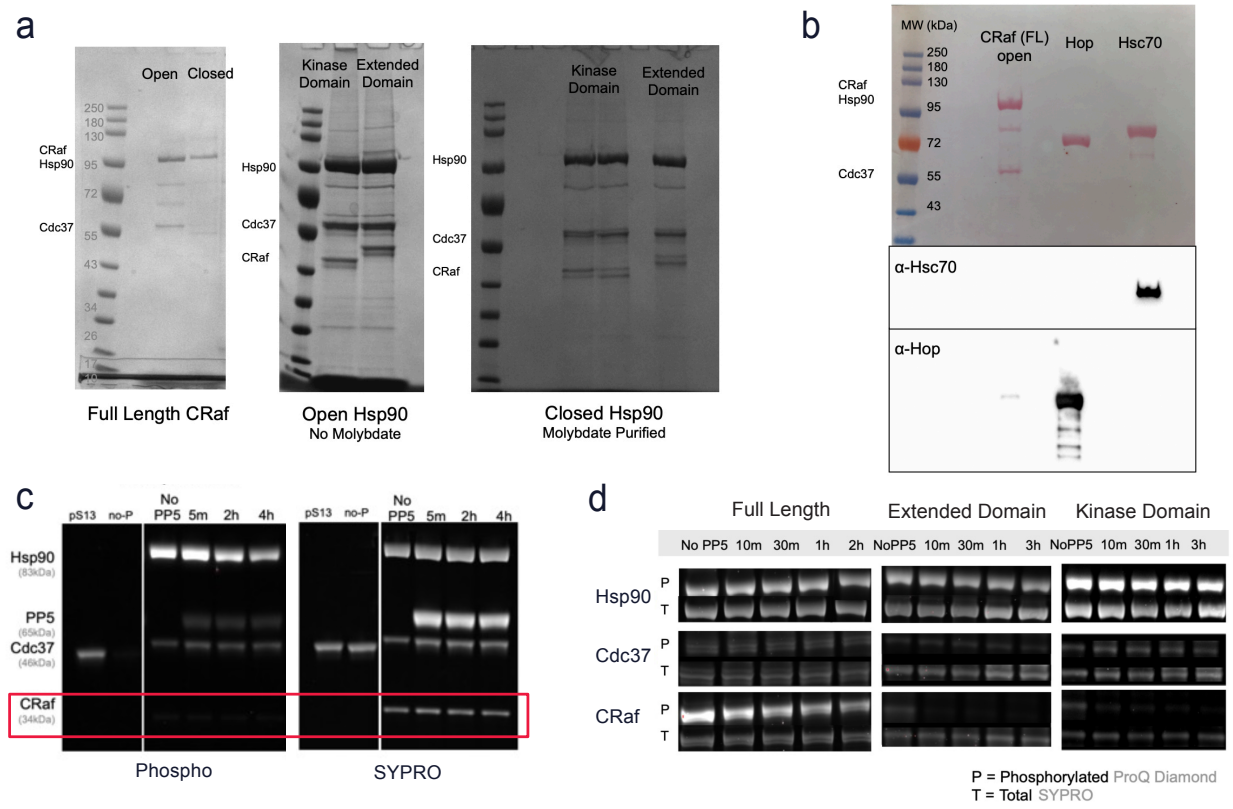

Fig. 3.5. Mammalian Hsp90:Cdc37:CRaf$^{304-648}$ complex ideal for biochemical studies.

a Hsp90:Cdc37:CRaf complexes with different CRaf lengths can be purified from Expi HEK293 cells. Complexes can be stabilized in a "Closed" conformation through Molybdate binding, but "Open" complexes are metastable in a closed state while on ice. **b** A distinct extra bands can be seen in all purified complexes, and western blots against both Hsc70/Hsp70 and Hop show the band may correspond to Hop. Positive controls are included. **c,d** ProQ Diamond stain shows phosphorylated species. **c** Purification of yeast Hsp90:Cdc37:CRaf$^{336-618}$ complex shows very faint phosphorylation signal. PP5 addition does not lead to Cdc37 dephosphorylation, but may lead to Hsp90 dephosphorylation. Further studies are recommended. **d** Complexes with Hsp90:Cdc37 and Full length, Extended domain or Kinase domain CRaf show slight phosphorylation of CRaf which becomes quickly dephosphorylated by PP5. The CRaf Extended domain complex shows the fastest CRaf dephosphorylation.

Two extra bands were visible in the SDS gels of the purified components. A western blot testing against Hsc70 and Hop was run to attempt to identify these two bands that ran at around 60kDa and 75kDa (Fig. 3.5b). Interestingly, and as might be expected from immortalized cell

lines, Hop lit up in the Hsp90:Cdc37:CRaf complex lane as well as in our positive control. Hop is a TPR binding protein and might have been bound to the MEEVD tails of Hsp90. The Hsc70 antibody bound to the positive control, but did not show signal in the Hsp90:Cdc37:CRaf lane. More experiments are required to identify this band and see if it is of biological interest.

After purification of the Hsp90:Cdc37:CRaf complexes, they were tested for PP5 dephosphorylation. While CRaf showed phosphorylation signal for all construct lengths, the CRaf^{ExtD} was promptly dephosphorylated. While the phosphorylation signal of full length CRaf also decreased, the total protein stain showed a decrease in CRaf concentration throughout the experimental timeframe. The lack stability of the full length CRaf led to the conclusion that CRaf^{ExtD} might be the best complex to use for biochemical characterization of PP5.

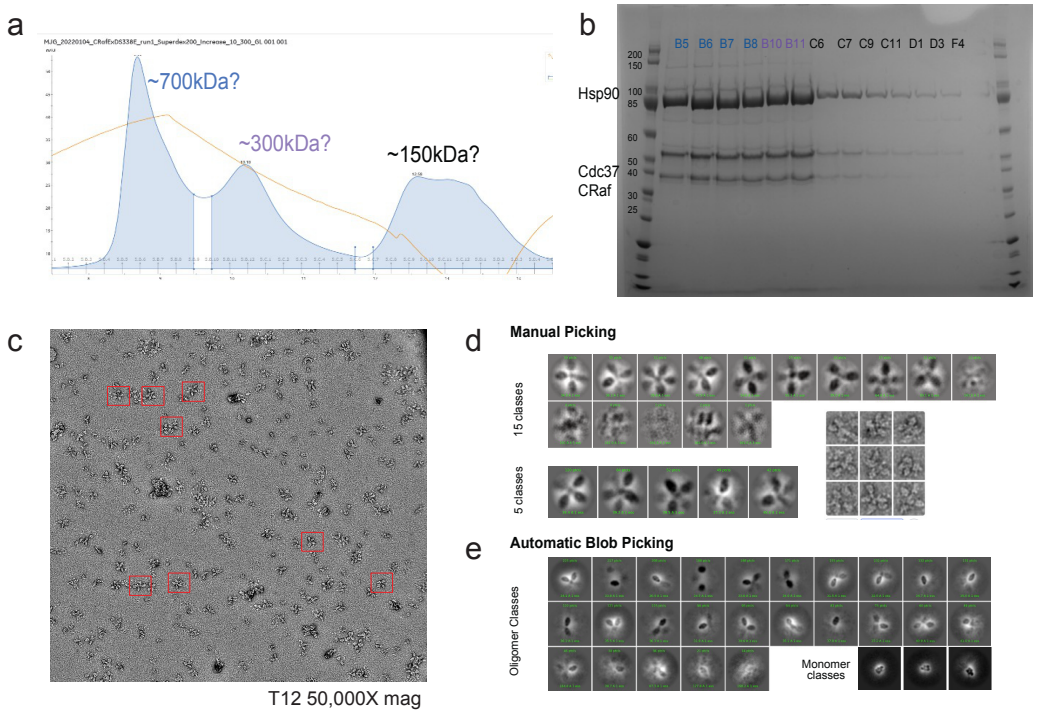

Fig. 3.6. Hsp90:Cdc37:CRaf^{ExtD} complex forms larger complex upon initial purification.

a Sizing run (S200 10/300) of Strep-Tag pulled Hsp90:Cdc37:CRaf$^{ExtD\ S338E}$ shows three predominant peaks, the first two peaks have similar stoichiometries (**b**) but different molecule sizes. c Fractions of the ~700kDa peak were

imaged in negative stain grids and showed “flower-like” complexes as well as smaller dispersed complexes. **d** Manual picking of these “flower-like” complexes, (**e**) or automatic gaussian blob picking led to flower like oligomers of Hsp90 complexes and monomer Hsp90 complexes.

During large scale purification of the Hsp90:Cdc37:CRaf^{ExtD} complex, an interesting larger peak of protein was visible through size exclusion (Fig. 3.6a). When these samples were run on an SDS gel, they appeared to have similar components to the next peak of expected size (~300kDa) (Fig. 3.6b). When these larger fractions were visualized through negative stain grids, flower-like classes could be visualized on the micrographs (Fig. 3.6c). When picked manually or automatically, these particles averaged out into 2D classes that looked flower-like as well (Fig. 3.6d,e). These particles were later screened on cryoEM grids and did not show these flower-like particles or classes, which suggests that the complexes might be stabilized by negative stain or that the interactions visualized may be weak in nature. Another possible explanation for these classes, is that the Hsp90:Cdc37:CRaf complexes are expressed through automatically cleaving P2A sequences and these inter-protein sequences might not have cleaved fully. More experiments are required to make sense of this fun observation.

While the phosphorylation gel stain showed clearly visible dephosphorylation of CRaf by PP5, a better readout was required to fully characterize PP5 specificity and activity. Phosphorylation specific antibodies were acquired to test dephosphorylation through western blots. An initial test was done within the cellular context. The cells were lysed after expression of Hsp90:Cdc37:CRaf complexes and/or PP5 and tested for phosphorylation at the S338 position (Fig. 3.7a). Hsp90:Cdc37:CRaf^{ExtD} complexes expressed with the inactive PP5^{H304A}, showed antibody signal at for pS338. Hsp90:Cdc37:CRaf^{ExtD} complexes expressed with wildtype PP5 showed no phosphorylation, presumably because of efficient PP5 dephosphorylation. Cells

expressing Hsp90:Cdc37:CRaf$^{ExtD\ S338E}$ complexes showed no phosphorylation of S338 because of their inability to become phosphorylated at this mutated residue. Finally, the singly expressed Hsp90:Cdc37:CRaf^{ExtD} complex showed strong phosphorylation at the S338 site.

All of these Hsp90:Cdc37:CRaf^{ExtD} complexes were also tested for CRaf presence through Ponceau stain, ensuring CRaf was not getting degraded. Through these experiments, an Hsp90:Cdc37:CRaf^{ExtD} complex expression time of around 72 hours was chosen for future expression. A second antibody against CRaf^{pS621} was also used as a control for pS338 phosphorylation, and all samples with or without PP5 showed constant pS621 presence. Interestingly, Hsp90:Cdc37:CRaf^{ExtD} complexes incubated with wildtype PP5 showed a slight decrease in pS621 phosphorylation as compared to PP5^{H304A}. This observation was later recreated in-vitro (see Chapter 4).

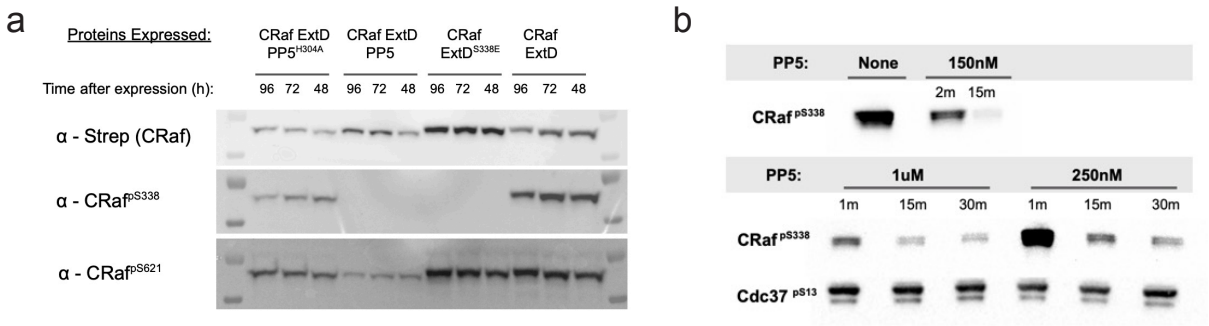

Fig. 3.7. PP5 dephosphorylates CRaf^{pS338} in cells and in vitro.

a Expression of Hsp90:Cdc37:CRaf$^{304-648}$ + PP5^{H304A}, Hsp90:Cdc37:CRaf$^{304-648}$ + PP5, Hsp90:Cdc37:CRaf$^{304-648}$ S338E, or Hsp90:Cdc37:CRaf$^{304-648}$ allows for in-vivo the testing of phosphospecific CRaf^{pS338} antibodies. The phosphatase dead PP5^{H304A} does not dephosphorylate CRaf^{pS338}, while PP5^{WT} does. CRaf^{pS338E} does not show S338 phosphorylation. **b** In-vitro dephosphorylation shows PP5 dephosphorylation of CRaf^{pS338} in purified Hsp90:Cdc37:CRaf complexes. PP5 concentrations were optimized to show a large dynamic range in future experiments.

Next, we tested the phosphorylation of purified Hsp90:Cdc37:CRaf^{ExtD} complexes. PP5 incubation with Hsp90:Cdc37:CRaf^{ExtD} complexes led to a decrease in pS338 signal. These initial western blots led to the establishment of ideal PP5 concentration ranges used to measure PP5 phosphatase activity.

Because the yeast purified Hsp90:Cdc37:CRaf^{KD} complex had been previously optimized for cryoEM freezing and could be reliably imaged and averaged, initial structural efforts were taken with this complex regardless of the apparent lack of phosphorylation seen through phosphorylation stained gels. The shorter CRaf kinase domain ensured a more homogeneous population of particles, and an easier biochemical set-up. This complex was incubated with E. coli purified PP5, or the E. coli purified phosphatase dead PP5^{H304A}. Both variants of PP5 were well crosslinked to the Hsp90:Cdc37:CRaf complex (Fig. 3.8a). Initial overnight collections of these samples did not show PP5 density in their 2D or 3D classes, so the amount of PP5 present while crosslinking was increased to 2X or 4X the amount of Hsp90:Cdc37:CRaf complex (Fig. 3.8b). Larger concentrations of PP5 crosslink to higher molecular weight bands and higher molecular weight complexes visualized after size exclusion chromatography through mass photometry (Fig. 3.8c,d). The larger species present in both the SDS gel and the mass photometry suggest that two PP5 molecules might be binding to one Hsp90 complex. None of the densities seen from these or the subsequent datasets showed more than a single PP5 molecule bound per Hsp90 complex, which might suggest that PP5 is binding through its TPR domain to the MEEVD tail of one of the Hsp90 protomers. This tethering would be too flexible to visualize through cryoEM reconstruction.

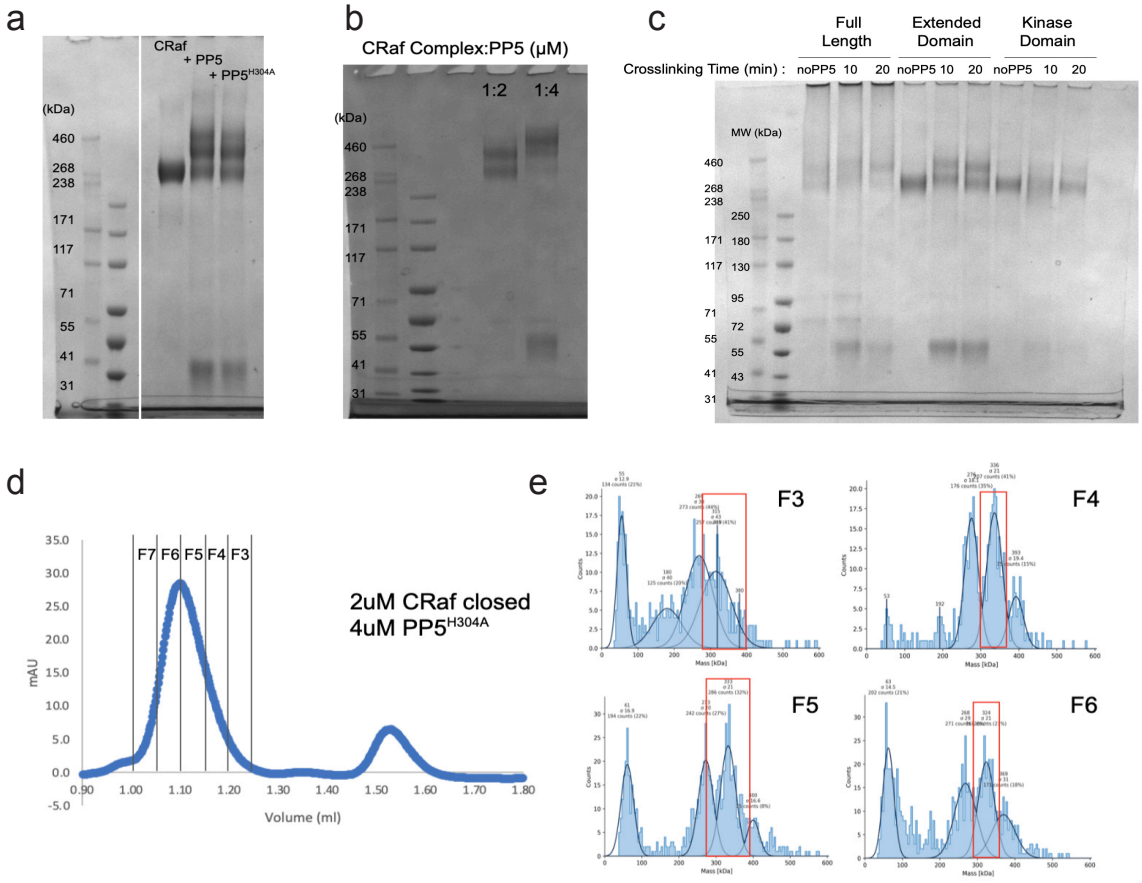

Fig. 3.8. Mammalian and yeast Hsp90:Cdc37:CRaf:PP5 complex can be crosslinked.

a Mammalian CRaf Extended domain (CRaf$^{304-648}$) Hsp90:Cdc37:CRaf:PP5 complex shows ideal crosslinking conditions. Full Length complex leads to protein signal in the well, suggesting unstable or aggregated complex, while Kinase domain shows limited crosslinking. **b** Previously cryoEM-screened Yeast Hsp90:Cdc37:CRaf$^{336-618}$ complexes crosslink to PP5. **c** Increasing the amount of PP5 present with complex while crosslinking leads to a complex larger than expected for a single PP5 binding. **d** Size Exclusion Chromatography (S200) and Mass photometry shows a clear peak with particles at around the expected 304kDa molecular weight. These fractions were used for further structural characterization.

While the yeast Hsp90:Cdc37:CRaf complex crosslinked well the PP5, interest in capturing an active conformation of PP5 led to the optimization of mammalian complex crosslinking. Full length, extended domain, or kinase domain complexes were crosslinked with catalytically dead PP5 (Fig.3.8c). Crosslinking of the full length CRaf complex to PP5 led to

dark protein signal by the gel well, suggesting that the denatured sample was too aggregated to enter the gel. This may be due to the lack of stability of the full length CRaf complex. The kinase domain of CRaf showed minimal crosslinking at the conditions tested, but the extended domain of CRaf crosslinked as thoroughly as was seen by the yeast complexes. Although a large dataset had already been collected for the yeast Hsp90:Cdc37:CRaf complex crosslinked to $PP5^{H304A}$, freezing optimization, and grid screening allowed for a small overnight collection of the mammalian Hsp90:Cdc37:$CRaf^{ExtD}$ complex crosslinked to $PP5^{aJ\ deletion}$ (see Chapter 4).

Hsp90:Cdc37:Kinase complexes fall apart at elevated temperatures

Previous experiments found that molybdate could replace the gamma phosphate of ATP upon ATP hydrolysis of a closed Hsp90 complex and lock Hsp90 in a closed state. Purifying Hsp90-kinase complexes under these conditions has enabled the study of Hsp90-Kinase interactions for years. Expecting an open Hsp90 complex, the structural determination of a molybdate free Hsp90:Cdc37:Her2 complex by D. Coutandin did not show an "open" Hsp90 complex, but instead a closed Hsp90 conformation. In this structure, one of the Hsp90 protomers was bound to an ATP molecule, while the other was bound to an ADP molecule. This suggests that by purifying Hsp90:Cdc37:Kinase complexes through the pulldown of the Strep-tagged Kinase, we are selecting for complexes tightly bound to Hsp90 and Cdc37 in a metastably closed state.

We decided to study the stability of Hsp90:Cdc37:Kinase complexes by exploring the rate at which Hsp90 releases ADP or ATP. To do this we observed the rate at which an Hsp90 covalent inhibitor bound the Hsp90 active site (Cuesta et al., 2020), and simultaneously studied the rate of

complex dissociation using a mass photometer. The small molecule was used to measure the availability of the ATP binding pocket in the N-terminal domain of Hsp90, and therefore the rate of "openness" of Hsp90. The Hsp90:Cdc37:Her2 complex was incubated at two different temperatures and Hsp90 inhibitor bound the complex more strongly at the higher temperature (30°C, Fig. 3.9a,c), indicative of the higher rate of Hsp90 opening at higher temperatures. The same Hsp90:Cdc37:Her2 complexes were then incubated at different temperatures with or without molybdate, and placed on a mass photometer to measure the populations of differently sized complexes in solution (Fig 3.9a, b). The mass photometer results showed peaks corresponding to the Hsp90:Cdc37:Her2 complex (~ 250kDa), Hsp90 dimers, Hsp90 monomers, and smaller proteins likely Cdc37 and the Her2 kinase domain. Through time the Hsp90:Cdc37:Her2 complex peak would fall apart. This effect was even more pronounced at a higher temperature (30°C). When molybdate salt was added to these complexes, a stabilization of the full complex could be seen.

Fig. 3.9. Elevated temperatures contribute to Hsp90:Cdc37:Kinase complex dissociation.

a Hsp90 opening was tracked by covalent inhibitor binding (Liquid Chromatography Mass Spectrometry (LCMS)), or complex dissociation as measured by mass photometry. Hsp90:Cdc37:Kinase complex stability was measured at different temperatures (20°C, 30°C or Molybdate trapped 30°C) as a function of time, and higher temperatures led to faster complex breakdown. **b, c** Mass photometry data and LCMS data examples are included.

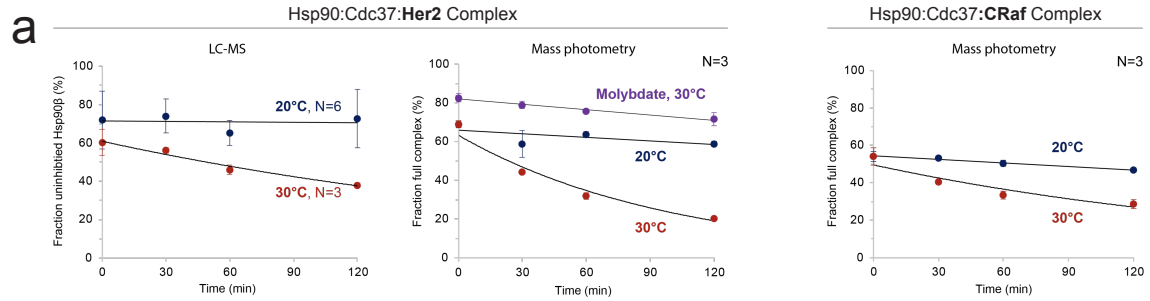
a
Hsp90:Cdc37:Her2 Complex
Hsp90:Cdc37:CRaf Complex
LC-MS
Mass photometry
N=3
Fraction uninhibited Hsp90β (%)
Fraction full complex (%)
Time (min)
20°C, N=6
30°C, N=3
Molybdate, 30°C
20°C
30°C

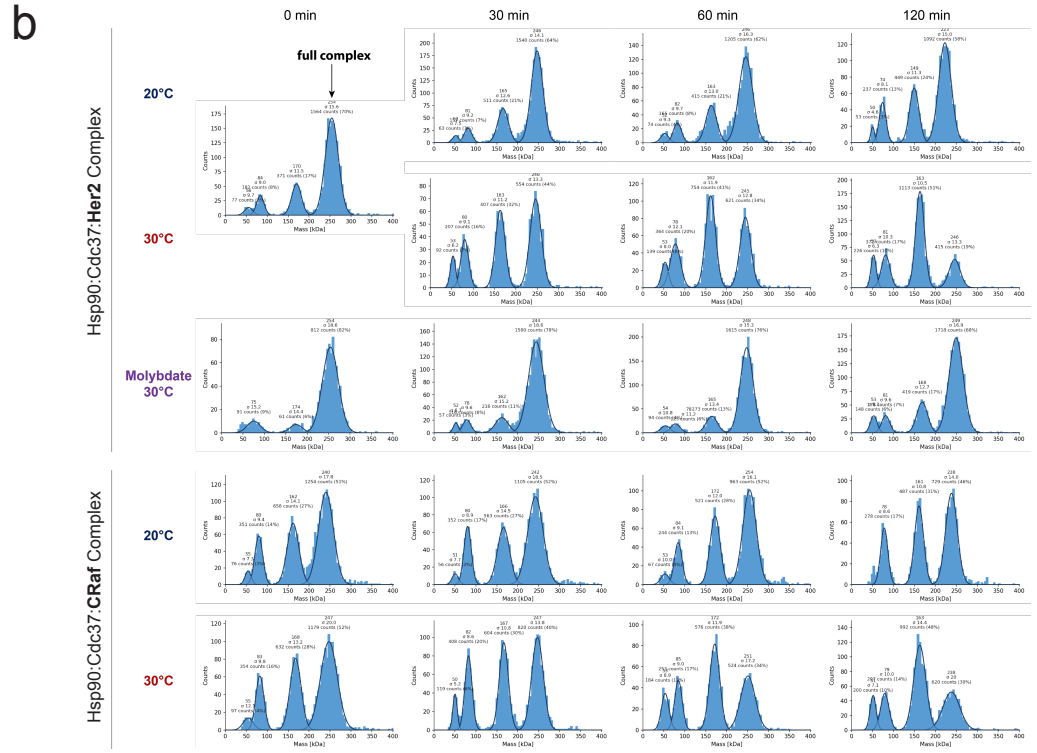
b
0 min
30 min
60 min
120 min
full complex
Hsp90:Cdc37:Her2 Complex
Hsp90:Cdc37:CRaf Complex
20°C
30°C
Molybdate 30°C
Counts
Mass (kDa)

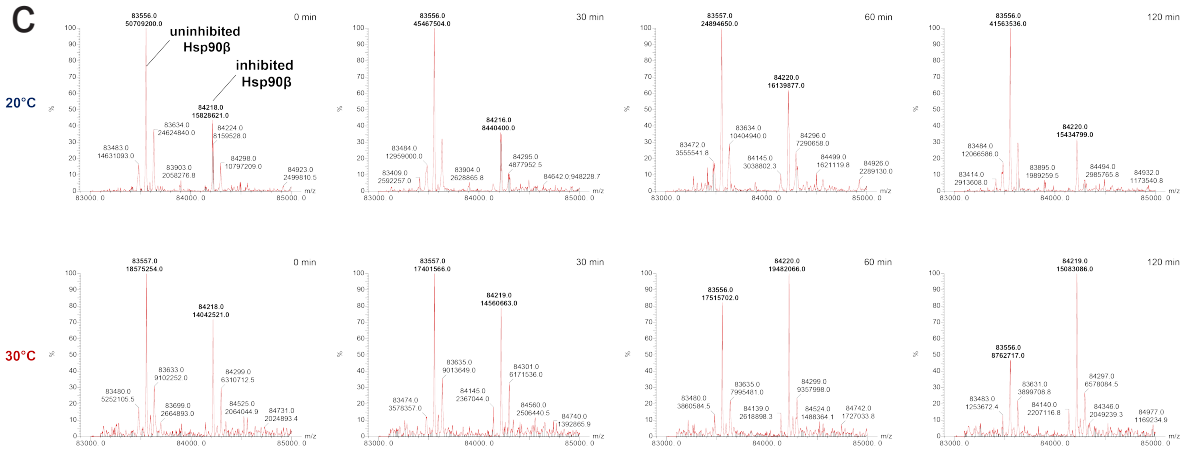
c
0 min
30 min
60 min
120 min
20°C
30°C
uninhibited Hsp90β
inhibited Hsp90β
m/z

CK2 phosphorylated Hsp90 doesn't get dephosphorylated by PP5

Hsp90 interacts with a wide range of cochaperones, chaperones and protein clients in many distinct ways. Hsp90 activity is modulated to interact with the right set of interactors and clients at the right time. Phosphorylation on Hsp90 (Mollapour & Neckers, 2012), but also its cochaperones and clients has been shown to act as a mechanism of Hsp90 regulation (Bachman et al., 2018; Miyata & Nishida, 2004; Röhl et al., 2015; Xu et al., 2012). Ppt1, the yeast homolog of PP5, binds Hsp90 and has been shown to directly dephosphorylate CK2 phosphorylated Hsp90 (Wandinger et al., 2006). We decided to repeat these experiments with human Hsp90, CK2 and PP5.

Phosphorylation gel stain was used to map the phosphorylation state of Hsp90 and its cochaperones through these experiments. E. coli purified Hsp90 is not phosphorylated and shows only background signal in the gels used. CK2 bought from N.E.B. was used following the included protocol. Hsp90, Hsp90:Cdc37^{pS13} and Hsp90:Cdc37 were all phosphorylated by CK2 at different intensities as compared to the CK2 free control (Fig. 3.10a). Interestingly, the Hsp90:Cdc37^{pS13} sample was the most heavily phosphorylated, suggesting that the phosphorylated Cdc37 might help boost CK2 activity on Hsp90. More experiments are required to test this hypothesis.

PP5 was then added to the phosphorylated samples and tested for its ability to dephosphorylate both Hsp90 and Cdc37 (Fig. 3.10b). PP5 did not seem to be able to dephosphorylate Hsp90, although it did dephosphorylate Cdc37 as has been shown previously. Although PP5 is present in large excess of CK2, CK2 was not purified out of the samples so further experiments need to be done to ensure that CK2 is not quickly re-phosphorylating Hsp90.

Hsp90 phosphorylation has been shown to modify the way cochaperones interact with Hsp90, so preliminary size exclusion chromatography experiments were run to compare the strength of association between Hsp90 and Cdc37. Hsp90 and CK2-phosphorylated Hsp90 both interacted with Cdc37 in a similar way (Fig. 3.10c). More sensitive experiments would be required to test finer affinity ranges. Much is left to do in to understand the PP5-dependent dephosphorylation of Hsp90.

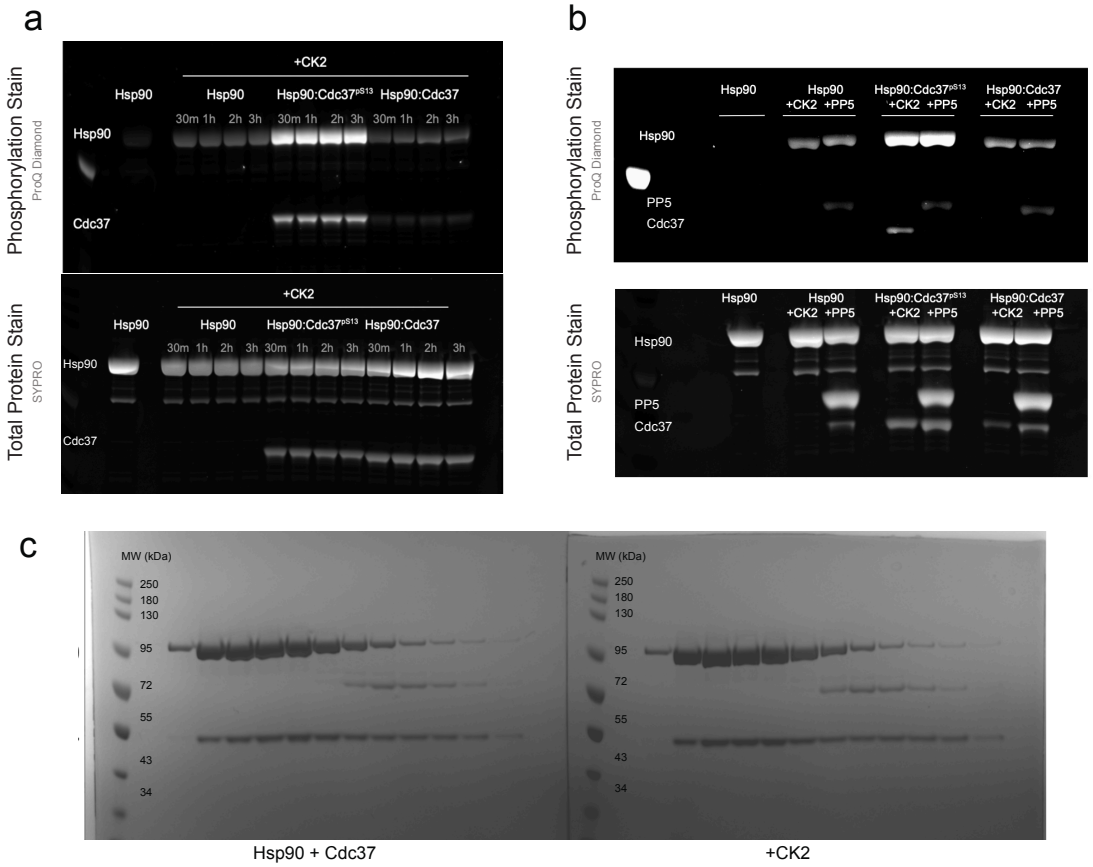

Fig. 3.10. PP5 does not dephosphorylate CK2 phosphorylated Hsp90.

A CK2 phosphorylates Hsp90 when Cdc37pS13 is present, but not if unphosphorylated Cdc37 or Hsp90 alone are present. **b** PP5 dephosphorylates Cdc37 but not CK2 phosphorylated Hsp90. It's important to note that CK2 has not been removed from the reaction and might therefore be competing with the excess PP5 dephosphorylation. **c** CK2 phosphorylated Hsp90 binds Cdc37^{pS13} similarly in a similar way to dephosphorylated Hsp90 as seen by size exclusion chromatography (S200) elution.

References

Abbas-Terki, T., Briand, P. A., Donzé, O., & Picard, D. (2002). The Hsp90 Co-Chaperones Cdc37 and Sti1 Interact Physically and Genetically. *383*(9), 1335-1342. https://doi.org/doi:10.1515/BC.2002.152

Bachman, A. B., Keramisanou, D., Xu, W., Beebe, K., Moses, M. A., Vasantha Kumar, M. V., Gray, G., Noor, R. E., van der Vaart, A., Neckers, L., & Gelis, I. (2018). Phosphorylation induced cochaperone unfolding promotes kinase recruitment and client class-specific Hsp90 phosphorylation. *Nature Communications*, *9*(1), 265. https://doi.org/10.1038/s41467-017-02711-w

Chen, M. X., McPartlin, A. E., Brown, L., Chen, Y. H., Barker, H. M., & Cohen, P. T. (1994). A novel human protein serine/threonine phosphatase, which possesses four tetratricopeptide repeat motifs and localizes to the nucleus. *The EMBO Journal*, *13*(18), 4278-4290. https://doi.org/10.1002/j.1460-2075.1994.tb06748.x

Chen, S., Sullivan, W. P., Toft, D. O., & Smith, D. F. (1998). Differential interactions of p23 and the TPR-containing proteins Hop, Cyp40, FKBP52 and FKBP51 with Hsp90 mutants. *Cell Stress Chaperones*, *3*(2), 118-129. https://doi.org/10.1379/1466-1268(1998)003<0118:diopat>2.3.co;2

Cuesta, A., Wan, X., Burlingame, A. L., & Taunton, J. (2020). Ligand Conformational Bias Drives Enantioselective Modification of a Surface-Exposed Lysine on Hsp90. *Journal of the American Chemical Society*, *142*(7), 3392-3400. https://doi.org/10.1021/jacs.9b09684

Harst, A., Lin, H., & Obermann, Wolfgang M. J. (2005). Aha1 competes with Hop, p50 and p23 for binding to the molecular chaperone Hsp90 and contributes to kinase and hormone

receptor activation. *Biochemical Journal*, *387*(3), 789-796. https://doi.org/10.1042/BJ20041283

Lee, K., Thwin, A. C., Nadel, C. M., Tse, E., Gates, S. N., Gestwicki, J. E., & Southworth, D. R. (2021). The structure of an Hsp90-immunophilin complex reveals cochaperone recognition of the client maturation state. *Molecular Cell*, *81*(17), 3496-3508.e3495. https://doi.org/10.1016/j.molcel.2021.07.023

Miyata, Y., & Nishida, E. (2004). CK2 Controls Multiple Protein Kinases by Phosphorylating a Kinase-Targeting Molecular Chaperone, Cdc37. *Molecular and Cellular Biology*, *24*(9), 4065-4074. https://doi.org/10.1128/MCB.24.9.4065-4074.2004

Miyata, Y., & Nishida, E. (2007). Analysis of the CK2-dependent phosphorylation of serine 13 in Cdc37 using a phospho-specific antibody and phospho-affinity gel electrophoresis: Cdc37 phosphorylation by CK2 and signaling kinases. *FEBS Journal*, *274*(21), 5690-5703. https://doi.org/10.1111/j.1742-4658.2007.06090.x

Mollapour, M., & Neckers, L. (2012). Post-translational modifications of Hsp90 and their contributions to chaperone regulation. *Biochimica et Biophysica Acta (BBA) - Molecular Cell Research*, *1823*(3), 648-655. https://doi.org/https://doi.org/10.1016/j.bbamcr.2011.07.018

Noddings, C. M., Johnson, J. L., & Agard, D. A. (2023). *Cryo-EM reveals how Hsp90 and FKBP immunophilins co-regulate the Glucocorticoid Receptor* [preprint]. http://biorxiv.org/lookup/doi/10.1101/2023.01.10.523504

Ramsey, A. J., & Chinkers, M. (2002). Identification of Potential Physiological Activators of Protein Phosphatase 5. *Biochemistry*, *41*(17), 5625-5632. https://doi.org/10.1021/bi016090h

Ramsey, A. J., Russell, L. C., Whitt, S. R., & Chinkers, M. (2000). Overlapping Sites of Tetratricopeptide Repeat Protein Binding and Chaperone Activity in Heat Shock Protein 90*. *Journal of Biological Chemistry*, *275*(23), 17857-17862. https://doi.org/https://doi.org/10.1074/jbc.M001625200

Röhl, A., Tippel, F., Bender, E., Schmid, A. B., Richter, K., Madl, T., & Buchner, J. (2015). Hop/Sti1 phosphorylation inhibits its co-chaperone function. *EMBO reports*, *16*(2), 240-249.

Schopf, F. H., Biebl, M. M., & Buchner, J. (2017). The HSP90 chaperone machinery. *Nature Reviews Molecular Cell Biology*, *18*(6), 345-360. https://doi.org/10.1038/nrm.2017.20

Shao, J., Irwin, A., Hartson, S. D., & Matts, R. L. (2003). Functional Dissection of Cdc37: Characterization of Domain Structure and Amino Acid Residues Critical for Protein Kinase Binding. *Biochemistry*, *42*(43), 12577-12588. https://doi.org/10.1021/bi035138j

Shao, J., Prince, T., Hartson, S. D., & Matts, R. L. (2003). Phosphorylation of Serine 13 Is Required for the Proper Function of the Hsp90 Co-chaperone, Cdc37. *Journal of Biological Chemistry*, *278*(40), 38117-38120. https://doi.org/10.1074/jbc.C300330200

Shiau, A. K., Harris, S. F., Southworth, D. R., & Agard, D. A. (2006). Structural Analysis of E. coli hsp90 Reveals Dramatic Nucleotide-Dependent Conformational Rearrangements. *Cell*, *127*(2), 329-340. https://doi.org/https://doi.org/10.1016/j.cell.2006.09.027

Skarra, D. V., Goudreault, M., Choi, H., Mullin, M., Nesvizhskii, A. I., Gingras, A. C., & Honkanen, R. E. (2011). Label-free quantitative proteomics and SAINT analysis enable interactome mapping for the human Ser/Thr protein phosphatase 5. *Proteomics*, *11*(8), 1508-1516.

Swingle, M. R., Honkanen, R. E., & Ciszak, E. M. (2004). Structural Basis for the Catalytic Activity of Human Serine/Threonine Protein Phosphatase-5. *Journal of Biological Chemistry*, *279*(32), 33992-33999. https://doi.org/10.1074/jbc.M402855200

Taipale, M., Jarosz, D. F., & Lindquist, S. (2010). HSP90 at the hub of protein homeostasis: emerging mechanistic insights. *Nature Reviews Molecular Cell Biology*, *11*(7), 515-528. https://doi.org/10.1038/nrm2918

Vaughan, C. K., Mollapour, M., Smith, J. R., Truman, A., Hu, B., Good, V. M., Panaretou, B., Neckers, L., Clarke, P. A., Workman, P., Piper, P. W., Prodromou, C., & Pearl, L. H. (2008). Hsp90-Dependent Activation of Protein Kinases Is Regulated by Chaperone-Targeted Dephosphorylation of Cdc37. *Molecular Cell*, *31*(6), 886-895. https://doi.org/10.1016/j.molcel.2008.07.021

Verba, K. A., Wang, R. Y.-R., Arakawa, A., Liu, Y., Shirouzu, M., Yokoyama, S., & Agard, D. A. (2016). Atomic structure of Hsp90-Cdc37-Cdk4 reveals that Hsp90 traps and stabilizes an unfolded kinase. *Science*, *352*(6293), 1542-1547. https://doi.org/10.1126/science.aaf5023

von Kriegsheim, A., Pitt, A., Grindlay, G. J., Kolch, W., & Dhillon, A. S. (2006). Regulation of the Raf–MEK–ERK pathway by protein phosphatase 5. *Nature Cell Biology*, *8*(9), 1011-1016. https://doi.org/10.1038/ncb1465

Wandinger, S. K., Suhre, M. H., Wegele, H., & Buchner, J. (2006). The phosphatase Ppt1 is a dedicated regulator of the molecular chaperone Hsp90. *The EMBO Journal*, *25*(2), 367-376. https://doi.org/10.1038/sj.emboj.7600930

Wang, R. Y.-R., Noddings, C. M., Kirschke, E., Myasnikov, A. G., Johnson, J. L., & Agard, D. A. (2022). Structure of Hsp90–Hsp70–Hop–GR reveals the Hsp90 client-loading mechanism. *Nature*, *601*(7893), 460-464. https://doi.org/10.1038/s41586-021-04252-1

Xu, W., Mollapour, M., Prodromou, C., Wang, S., Scroggins, Bradley T., Palchick, Z., Beebe, K., Siderius, M., Lee, M.-J., Couvillon, A., Trepel, Jane B., Miyata, Y., Matts, R., & Neckers, L. (2012). Dynamic Tyrosine Phosphorylation Modulates Cycling of the HSP90-P50CDC37-AHA1 Chaperone Machine. *Molecular Cell*, *47*(3), 434-443. https://doi.org/https://doi.org/10.1016/j.molcel.2012.05.015

Yang, J., Roe, S. M., Cliff, M. J., Williams, M. A., Ladbury, J. E., Cohen, P. T. W., & Barford, D. (2005). Molecular basis for TPR domain-mediated regulation of protein phosphatase 5. *The EMBO Journal*, *24*(1), 1-10. https://doi.org/10.1038/sj.emboj.7600496

Chapter 4

Hsp90 provides a platform for kinase dephosphorylation by PP5

Abstract

The Hsp90 molecular chaperone collaborates with the phosphorylated Cdc37 cochaperone for the folding and activation of its many client kinases. As with many kinases, the Hsp90 client kinase CRaf is activated by phosphorylation at specific regulatory sites. The cochaperone phosphatase PP5 dephosphorylates CRaf but also Cdc37 in an Hsp90-dependent manner. Although dephosphorylating Cdc37 has been proposed as a mechanism for releasing Hsp90-bound kinases, here we show that Hsp90 bound kinases sterically inhibit Cdc37 dephosphorylation indicating kinase release must occur before Cdc37 dephosphorylation. Our cryo-EM structure of PP5 in complex with Hsp90:Cdc37:CRaf reveals how Hsp90 both activates PP5 and scaffolds its association with the bound CRaf to dephosphorylate phosphorylation sites neighboring the kinase domain. Thus, we directly show how Hsp90's role in maintaining protein

homeostasis goes beyond folding and activation to include post translationally modifying its client kinases.

Introduction

Maintaining protein homeostasis is a critical function for all organisms and relies on a broad array of proteins including molecular chaperones (Hartl et al., 2011). The Heat shock protein Hsp90 is a molecular chaperone required for the folding and activation of over 10% of the human proteome (Taipale et al., 2010; Taipale et al., 2012). Hsp90's "client" proteins are enriched in signaling proteins such as protein kinases, transcription factors, and steroid hormone receptors. This leads Hsp90 to play an important role in organismal health and disease. Importantly, more than half of all human kinases depend on Hsp90 and the Hsp90 co-chaperone Cdc37 for their folding and activation (Kimura et al., 1997). The role of Hsp90 in kinase activation goes beyond folding and includes facilitating alterations in posttranslational modifications. Through its regulation of both kinase folding and kinase dephosphorylation, Hsp90 can modulate essential signaling pathways.

One such critical Hsp90-dependent pathway is the Ras-MAPK pathway involved in regulating cellular proliferation (Grammatikakis et al., 1999; Wartmann & Davis, 1994). When dysregulated, this pathway is often implicated in cellular malignancy (Maurer et al., 2011). Raf kinases are part of this pathway, and act to propagate growth hormone signals from the membrane bound Ras GTPase to MEK and ERK kinases which can lead to signal amplification (Wellbrock et al., 2004). Pathway activation requires Raf kinase dimerization which is mediated by phosphorylation of the Raf kinase acidic N-terminus (Diaz et al., 1997; Hu et al., 2013;

Mason, 1999). Thus, dephosphorylation of this acidic N-terminus may then lead to pathway inactivation (Cutler et al., 1998).

While Raf kinase activation has been extensively studied, Raf inactivation is less well understood. Importantly, for RAF proto-oncogene serine/threonine-protein kinase (CRaf or RAF-1), a member of the Raf family, the Hsp90 cochaperone, Serine/threonine-protein phosphatase 5 (PP5) has been directly implicated in its dephosphorylation and inactivation(von Kriegsheim et al., 2006). More specifically, PP5 was shown to pulldown with CRaf and specifically dephosphorylate phosphoserine 338 ($CRaf^{pS338}$) during Ras-MAPK pathway activation. Similarly, siRNA PP5 knockdown led to a specific increase in S338 phosphorylation. Based on these results, PP5 was hypothesized to play a key role in CRaf inactivation.

PP5 is a serine-threonine phosphatase from the PPP family which consists of a Tetratricopeptide (TPR) domain N-terminal to the catalytic phosphatase domain (Becker et al., 1994; Chen et al., 1994). The TPR domain sits directly atop the catalytic domain, sterically blocking substrate binding and access to the active site (Swingle et al., 2004; Yang et al., 2005). The inhibitory αJ helix on the catalytic domain stabilizes the autoinhibited PP5 state through hydrophobic interactions with the TPR domain (Kang et al., 2001). Like other TPR-cochaperones, the PP5 TPR domain binds the Hsp90 C-terminal MEEVD tail, in this case leading to PP5 activation (Russell et al., 1999; Yang et al., 2005). A TPR domain mutation that blocks MEEVD binding abrogates the dephosphorylation of $CRaf^{pS338}$ and inhibits PP5 coelution with CRaf kinase (von Kriegsheim et al., 2006). These results strongly suggest that Hsp90 plays a key role in CRaf dephosphorylation by controlling when and where PP5 becomes activated. In addition to CRaf, PP5 dephosphorylates numerous other Hsp90 clients, presumably while they

are bound to Hsp90 (Ali et al., 2004; Amable et al., 2011; Morita et al., 2001; Wechsler et al., 2004; Zhang et al., 2005; Zuo et al., 1998; Zuo et al., 1999).

Ppt1, the yeast homolog of PP5 has been shown to dephosphorylate yeast Hsp90 itself (Wandinger et al., 2006). This led Vaughan et. al. to hypothesize that PP5 might dephosphorylate the Hsp90 cochaperone Cdc37 which must be phosphorylated on S13 ($Cdc37^{pS13}$) to function in kinase activation (Bandhakavi et al., 2003; Miyata & Nishida, 2004, 2007; Shao, Irwin, et al., 2003; Shao, Prince, et al., 2003). Cdc37 is a kinase-specific Hsp90 cochaperone which binds and destabilizes kinase domains, enabling their recruitment into Hsp90:Cdc37:kinase complexes (Keramisanou et al., 2016). Hsp90:Cdc37:kinase complexes purified from yeast, baculovirus or mammalian cells are invariably phosphorylated on $Cdc37^{S13}$ (Miyata & Nishida, 2007; Vaughan et al., 2008). It has also been shown that the mutation of $Cdc37^{S13}$ leads to a decrease in Hsp90 and kinase pulldowns (Miyata & Nishida, 2004, 2007). Finally, structural analysis of Hsp90:Cdc37:kinase complexes reveals that $Cdc37^{pS13}$ is required to stabilize the Cdc37 N-terminal domain and to facilitate interactions with Hsp90 (Verba et al., 2016).

Without Hsp90 activation, PP5 by itself cannot dephosphorylate isolated Cdc37 or Cdc37 within a Cdc37:Cdk4 complex (Vaughan et al., 2008). PP5 can, however, dephosphorylate Cdc37 in the context of a purified Hsp90:Cdc37:Cdk4 complex whereas non-specific phosphatases cannot (Vaughan et al., 2008). This led to the hypothesis that PP5 must dephosphorylate Cdc37 while it is bound to an Hsp90:Cdc37:kinase complex and that it can thus facilitate kinase modification or release from the Hsp90 complex.

To further understand the molecular mechanisms by which PP5 is activated and selects its target substrates, we solved the atomic resolution cryo-EM structure of a human Hsp90:Cdc37:CRaf:PP5 complex and biochemically explored PP5-dependent dephosphorylation

of both CRaf and Cdc37. Surprisingly, this revealed that while CRaf could be readily dephosphorylated by Hsp90-activated PP5, Cdc37 could only be dephosphorylated by Hsp90 activated PP5 in the absence of bound kinase. Through this work we propose a mechanism for PP5 activation; we suggest that PP5 does not serve as a kinase release factor but instead blocks kinase rebinding to previously accessed Hsp90:Cdc37 complexes.

Results

Only kinase free Hsp90-Cdc37 complex can be dephosphorylated by PP5.

PP5 is reported to specifically dephosphorylate CRaf^{pS338} in-vivo while leaving other essential CRaf phosphosites unaltered. Phosphorylated CRaf can be purified in Hsp90:Cdc37:CRaf complexes, and CRaf^{pS338} can subsequently be dephosphorylated in-vitro by PP5 (Stancato et al., 1993). Unless otherwise noted, truncated CRaf$^{304-648}$ complexes (Hsp90:Cdc37:CRaf$^{304-648}$) were used to measure PP5 driven dephosphorylation. The phosphorylation state of CRaf kinase was quantitatively assessed using specific phosphosite antibodies directed against CRaf^{pS338}(N-terminal to the kinase domain), and the control phosphosite CRaf^{pS621} (C-terminal to the kinase domain) (Sup. Fig. 1). Additionally, Cdc37 dephosphorylation was probed using Cdc37^{pS13} specific antibodies (von Kriegsheim et al., 2006).

PP5 activity was followed by incubating *E. coli* purified PP5 with mammalian purified Hsp90:Cdc37:CRaf complexes (Fig. 1a, Sup. Fig. 2). CRaf^{pS338} was promptly dephosphorylated. Surprisingly, the CRaf^{pS621} control site was also rapidly dephosphorylated, although at about 40% the rate of CRaf^{pS338}. Contrary to our expectations, Cdc37^{pS13} was not measurably dephosphorylated upon PP5 addition. These results corroborate structural data showing that Cdc37^{pS13} is inaccessible within the complex, yet contradict previous in vitro biochemical

experiments (Verba et al., 2016). With substantially longer incubations at 37° C (vs RT) we can observe Cdc37^{pS13} dephosphorylation. However, size exclusion analysis suggests that this is due to partial complex dissociation at 37° C (Sup. Fig 3).

To probe the factors contributing to the inaccessibility of Cdc37^{pS13}, we systematically explored the impact of the Hsp90 nucleotide state and the role that the kinase plays in Cdc37^{pS13} dephosphorylation. As shown by cryo-EM, Hsp90 appears closed in the natively isolated Hsp90:Cdc37:kinase complexes, leaving Cdc37^{pS13} inaccessible (Verba et al., 2016). In principle, by leaving out the nucleotide in an in vitro reconstitution (Hsp90^{open}), it should be possible to form Hsp90 open-state complexes. Unfortunately, it has not yet been possible to reconstitute CRaf assembly into an Hsp90 complex in vitro. However, it is possible to assemble Hsp90:kinase domain complexes using the heavily mutated and solubilized Braf kinase domain (Polier et al., 2013; Tsai et al., 2008). Hsp90, Cdc37, and Braf were expressed and purified from *E. coli*, and Cdc37 was phosphorylated by CK2 before a final purification. We reconstituted an Hsp90:Cdc37:Braf complex by mixing and incubating for 30min at 4°C (Polier et al., 2013). Dephosphorylation of Cdc37^{pS13} upon addition of PP5 was again quantitated (Fig. 1b). To our surprise, PP5 was unable to dephosphorylate Cdc37^{pS13} reconstituted into Hsp90^{open} Hsp90:Cdc37:Braf complexes.

To test if Braf might sterically occlude PP5 from dephosphorylating Cdc37, we repeated the experiment without the kinase present. Notably, Hsp90 bound Cdc37^{pS13} was rapidly dephosphorylated by PP5 without the presence of any nucleotide. We reasoned that if kinase steric hinderance were the main factor limiting Cdc37^{pS13} dephosphorylation, then closing Hsp90 without Braf present might allow PP5 access to Cdc37^{pS13}. Hsp90 was incubated with AMPPNP and allowed to shift to a stabilized closed conformation as has been shown previously (Lee et al.,

2021). Once Hsp90 shifted to a closed conformation, Cdc37^{pS13} was added and dephosphorylation was measured. Interestingly, Hsp90^{closed}:Cdc37^{pS13} was dephosphorylated at about half the rate as Hsp90^{open}:Cdc37^{pS13}, suggesting that while the Hsp90 conformational state contributes to the occlusion of Cdc37^{pS13}, kinase presence or absence dominates PP5 activity on Cdc37^{pS13}.

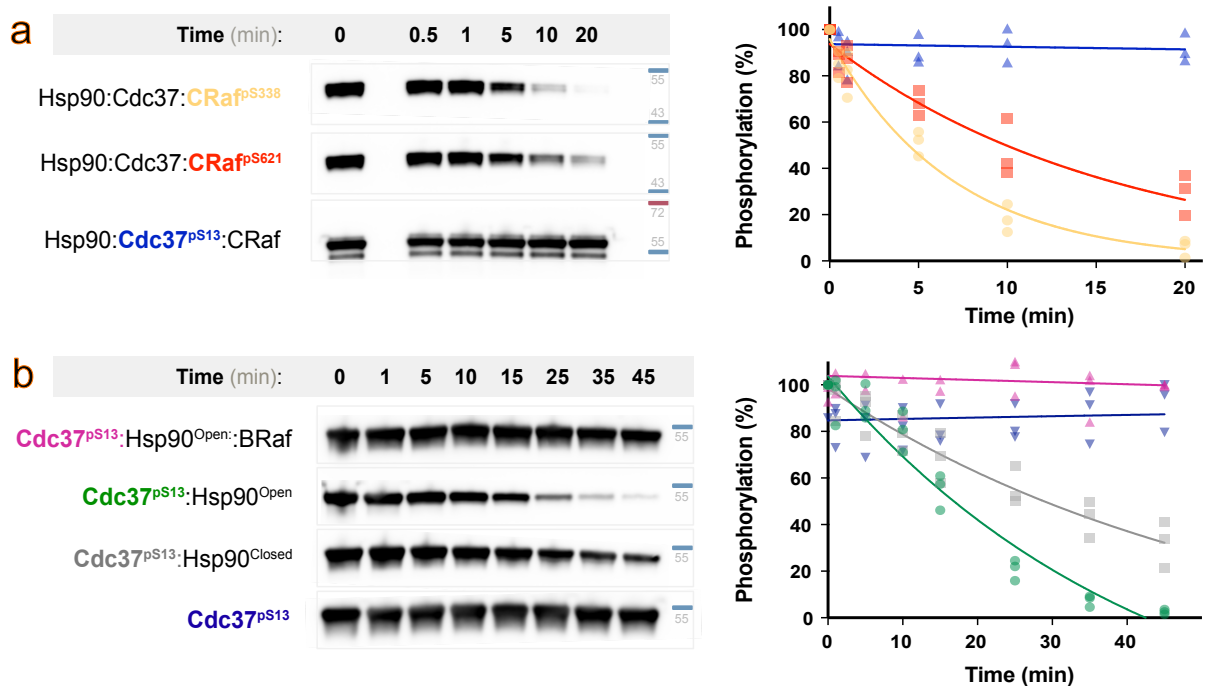

Fig. 4.1. Kinase sterically blocks Cdc37 dephosphorylation.

a Mammalian purified Hsp90:Cdc37:CRaf complex (1.5µM) was incubated with PP5 (75nM) at 25°C. The dephosphorylation of CRaf^{pS338}, CRaf^{pS621} and Cdc37^{pS13} were assayed by 85hosphor-specific blotting (n=3, rate ± SEM). CRaf^{pS338} was preferentially dephosphorylated (yellow, 0.147 ± 0.012 min^{-1}), CRaf^{pS621} was more slowly dephosphorylated (red, 0.063 ± 0.006 min^{-1}), while Cdc37^{pS13} dephosphorylation was not apparent (blue, 0.001 ±0.002 min^{-1}). Both native and tagged Cdc37 are visible in the α-Cdc37^{pS13} blot. **b** Cdc37^{pS13} (3µM) was incubated with equimolar complex components (Hsp90$^{open\ dimer}$, Hsp90$^{closed\ dimer}$, Braf) and PP5 (750nM) at 25°C (n=3, rate ± SEM). Cdc37^{pS13} dephosphorylation was assayed by α-Cdc37^{pS13} blotting. There is no dephosphorylation when Braf kinase is added to the Hsp90^{open}:Cdc37^{pS13} complex (magenta, 0 min^{-1}). PP5 dephosphorylates Cdc37^{pS13} bound to Hsp90^{open} (green, 0.024 ± 0.009 min^{-1}) faster than when bound to Hsp90^{closed} (gray, 0.018 ± 0.01 min^{-1}). PP5 doesn't

dephosphorylate Cdc37^{pS13} when Hsp90 is absent (blue, 0.004 ± 0.37 min^{-1}). All Western blot data available in Supplementary Information, and quantified data available in the provided Source Data file.

PP5 becomes activated and uses Hsp90 as a dephosphorylation scaffold.

Motivated by the high levels of PP5 activity on CRaf, we set out to determine the atomic structure of PP5 dephosphorylation in action. Various steps were taken to reduce sample heterogeneity, and protect the complex from dissociation at the air-water interface: (1) Following from previous cryo-EM studies, natively isolated Hsp90^{closed}:Cdc37:CRaf complexes containing just the CRaf kinase domain (CRaf^{KD}, residues 336-618) were used, (2) the catalytically inactive PP5 mutant PP5^{H304A} was used to stabilize substrate-bound PP5 without dephosphorylating CRaf (Swingle et al., 2004; von Kriegsheim et al., 2006), and (3) the complex was chemically crosslinked and frozen on grids covered with a monolayer of graphene oxide derivatized with amino-PEG groups (Sup. Fig. 4) (Wang, Liu, et al., 2020; Wang, Yu, et al., 2020). A large single particle data set was collected and processed using cryoSPARC and RELION (Punjani et al., 2017; Scheres, 2012).

Despite having a biochemically homogeneous crosslinked sample, data processing indicated a conformationally heterogeneous complex requiring significant 3D classification and refinement yielding a 3.8 Å map (Fig. 2a). In this map, Hsp90 sidechains could be readily interpreted and more detail for Cdc37 and the kinase was observed than in our previous, lower resolution Hsp90:Cdc37:Cdk4 kinase complex structure (Verba et al., 2016). As expected from the Cdk4 kinase complex, and further seen in the recent CRaf kinase complex (García-Alonso et al., 2022), the CRaf^{KD} kinase domain in our structure was split into its distinct lobes, threaded through the Hsp90 lumen and stabilized by Cdc37. This new map shows a closed Hsp90, with the CRaf^{KD} C-lobe extending from the Hsp90 lumen on one side while the prominent Cdc37 N-

terminal coiled-coil projects away from the opposite complex surface. In the refined CRaf map we could observe the β4-strand from the kinase N-lobe bound to a groove in the $Cdc37^{MD}$ as has been shown in recent work (García-Alonso et al., 2022). Beyond these features within the kinase complex, two new densities were visible. The first sits near the Hsp90 C-terminal domains ($Hsp90^{CTD}$) and the second reaches towards the CRaf C-lobe and the Hsp90 middle domain ($Hsp90^{MD}$) of protomer A. Focused local 3D classification around the newfound densities and subsequent refinement provided higher resolution views resulting in the composite map shown in Fig. 2a (Sup. Fig. 5).

A complete atomic model (Fig. 2b) constructed using the consensus and composite maps clearly revealed a PP5 conformation quite distinct from that found in the autoinhibited crystal structure (Fig. 2c) (Das, 1998; Yang et al., 2005). Instead of sitting atop the PP5 catalytic domain active site, the PP5 TPR domain was disassociated from its catalytic domain and interacted with both $Hsp90^{CTD}$s (Sup. Movie 1). A low-resolution linker could be seen joining the two domains (Fig. 2d).

The PP5 TPR domain α7 helix made an end-on interaction with Hsp90, nestled into a groove between the two $Hsp90^{CTD}$s (Fig 2d). This interaction leads to a modest widening of the $Hsp90^{CTD}$ groove as compared to the Hsp90:Cdc37:CRaf structure (García-Alonso et al., 2022) (Sup. Fig. 6). Fitting the TPR domain from the autoinhibited PP5 crystal structure into our Hsp90 bound structure revealed slight TPR domain rearrangements, but a substantial steric clash between the PP5 catalytic domain and the kinase if the catalytic domain were to remain in this inhibited position (Fig. 2e). Therefore, Hsp90 binding to the PP5 TPR domain likely prompts TPR domain-catalytic domain reorganization and potentially drives domain separation leading to the active PP5 conformation seen here.

Surprisingly, the PP5 catalytic domain was not located near the readily dephosphorylated CRaf^{pS338} but was instead located on the opposite side of the Hsp90 dimer, with the PP5 active site facing the CRaf C-lobe. Although CRaf^{617} and CRaf^{618} are disordered in our focused maps, a CRaf low resolution mainchain density can be traced near the PP5 active site in some classes (Fig. 4d,e). This would place CRaf^{pS621} near the PP5 active site, making pS621 readily accessible for PP5 dephosphorylation. Combined with our dephosphorylation data (Fig 1a), this indicates that PP5 would be able to dephosphorylate CRaf^{pS621} while bound to Hsp90.

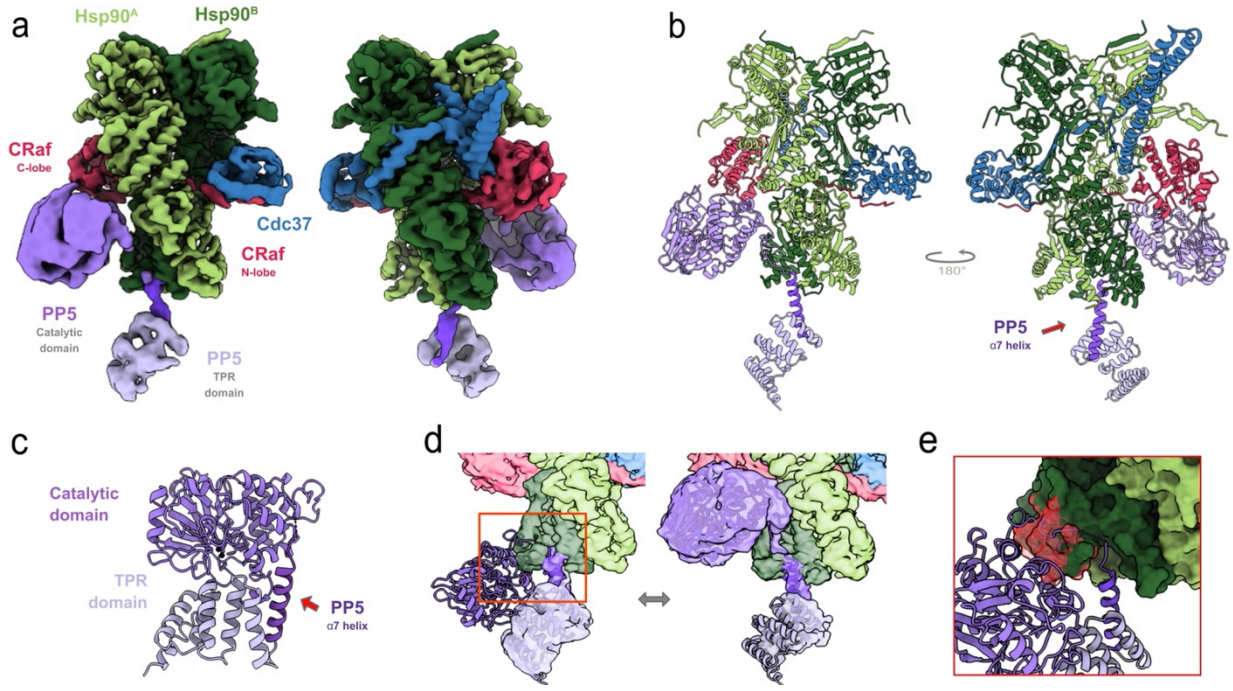

Fig. 4.2. Hsp90 activates PP5, acting as a phosphatase scaffold.

A CryoEM composite map and Hsp90:Cdc37:CRaf:PP5 complex model (b) shows unfolded CRaf kinase (magenta) threaded through the closed Hsp90 dimer lumen (green), and embraced by Cdc37 (blue). PP5 is in an active conformation as its TPR domain (lavender) interacts with the Hsp90 CTDs, while the PP5 catalytic domain (purple) is near the Hsp90^{MD} and the CRaf C-lobe. c In the PP5 crystal structure (PDB: 1WAO [PDB DOI: 10.2210/pdb1WAO/pdb]) the PP5 active site is occluded when not bound to Hsp90. D Overlaying the autoinhibited PP5 structure with the activated structure reveals PP5-Hsp90 steric clashes (e, in red) that would require rearrangement of the PP5 domain interface, possibly driving PP5 activation.

PP5's TPR domain interacts extensively with Hsp90's C-terminal domains via an extended helix.

In its activated conformation, the PP5 α7 helix bound in the amphipathic grove formed by $Hsp90^{CTD}$ helices from both protomers (Fig. 3a). Binding at this interface stabilized and elongated the C-terminal end of the α7 helix by a turn (Sup. Fig. 7b). Interactions with Hsp90 are electrostatic superficially, and hydrophobic deep within the CTD groove (Fig. 3b,c). The PP5 linker connecting the catalytic domain to the α7 helix has conserved acidic residues ($PP5^{D155}$ and $PP5^{E156}$) that lie in close proximity to $Hsp90^{R679}$ and $Hsp90^{R682}$ (Fig. 3c, Sup. Fig. 7d), stabilizing the α7 helix within the Hsp90 amphipathic groove. Here, the $PP5^{F148}$ and $PP5^{I152}$ residues which were solvent exposed and disordered in the PP5 autoinhibited state (Sup. Fig. 7a), were stabilized by Hsp90 hydrophobic residues ($Hsp90^{A}$: L638, L654, L657 and $Hsp90^{B}$: I680, I684, M683, L686) (Fig. 3d).

Density corresponding to the $Hsp90^{A}$ tail can be seen extending beyond the last $Hsp90^{CTD}$ α helix towards the PP5 TPR domain (Fig. 3d). While poorly resolved, the charge complementarity between the $Hsp90^{A}$ tail ($Hsp90^{D691-E694}$) and basic residues on the PP5 TPR domain ($PP5^{R150}$, $PP5^{R113}$, $PP5^{R117}$) suggest that Hsp90 and PP5 interact beyond the α7 helix (Fig. 3e). This electrostatic interaction may guide the Hsp90 tail towards the PP5 MEEVD binding site, for which heterogeneous density is visible in our map (Sup. Fig. 7e).

The "entrance" for the TPR α7 helix on the Hsp90 CTD pyramidal groove measures approximately 13 Å wide when Hsp90 is in a closed position, but contracts by almost 3 Å when Hsp90 is in the Hsp90 partially open conformation found in the Hsp90:Hsp70:Hop:GR client

loading state (Sup. Fig. 6) (Wang et al., 2022). This suggests that PP5 binding might be substantially weaker in the fully open apo state or the partially open client loading state.

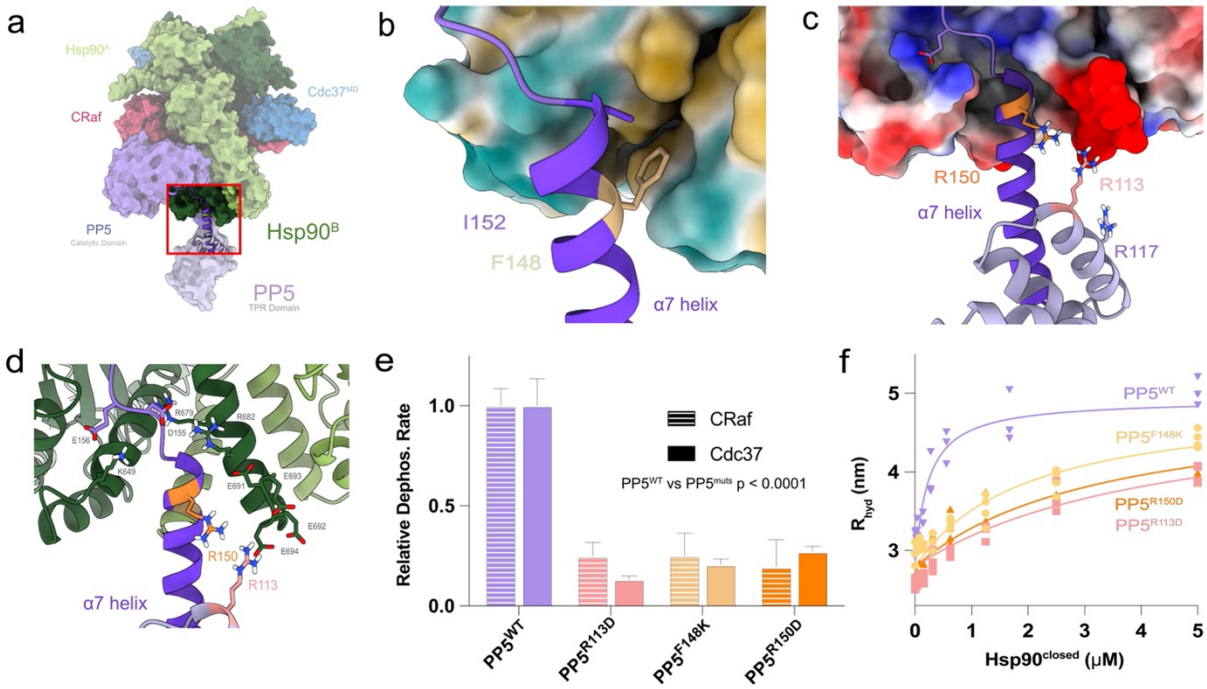

Fig. 4.3. Distinct TPR a7 helix – Hsp90 C-terminal domain interaction mode.

a The PP5 TPR domain interacts with the amphipathic Hsp90 dimer C-terminal groove. **b** Hydrophobic residues $PP5^{F148}$ and $PP5^{I152}$ bind the Hsp90 hydrophobic CTD groove, while (**c, d**) $PP5^{R113}$ and $PP5^{R150}$ electrostatically interact with the Hsp90 acidic tail. **e** Mutations to key TPR residues significantly decrease PP5 dephosphorylation of both $Cdc37^{pS13}$ and $CRaf^{pS338}$ substrates (mean rates ± SEM (min^{-1}) reported, CRaf: $PP5^{WT}$ = 0.19 ± 0.016, $PP5^{R113D}$ = 0.046 ± 0.013, $PP5^{F148K}$ = 0.05 ± 0.02, $PP5^{R150D}$ = 0.04 ± 0.03, Cdc37: $PP5^{WT}$ = 0.043 ± 0.006, $PP5^{R113D}$ = 0.006 ± 0.001, $PP5^{F148K}$ = 0.009 ± 0.001, $PP5^{R150D}$=0.012 ± 0.001). The differences between PP5 mutants and $PP5^{WT}$ were significant in an Ordinary one-way ANOVA (CRaf: n=3, $p < 0.0001$; Cdc37: $n^{mutants}$=3, n^{WT}=4, $p < 0.0001$) with a Dunnett test for multiple hypothesis testing ($PP5^{WT}$ vs $PP5^{muts}$ $p < 0.0001$). **f** Mutations to key TPR residues decrease $Hsp90^{closed}$:PP5 complex formation measured by FCS hydrodynamic radius. $Hsp90^{closed}$ dimer concentrations were used for K_D evaluation. Hsp90:PP5 K_D's were solved by nonlinear regression, (K_D ± SEM (μM) reported, $n^{mutants}$=4, n^{WT}=3: $PP5^{WT}$ = 0.23 ± 0.04; $PP5^{R113D}$ =4.3 ± 0.8; $PP5^{F148K}$ = 2.0 ± 0.4; $PP5^{R150D}$ = 3.3 ± 0.6). R_{hyd}max and R_{hyd}PP5 were fit globally, an Ordinary one-way ANOVA showed significant differences (F = 9.8, $p < 0.0001$) with a Dunnett's multiple hypothesis test for comparison of individual interactions ($PP5^{WT}$ vs $PP5^{F148K}$ p = 0.09, vs $PP5^{R113D}$ p = <0.0001, vs $PP5^{R150D}$ p = 0.0006). Source data are provided as a Source Data file.

To determine the functional significance of the PP5-Hsp90^{CTD} interactions observed here, we mutated three key residues (PP5^{R113D}, PP5^{F148K}, PP5^{R150D}) and assessed their impact on both CRaf^{pS338} and Hsp90^{open}:Cdc37^{pS13} dephosphorylation (Fig. 3e and Sup. Figs. 7a, 8). All three individual mutations led to ~3-fold reduction in dephosphorylation rate for CRaf^{pS338} and a greater impairment for Hsp90^{open}:Cdc37^{pS13} . We next tested the binding of each PP5 mutant to increasing concentrations of closed Hsp90 dimers through Fluorescence Correlation Spectroscopy (Fig. 3f). All three mutations led to a decrease in Hsp90^{closed}:PP5 complex formation, with an approximate 8-fold decrease in Hsp90^{closed}:PP5 binding affinity. These findings confirm the broad importance of the PP5^{TPR}-Hsp90 interaction for substrate dephosphorylation, and suggest similar Hsp90^{CTD}:PP5^{TPR} interfaces are used during dephosphorylation of both Hsp90^{open}:Cdc37^{pS13} and Hsp90:Cdc37:CRaf complexes.

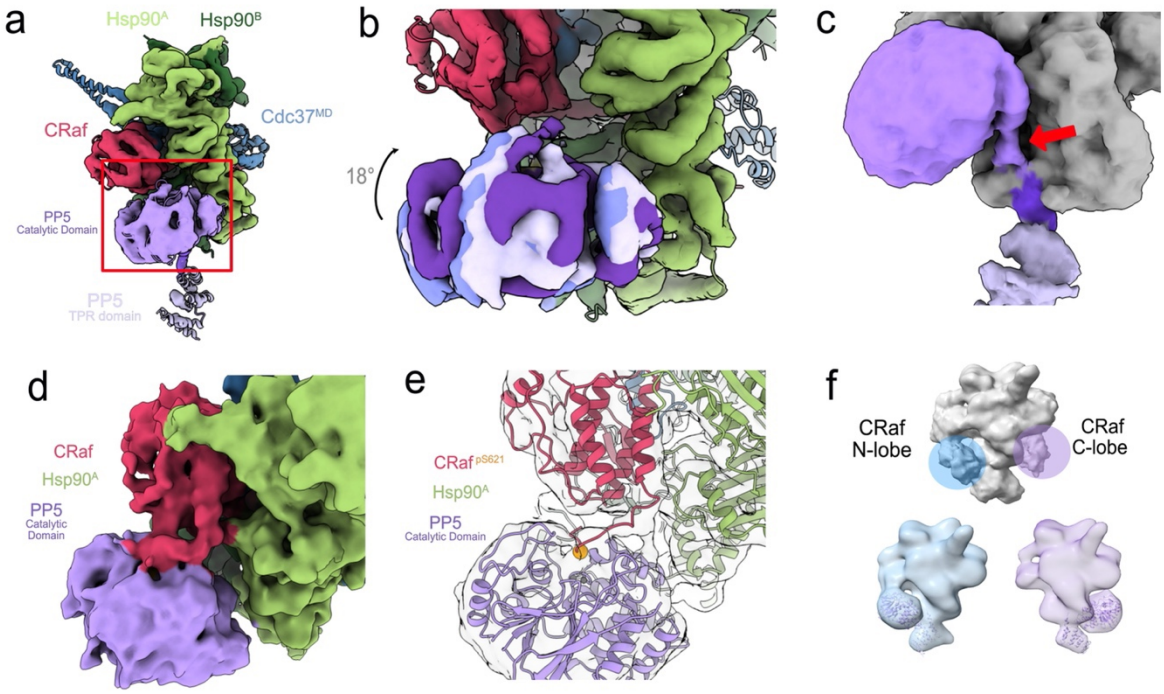

Fig. 4.4. Heterogeneous PP5 catalytic domain in position for CRaf^{pS621} dephosphorylation.

a The PP5 catalytic domain sits by Hsp90^{MD} allowing for CRaf kinase dephosphorylation. **b** Multiple PP5 conformations can be teased apart through focused classification. Anchored by its TPR domain, PP5 is flexibly held

in proximity to the CRaf^{pS621}. **C** In some classes, the PP5 linker can be seen leaving the Hsp90 CTD groove and leading up to the PP5 active site. **d** A frame from a 3D variability analysis movie (Sup. Movie 3) shows density spanning between the C-terminus of CRaf and the PP5 active site. **e** Focused classification of the interface between the CRaf C-lobe and the catalytic domain yields a similar class. A model was fit based on the substrate bound PP5 crystal structure (PDB: 5HPE [PDB DOI: 10.2210/pdb5HPE/pdb]) to show how CRaf^{pS621} substrate may be positioned right at the PP5 active site. **f** Low resolution volumes from the longer Hsp90:Cdc37:CRaf$^{304-648\ S338E}$:PP5 $^{\alpha J\ del}$ complex used in the biochemical experiments shows density for the PP5 catalytic domain interacting with both the CRaf N-lobe and the C-Raf C-lobe multiple PP5 orientations. The heterogeneity seen in the upper panel (gray) can be resolved into complexes having either the N-terminal or C-terminal interactions (bottom, purple and blue).

Hsp90 positions the PP5 catalytic domain to efficiently dephosphorylate CRaf^{pS621}.

While the PP5 catalytic domain is readily visible in our maps (Fig. 4a), the limited Hsp90^{MD}:PP5 interface size (< ~330 Å^2) and the multiple conformations of PP5 seen through 3D local classification and 3D variability analysis (Fig. 4b, Sup. Movie 2) suggest that the catalytic domain is only weakly stabilized by the Hsp90:kinase complex (Punjani & Fleet, 2021). Localization is likely aided by tethering of the PP5 catalytic domain to the strongly bound TPR domain and by interactions between the catalytic domain and its CRaf substrate.

In our high-resolution structure, the PP5 active site faces towards the CRaf C-lobe. While the PP5 catalytic domain can be easily visualized, density near the PP5 active site is quite heterogeneous. 3D variability analysis (Sup. Movie 3) was performed on the PP5 containing particles, which led to the visualization of density extending from the C-terminal CRaf alpha helix towards the PP5 active site (Fig. 4d). Further focused classification of the CRaf:PP5 interface revealed a class with continuous density extending from the last well resolved helical residue in the CRaf C-terminus (CRaf^{616}) to within 8 Å of the PP5 active site (Fig. 4e). While our sample doesn't demonstrate the CRaf^{pS621} dephosphorylation, a plausible model was constructed

based on the covalently bound PP5:substrate crystal structure (PDB: 5HPE [PDB DOI: 10.2210/pdb5HPE/pdb]).

While heterogeneous density existed on the N-lobe region of CRaf, no high-resolution classes could be seen in which the PP5 catalytic domain interacted with the CRaf N-lobe. We suggest this is a consequence of using the truncated $CRaf^{KD}$ construct for our cryo-EM studies, whereas the longer $CRaf^{304-648}$ construct was used in the biochemical experiments. Thus, visualization of a stable PP5 binding to the N-terminal CRaf substrate might necessitate a more stably interacting CRaf N-lobe. This suggests that the residues N-terminal to the C-terminal tail may stabilize the CRaf:PP5 catalytic domain interaction, while the residues C-terminal to the $CRaf^{pS338}$ site in our construct may not be sufficient for stable PP5 interaction. To test this hypothesis, a new sample was prepared which included the longer CRaf construct, a glutamic acid in the place of the pS338 phosphoserine, and a more activatable PP5 construct with a truncated αJ helix (see below). This Hsp90:Cdc37: $CRaf^{304-648}$:$PP5^{\alpha J\ del}$ sample was prepared as outlined previously (Sup. Fig. 4) and a limited dataset collected.

Although significantly fewer particles were available, 3D classification of this new dataset immediately demonstrated two distinct TPR orientations and catalytic domain density on either side of the Hsp90 dimer. Further focused classification yielded low-resolution maps having the catalytic domain either in close proximity to the C-lobe as seen previously, or as predicted, in close proximity to the CRaf N-lobe (Fig. 4f).

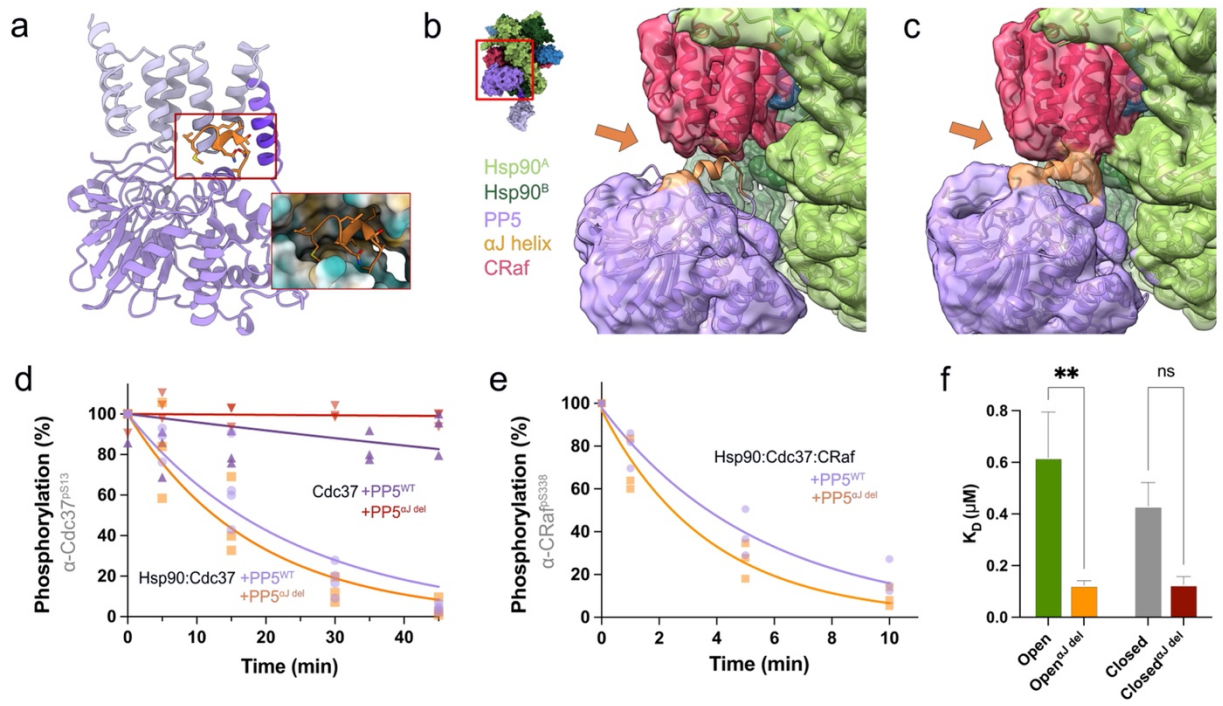

Fig. 4.5. Deletion of PP5's aJ helix increases rate of dephosphorylation.

a In its inhibited conformation, the PP5 αJ helix (orange) lies at the hydrophobic interface between the PP5 catalytic and TPR domains. **b** While initial focused classification around PP5 showed no αJ helix density, **c** further classification showed potential αJ helix density near the PP5 catalytic domain. **d** PP5 $^{\alpha J\ del}$ does not dephosphorylate Cdc37 without Hsp90 present (Rates ± S.E.M. reported (min^{-1}), 0.0 ± 0.0), but PP5$^{\alpha J\ del}$ dephosphorylates Cdc37 while bound to Hsp90 at a slightly higher rate than PP5^{WT} (0.055 ± 0.007 vs 0.043 ± 0.006). An Ordinary one-way ANOVA found differences significant ($F = 29.40$, $p < 0.0001$), while Dunnett's multiple comparisons test showed significance between Hsp90-free complexes and Hsp90:PP5^{WT} complexes ($p < 0.0001$), but not between PP5 $^{\alpha J\ del}$ and PP5^{WT} (0.055 ± 0.007 and 0.043 ± 0.006, $p = 0.17$). **e** PP5 $^{\alpha J\ del}$ led to a slight increase in CRaf^{pS338} dephosphorylation as compared to PP5^{WT} (0.28 ± 0.03 vs 0.187 ± 0.016 min^{-1}, two-tailed unpaired t-test: $t = 2.9$, d.f. = 20, $p = 0.009$). **f** The binding affinity of fluorescently labelled PP5^{WT} or PP5 $^{\alpha J\ del}$ to Hsp90^{open} or Hsp90^{closed} was measured through FCS (n=3, K_D ± S.E.M. (μM) reported). Significant difference between the K_D's of PP5^{WT} and PP5 $^{\alpha J\ del}$ to Hsp90^{open} and Hsp90^{closed} was found in a an Ordinary one-way ANOVA ($F = 5.3$, $p = 0.002$), with a Šídák's multiple comparisons test comparing individual interactions (Hsp90^{open}:PP5^{WT} vs PP5$^{\alpha J\ del}$ = 0.62 ± 0.17 vs 0.12 ± 0.018, $p = 0.0022$ and Hsp90^{closed}:PP5^{WT} vs PP5$^{\alpha J\ del}$ = 0.43 ± 0.09 vs 0.13±0.03, $p = 0.11$). Source data has been provided as a Source Data file.

PP5$^{\alpha J\ helix}$ is displaced upon interaction with Hsp90:Cdc37:CRaf complex

The PP5 C-terminal αJ helix (orange) makes stabilizing interdomain interactions in the autoinhibited PP5 crystal structure (Fig. 5a). Focused classification with of the PP5 catalytic domain yielded a class of Hsp90:PP5 complexes in which no αJ helix density could be visualized (Fig. 5b). Further focused classification from this particle stack yielded one smaller class with potential low-resolution density for the αJ helix (Fig. 5b, orange). This low-resolution density also connects to the CRaf C-terminal tail and the PP5 catalytic domain. This is likely a superposition of density corresponding to an ordered αJ helix and another for the CRaf C-terminal tail. Given the small number of particles, it was not possible to further resolve this density. Previous work has suggested that the αJ helix rearranges and becomes disordered upon PP5 activation (Oberoi et al., 2016; Yang et al., 2005).

From these observations we hypothesize that removal of the αJ helix would help activate PP5. To test this, we truncated the last 10 residues of PP5 (PP5$^{\alpha J\ del}$). As shown in Fig 5c, deletion of the αJ helix was insufficient to activate PP5 in the absence of Hsp90 (Fig. 5c). However, PP5$^{\alpha J\ del}$ did lead to a slight increase in the rates of CRaf^{pS338} and Cdc37^{pS13} dephosphorylation in the context of the relevant Hsp90 complexes.

To test whether this increase in dephosphorylation rate was due to a higher Hsp90:PP5 affinity, we compared the binding affinities of trace fluorescent PP5 to PP5 $^{\alpha J\ del}$ in the context of Hsp90^{open} and Hsp90^{closed}. As predicted, a sharp drop in apparent K_D was seen upon deleting the αJ helix, a finding which correlates well to Hsp90:PP5 and Hsp90:PP5 $^{\alpha J\ del}$ sizing traces (Sup. Fig. 9). These results suggest that the αJ helix is primarily involved in stabilizing the closed and inactive PP5 conformation, rather than being involved in Hsp90 binding. Thus, its role is to stabilize the autoinhibited state, minimizing dephosphorylation from free PP5.

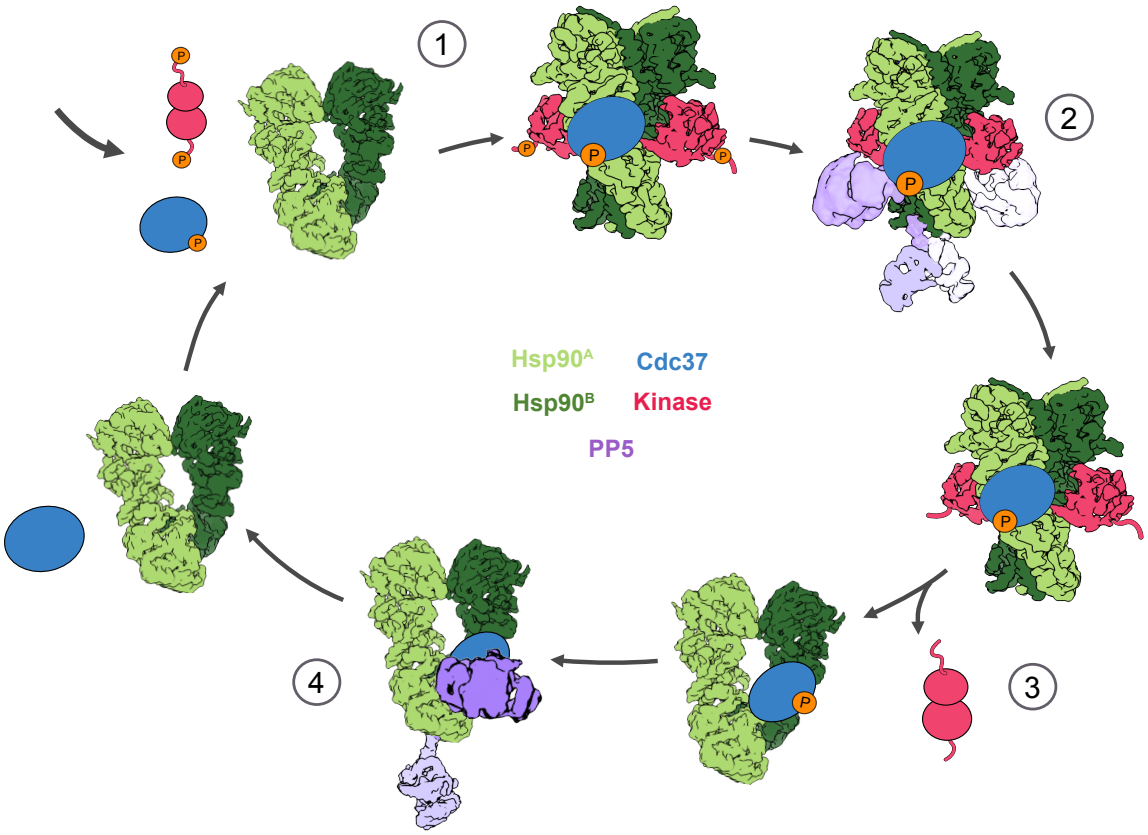

Fig. 4.6. Model of PP5's role in kinase and Cdc37 dephosphorylation.

Steric blocking of Cdc37^{pS13} dephosphorylation by kinase clients suggests that Cdc37 can only be dephosphorylated once the kinase has exited the Hsp90 complex. Our model goes as follows: (1) Cdc37^{pS13} first recruits the kinase to Hsp90 for folding or modification. (2) PP5 can then dephosphorylate CRaf, binding to Hsp90 in either direction to allow for the removal of phosphate groups on either side of the Hsp90-bound kinase. (3) After dephosphorylation of CRaf and potential conformational modifications by Hsp90, the phosphorylation free kinase can be released. (4) As the kinase is released from Hsp90, Cdc37^{pS13} may remain bound to Hsp90 until it's dephosphorylated by PP5. This would allow for a unidirectional Hsp90-kinase cycle.

Discussion

PP5 is a unique member of the PPP family of phosphatases in that it contains a catalytic domain and a regulatory substrate-targeting TPR domain within the same protein (Golden et al.,

2008). Hsp90 offers PP5 the benefits of increased regulation and productive substrate positioning. In some cases, Hsp90 may even unfold the client, exposing phosphorylation sites that would otherwise be inaccessible.

PP5 has been shown to act as a negative regulator of numerous Hsp90 clients, including ASK1 kinase in oxidative stress, ATM kinase in DNA double strand break stress, and Chk1 kinase in UV induced stress (Ali et al., 2004; Amable et al., 2011; Morita et al., 2001). Not limited to kinases, PP5 also inactivates other Hsp90 clients such as Hsf1, p53 and the glucocorticoid receptor in an Hsp90 dependent manner (Conde et al., 2005; Zuo et al., 1998; Zuo et al., 1999).

We set out to understand how Hsp90 activates PP5, and how Hsp90 can help position PP5 for efficient client dephosphorylation. Our Hsp90:Cdc37:CRaf^{KD}:PP5 complex structure illustrates the molecular mechanism underlying both of these activities. The PP5 TPR and catalytic domains are separately bound to Hsp90, liberating the PP5 active site for activity and placing the phosphatase domain near its substrates. The PP5 TPR domain facilitates this by uniquely binding its α7 helix within the Hsp90^{CTD} groove. While the same Hsp90 groove is used to bind to the TPR containing Fkbp51 and Fkbp52 cochaperones (Sup. Fig. 6d-i) (Lee et al., 2021), the specialized PP5 α7 helix lies parallel to the Hsp90 dimer axis, rotated almost 90° from the α7 helix orientation seen in the Hsp90:Fkbp51/52 complexes (Lee et al., 2021; Noddings et al., 2023).

The PP5 catalytic domain approaches the CRaf C-lobe, where the CRaf^{pS621} phosphosite can be dephosphorylated by PP5. While the shorter CRaf^{KD} likely precluded the visualization of PP5:CRaf^{pS338} interactions in our structure, the use of the longer CRaf$^{304-648}$ construct in our activity assays demonstrates efficient dephosphorylation of both CRaf^{pS338} and CRaf^{pS621} by PP5.

From this we suggest that the catalytic domain could alternatively bind to the opposite site on the $Hsp90^{B}$ protomer, positioning it near the CRaf N-lobe. This is supported by low resolution cryo-EM densities showing that PP5 can orient itself on either face of Hsp90 and reach both ends of the scaffolded substrate (Figs. 4f, 6). This work was corroborated by recent work by Oberoi et al which uses mass spectrometry to show how PP5 can dephosphorylate a substantial number of phosphorylation sites both N-terminal and C-terminal to the BRaf kinase domain (Oberoi et al., 2022).

While our work clearly implicates PP5 in both $CRaf^{pS338}$ dependent inactivation, and in the dephosphorylation of CRaf's "maturity marker", $CRaf^{pS621}$ (Dhillon et al., 2009) , we note that PP5 only minimally alters $CRaf^{pS621}$ levels in vivo (von Kriegsheim et al., 2006). This could be due to the lack of specific inhibitory factors or more rapid re-phosphorylation of $CRaf^{pS621}$. Additional studies are clearly called for.

Surprisingly, while previous work showed that $Cdc37^{pS13}$ could be dephosphorylated by PP5 (Vaughan et al., 2008), this was not the case in our molybdate stabilized $Hsp90^{closed}$:Cdc37:CRaf complexes. The phosphate on $Cdc37^{pS13}$ makes important Cdc37:Hsp90 stabilizing interactions in the various $Hsp90^{closed}$:Cdc37:Kinase structures acquired to date (García-Alonso et al., 2022; Verba et al., 2016). These interactions render $Cdc37^{pS13}$ inaccessible to PP5 dephosphorylation and explain our current results. Additionally, our current structure and biochemistry shows that the removal of the bound kinase, or a large rearrangement of Cdc37 would be required for PP5 to reach the phosphorylation site on Cdc37.

Previous results in which Cdc37 is dephosphorylated by PP5 may be explained by complex dissociation due to longer reaction times at elevated temperatures. Indeed, in our hands, longer

experimental timeframes and higher temperatures led to both Cdc37^{pS13} dephosphorylation and complex dissociation (Sup. Fig. 3).

In our experiments, kinases sterically block the dephosphorylation of Cdc37 by PP5. This negates the hypothesis that PP5 can dephosphorylate Cdc37 in an Hsp90:Cdc37:kinase complex, leading to kinase release. Instead, we propose a model in which PP5 only dephosphorylates Cdc37 once the kinase has been released, thereby resetting Cdc37^{pS13} phosphorylation and preventing immediate kinase re-recruitment (Fig. 6). This would enhance directionality to the Hsp90-kinase cycle and allow Hsp90 to release the dephosphorylated kinase in a reset "basal" phosphorylation state.

In summary, Hsp90's role in maintaining protein homeostasis goes beyond folding and activation to include facilitating client post-translational modification. Through the Hsp90:Cdc37:CRaf^{KD}:PP5 cryo-EM structure, we further understand how Hsp90 activates PP5 and provides a scaffold for substrate dephosphorylation. Our biochemistry efforts suggest that PP5 may directly reset kinase dephosphorylation, while influencing Cdc37's kinase recruitment to Hsp90. Further work will be required to provide a more complete mechanistic description of Cdc37^{pS13} dephosphorylation.

Methods

Data analysis and figure preparation

All figures were assembled using Affinity Designer v1.10.5. UCSF ChimeraX v.1.2.5 was used to render the structural data included in our figures(Goddard et al., 2018; Pettersen et al., 2021). All graphs and charts were created using Prism v.9.3.1 (GraphPad).

The western blot data was quantified using ImageJ 1.53k(Schneider et al., 2012), and moved into Prism for further normalization to a PP5 free control (100%) and analysis. The data was displayed and fit to a one-phase decay model (Y_0= 100%, Plateau = 0%) to obtain a decay rate (K min^{-1}). These rates were then statistically compared in Prism (Ordinary one-way ANOVA test, two-tailed One sample t and Wilcoxson test). PP5 mutant dephosphorylation rates were normalized to wild type PP5 dephosphorylation rates to simplify reader analysis.

The CorTector SX100 Fluorescence Correlation Spectroscopy (FCS) data analysis software Correlation Analysis (v.3.5.010722, LightEdge Technologies, Beijing, China) was used to analyze the FCS data. Data was curated, removing large fluorescent outliers from the single molecule data. The means of the calculated radii of hydration (R_{hyd}) were then further analyzed using Prism v.9.3.1 (GraphPad). Triplicate data was averaged, plotted, and the K_D parameter was fit using a One site Total binding model. Ordinary one-way ANOVA's were used to test for difference in K_D's.

Individual component expression and purification

The Hsp90, Cdc37, PP5, and BRaf plasmids were transfected into *E. coli* BL21 cells, and plated on antibiotic agarose plates. Overnight cultures of one colony were grown in Terrific Broth media (TB media), after which 10 mL of culture were transferred into 2-6 L of TB media. Once the cultures grew to an $O.D._{600}$ of 0.6, cells were allowed to shake (180 R.P.M.) at 16°C for an hour after which they were induced with 1 mM IPTG. The temperature of the cultures was then raised to 18°C and allowed to shake overnight (160 R.P.M.). The pellets were then spun down (4,500 xg for 10 min) and frozen until protein purification.

The thawed pellets were then resuspended with Lysis Buffer (500 mM NaCl, 50 mM Tris pH 7.8, 5% Imidazole, 5% glycerol, 1 Protease Inhibitor Tablet / 50 mL of pellet suspension, 0.5 mM TCEP), and the sample was sonicated in an ice bath for five cycles, 1 minute/cycle, with at least a minute between cycles. The sample was then spun down at 35,000 xg for 30 min at 4°C. The lysate was then run through HisTrap FF (5mL) Nickel columns (1-2 columns) at 5 ml/min. The column was loaded onto an AKTA FPLC instrument and washed with Wash Buffer (50 mM Tris pH 7.8, 250 mM NaCl, 0.5 mM TCEP, 5% glycerol, 30 mM Imidazole, PP5 buffer included 1 mM Manganese), and then eluted with Elution Buffer (Wash Buffer with 10% glycerol and 400 mM Imidazole). The purified lysate was then concentrated down to 5-7 mL of lysate using a Centricon tube, and subsequently cleaved overnight (3C or TEV depending on plasmid).

The cleaved sample was diluted down to ~50 mL using Low Salt Buffer (20 mM Tris pH 8.0, 1mM EDTA, 0.5 mM TCEP, 5% Glycerol, PP5 buffer included 1mM Manganese), filtered, and loaded onto a 50 mL superloop. This sample was then run through an AKTA FPLC MonoQ 10/100 column (Cytiva), eluting through a salt gradient (0-1 M NaCl). An SDS PAGE Gel was run to select the peaks of interest, which were isolated and concentrated down to ~250 μL. The sample was then filtered and loaded onto a Superdex 200 16/600 (Cytiva) column in Storage Buffer (20 mM Hepes, 150 mM KCl, 1 mM EDTA, 1 mM TCEP, 5% glycerol). The cleanest protein fractions as dictated by an SDS PAGE Gel were concentrated and flash frozen in liquid nitrogen for storage at -80°C.

BRaf purification was slightly modified to improve kinase solubility: 0.75% IGEPAL was added to the Lysis Buffer, 20 mM HEPES was used instead of 20 mM Tris throughout the purification, and 10% Glycerol was used. BRaf was not cleaved overnight, and so the purification process took place in one day.

Complex expression and purification

Hsp90:Cdc37:CRaf complexes were purified from either yeast (sample used for main Hsp90:Cdc37:CRaf:PP5 structure) or mammalian cells (sample used for biochemistry and low resolution structure).

Yeast expression: Constructs were cloned into a 83 nu yeast expression vector, and transformed into JEL1 yeast strain using Zymo Research EZ transformation protocol and plated onto SD-His plates. After 3 days a colony was expanded into 200 mL overnight cultures. 1 L of YPGL media was inculcated with 10 mL of overnight culture. Cultures were induced with 2 % w/v galactose at an $O.D._{600}$ of 0.6 – 0.8 to induce expression. Temperature was reduced to 16°C and cultures were pelleted after 18 hours (4,500 xg for 5 min). Pellets were resuspended in minimal yeast resuspension buffer (20 mM HEPES-KOH pH 7.5, 150 mM KCl, 10% glycerol) and frozen drop wise into a container of liquid nitrogen.

Mammalian expression: Constructs were cloned into a pcDNA3.1 expression vector. Mammalian HEK293 cells were seeded at 0.5 M/mL and allowed to reach a confluency of 3 M/mL. Media was exchanged three hours before transfection and cells were allowed to recover. The Expi293™ Expression system kit and protocol was used for transformation. Cells were allowed to grow for 48 - 72 hours before they were spun down at 5,000 xg, reconstituted with PBS and frozen dropwise into liquid nitrogen.

The frozen yeast or mammalian cell drops were then ground in a cryoMill for 5 cycles (Precool 5 min, Run 1:30 min, Cool 2 min, 10 cps Rate). The samples were reconstituted with Strep Binding Buffer (20 mM HEPES, 150 mM KCl, 10 mM MgCl, 1 mM TCEP, 10% glycerol, 0.05% Tween) with NaMo (20 mM) added when purifying the more stable “closed” Hsp90

complex. The sample was loaded onto a StrepTrap HP (Cytiva, 5 mL) column at a rate of 5 ml/min and subsequently washed with 20 mL of Strep Binding Buffer in an AKTA FPLC instrument at a flow rate of 5 ml/min and then eluted with 10 mL of Elution Buffer (Strep Binding Buffer with 10 mM Desthiobiotin). The elution fractions were then concentrated down to 250 μL and loaded onto the Superdex 200 16/600 (Cytiva) column. After running the sample through the column using Storage Buffer (20 mM Hepes, 150 mM KCl, 1 mM EDTA, 1 mM TCEP, 5% glycerol), and SDS PAGE Gel was run to choose the peak to be concentrated, flash frozen with liquid nitrogen and finally stored at -80°C.

Dephosphorylation Assays

PP5 Dephosphorylation reactions were carried out in Reaction Buffer (20 mM Hepes, 50 mM KCl, 10 mM Mg2Cl, 1 mM TCEP, 1 mM EDTA) in PCR tubes. Buffer exchanged Hsp90:Cdc37:CRaf, Hsp90:Cdc37, $Hsp90^{Open}$ or $Hsp90^{Closed}$ complexes were placed on a 25°C thermocycler (~1 min) before PP5 addition. The reaction began after PP5 was added and the sample was thoroughly mixed. Sample was removed from the thermocycler at each timepoint, and the reaction was quenched using SDS-DTT. Each reaction was repeated at least three distinct times with newly prepared sample. Dephosphorylation conditions were optimized such that the PP5 concentrations used were ideal for western blot visualization. 3 μM of $Cdc37^{pS13}$ and equimolar constituents were used for Cdc37 blots, with a final addition of 750nM of $PP5^{WT}$ or $PP5^{mutant}$. 1.5 μM of Hsp90:Cdc37:CRaf complex with 75 nM of PP5 were used for Fig. 1 experiments, while 3 μM of Hsp90:Cdc37:CRaf complex and 150 nM PP5 were used for $PP5^{mutant}$ experiments.

The samples were run on Bolt™ 4-12% Bis-Tris gels (140 V, 65 min) using the Color Protein Standard, (NEB# P7712, Broad Range (10-250 kDa)) for molecular weight differentiation. The gels were next transferred using Invitrogen's iBlot® Gel Transfer Stacks (Nitrocellulose), following the transfer kit protocol (10 min transfer) and then stained with Ponzo stain for ~5 min to ensure equal protein transfer and constant protein concentrations (Sup. Figs. 2, 9). The membranes were then incubated with 5% milk on a room temperature nutator for one hour. Primary antibodies against $Cdc37^{pS13}$ (1:5000 Phospho-CDC37 (Ser13) (D8P8F) Rabbit mAb #13248), $CRaf^{pS338}$ (1:1000, # MA5-15176 Phospho-c-Raf (Ser338) Monoclonal Antibody(E.838.4)) or $CRaf^{pS621}$(1:1000, #MA5-33196 Phospho-c-Raf (Ser621) Recombinant Rabbit Monoclonal Antibody) were then added to the membrane with 5% milk and nutated overnight at 4°C. The membrane was next washed with TBST (80mM Tris Base, 550mM NaCl, 1% Tween 20 (v/w)) three times, 15 min/wash. HRP Secondary antibody was then added to the membrane (1:10000, Anti-Rabbit NA9340V GE Healthcare UK Limited) and allowed to incubate on a nutator for 1h at RT. Next, the membrane was washed three times with TBST for 15 min/wash and exposed using the Thermofisher protocol and chemiluminescent agents (Pierce™ ECL Western Blotting Substrate, Catalog number: 32109).

An Azure biosystems imager was used to capture ponzo and chemiluminescence Western Blot images. The images were then analyzed using the ImageJ software(Schneider et al., 2012). Each sample was run at least three separate times to ensure replicability. The western blots were then normalized by the phosphorylated control sample (not incubated with PP5) using the Prism software. A one-phase linear decay curve was fit to dephosphorylation vs time data, and the rates

of decay were compared using an ordinary one-way ANOVA test within Prism. Multiple hypothesis testing was carried out within Prism. For visualization purposes, dephosphorylation rates for mutants were normalized to wiltype rates. All these values were then plotted with standard error of the mean error bars.

Hsp90:Cdc37:CRaf^{KD}:PP5 CryoEM Sample Preparation

Yeast purified Hsp90:Cdc37:CRaf$^{336-618}$ complex was incubated with PP5^{H304A} for 30 min on ice, then brought to room temperature and mixed with 0.05% glutaraldehyde (15 min). The reaction was quenched with 50 mM Tris buffer pH 8. The sample was then filtered (PVDF 0.1μm), and 25 μL of sample was injected into the Ettan liquid chromatography system, where it ran through the Superdex 200 3.2/200 column (Cytiva) in running buffer (20mM Hepes pH 7.5, 50mM KCl, 1mM EDTA and 1mM TCEP). The fractions with Hsp90:Cdc37:CRaf:PP5^{H304A} complex were separated from the PP5 excess, concentrated to ~300nM and added to grids (Quantifoil R1.2/1.3, gold, covered with a monolayer of graphene oxide derivatized with amino-PEG groups) in a FEI Vitrobot chamber (3μL of sample, 10°C, 100% humidity, 30s Wait Time, 3s Blot Time, -2 Blot Force) and plunged into liquid ethane (Wang, Liu, et al., 2020; Wang, Yu, et al., 2020). Frozen grids were then stored in liquid nitrogen.

CryoEM data acquisition and data processing

4160 micrographs were collected using SerialEM v.3.8-beta at 105,000X magnification on a Titan Krios G3 (Thermo Fischer Scientific) with a Gatan K2 camera (0.835 Å/pix pixel size) at -

0.8--1.8 μm defocus, 16 e-/pix*s, 0.025 sec/frame, per frame dose of 0.57e/A^2*frame accumulating to a total dose of 69 $e^-/Å^2$.

The micrographs were motion corrected using UCSF Motioncor2, and their CTF estimated using CTFFIND-4.1 (Rohou & Grigorieff, 2015; Zheng et al., 2017). Only micrographs with a CTF fit <5Å were kept for gaussian blob autopicking in the cryoSPARC software (v.3.3.2). The particles were then 2D classified to remove high-resolution artifact particles, while the rest of the classes were kept for the next round of classification (Punjani et al., 2017). The particles were then exported from cryoSPARC using csparc2star (Asarnow et al., 2019). The coordinates were used to re-extract particles in the RELION software (v.3.1.3), where 3D classification took place(Scheres, 2012). An Hsp90:Cdc37:Cdk4 C-lobe model (low pass filtered from PDB: 5FWK [PDB DOI: 10.2210/pdb5FWK/pdb]) was used for classification and refinement.

After one round of binned 3D classification, a particle stack of approximately 1M Hsp90-like particles was further refined and then unbinned to yield a high resolution Hsp90 map. Masks were created to subtract regions of interest around Hsp90, and those subtracted stacks were focused classified without alignment. Classes of interest were un-subtracted and refined, and the process was continued iteratively until no improvement in resolution was seen. Subsequently, cycles of post-processing, per particle CTF refinement and refinement were repeated until no there was no resolution improvement.

Model building and refinement

Hsp90:Cdc37:kinase cryo-EM structures (PDB: 5FWK [PDB DOI: 10.2210/pdb5FWK/pdb], unpublished D. Coutandin) and PP5 crystal structures (PDB: 1WAO [PDB DOI: 10.2210/pdb1WAO/pdb], 5HPE[PDB DOI: 10.2210/pdb5HPE/pdb], 1S95 [PDB DOI: 10.2210/pdb1S95/pdb]) were used for model building. The PP5 linker was built using

RosettaCM after whole domain docking of both PP5 domains (Song et al., 2013; Wang et al., 2016). The Cdc37^{MD} model from PDB model 5FWK [PDB DOI: 10.2210/pdb5FWK/pdb] was improved by rebuilding Cdc37 using RosettaCM and ISOLDE (Croll, 2018). PhenixRefine was used after model docking/building (Liebschner et al., 2019), and RosettaRelax was used to model lower resolution parts of the model. ISOLDE (v.1.2) was finally used to improve clashes, Ramachandran outliers, and rotamer fits. Different B-factor sharpened maps were used to build the models depending on different resolution areas on the map.

FCS binding assays

E. coli purified PP5 (~50 μM) was incubated with 0.8X malemide Alexa488 dye for ~6 hours at 4°C on a nutator. The sample was then buffer exchanged using a 7MWCO Zeba^{TM} Spin Desalting Column, and subsequently purified using a Superdex 200 3.2/300 column (Cytiva). The dilute sample was then aliquoted and flash frozen in liquid nitrogen for future use.

The thawed sample was spun down to remove aggregates and added at a constant final concentration of ~20 nM to varying concentrations of Hsp90^{open}, Hsp90^{closed}, Hsp90:Cdc37, or Hsp90:Cdc37:CRaf$^{304-648}$. Samples were placed on microscope cover glass slides (High Precision, Deckgläser 22 x 22 mm, 170±5 μm No. 1.5H) and mounted on a CorTector SX100 instrument (LightEdge Technologies, Beijing, China) equipped with a 488 nm laser. Three replicates of 10-20 10s autocorrelation measurements per sample were recorded at room temperature. Aggregate data was discarded through curve analysis. Atto488 dye was used to calibrate the measurement volume (S). The mean of the 10-20 replicate autocorrelation

measurements was then fit to an equation which accounts for single 3D diffusion and triplet dynamics, starting at autocorrelation values of 0.001ms.

$$(1) \qquad G(\tau) = \frac{1 - T + T * e^{\frac{-\tau}{\tau T}}}{1 - T} * \frac{1}{N} * \frac{1}{1 + \frac{\tau}{\tau_D}} * \frac{1}{\sqrt{1 + \frac{\tau}{\tau_D * S^2}}}$$

From these parameters, the radius of hydration (R_{hyd}) of each sample was calculated, and the values were plotted against the Hsp90 species concentration. Three replicates were then averaged, plotted, and fit with a one site – total binding nonlinear regression equation in Prism to obtain an approximate K_D value:

$$(2) \qquad Y = \mathrm{R_{hyd}Complex_{max}} * \frac{X}{K_D + X} + \mathrm{R_{hyd}PP5}$$

The background R_{hyd} of $PP5_{free}$ ($R_{hyd}PP5$) value was fit globally amongst all samples, and the mutant samples were fit with the same $R_{hyd}Complex_{max}$. Different K_D values were then compared to each other and assessed for significant difference using Prism's ordinary one-way ANOVA, with Šídák's multiple comparisons to compare between Open/Closed and $Open^{aJ\ del}$/$Closed^{aJ\ del}$.

Data Availability

The raw western blot images can be found in the Supplementary Figures included in this publication. The western blot and FCS data used are available in the provided Data Source file (SourceData.xlsx) included in this publication.

The cryo-EM maps generated in this study were deposited in the Electron Microscopy DataBank (EMDB) and atomic coordinate models generated were deposited in the Protein Data Bank (PDB).

Below are the PDB accession codes and corresponding EMDB composite maps:

Hsp90:Cdc37:CRaf:PP5 Composite map I: PDB 8GFT[ ], EMDB: EMD-29984

Hsp90:Cdc37:CRaf:PP5 Composite map II: PDB 8GAE[ ], EMDB: EMD-29895

Below are the EMDB accession codes for the following focus classified maps:

PP5 catalytic domain, Consensus map I: EMDB: EMD-29973

PP5 catalytic domain and kinase domain, Consensus map II: EMDB: EMD-29976

PP5 TPR domain: EMDB: EMD-29957

Cdc37 Middle domain: EMDB: EMD-29949

Models used for model building and data analysis in this manuscript and in our supplementary files can be found in the PDB: 5FWK [PDB DOI: 10.2210/pdb5FWK/pdb], 1WAO [PDB DOI: 10.2210/pdb1WAO/pdb], 5HPE [PDB DOI: 10.2210/pdb5HPE/pdb], 1S95 [PDB DOI: 10.2210/pdb1S95/pdb], 6Q3Q [PDB DOI: 10.2210/pdb6Q3Q/pdb], 7KW7[PDB DOI: 10.2210/pdb7KW7/pdb], 7L7I [PDB DOI: 10.2210/pdb7L7I/pdb]

Acknowledgements

We thank Agard Lab members for many helpful discussions; E. Nieweglowska for her mentorship and guidance; M. Tabios for his support and encouragement; C. Nowotny, D. Mozumdar and M. Moritz for help with Western blots; T. Kortemme and J. Gestwicki for their mentorship; C. Noddings, S. Pourmal, X. Liu, D. Asarnov for their help with CryoEM data processing; D. Bulkley, G. Gilbert, and Z. Yu from the W.M. Keck Foundation Advanced Microscopy Laboratory at the University of California, San Francisco (UCSF) for EM facility maintenance and help with data collection; M. Harrington and J. Baker-LePain for computational support with the UCSF Wynton Cluster. This work was supported in by NIH grant

R35GM118099 (D.A.A.) and NIH grants 1S10OD026881, 1S10OD020054, and 1S10OD021741 to the UCSF cryoEM facility.

Author Contributions Statement

M.J-G designed and executed protein preparation, biochemical experiments, cryo-EM sample preparation, data collection, data processing and model building. C.A.N. helped express yeast and mammalian constructs. D.C. optimized yeast Hsp90:Cdc37:CRaf^{KD} expression and purification. F.W. optimized grids used for cryo-EM, M.T. cloned PP5 mutants. D.A.A. edited, mentored, provided funding, and gave scientific advice throughout the project.

Inclusion & Ethics Statement

All research has taken place at University of California, San Francisco (UCSF), by local UCSF researchers. No human or animal subjects were used in our study. This research does not provide risk to the researchers. Nature Communications is an open-source journal, and this work will be available to all with internet access. (See Data Availability Statement above for more.)

Supplementary Figures

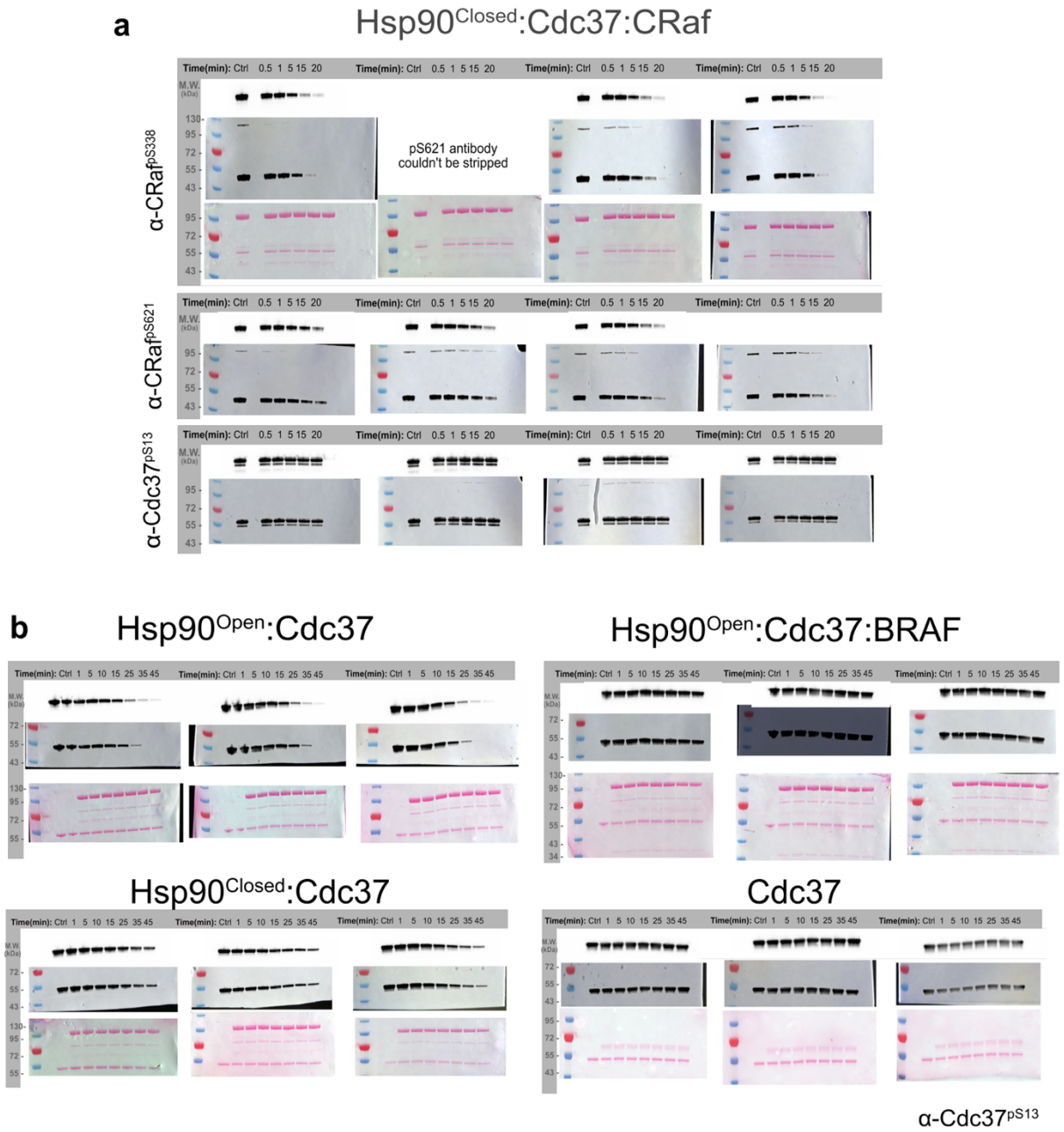

Sup. Fig. 1. Figure 1 Western blot replicate data.

a Purified CRaf-complex (1.5 μM) was incubated with PP5 (75 nM) at 25°C, ran on a gel transferred to a nitrocellulose membrane, ponzo stained and blotted for α-CRaf^{pS338}, α-CRaf^{pS621}, and α-Cdc37^{pS13}. **b** Reconstituted complex (3 μM) was incubated with PP5 (750 nM) at 25°C, ran on a gel, transferred to a nitrocellulose membrane, ponzo stained and blotted for α-Cdc37^{pS13}. Equal amounts of protein can be seen in ponzo stained membrane

throughout experimental timepoints. Blot strips were processed in parallel, and all were normalized by the phosphorylation signal of the internal control which has not been in contact with PP5.

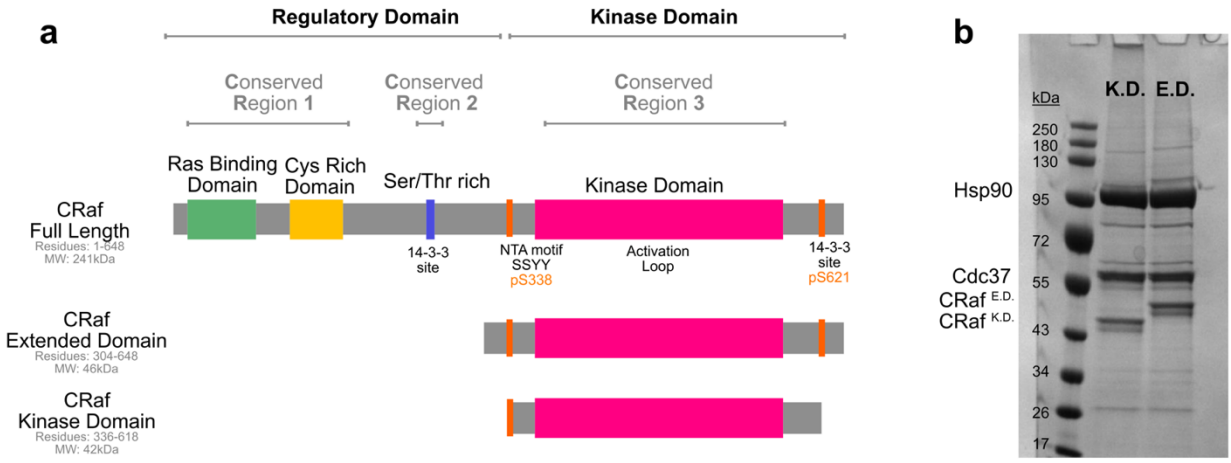

Sup. Fig. 2. CRaf topology and constructs.

a CRaf consists of a Regulatory and Kinase domain. The CRaf regulatory domain contains a Ras Binding Domain, a Cysteine Rich Domain, and important phosphorylation sites such as pS259 and pS621 which bind 14-3-3 chaperones. The CRaf kinase domain consists of two lobes, the beta sheet heavy N-lobe and alpha helical C-lobe. ATP binds between these two lobes. Important phosphorylation sites around the kinase domain are highlighted in orange and consist of the N-terminal pS338 and the C-terminal pS621. Two shorter CRaf constructs were used to increase solubility of CRaf and enable further biochemistry. The Extended domain ($CRaf^{ED}$) was used for all biochemical experiments, while the Kinase domain ($CRaf^{KD}$) was used for structural characterization. **b** Hsp90:Cdc37:CRaf complexes were purified from Expi HEK293 cells, a process repeated with similar results more than five times.

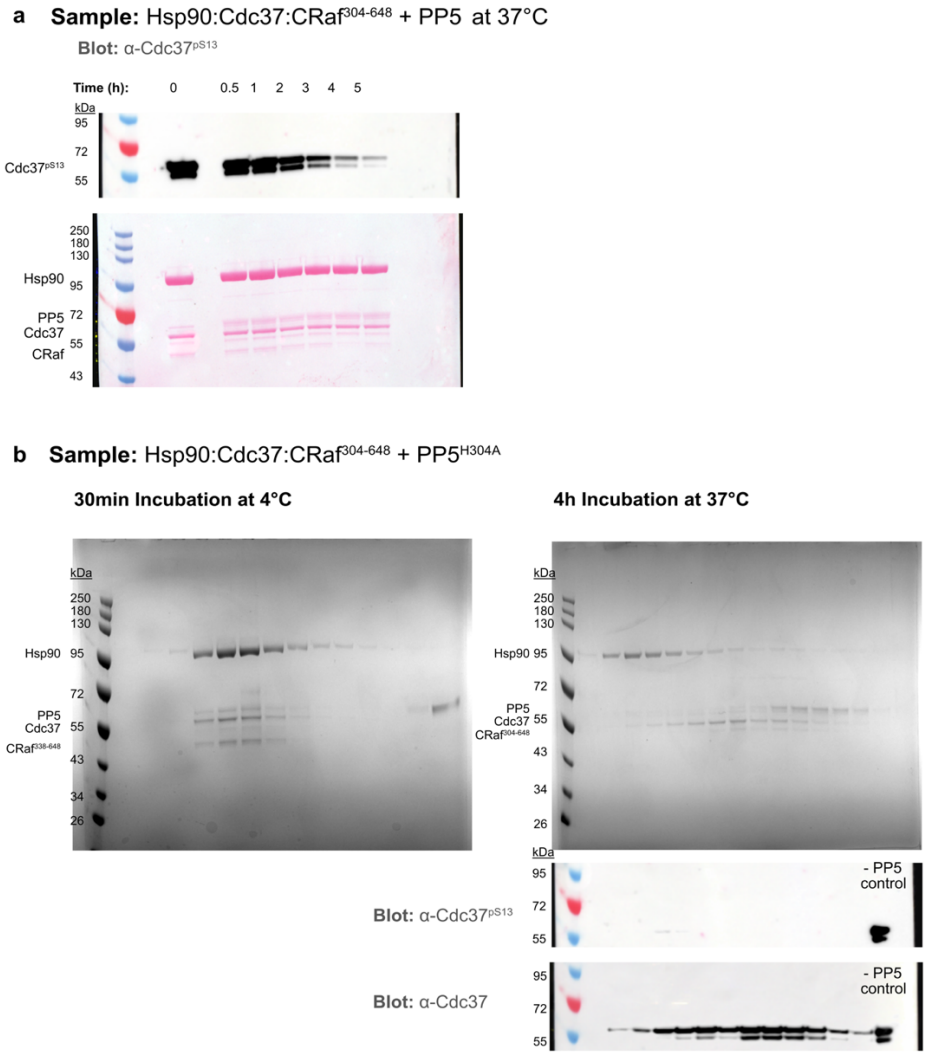

Sup. Fig. 3. Cdc37 becomes dephosphorylated by PP5 at high temperatures.

a Hsp90:Cdc37pS13:CRaf$^{304-648}$ complex (2 μM) was incubated with PP5 (2 μM) at 37°C. The reaction was quenched by SDS:DTT at differing timepoints. The sample was then run on a gel, transferred to a nitrocellulose membrane, ponzo stained and blotted for α-Cdc37^{pS13}. These results were seen three times. **b** Hsp90:Cdc37:CRaf:PP5 complexes were run through a Superdex 200 column after incubation for 30 min at 4°C or for 4h at 37°C. Complex dissociation and PP5 dephoshorylation can be seen in the gel trace of the 37°C incubated sample, which show larger complexes on the left side of the gel and smaller complexes on the right side of the gel. Slight Cdc37^{pS13} phosphorylation can be seen where the complex remains intact as seen by the Western blots provided. This experiment was repeated twice.

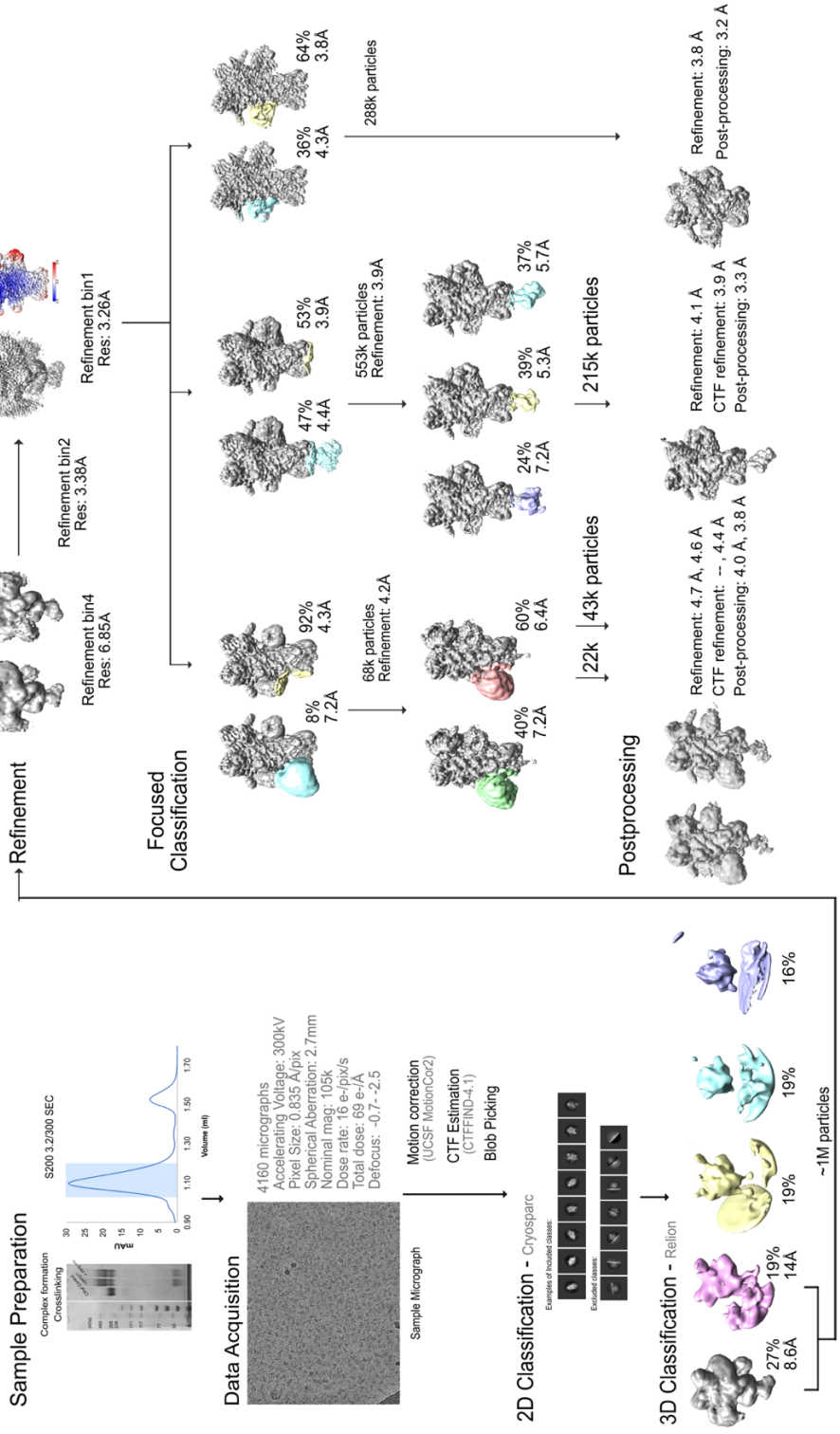

Sup. Fig. 4. Sample preparation and cryo-EM data processing.

The human Hsp90:Cdc37:CRaf complex was purified from yeast, and human $PP5^{H304A}$ was purified from E. coli. The Hsp90:Cdc37:CRaf complex (2 μM) was mixed with $PP5^{H304A}$ (6 μM) for 30 min on ice, and then brought to room temperature and crosslinked with glutaraldehyde (0.05%, 15 min, quenched with 50 mM Tris pH 7.8). The crosslinked complex was then run over an S200 column (3.2/300) to remove excess PP5. The fractions from the major peak (~1.1 mL) were collected and concentrated 3 fold. This sample was frozen on PEG Amino functionalized gold carbon quantifoil grids using a Vitrobot (10C, 100% humidity, 30s Wait Time, 3s Blot Time, -2 Blot Force). 4160 micrographs were acquired using a Krios microscope (105,000X magnification). The images were then motion corrected (MotionCor2), and their CTF estimated (CTFFIND-4.1). Micrographs with a CTF fit <5Å were kept for cryoSPARC gaussian blob picking. The particles were then 2D classified to remove high resolution artifact particles and ensure sample quality. Selected 2D classes were then imported into RELION (using csparc2star by D. Asarnov) for further 3D classification. One round of classification led to ~1M Hsp90-like particles, which were then refined and unbinned. Focused classification with subtraction, Refinement and Postprocessing led to the final maps used for composite map creation and model fitting.

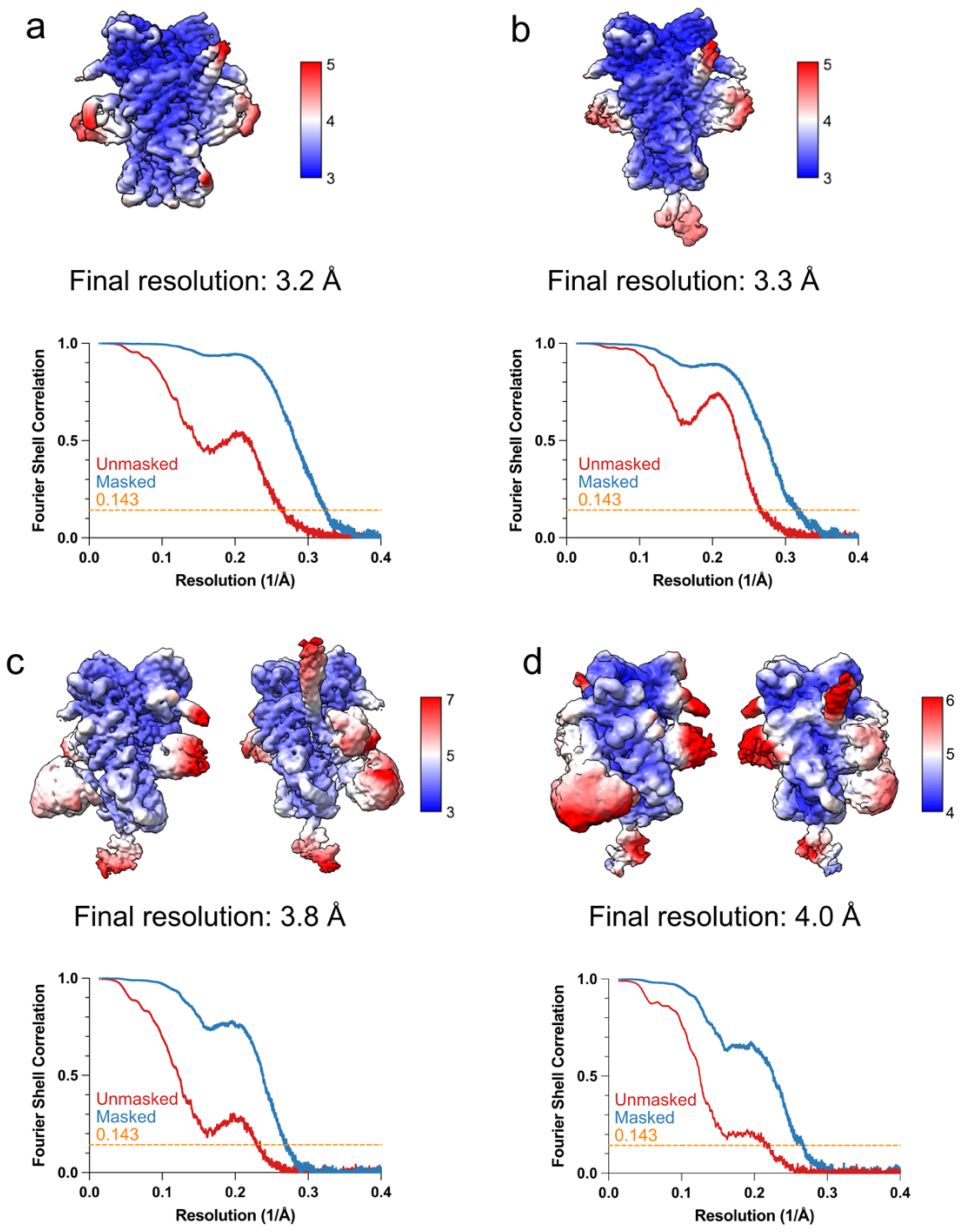

Sup. Fig. 5. Focused classification maps used for composite map creation.

Focused classification on the CRaf N-lobe (**a**), the TPR domain of PP5 (**b**), and two alternate PP5 conformations (**c,d**) yielded the final maps used to create the two composite models in this work. The maps included **a, b** and either **c** or **d**. The volumes shown here were post-processed in RELION to give the final resolutions reported. The FSC curves were obtained using the phenix software (Mtriage).

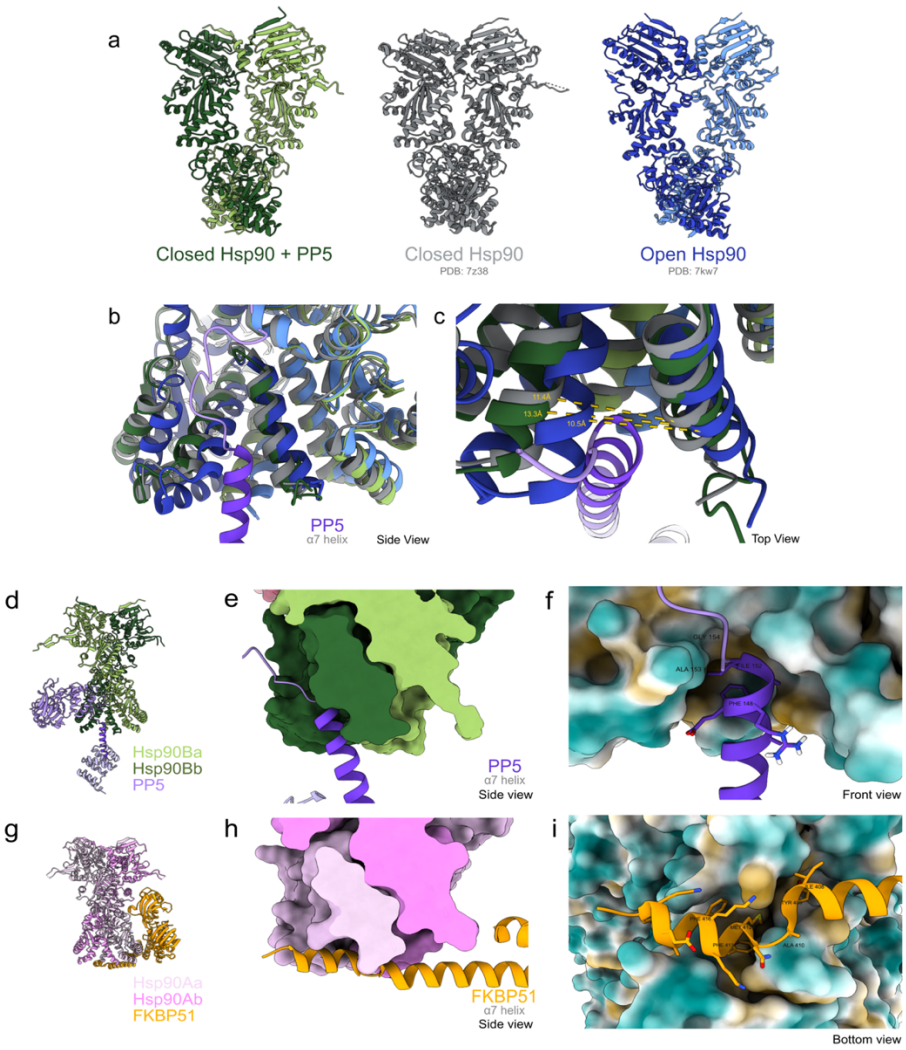

Sup. Fig. 6. Comparison between Hsp90 conformations, and differently binding cochaperones.

a Closed Hsp90 dimer as seen in our current work is contrasted with the Hsp90:Cdc37:CRaf complex (PDB: 7z38 [PDB DOI: 10.2210/pdb7Z38/pdb]) and the loading complex semi-open Hsp90 dimer (PDB: 7kw7 [PDB DOI: 10.2210/pdb7KW7/pdb]). **b,c** A closer view of the $Hsp90^{CTD}$ shows the rearrangements that occur between the Hsp90 CTD groove that binds PP5s α7 helix. The Hsp90 CTD groove varies in size ($Hsp90^{closed}$:PP5 > $Hsp90^{closed}$ > $Hsp90^{semi\text{-}open}$); $Hsp90^{closed}$:PP5 allows PP5 binding in its enlarged CTD groove. **d,i** Hsp90 interacts with PP5 and FKBP51 via TPR domain:Hsp90 C-terminal interactions. **e,h** The cochaperone's α7 helices interact with the Hsp90 C-terminal groove at an almost ~90° angle difference from each other. **f,i** Numerous FKBP51 α7 helix hydrophobic residues are buried in the Hsp90:FKBP51 interface, while only two hydrophobic residues are buried in the Hsp90:PP5 interface.

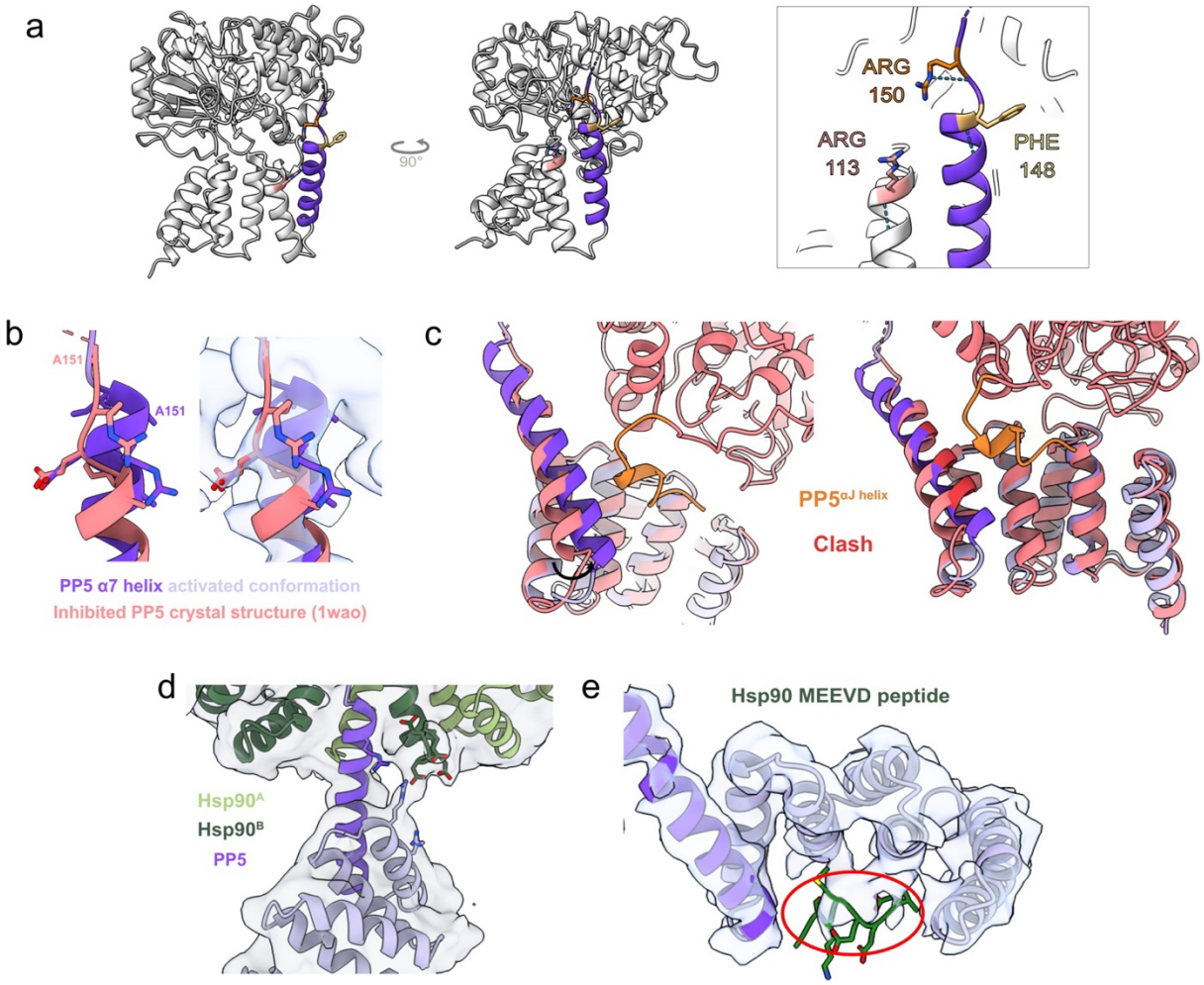

Sup. Fig. 7. Hsp90 binding leads to PP5 TPR domain rearrangement.

a The PP5 TPR mutants are more than 8Å away from the PP5 catalytic site. The α7 helix on the TPR domain binds to Hsp90's C-terminal domains. **b** PP5 α7 helix binding to $Hsp90^{CTD}$ leads to the elongation of the PP5 α7 helix as it makes stabilizing interactions with Hsp90. **c** Overlay of PP5's TPR domain in an inhibited (PDB: 1wao) or active state shows PP5 α7 helix movement towards the PP5 αJ helix of PP5's catalytic domain. Potential clash (red) between these two helices might contribute to αJ helix inhibition release. **d** Density can be seen for the interaction between the negatively charged Hsp90 tail and the positively charged patch on TPR domain. **e** Partial density can be seen for the Hsp90 MEEVD peptide as it interacts with PP5's basic patch. A homologous structure of a TPR-MEEVD interaction was docked to highlight the location of key MEEVD binding residues on PP5. (PDB: 6q3q [PDB DOI: 10.2210/pdb6Q3Q/pdb]).

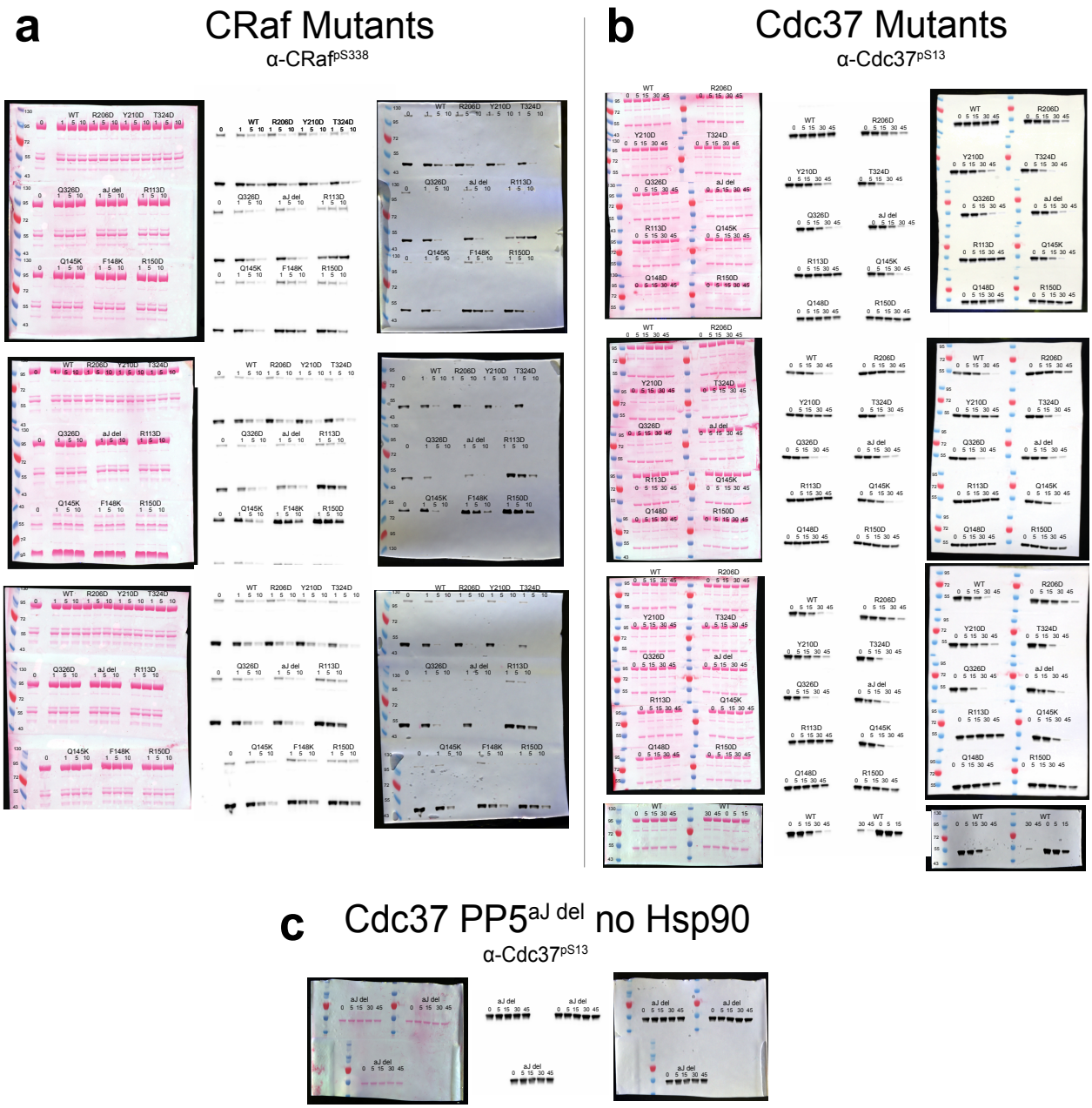

Sup. Fig. 8. Mutant western blot replicate data.

PP5 mutants were tested for rates of dephosphorylation as described in Supplementary Fig. 1. **a** Mammalian purified Hsp90^{closed}:Cdc37:CRaf^{ED} (3 μM) was incubated with PP5 mutant (150 nM). **b** E. coli purified, CK2 phosphorylated Cdc37^{pS13} (3 μM) was incubated with Hsp90 and PP5 mutants (750 nM). Additional mutants not considered in the manuscript are included here. **c** Cdc37 (3 μM) was incubated with PP5 $^{\alpha J\ del}$ (750 nM) in the absence of Hsp90.

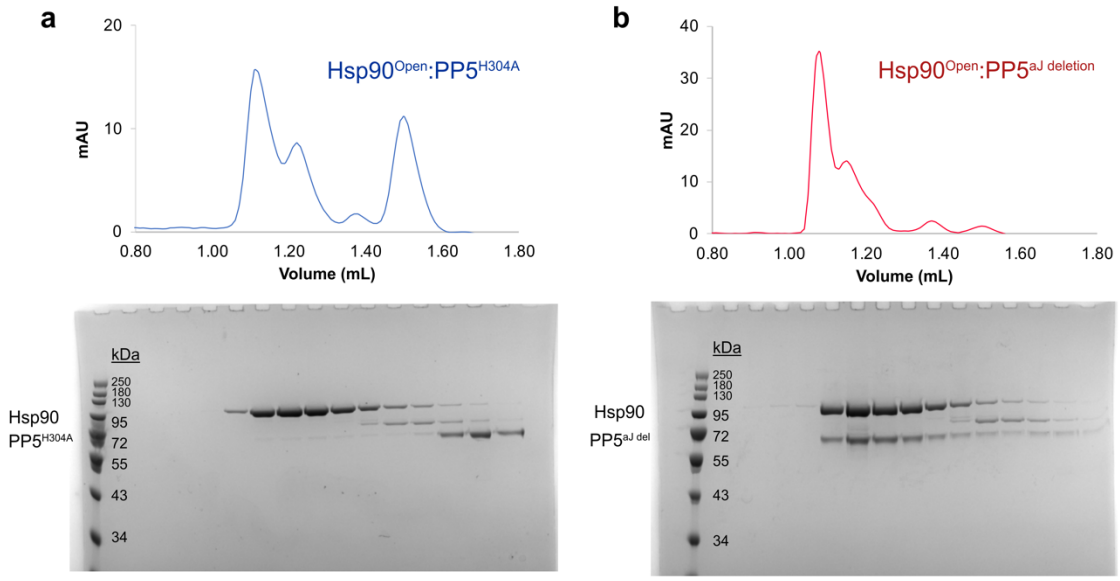

Sup. Fig. 9. aJ helix truncation leads to increased Hsp90:PP5 complex coelution.

Hsp90 dimer (6 μM) was incubated with either catalytically dead $PP5^{H304A}$ or PP5 $^{\alpha J\ del}$ (6 μM) at 4°C for 30 min before loading the sample onto the S200 3.2/300 column in SEC buffer (20 mM HEPES, 50 mM KCl, 10m $MgCl_2$, 1 mM EDTA, 1 mM TCEP) and allowed to flow through at a flow rate of 0.04ml/min. 50 μL aliquots were eluted and ran on SDS gels for component visualization. **a** $PP5^{H304A}$ loosely coelutes with Hsp90, while **b** PP5 $^{\alpha J\ del}$ strongly coelutes with Hsp90. This result was repeated twice.

References

Ali, A., Zhang, J., Bao, S., Liu, I., Otterness, D., Dean, N. M., Abraham, R. T., & Wang, X.-F. (2004). Requirement of protein phosphatase 5 in DNA-damage-induced ATM activation. *Genes & Development*, *18*(3), 249-254. https://doi.org/10.1101/gad.1176004

Amable, L., Grankvist, N., Largen, J. W., Ortsäter, H., Sjöholm, Å., & Honkanen, R. E. (2011). Disruption of Serine/Threonine Protein Phosphatase 5 (PP5:PPP5c) in Mice Reveals a Novel Role for PP5 in the Regulation of Ultraviolet Light-induced Phosphorylation of Serine/Threonine Protein Kinase Chk1 (CHEK1). *Journal of Biological Chemistry*, *286*(47), 40413-40422. https://doi.org/10.1074/jbc.M111.244053

Asarnow, D., Palovcak, E., & Cheng, Y. (2019). *asarnow/pyem: UCSF pyem v0.5*. In (Version v0.5) Zenodo. https://zenodo.org/record/3576630

Bandhakavi, S., McCann, R. O., Hanna, D. E., & Glover, C. V. C. (2003). A Positive Feedback Loop between Protein Kinase CKII and Cdc37 Promotes the Activity of Multiple Protein Kinases. *Journal of Biological Chemistry*, *278*(5), 2829-2836. https://doi.org/10.1074/jbc.M206662200

Becker, W., Kentrup, H., Klumpp, S., Schultz, J. E., & Joost, H. G. (1994). Molecular cloning of a protein serine/threonine phosphatase containing a putative regulatory tetratricopeptide repeat domain. *Journal of Biological Chemistry*, *269*(36), 22586-22592. https://doi.org/10.1016/S0021-9258(17)31686-1

Chen, M. X., McPartlin, A. E., Brown, L., Chen, Y. H., Barker, H. M., & Cohen, P. T. (1994). A novel human protein serine/threonine phosphatase, which possesses four tetratricopeptide repeat motifs and localizes to the nucleus. *The EMBO Journal*, *13*(18), 4278-4290. https://doi.org/10.1002/j.1460-2075.1994.tb06748.x

Conde, R., Xavier, J., McLoughlin, C., Chinkers, M., & Ovsenek, N. (2005). Protein Phosphatase 5 Is a Negative Modulator of Heat Shock Factor 1. *Journal of Biological Chemistry*, *280*(32), 28989-28996. https://doi.org/10.1074/jbc.M503594200

Croll, T. I. (2018). ISOLDE : a physically realistic environment for model building into low-resolution electron-density maps. *Acta Crystallographica Section D Structural Biology*, *74*(6), 519-530. https://doi.org/10.1107/S2059798318002425

Cutler, R. E., Stephens, R. M., Saracino, M. R., & Morrison, D. K. (1998). Autoregulation of the Raf-1 serine/threonine kinase. *Proceedings of the National Academy of Sciences*, *95*(16), 9214-9219. https://doi.org/10.1073/pnas.95.16.9214

Das, A. K. (1998). The structure of the tetratricopeptide repeats of protein phosphatase 5: implications for TPR-mediated protein-protein interactions. *The EMBO Journal*, *17*(5), 1192-1199. https://doi.org/10.1093/emboj/17.5.1192

Dhillon, A. S., Yip, Y. Y., Grindlay, G. J., Pakay, J. L., Dangers, M., Hillmann, M., Clark, W., Pitt, A., Mischak, H., & Kolch, W. (2009). The C-terminus of Raf-1 acts as a 14-3-3-dependent activation switch. *Cellular Signalling*, *21*(11), 1645-1651. https://doi.org/10.1016/j.cellsig.2009.07.001

Diaz, B., Barnard, D., Filson, A., MacDonald, S., King, A., & Marshall, M. (1997). Phosphorylation of Raf-1 serine 338-serine 339 is an essential regulatory event for Ras-dependent activation and biological signaling. *Molecular and Cellular Biology*, *17*(8), 4509-4516. https://doi.org/10.1128/MCB.17.8.4509

García-Alonso, S., Mesa, P., Ovejero, L. d. l. P., Aizpurua, G., Lechuga, C. G., Zarzuela, E., Santiveri, C. M., Sanclemente, M., Muñoz, J., Musteanu, M., Campos-Olivas, R., Martínez-Torrecuadrada, J., Barbacid, M., & Montoya, G. (2022). Structure of the RAF1-

HSP90-CDC37 complex reveals the basis of RAF1 regulation. *Molecular Cell*, *82*(18), 3438-3452.e3438. https://doi.org/10.1016/j.molcel.2022.08.012

Golden, T., Swingle, M., & Honkanen, R. E. (2008). The role of serine/threonine protein phosphatase type 5 (PP5) in the regulation of stress-induced signaling networks and cancer. *Cancer and Metastasis Reviews*, *27*(2), 169-178. https://doi.org/10.1007/s10555-008-9125-z

Grammatikakis, N., Lin, J.-H., Grammatikakis, A., Tsichlis, P. N., & Cochran, B. H. (1999). p50 ^{cdc37} Acting in Concert with Hsp90 Is Required for Raf-1 Function. *Molecular and Cellular Biology*, *19*(3), 1661-1672. https://doi.org/10.1128/MCB.19.3.1661

Hartl, F. U., Bracher, A., & Hayer-Hartl, M. (2011). Molecular chaperones in protein folding and proteostasis. *Nature*, *475*(7356), 324-332. https://doi.org/10.1038/nature10317

Hu, J., Stites, Edward C., Yu, H., Germino, Elizabeth A., Meharena, Hiruy S., Stork, Philip J. S., Kornev, Alexandr P., Taylor, Susan S., & Shaw, Andrey S. (2013). Allosteric Activation of Functionally Asymmetric RAF Kinase Dimers. *Cell*, *154*(5), 1036-1046. https://doi.org/10.1016/j.cell.2013.07.046

Kang, H., Sayner, S. L., Gross, K. L., Russell, L. C., & Chinkers, M. (2001). Identification of Amino Acids in the Tetratricopeptide Repeat and C-Terminal Domains of Protein Phosphatase 5 Involved in Autoinhibition and Lipid Activation. *Biochemistry*, *40*(35), 10485-10490. https://doi.org/10.1021/bi010999i

Keramisanou, D., Aboalroub, A., Zhang, Z., Liu, W., Marshall, D., Diviney, A., Larsen, Randy W., Landgraf, R., & Gelis, I. (2016). Molecular Mechanism of Protein Kinase

Recognition and Sorting by the Hsp90 Kinome-Specific Cochaperone Cdc37. *Molecular Cell*, *62*(2), 260-271. https://doi.org/10.1016/j.molcel.2016.04.005

Kimura, Y., Rutherford, S. L., Miyata, Y., Yahara, I., Freeman, B. C., Yue, L., Morimoto, R. I., & Lindquist, S. (1997). Cdc37 is a molecular chaperone with specific functions in signal transduction. *Genes & Development*, *11*(14), 1775-1785. https://doi.org/10.1101/gad.11.14.1775

Lee, K., Thwin, A. C., Nadel, C. M., Tse, E., Gates, S. N., Gestwicki, J. E., & Southworth, D. R. (2021). The structure of an Hsp90-immunophilin complex reveals cochaperone recognition of the client maturation state. *Molecular Cell*, *81*(17), 3496-3508.e3495. https://doi.org/10.1016/j.molcel.2021.07.023

Liebschner, D., Afonine, P. V., Baker, M. L., Bunkóczi, G., Chen, V. B., Croll, T. I., Hintze, B., Hung, L.-W., Jain, S., McCoy, A. J., Moriarty, N. W., Oeffner, R. D., Poon, B. K., Prisant, M. G., Read, R. J., Richardson, J. S., Richardson, D. C., Sammito, M. D., Sobolev, O. V., . . . Adams, P. D. (2019). Macromolecular structure determination using X-rays, neutrons and electrons: recent developments in Phenix. *Acta Crystallographica Section D Structural Biology*, *75*(10), 861-877. https://doi.org/10.1107/S2059798319011471

Mason, C. S. (1999). Serine and tyrosine phosphorylations cooperate in Raf-1, but not B-Raf activation. *The EMBO Journal*, *18*(8), 2137-2148. https://doi.org/10.1093/emboj/18.8.2137

Maurer, G., Tarkowski, B., & Baccarini, M. (2011). Raf kinases in cancer–roles and therapeutic opportunities. *Oncogene*, *30*(32), 3477-3488. https://doi.org/10.1038/onc.2011.160

Miyata, Y., & Nishida, E. (2004). CK2 Controls Multiple Protein Kinases by Phosphorylating a Kinase-Targeting Molecular Chaperone, Cdc37. *Molecular and Cellular Biology*, *24*(9), 4065-4074. https://doi.org/10.1128/MCB.24.9.4065-4074.2004

Miyata, Y., & Nishida, E. (2007). Analysis of the CK2-dependent phosphorylation of serine 13 in Cdc37 using a phospho-specific antibody and phospho-affinity gel electrophoresis: Cdc37 phosphorylation by CK2 and signaling kinases. *FEBS Journal*, *274*(21), 5690-5703. https://doi.org/10.1111/j.1742-4658.2007.06090.x

Morita, K., Saitoh, M., Tobiume, K., Matsuura, H., Enomoto, S., Nishitoh, H., & Ichijo, H. (2001). Negative feedback regulation of ASK1 by protein phosphatase 5 (PP5) in response to oxidative stress. *The EMBO Journal*, *20*(21), 6028-6036. https://doi.org/10.1093/emboj/20.21.6028

Noddings, C. M., Johnson, J. L., & Agard, D. A. (2023). *Cryo-EM reveals how Hsp90 and FKBP immunophilins co-regulate the Glucocorticoid Receptor* [preprint]. http://biorxiv.org/lookup/doi/10.1101/2023.01.10.523504

Oberoi, J., Aran-Guiu, X., Outwin, E. A., Schellenberger, P., Roumeliotis, T. I., Choudhary, J. S., & Pearl, L. H. (2022). *HSP90-CDC37-PP5 forms a structural platform for kinase dephosphorylation* [preprint]. http://biorxiv.org/lookup/doi/10.1101/2022.05.03.490524

Oberoi, J., Dunn, D. M., Woodford, M. R., Mariotti, L., Schulman, J., Bourboulia, D., Mollapour, M., & Vaughan, C. K. (2016). Structural and functional basis of protein phosphatase 5 substrate specificity. *Proceedings of the National Academy of Sciences*, *113*(32), 9009-9014. https://doi.org/10.1073/pnas.1603059113

Polier, S., Samant, R. S., Clarke, P. A., Workman, P., Prodromou, C., & Pearl, L. H. (2013). ATP-competitive inhibitors block protein kinase recruitment to the Hsp90-Cdc37 system. *Nature Chemical Biology*, *9*(5), 307-312. https://doi.org/10.1038/nchembio.1212

Punjani, A., & Fleet, D. J. (2021). 3D variability analysis: Resolving continuous flexibility and discrete heterogeneity from single particle cryo-EM. *Journal of Structural Biology*, *213*(2), 107702. https://doi.org/10.1016/j.jsb.2021.107702

Punjani, A., Rubinstein, J. L., Fleet, D. J., & Brubaker, M. A. (2017). cryoSPARC: algorithms for rapid unsupervised cryo-EM structure determination. *Nature Methods*, *14*(3), 290-296. https://doi.org/10.1038/nmeth.4169

Rohou, A., & Grigorieff, N. (2015). CTFFIND4: Fast and accurate defocus estimation from electron micrographs. *Journal of Structural Biology*, *192*(2), 216-221. https://doi.org/10.1016/j.jsb.2015.08.008

Russell, L. C., Whitt, S. R., Chen, M.-S., & Chinkers, M. (1999). Identification of Conserved Residues Required for the Binding of a Tetratricopeptide Repeat Domain to Heat Shock Protein 90. *Journal of Biological Chemistry*, *274*(29), 20060-20063. https://doi.org/10.1074/jbc.274.29.20060

Scheres, S. H. W. (2012). RELION: Implementation of a Bayesian approach to cryo-EM structure determination. *Journal of Structural Biology*, *180*(3), 519-530. https://doi.org/10.1016/j.jsb.2012.09.006

Shao, J., Irwin, A., Hartson, S. D., & Matts, R. L. (2003). Functional Dissection of Cdc37: Characterization of Domain Structure and Amino Acid Residues Critical for Protein Kinase Binding. *Biochemistry*, *42*(43), 12577-12588. https://doi.org/10.1021/bi035138j

Shao, J., Prince, T., Hartson, S. D., & Matts, R. L. (2003). Phosphorylation of Serine 13 Is Required for the Proper Function of the Hsp90 Co-chaperone, Cdc37. *Journal of Biological Chemistry*, *278*(40), 38117-38120. https://doi.org/10.1074/jbc.C300330200

Song, Y., DiMaio, F., Wang, Ray Y.-R., Kim, D., Miles, C., Brunette, T., Thompson, J., & Baker, D. (2013). High-Resolution Comparative Modeling with RosettaCM. *Structure*, *21*(10), 1735-1742. https://doi.org/10.1016/j.str.2013.08.005

Stancato, L. F., Chow, Y. H., Hutchison, K. A., Perdew, G. H., Jove, R., & Pratt, W. B. (1993). Raf exists in a native heterocomplex with hsp90 and p50 that can be reconstituted in a cell-free system. *Journal of Biological Chemistry*, *268*(29), 21711-21716. https://doi.org/10.1016/S0021-9258(20)80600-0

Swingle, M. R., Honkanen, R. E., & Ciszak, E. M. (2004). Structural Basis for the Catalytic Activity of Human Serine/Threonine Protein Phosphatase-5. *Journal of Biological Chemistry*, *279*(32), 33992-33999. https://doi.org/10.1074/jbc.M402855200

Taipale, M., Jarosz, D. F., & Lindquist, S. (2010). HSP90 at the hub of protein homeostasis: emerging mechanistic insights. *Nature Reviews Molecular Cell Biology*, *11*(7), 515-528. https://doi.org/10.1038/nrm2918

Taipale, M., Krykbaeva, I., Koeva, M., Kayatekin, C., Westover, Kenneth D., Karras, Georgios I., & Lindquist, S. (2012). Quantitative Analysis of Hsp90-Client Interactions Reveals Principles of Substrate Recognition. *Cell*, *150*(5), 987-1001. https://doi.org/10.1016/j.cell.2012.06.047

Tsai, J., Lee, J. T., Wang, W., Zhang, J., Cho, H., Mamo, S., Bremer, R., Gillette, S., Kong, J., Haass, N. K., Sproesser, K., Li, L., Smalley, K. S. M., Fong, D., Zhu, Y.-L., Marimuthu, A., Nguyen, H., Lam, B., Liu, J., . . . Bollag, G. (2008). Discovery of a selective inhibitor

of oncogenic B-Raf kinase with potent antimelanoma activity. *Proceedings of the National Academy of Sciences*, *105*(8), 3041-3046. https://doi.org/10.1073/pnas.0711741105

Vaughan, C. K., Mollapour, M., Smith, J. R., Truman, A., Hu, B., Good, V. M., Panaretou, B., Neckers, L., Clarke, P. A., Workman, P., Piper, P. W., Prodromou, C., & Pearl, L. H. (2008). Hsp90-Dependent Activation of Protein Kinases Is Regulated by Chaperone-Targeted Dephosphorylation of Cdc37. *Molecular Cell*, *31*(6), 886-895. https://doi.org/10.1016/j.molcel.2008.07.021

Verba, K. A., Wang, R. Y.-R., Arakawa, A., Liu, Y., Shirouzu, M., Yokoyama, S., & Agard, D. A. (2016). Atomic structure of Hsp90-Cdc37-Cdk4 reveals that Hsp90 traps and stabilizes an unfolded kinase. *Science*, *352*(6293), 1542-1547. https://doi.org/10.1126/science.aaf5023

von Kriegsheim, A., Pitt, A., Grindlay, G. J., Kolch, W., & Dhillon, A. S. (2006). Regulation of the Raf–MEK–ERK pathway by protein phosphatase 5. *Nature Cell Biology*, *8*(9), 1011-1016. https://doi.org/10.1038/ncb1465

Wandinger, S. K., Suhre, M. H., Wegele, H., & Buchner, J. (2006). The phosphatase Ppt1 is a dedicated regulator of the molecular chaperone Hsp90. *The EMBO Journal*, *25*(2), 367-376. https://doi.org/10.1038/sj.emboj.7600930

Wang, F., Liu, Y., Yu, Z., Li, S., Feng, S., Cheng, Y., & Agard, D. A. (2020). General and robust covalently linked graphene oxide affinity grids for high-resolution cryo-EM. *Proceedings of the National Academy of Sciences*, *117*(39), 24269-24273. https://doi.org/10.1073/pnas.2009707117

Wang, F., Yu, Z., Betegon, M., Campbell, M. G., Aksel, T., Zhao, J., Li, S., Douglas, S. M., Cheng, Y., & Agard, D. A. (2020). Amino and PEG-amino graphene oxide grids enrich and protect samples for high-resolution single particle cryo-electron microscopy. *Journal of Structural Biology*, *209*(2), 107437. https://doi.org/10.1016/j.jsb.2019.107437

Wang, R. Y.-R., Noddings, C. M., Kirschke, E., Myasnikov, A. G., Johnson, J. L., & Agard, D. A. (2022). Structure of Hsp90–Hsp70–Hop–GR reveals the Hsp90 client-loading mechanism. *Nature*, *601*(7893), 460-464. https://doi.org/10.1038/s41586-021-04252-1

Wang, R. Y.-R., Song, Y., Barad, B. A., Cheng, Y., Fraser, J. S., & DiMaio, F. (2016). Automated structure refinement of macromolecular assemblies from cryo-EM maps using Rosetta. *eLife*, *5*, e17219. https://doi.org/10.7554/eLife.17219

Wartmann, M., & Davis, R. J. (1994). The native structure of the activated Raf protein kinase is a membrane-bound multi-subunit complex. *The Journal of Biological Chemistry*, *269*(9), 6695-6701. http://www.ncbi.nlm.nih.gov/pubmed/8120027

Wechsler, T., Chen, B. P. C., Harper, R., Morotomi-Yano, K., Huang, B. C. B., Meek, K., Cleaver, J. E., Chen, D. J., & Wabl, M. (2004). DNA–PKcs function regulated specifically by protein phosphatase 5. *Proceedings of the National Academy of Sciences*, *101*(5), 1247-1252. https://doi.org/10.1073/pnas.0307765100

Wellbrock, C., Karasarides, M., & Marais, R. (2004). The RAF proteins take centre stage. *Nature Reviews Molecular Cell Biology*, *5*(11), 875-885. https://doi.org/10.1038/nrm1498

Yang, J., Roe, S. M., Cliff, M. J., Williams, M. A., Ladbury, J. E., Cohen, P. T. W., & Barford, D. (2005). Molecular basis for TPR domain-mediated regulation of protein phosphatase 5. *The EMBO Journal*, *24*(1), 1-10. https://doi.org/10.1038/sj.emboj.7600496

Zhang, J., Bao, S., Furumai, R., Kucera, K. S., Ali, A., Dean, N. M., & Wang, X.-F. (2005). Protein Phosphatase 5 Is Required for ATR-Mediated Checkpoint Activation. *Molecular and Cellular Biology*, *25*(22), 9910-9919. https://doi.org/10.1128/MCB.25.22.9910-9919.2005

Zheng, S. Q., Palovcak, E., Armache, J.-P., Verba, K. A., Cheng, Y., & Agard, D. A. (2017). MotionCor2: anisotropic correction of beam-induced motion for improved cryo-electron microscopy. *Nature Methods*, *14*(4), 331-332. https://doi.org/10.1038/nmeth.4193

Zuo, Z., Dean, N. M., & Honkanen, R. E. (1998). Serine/Threonine Protein Phosphatase Type 5 Acts Upstream of p53 to Regulate the Induction of p21WAF1/Cip1 and Mediate Growth Arrest. *Journal of Biological Chemistry*, *273*(20), 12250-12258. https://doi.org/10.1074/jbc.273.20.12250

Zuo, Z., Urban, G., Scammell, J. G., Dean, N. M., McLean, T. K., Aragon, I., & Honkanen, R. E. (1999). Ser/Thr Protein Phosphatase Type 5 (PP5) Is a Negative Regulator of Glucocorticoid Receptor-Mediated Growth Arrest. *Biochemistry*, *38*(28), 8849-8857. https://doi.org/10.1021/bi990842e

Chapter 5

Future Directions

Hsp90 kinase loading

While many attempts to visualize a Kinase Loading Complex were undertaken, the kinase used for these experiments was not the prototypical kinase. sBRaf is easy to work with in a test tube, but clearly has properties that make it quite different from most kinases. The follow the next steps of the work shown here, I would be interested in doing one of two things (1) following the work of Arlander et al. closely, and attempting to more closely reproduce the processes seen with Chk1 kinase or (2) studying the cell biology of this process in cells further before attempting a reconstitution (Arlander et al., 2006). Finally, (3) studying the dynamics and conformational changes in kinases through FRET labeling, Hydrogen-Deuterium exchange, or single molecule atomic force microscopy would greatly contribute to understanding what Hsp90's role is in the kinase chaperone cycle. I will briefly go over ideas for each of these concepts.

Arlander et al. tested kinase chaperone activity by measuring kinase phosphorylation (Arlander et al., 2006), something we didn't measure in our experiments. Chaperones are present in high concentrations in the cell, and the Hsp90 complexes formed may be short lived. For this reason, focusing on visualizing complexes may not be the best way to test for the functionality of

the system. In the aggregation experiments conducted, chaperones were shown to keep sBRaf in its soluble state longer, limiting aggregation. This suggests that kinases are indeed interacting with the chaperones, even if the interaction is hard to isolate. By seeing kinase activity, we would better be able to classify chaperone function and work to biochemically capture the state of interest for cryoEM. Starting with the known Chk1 system and attempting to reproduce Arlander et al.'s results would be a great idea. In our hands, Chk1 stability when purified in E. coli was questionable. The next steps to Chk1 purification might be to add a solubility tag or use another expression system.

Hsp90 plays many roles in client function, and while we have discovered that PP5 can use Hsp90 as a scaffold for dephosphorylation of kinase clients, there is still much more to learn. At what point does Hsp90 interact with protein kinases? There is proof that some kinases require Hsp90 for their initial folding and activation, while other kinases interact with Hsp90 throughout their lifespan. Other Hsp90 cochaperones such as the FKBP's have been shown to be important for Hsp90-client translocation into the nucleus. Might kinases be using Hsp90 to aide in transport to the membrane or to other compartments? Does Hsp90 binding lead to kinase inactivation? Or do kinases bind Hsp90 when they're inactive and on pathway for activation? Might Hsp90 do both depending on the phosphorylation state of the kinase or which cochaperones are involved?

All these questions can be answered through careful cell biology and biochemistry. Kinase phosphorylation patterns can be used as read-outs of kinase activation state. By understanding when Hsp90 interacts with which phosphorylated state – we might get closer to understanding Hsp90's function in kinase interactions. Alternatively, Hsp90-Kinase colocalization through FRET may allow the visualization of Hsp90-Kinase interactions at the cytosol or at the cell membrane. Kinase translation stalling via small molecule inhibitors, Hsp90

inhibition, and kinase pathway activation might illustrate changes in Hsp90-Kinase interaction localization.

To study the nature of the kinase conformational changes due to Hsp90, a more detailed study of kinase conformational rearrangement would be required. Work by Ruth Röck et al. explored “open” vs “closed” kinase conformational change through a protein-fragment complementation assay (Röck et al., 2019). Through this assay, the group could distinguish between a closed inhibited kinase and a more stretched out active kinase. In these cell-based assays, different drug’s effects on Hsp90 conformations could be tested. I propose that a similar assay could be paired with Hsp90 inhibition or fluorescence to see Hsp90 interactions with distinct kinase states. Similar FRET assays with kinase labelling on either end of the kinase, hydrogen deuterium experiments, or measurements of forces exerted by Hsp90 might illustrate different kinase conformational modifications before and after Hsp90 interactions.

Hsp90-Cdc37 Interactions

The interaction between Hsp90 and Cdc37 has been studied for years. Crystallography and cryoEM studies show two highly distinct Cdc37 binding conformations, and NMR studies begin exploring the dynamics behind Cdc37’s role as a kinase adaptor (Keramisanou et al., 2016; Roe et al., 2004; Verba et al., 2016). The first crystal structure of a Hsp90:Cdc37 complex, involved only the Hsp90 N-terminal domain and the C-terminal domain of Cdc37 (Roe et al., 2004). In this structure, the Cdc37 C-terminal domain packs against the Hsp90 N-terminal domain lid. Subsequent cryoEM studies showed that Cdc37 and Hsp90 could indeed form a complex when aided by a present kinase, but these complexes did not show density for the Cdc37 C-terminal domain and instead showed the Cdc37 N-terminal domain wrapped around

Hsp90, with a flexible middle domain flexibly present where the kinase N-lobe leaves the Hsp90 lumen (Verba et al., 2016). These two complexes begin to show the flexibility of Cdc37, and the various mechanisms of interaction that these two proteins can partake in.

Our work studying how PP5 dephosphorylates the Hsp90:Cdc37 complex shows that PP5 can dephosphorylate Cdc37 while it is bound to Hsp90, without kinase presence. The PP5 α7 helix binds the Hsp90 C-terminal domain groove, an interaction surface available to PP5 because of Hsp90 closure. Mutations of the PP5 α7 helix inhibit PP5 interaction with CRaf, but also with Cdc37 in a Hsp90:Cdc37 complex. This suggests that the conserved mechanism of PP5 binding may apply to PP5 dephosphorylation of Cdc37 in the Hsp90:Cdc37 complex. Not only this, but the dephosphorylation of Cdc37 might permit different conformations of Cdc37 interaction with Hsp90. To further understand these interactions, negative stain and preliminary cryoEM grids were created with the Hsp90:Cdc37 or Hsp90:Cdc37:PP5 complexes. While the Hsp90:Cdc37:PP5 complex showed clear particles, averaging out of such a heterogeneous complex made achieving high resolution complicated. This led me to attempt to understand the structure of Hsp90:Cdc37 without PP5 present. In preliminary negative stain results, it appears as if Hsp90 is held in a semi-open state when bound to Cdc37. The stabilization of the Hsp90 open state by Cdc37 might allow for visualization of an open Hsp90 complex, a complex too heterogeneous for visualization without stabilizing cochaperones. Efforts to push this complex forward would have many benefits for model creation and understanding Hsp90-Kinase interactions.

The role of Cdc37 phosphorylation in Kinase chaperoning

Cdc37 has a key phosphorylation at its N-terminus (S13) shown through mutation to be essential for kinase recruitment (Miyata & Nishida, 2004, 2007). The reason why this phosphorylation is essential has yet to be worked out, but we suggest that Cdc37 dephosphorylation might be a key part of the kinase recruitment process, keeping Cdc37^{pS13} attached to Hsp90 until the folded kinase leaves the complex and PP5 dephosphorylates Cdc37^{pS13}. The Hsp90:Cdc37 interaction has been proposed to happen with a stoichiometry of 1:1 or 1:2. For this reason, and for the complex's large conformational heterogeneity, affinity studies may require more than an ITC measurement to work out. Establishing a good affinity measurement system, ideally one that can differentiate between on and off rates would be incredibly helpful in the elucidation of a Hsp90-Kinase interaction mechanism by distinguishing between interactions with the phosphorylated and non-phosphorylated Cdc37.

Mechanism of PP5 substrate dephosphorylation – Kinase, GR and beyond

Another group published a biorxiv paper halfway through my investigation of the Hsp90:Cdc37:CRaf complex bound to PP5 (Oberoi et al., 2022), which led us to publish the yeast complex bound to E. coli PP5 at high resolution. At the time, improved samples (Hsp90:Cdc37:CRaf$^{304\text{-}648\ S338E}$:PP5$^{aJ\ del}$ or Hsp90:Cdc37:CRaf$^{304\text{-}648\ S338E}$:PP5^{H304A}) had been optimized and were ready to be placed on the microscope. The low-resolution structure acquired at the time (Fig. 4.4f) allowed superficial understanding of alternate PP5 conformations, but using a longer CRaf or even a full length CRaf complex might lead to fuller story about PP5 dephosphorylation. More micrographs or more particles might show an active PP5 and potentially even different populations of CRaf phosphorylation engagement. Furthermore,

understanding the PP5 active site – substrate engagement might explain why PP5 binds certain kinases while not others. This project would require little optimization past what is described in Chapter 4 and would be a great training project. If a larger number of particles does not yield high resolution PP5-CRaf engagement, playing around with disulfide bonded active sites might yield interesting results as well (Following the work of D. Southworth et al. with Hsp90:Hop interactions) (Southworth & Agard, 2011).

Through the work done by us and the Pearle Lab, PP5 has been shown to dephosphorylate in a rather non-specific manner (Oberoi et al., 2022). These observations might be explained by the high concentrations of PP5 used in the Pearle lab's experiments, or the in-vitro environment used by both our lab and the Pearle Lab. The difference between phosphorylation rates of different phosphorylation sites on CRaf seen in our work (Chapter 4) suggests that PP5 might have substrate preference. What determines this preference? The creation of constructs in which all phosphorylation sites but one are modified (S to A mutations) may explain substrate preference by PP5. The biophysics of this interaction, its dependence on linker length and substrate proximity may teach us more about the PP5 dephosphorylation mechanism. Additionally, while previous cellular studies by Kriegsheim et al. and our pulldowns (Fig. 3.7a), showed high specificity towards the CRaf pS338 phosphorylation site, that was not seen in our in vitro studies (Fig. 4.1) (von Kriegsheim et al., 2006). What might this specificity be due to? Are there important cofactors involved in giving PP5 specificity, and if so, may they also be Hsp90 cochaperones as explored in Chapter 3? Pulldowns of CRaf in cells expressing PP5 and the Hsp90:Cdc37:CRaf complex, followed by consequent mass spectrometry of additional bands coeluting with the complexes might yield some of these answers.

To further understand how PP5 interacts with other Hsp90 clients, rotation students in the lab, Claire Kokontis and Estelle Ronayane , showed that PP5 could also bind to an Hsp90-GR complex (More in Chari Noddings Thesis). While the Glucocorticoid Receptor (GR) construct used did not contain the phosphorylated residues of interest, nor did it contain any phosphorylation sites, PP5 could be seen bound to Hsp90 following their cryoEM analysis. This project could greatly benefit from a full-length GR construct, ideally a mammalian expressed GR construct with phosphorylation sites or a construct with phosphomimetics. Using mammalian GR and PP5 constructs available in the lab, co-expression of GR and PP5 followed by a pulldown straight from mammalian cells would be worth trying. Dephosphorylation rates and GR localization due to these phosphorylation sites would also be very valuable as existing experiments contradict each other's results.

PP5 has been shown to dephosphorylate Hsp90. In our work, PP5 seemed to dephosphorylate Hsp90 when purified from Hsp90:Cdc37:CRaf$^{\text{Full Length}}$ complexes, but not in Extended domain or Kinase domain complexes (Fig. 3.5). More could be learned from these experiments as these were not repeated. In-vitro experiments were also tried. These preliminary experiments showed that while CK2 can phosphorylate Hsp90 (especially in the presence of Cdc37), PP5 does not seem to dephosphorylate the CK2 phosphorylated Hsp90. These experiments were done with minimal amounts of CK2 and high concentrations of PP5, but CK2 was never removed from the samples stained and studied for phosphorylation. A logical next step would be to test PP5 dephosphorylation of Hsp90 after CK2 removal by pulldowns or size exclusion. Hsp90 phosphorylation and dephosphorylation has been studied in yeast and mammalian cells, so previously mapped out phosphomimetics could be purified, and the Hsp90 complexes closed as shown previously (Lee et al., 2021). This would then allow the incubation

of Hsp90 with PP5 to place the complex on grids and enquire further onto PP5 dephosphorylation of Hsp90.

Many many future directions exist from this work, and I'm excited to see where the field takes the study of Hsp90-Kinase interactions.

References

Arlander, S. J. H., Felts, S. J., Wagner, J. M., Stensgard, B., Toft, D. O., & Karnitz, L. M. (2006). Chaperoning Checkpoint Kinase 1 (Chk1), an Hsp90 Client, with Purified Chaperones. *Journal of Biological Chemistry*, *281*(5), 2989-2998. https://doi.org/10.1074/jbc.M508687200

Keramisanou, D., Aboalroub, A., Zhang, Z., Liu, W., Marshall, D., Diviney, A., Larsen, Randy W., Landgraf, R., & Gelis, I. (2016). Molecular Mechanism of Protein Kinase Recognition and Sorting by the Hsp90 Kinome-Specific Cochaperone Cdc37. *Molecular Cell*, *62*(2), 260-271. https://doi.org/10.1016/j.molcel.2016.04.005

Lee, K., Thwin, A. C., Nadel, C. M., Tse, E., Gates, S. N., Gestwicki, J. E., & Southworth, D. R. (2021). The structure of an Hsp90-immunophilin complex reveals cochaperone recognition of the client maturation state. *Molecular Cell*, *81*(17), 3496-3508.e3495. https://doi.org/10.1016/j.molcel.2021.07.023

Miyata, Y., & Nishida, E. (2004). CK2 Controls Multiple Protein Kinases by Phosphorylating a Kinase-Targeting Molecular Chaperone, Cdc37. *Molecular and Cellular Biology*, *24*(9), 4065-4074. https://doi.org/10.1128/MCB.24.9.4065-4074.2004

Miyata, Y., & Nishida, E. (2007). Analysis of the CK2-dependent phosphorylation of serine 13 in Cdc37 using a phospho-specific antibody and phospho-affinity gel electrophoresis: Cdc37 phosphorylation by CK2 and signaling kinases. *FEBS Journal*, *274*(21), 5690-5703. https://doi.org/10.1111/j.1742-4658.2007.06090.x

Oberoi, J., Aran-Guiu, X., Outwin, E. A., Schellenberger, P., Roumeliotis, T. I., Choudhary, J. S., & Pearl, L. H. (2022). *HSP90-CDC37-PP5 forms a structural platform for kinase dephosphorylation* [preprint]. http://biorxiv.org/lookup/doi/10.1101/2022.05.03.490524

Röck, R., Mayrhofer, J. E., Torres-Quesada, O., Enzler, F., Raffeiner, A., Raffeiner, P., Feichtner, A., Huber, R. G., Koide, S., Taylor, S. S., Troppmair, J., & Stefan, E. (2019). BRAF inhibitors promote intermediate BRAF(V600E) conformations and binary interactions with activated RAS. *Science Advances*, *5*(8), eaav8463. https://doi.org/10.1126/sciadv.aav8463

Roe, S. M., Ali, M. M. U., Meyer, P., Vaughan, C. K., Panaretou, B., Piper, P. W., Prodromou, C., & Pearl, L. H. (2004). The Mechanism of Hsp90 Regulation by the Protein Kinase-Specific Cochaperone p50cdc37. *Cell*, *116*(1), 87-98. https://doi.org/https://doi.org/10.1016/S0092-8674(03)01027-4

Southworth, Daniel R., & Agard, David A. (2011). Client-Loading Conformation of the Hsp90 Molecular Chaperone Revealed in the Cryo-EM Structure of the Human Hsp90:Hop Complex. *Molecular Cell*, *42*(6), 771-781. https://doi.org/https://doi.org/10.1016/j.molcel.2011.04.023

Verba, K. A., Wang, R. Y.-R., Arakawa, A., Liu, Y., Shirouzu, M., Yokoyama, S., & Agard, D. A. (2016). Atomic structure of Hsp90-Cdc37-Cdk4 reveals that Hsp90 traps and stabilizes an unfolded kinase. *Science*, *352*(6293), 1542-1547. https://doi.org/10.1126/science.aaf5023

von Kriegsheim, A., Pitt, A., Grindlay, G. J., Kolch, W., & Dhillon, A. S. (2006). Regulation of the Raf–MEK–ERK pathway by protein phosphatase 5. *Nature Cell Biology*, *8*(9), 1011-1016. https://doi.org/10.1038/ncb1465

Appendix

Methods

Buffers

Buffer Stocks

1M Tris pH 7.8

1M HEPES pH 7.5 (stored frozen)

4M NaCl

2M KCl

1M $MgCl_2$

0.1M $MnCl_2$

75% Glycerol

0.5M TCEP (stored frozen)

Binding Buffer – used for E. coli pellet resuspension

50mM Tris pH 7.8

500mM NaCl

5% Glycerol

5mM Imidazol pH 7.8

1 cOmplete Protease Inhibitor Cocktail tablet Roche/50mL E. coli pellet

0.5mM TCEP

0.75% IGEPAL for kinase prep only

Nickel Wash Buffer –

50mM Tris pH 7.8 (or 20mM HEPES for kinases)

250mM NaCl

0.5mM TCEP

5% Glycerol

30mM Imidazole pH 7.8 if 6X His or 50mM Imidazole pH 7.8 if 10X His

Nickel Elution Buffer –

50mM Tris pH 7.8 (or 20mM HEPES for kinases)

250mM NaCl

0.5mM TCEP

10% Glycerol

400mM Imidazole pH 7.8

Anion Exchange Buffer Low Salt –

20mM Tris pH 8.0

0.5mM EDTA

0.5mM TCEP

5% Glycerol

2mM $MgCl_2$

Anion Exchange Buffer High Salt –

20mM Tris pH 8.0

0.5mM EDTA

0.5mM TCEP

5% Glycerol

2mM MgCl2

1M NaCl

Protein Storage Buffer –

20 mM HEPES pH 7.5

150 mM KCl

10 mM MgCl2

0.5 mM TCEP

1 mM EDTA

2.5% Glycerol

Reaction Buffer –

20 mM HEPES pH 7.5

50 mM KCl

10 mM MgCl2

0.5 mM TCEP

1 mM EDTA

Maleimide dye protein labeling buffer –

20 mM HEPES pH 7.5

150 mM KCl

10 mM MgCl2

2.5% Glycerol

Individual protein expression

The Hsp90, Cdc37, PP5, and sBRaf plasmids were transfected into *E. coli* BL21 cells, and plated on antibiotic agarose plates. Overnight cultures of one colony were grown in Terrific Broth media (TB media), after which 10 mL of culture were transferred into 2-6 L of TB media. Once the cultures grew to an $O.D._{600}$ of 0.6, cells were allowed to shake (180 R.P.M.) at 16°C for an hour after which they were induced with 1 mM IPTG. The temperature of the cultures was then raised to 18°C and allowed to shake overnight (160 R.P.M.). The pellets were then spun down (4,500 xg for 10 min) and frozen until protein purification.

Individual protein purification

The thawed pellets were then resuspended with Lysis Buffer (500 mM NaCl, 50 mM Tris pH 7.8, 5% Imidazole, 5% glycerol, 1 Protease Inhibitor Tablet / 50 mL of pellet suspension, 0.5 mM TCEP), and the sample was sonicated in an ice bath for five cycles, 1 minute/cycle, with at least a minute between cycles. The sample was then spun down at 35,000 xg for 30 min at 4°C. The lysate was then run through HisTrap FF (5mL) Nickel columns (1-2 columns) at 5 ml/min. The column was loaded onto an AKTA FPLC instrument and washed with Wash Buffer (50 mM Tris pH 7.8, 250 mM NaCl, 0.5 mM TCEP, 5% glycerol, 30 mM Imidazole, PP5 buffer included 1

mM Manganese), and then eluted with Elution Buffer (Wash Buffer with 10% glycerol and 400 mM Imidazole). The purified lysate was then concentrated down to 5-7 mL of lysate using a Centricon tube, and subsequently cleaved overnight (3C or TEV depending on plasmid).

The cleaved sample was diluted down to ~50 mL using Low Salt Buffer (20 mM Tris pH 8.0, 1mM EDTA, 0.5 mM TCEP, 5% Glycerol, PP5 buffer included 1mM Manganese), filtered, and loaded onto a 50 mL superloop. This sample was then run through an AKTA FPLC MonoQ 10/100 column (Cytiva), eluting through a salt gradient (0-1 M NaCl). An SDS PAGE Gel was run to select the peaks of interest, which were isolated and concentrated down to ~250 μL. The sample was then filtered and loaded onto a Superdex 200 16/600 (Cytiva) column in Storage Buffer (20 mM Hepes, 150 mM KCl, 1 mM EDTA, 1 mM TCEP, 5% glycerol). The cleanest protein fractions as dictated by an SDS PAGE Gel were concentrated and flash frozen in liquid nitrogen for storage at -80°C.

sBRaf purification was slightly modified to improve kinase solubility: 0.75% IGEPAL was added to the Lysis Buffer, 20 mM HEPES was used instead of 20 mM Tris throughout the purification, and 10% Glycerol was used. BRaf was not cleaved overnight, and so the purification process took place in one day.

Protein complex expression

Hsp90:Cdc37:CRaf complexes were purified from either yeast (sample used for main Hsp90:Cdc37:CRaf:PP5 structure) or mammalian cells (sample used for biochemistry and low resolution structure).

Yeast expression: Constructs were cloned into a 83 nu yeast expression vector, and transformed into JEL1 yeast strain using Zymo Research EZ transformation protocol and plated onto SD-His plates. After 3 days a colony was expanded into 200 mL overnight cultures. 1 L of YPGL media was inculcated with 10 mL of overnight culture. Cultures were induced with 2 % w/v galactose at an $O.D._{600}$ of 0.6 – 0.8 to induce expression. Temperature was reduced to 16°C and cultures were pelleted after 18 hours (4,500 xg for 5 min). Pellets were resuspended in minimal yeast resuspension buffer (20 mM HEPES-KOH pH 7.5, 150 mM KCl, 10% glycerol) and frozen drop wise into a container of liquid nitrogen.

Mammalian expression: Constructs were cloned into a pcDNA3.1 expression vector. Mammalian HEK293 cells were seeded at 0.5 M/mL and allowed to reach a confluency of 3 M/mL. Media was exchanged three hours before transfection and cells were allowed to recover. The Expi293™ Expression system kit and protocol was used for transformation. Cells were allowed to grow for 48 - 72 hours before they were spun down at 5,000 xg, reconstituted with PBS and frozen dropwise into liquid nitrogen.

The frozen yeast or mammalian cell drops were then ground in a cryoMill for 5 cycles (Precool 5 min, Run 1:30 min, Cool 2 min, 10 cps Rate).

Protein complex purification

The protein complex samples were reconstituted with Strep Binding Buffer (20 mM HEPES, 150 mM KCl, 10 mM MgCl, 1 mM TCEP, 10% glycerol, 0.05% Tween) with NaMo (20 mM) added when purifying the more stable “closed” Hsp90 complex. The sample was loaded onto a StrepTrap HP (Cytiva, 5 mL) column at a rate of 5 ml/min and subsequently washed with 20 mL of Strep Binding Buffer in an AKTA FPLC instrument at a flow rate of 5 ml/min and then

eluted with 10 mL of Elution Buffer (Strep Binding Buffer with 10 mM Desthiobiotin). The elution fractions were then concentrated down to 250 μL and loaded onto the Superdex 200 16/600 (Cytiva) column. After running the sample through the column using Storage Buffer (20 mM Hepes, 150 mM KCl, 1 mM EDTA, 1 mM TCEP, 5% glycerol), and SDS PAGE Gel was run to choose the peak to be concentrated, flash frozen with liquid nitrogen and finally stored at -80°C.

Dephosphorylation Assays

PP5 Dephosphorylation reactions were carried out in Reaction Buffer (20 mM Hepes, 50 mM KCl, 10 mM Mg2Cl, 1 mM TCEP, 1 mM EDTA) in PCR tubes.

Phosphorylation Gel Stain – (1) Protein samples were run on SDS gels. (2) The gels were then fixed with 100mL of solution made up of 50% methanol and 10% acetic acid for 30 min, and then fresh buffer was added and allowed to incubate with the gel overnight. The gel got smaller. (3) The gel was then washed 3 times on a nutator for 10min with 100mL per wash. (4) From this step on, the gel was incubated in a dark container. The gel was then stained on a nutator with 60mL of Pro-Q Diamond stain (ThermoFisher) for 90min. (5) The gel was destained 3 ties, with 100mL of 20% acetonitrile, 50mM sodium acetate pH 4 solution on a nutator. (6) Finally, the gel was washed twice for 5 min each with 100mL of ultrapure water. The gel could then be imaged by excitation around 500nm. Once the gels had been stained to test levels of phosphorylation, remove the ultrapure water and incubate the gel in SYPRO Ruby gel stain overnight. The gel was then washed with 100mL of 10% methanol and 7% acetic acid for 30 min before imaging.

Phosphorylation specific Western blot - Buffer exchanged Hsp90:Cdc37:CRaf, Hsp90:Cdc37, $Hsp90^{Open}$ or $Hsp90^{Closed}$ complexes were placed on a 25°C thermocycler (~1 min) before PP5 addition. The reaction began after PP5 was added and the sample was

thoroughly mixed. Sample was removed from the thermocycler at each timepoint, and the reaction was quenched using SDS-DTT. Dephosphorylation conditions were optimized such that the PP5 concentrations used were ideal for western blot visualization. 3 μM of $Cdc37^{pS13}$ and equimolar constituents were used for Cdc37 blots, with a final addition of 750nM of $PP5^{WT}$ or $PP5^{mutant}$. 1.5 μM of Hsp90:Cdc37:CRaf complex with 75 nM of PP5 were used for Fig. 1 experiments, while 3 μM of Hsp90:Cdc37:CRaf complex and 150 nM PP5 were used for $PP5^{mutant}$ experiments.

The samples were run on Bolt™ 4-12% Bis-Tris gels (140 V, 65 min) using the Color Protein Standard, (NEB# P7712, Broad Range (10-250 kDa)) for molecular weight differentiation. The gels were next transferred using Invitrogen's iBlot® Gel Transfer Stacks (Nitrocellulose), following the transfer kit protocol (10 min transfer) and then stained with Ponzo stain for ~5 min to ensure equal protein transfer and constant protein concentrations (Sup. Figs. 2, 9). The membranes were then incubated with 5% milk on a room temperature nutator for one hour. Primary antibodies against $Cdc37^{pS13}$ (1:5000 Phospho-CDC37 (Ser13) (D8P8F) Rabbit mAb #13248), $CRaf^{pS338}$ (1:1000, # MA5-15176 Phospho-c-Raf (Ser338) Monoclonal Antibody(E.838.4)) or $CRaf^{pS621}$(1:1000, #MA5-33196 Phospho-c-Raf (Ser621) Recombinant Rabbit Monoclonal Antibody) were then added to the membrane with 5% milk and nutated overnight at 4°C. The membrane was next washed with TBST (80mM Tris Base, 550mM NaCl, 1% Tween 20 (v/w)) three times, 15 min/wash. HRP Secondary antibody was then added to the membrane (1:10000, Anti-Rabbit NA9340V GE Healthcare UK Limited) and allowed to incubate on a nutator for 1h at RT. Next, the membrane was washed three times with TBST for 15 min/wash and exposed using the Thermofisher protocol and chemiluminescent agents (Pierce™ ECL Western Blotting Substrate, Catalog number: 32109).

An Azure biosystems imager was used to capture Ponceau and chemiluminescence Western Blot images. The images were then analyzed using the ImageJ software (Schneider et

al., 2012). Each sample was run at least three separate times to ensure replicability. The western blots were then normalized by the phosphorylated control sample (not incubated with PP5) using the Prism software. A one-phase linear decay curve was fit to dephosphorylation vs time data, and the rates of decay were compared using an ordinary one-way ANOVA test within Prism. Multiple hypothesis testing was carried out within Prism. For visualization purposes, dephosphorylation rates for mutants were normalized to wildtype rates. All these values were then plotted with standard error of the mean error bars.

EM Sample Preparation

Complexes were incubated for 30 min on ice, then brought to room temperature and mixed with 0.05% glutaraldehyde (15 min). The reaction was quenched with 50 mM Tris buffer pH 8. The sample was then filtered (PVDF 0.1μm), and 25 μL of sample were injected into the Ettan liquid chromatography system, where it ran through the Superdex 200 3.2/200 column (Cytiva) in running buffer (20mM Hepes pH 7.5, 50mM KCl, 1mM EDTA and 1mM TCEP). The fractions with the complex of interest were separated from the PP5 excess, concentrated to ~300nM and added to grids.

Negative stain – 4μL of sample were added to glow discharged grids (PELCO easiGlow, 15mA, Glow: 30s, Hold: 30s; 300 mesh Cu) with a wait time of 30s. The sample was then blotted, placed sample down into a 40μL drop of water, blotted, placed into a 40μL drop of water for a couple of seconds, blotted, placed into a 40μL drop of uranyl formate, blotted, and placed into a 40μL drop of uranyl formate for a couple of seconds, blotted, dried by vacuum, and stored.

cryoEM - Sample was added to Quantifoil grids (R1.2/1.3, gold, covered with a monolayer of graphene oxide derivatized with amino-PEG groups) in a FEI Vitrobot chamber (3μL of sample, 10°C, 100% humidity, 30s Wait Time, 3s Blot Time, -2 Blot Force) and plunged into liquid ethane (F. Wang, Liu, et al., 2020; F. Wang, Yu, et al., 2020). Frozen grids were then stored in liquid nitrogen.

FCS assays

Purified proteins (~50μM) of interest were incubated with 0.8X malemide Alexa488 dye for ~6 hours at 4°C on a nutator. The sample was then buffer exchanged using a 7MWCO Zeba™ Spin Desalting Column, and subsequently purified using a Superdex 200 3.2/300 column (Cytiva). The dilute sample was then aliquoted and flash frozen in liquid nitrogen for future use. The thawed sample was spun down to remove aggregates and added at a constant final concentration of ~20 nM to the testing conditions of interest. Samples were placed on microscope cover glass slides (High Precision, Deckgläser 22 x 22 mm, 170±5 μm No. 1.5H) and mounted on a CorTector SX100 instrument (LightEdge Technologies, Beijing, China) equipped with a 488 nm laser. Autocorrelation measurements recorded at room temperature. Aggregate data was discarded through curve analysis. Atto488 dye was used to calibrate the measurement volume (S). The mean of various replicate autocorrelation measurements was then fit to an equation which accounts for single 3D diffusion and triplet dynamics, starting at autocorrelation values of 0.001ms.

$$(1) \qquad G(\tau) = \frac{1 - T + T * e^{\frac{-\tau}{\tau T}}}{1 - T} * \frac{1}{N} * \frac{1}{1 + \frac{\tau}{\tau_D}} * \frac{1}{\sqrt{1 + \frac{\tau}{\tau_D * S^2}}}$$

Plasmid Library

Cdc37

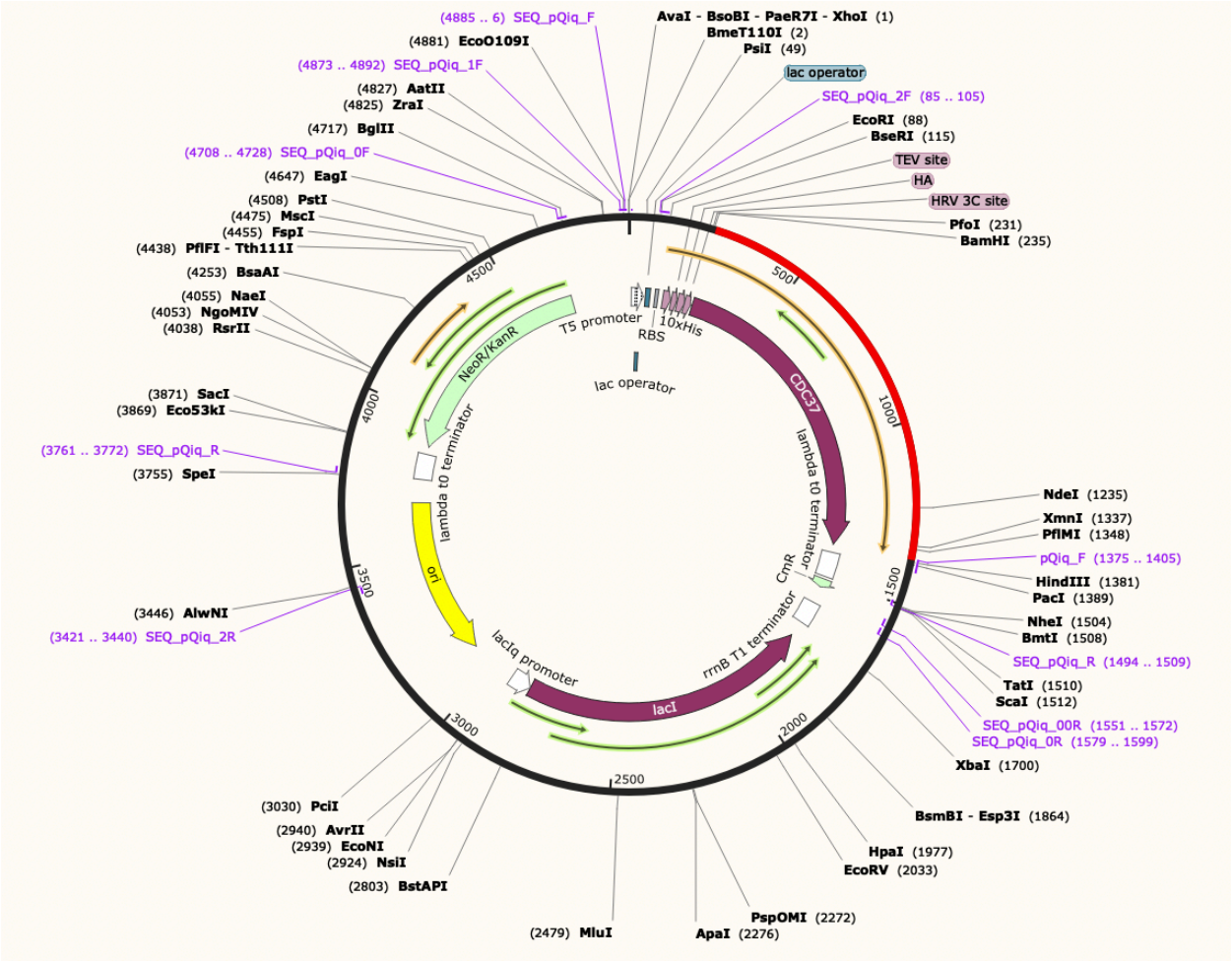

CTCGAGAAATCATAAAAAATTTATTTGCTTTGTGAGCGGATAACAATTATAATAGATTCAATTGTGAG
CGGATAACAATTTCACACAGAATTCATTAAAGAGGAGAAATTAACTatgagaggatcgcatcatcaccaccatcaccatcat
catcacggcGAAAATCTGTATTTTCAGGGTAGCTATCCGTATGATGTGCCGGATTATGCActggaagtgctgtttcaggg
tccgggatccATGGTTGATTACTCTGTTTGGGATCATATCGAAGTTTCAGATGATGAAGATGAAACTCATCC
AAACATTGATACAGCTTCTTTGTTTAGATGGAGACATCAAGCAAGAGTTGAAAGAATGGAACAATTCC
AAAAGGAAAAGGAAGAATTAGATAGAGGTTGTAGAGAGTGTAAGAGAAAGGTTGCTGAATGTCAAA
GAAAATTGAAGGAATTAGAAGTTGCTGAAGGTGGTAAAGCAGAATTGGAAAGATTACAAGCAGAAGC
TCAACAATTGAGAAAGGAAGAAAGATCATGGGAACAAAAATTGGAAGAAATGAGAAAGAAAGAAAA
ATCTATGCCATGGAACGTTGATACTTTGTCAAAGGATGGTTTTTCAAAATCTATGGTTAATACTAAACC
AGAAAAGACTGAAGAAGATTCAGAAGAAGTTAGAGAACAAAAGCATAAGACATTCGTTGAAAAGTAC
GAAAAACAAATTAAACATTTTGGCATGTTGAGAAGATGGGATGATTCTCAAAAGTATTTGTCAGATAA
CGTTCATTTGGTTTGTGAAGAAACTGCTAACTACTTAGTTATTTGGTGTATTGATTTGGAAGTTGAAGA

AAAGTGTGCTTTGATGGAACAAGTTGCACATCAAACAATCGTTATGCAATTCATTTTGGAATTGGCTA
AATCTTTAAAGGTTGATCCAAGAGCATGTTTCAGACAATTTTTCACTAAGATTAAAACAGCTGATAGA
CAATACATGGAAGGTTTTAATGATGAATTGGAAGCCTTTAAAGAAAGAGTTAGAGGTAGAGCTAAATT
GAGAATCGAAAAGGCAATGAAGGAATACGAAGAAGAGGAAAGAAAGAAAAGATTGGGTCCAGGTGG
TTTAGATCCAGTTGAAGTTTACGAATCTTTACCAGAAGAATTGCAAAAGTGTTTCGATGTTAAGGATGT
TCAAATGTTGCAAGATGCTATTTCTAAGATGGACCCAACTGATGCAAAGTACCATATGCAAAGATGTA
TTGATTCAGGTTTGTGGGTTCCAAATTCTAAAGCATCTGAAGCAAAAGAAGGTGAAGAAGCTGGTCCA
GGTGACCCATTGTTAGAAGCAGTTCCAAAAACTGGTGACGAAAAGGATGTTTCTGTTtaatgaaagcttaattaatg
aCTGAGCTTGGACTCCTGTTGATAGATCCAGTAATGACCTCAGAACTCCATCTGGATTTGTTCAGAACG
CTCGGTTGCCGCCGGGCGTTTTTTATTGGTGAGAATCCAAGCTAGCAGTACTGCGATGAGTGGCAGGG
CGGGGCGTAATTTTTTTAAGGCAGTTATTGGTGCCCTTAAACGCCTGGGGTAATGACTCTCTAGTTTGA
GGCATCAAATAAAACGAAAGGCTCAGTCGAAAGACTGGGCCTTTCGTTTTATCTGTTGTTTGTCGGTG
AACGCTCTCCTGAGTAGGACAAATCCGCCGCTCTAGAGATTTCCCTCGACAATTCGCGCTAACTTACAT
TAATTGCGTTGCGCTCACTGCCCGCTTTCCAGTCGGGAAACCTGTCGTGCCAGCTGCATTAATGAATCG
GCCAACGCGCGGGGAGAGGCGGTTTGCGTATTGGGCGCCAGGGTGGTTTTTCTTTTCACCAGTGAGAC
GGGCAACAGCTGATTGCCCTTCACCGCCTGGCCCTGAGAGAGTTGCAGCAAGCGGTCCACGCTGGTTT
GCCCCAGCAGGCGAAAATCCTGTTTGATGGTGGTTAACGGCGGGATATAACATGAGCTGTCTTCGGTA
TCGTCGTATCCCACTACCGAGATATCCGCACCAACGCGCAGCCCGGACTCGGTAATGGCGCGCATTGC
GCCCAGCGCCATCTGATCGTTGGCAACCAGCATCGCAGTGGGAACGATGCCCTCATTCAGCATTTGCA
TGGTTTGTTGAAAACCGGACATGGCACTCCAGTCGCCTTCCCGTTCCGCTATCGGCTGAATTTGATTGC
GAGTGAGATATTTATGCCAGCCAGCCAGACGCAGACGCGCCGAGACAGAACTTAATGGGCCCGCTAA
CAGCGCGATTTGCTGGTGACCCAATGCGACCAGATGCTCCACGCCCAGTCGCGTACCGTCTTCATGGG
AGAAAATAATACTGTTGATGGGTGTCTGGTCAGAGACATCAAGAAATAACGCCGGAACATTAGTGCA
GGCAGCTTCCACAGCAATGGCATCCTGGTCATCCAGCGGATAGTTAATGATCAGCCCACTGACGCGTT
GCGCGAGAAGATTGTGCACCGCCGCTTTACAGGCTTCGACGCCGCTTCGTTCTACCATCGACACCACC
ACGCTGGCACCCAGTTGATCGGCGCGAGATTTAATCGCCGCGACAATTTGCGACGGCGCGTGCAGGGC
CAGACTGGAGGTGGCAACGCCAATCAGCAACGACTGTTTGCCCGCCAGTTGTTGTGCCACGCGGTTGG
GAATGTAATTCAGCTCCGCCATCGCCGCTTCCACTTTTTCCCGCGTTTTCGCAGAAACGTGGCTGGCCT
GGTTCACCACGCGGGAAACGGTCTGATAAGAGACACCGGCATACTCTGCGACATCGTATAACGTTACT
GGTTTCACATTCACCACCCTGAATTGACTCTCTTCCGGGCGCTATCATGCCATACCGCGAAAGGTTTTG
CACCTTTCGATGGTGTCAACGTAAATGCATGCCGCTTCGCCTTCCCTAGGGCGTTCGGCTGCGGCGAGC
GGTATCAGCTCACTCAAAGGCGGTAATACGGTTATCCACAGAATCAGGGGATAACGCAGGAAAGAAC
ATGTGAGCAAAAGGCCAGCAAAAGGCCAGGAACCGTAAAAAGGCCGCGTTGCTGGCGTTTTTCCATA
GGCTCCGCCCCCCTGACGAGCATCACAAAAATCGACGCTCAAGTCAGAGGTGGCGAAACCCGACAGG
ACTATAAAGATACCAGGCGTTTCCCCCTGGAAGCTCCCTCGTGCGCTCTCCTGTTCCGACCCTGCCGCT
TACCGGATACCTGTCCGCCTTTCTCCCTTCGGGAAGCGTGGCGCTTTCTCATAGCTCACGCTGTAGGTA
TCTCAGTTCGGTGTAGGTCGTTCGCTCCAAGCTGGGCTGTGTGCACGAACCCCCCGTTCAGCCCGACCG
CTGCGCCTTATCCGGTAACTATCGTCTTGAGTCCAACCCGGTAAGACACGACTTATCGCCACTGGCAGC
AGCCACTGGTAACAGGATTAGCAGAGCGAGGTATGTAGGCGGTGCTACAGAGTTCTTGAAGTGGTGG
CCTAACTACGGCTACACTAGAAGGACAGTATTTGGTATCTGCGCTCTGCTGAAGCCAGTTACCTTCGG
AAAAAGAGTTGGTAGCTCTTGATCCGGCAAACAAACCACCGCTGGTAGCGGTGGTTTTTTTGTTTGCA
AGCAGCAGATTACGCGCAGAAAAAAAGGATCTCAAGAAGATCCTTTGATCTTTTCTACGGGGTCTGAC
GCTCAGTGGAACGAAAACTCACGTTAAGGGATTTTGGTCATGACTAGTGCTTGGATTCTCACCAATAA
AAAACGCCCGGCGGCAACCGAGCGTTCTGAACAAATCCAGATGGAGTTCTGAGGTCATTACTGGATCT
ATCAACAGGAGTCCAAGCGAGCTCTCGAACCCCAGAGTCCCGCTCAGAAGAACTCGTCAAGAAGGCG
ATAGAAGGCGATGCGCTGCGAATCGGGAGCGGCGATACCGTAAAGCACGAGGAAGCGGTCAGCCCAT
TCGCCGCCAAGCTCTTCAGCAATATCACGGGTAGCCAACGCTATGTCCTGATAGCGGTCCGCCACACC
CAGCCGGCCACAGTCGATGAATCCAGAAAAGCGGCCATTTTCCACCATGATATTCGGCAAGCAGGCAT
CGCCATGGGTCACGACGAGATCCTCGCCGTCGGGCATGCGCGCCTTGAGCCTGGCGAACAGTTCGGCT
GGCGCGAGCCCCTGATGCTCTTCGTCCAGATCATCCTGATCGACAAGACCGGCTTCCATCCGAGTACG
TGCTCGCTCGATGCGATGTTTCGCTTGGTGGTCGAATGGGCAGGTAGCCGGATCAAGCGTATGCAGCC
GCCGCATTGCATCAGCCATGATGGATACTTTCTCGGCAGGAGCAAGGTGAGATGACAGGAGATCCTGC
CCCGGCACTTCGCCCAATAGCAGCCAGTCCCTTCCCGCTTCAGTGACAACGTCGAGCACAGCTGCGCA
AGGAACGCCCGTCGTGGCCAGCCACGATAGCCGCGCTGCCTCGTCCTGCAGTTCATTCAGGGCACCGG
ACAGGTCGGTCTTGACAAAAAGAACCGGGCGCCCCTGCGCTGACAGCCGGAACACGGCGGCATCAGA
GCAGCCGATTGTCTGTTGTGCCCAGTCATAGCCGAATAGCCTCTCCACCCAAGCGGCCGGAGAACCTG

CGTGCAATCCATCTTGTTCAATCATGCGAAACGATCCTCATCCTGTCTCTTGATCAGATCTTGATCCCCT
GCGCCATCAGATCCTTGTCGGCAAGAAAGCCATCCAGTTTACTTTGCAGGGCTTCCCAACCTTACCAG
AGGGCGCCCCAGCTGGCAATTCCGACGTCTAAGAAACCATTATTATCATGACATTAACCTATAAAAAT
AGGCGTATCACGAGGCCCTTTCGTCTTCAC

sBRaf

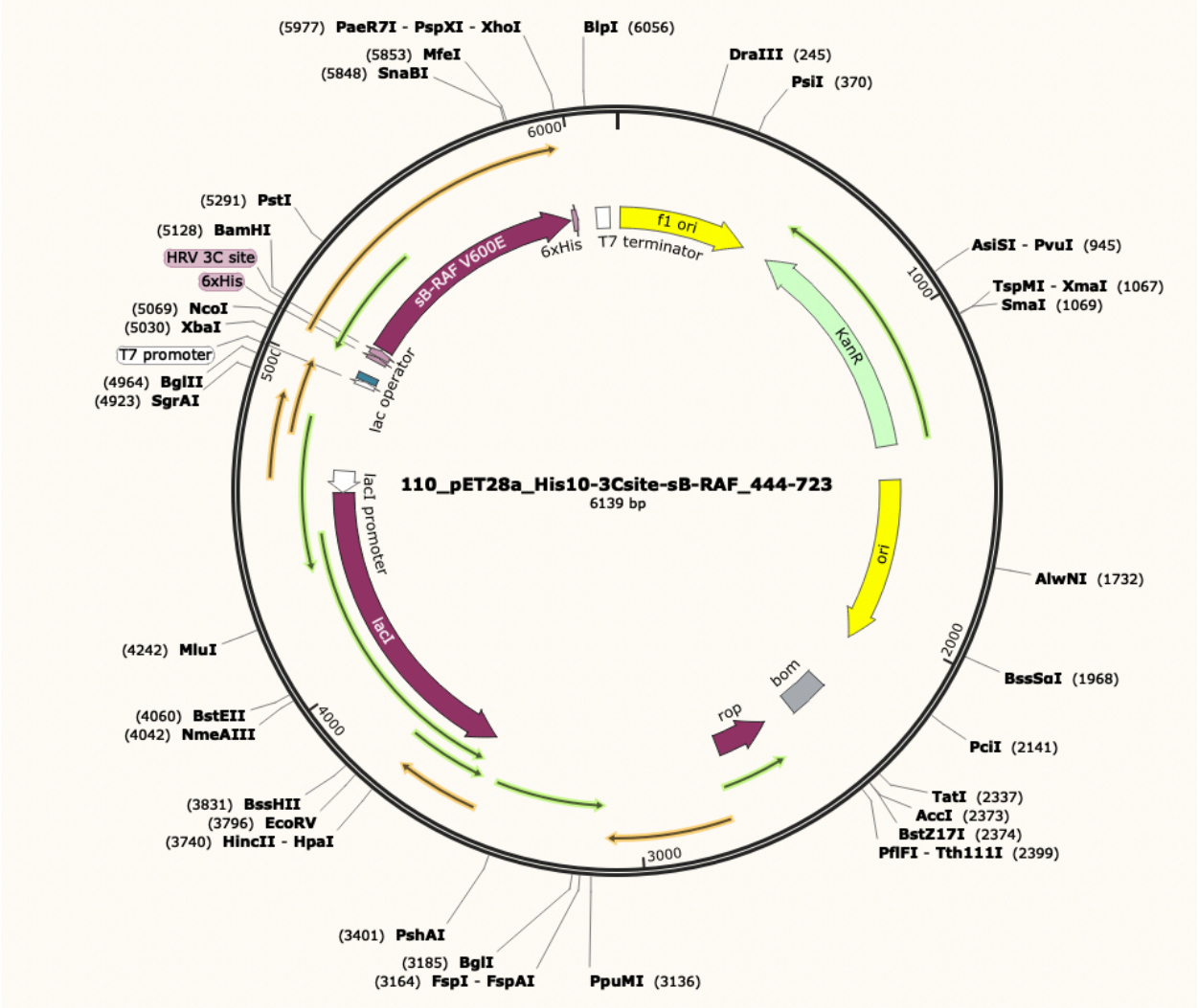

TGGCGAATGGGACGCGCCCTGTAGCGGCGCATTAAGCGCGGCGGGTGTGGTGGTTACGCGCAGCGTG
ACCGCTACACTTGCCAGCGCCCTAGCGCCCGCTCCTTTCGCTTTCTTCCCTTCCTTTCTCGCCACGTTCG
CCGGCTTTCCCCGTCAAGCTCTAAATCGGGGGCTCCCTTTAGGGTTCCGATTTAGTGCTTTACGGCACC
TCGACCCCAAAAAACTTGATTAGGGTGATGGTTCACGTAGTGGGCCATCGCCCTGATAGACGGTTTTT
CGCCCTTTGACGTTGGAGTCCACGTTCTTTAATAGTGGACTCTTGTTCCAAACTGGAACAACACTCAAC
CCTATCTCGGTCTATTCTTTTGATTTATAAGGGATTTTGCCGATTTCGGCCTATTGGTTAAAAAATGAGC
TGATTTAACAAAAATTTAACGCGAATTTTAACAAAATATTAACGTTTACAATTTCAGGTGGCACTTTTC

GGGGAAATGTGCGCGGAACCCCTATTTGTTTATTTTTCTAAATACATTCAAATATGTATCCGCTCATGA
ATTAATTCTTAGAAAAACTCATCGAGCATCAAATGAAACTGCAATTTATTCATATCAGGATTATCAATA
CCATATTTTTGAAAAAGCCGTTTCTGTAATGAAGGAGAAAACTCACCGAGGCAGTTCCATAGGATGGC
AAGATCCTGGTATCGGTCTGCGATTCCGACTCGTCCAACATCAATACAACCTATTAATTTCCCCTCGTC
AAAAATAAGGTTATCAAGTGAGAAATCACCATGAGTGACGACTGAATCCGGTGAGAATGGCAAAAGT
TTATGCATTTCTTTCCAGACTTGTTCAACAGGCCAGCCATTACGCTCGTCATCAAAATCACTCGCATCA
ACCAAACCGTTATTCATTCGTGATTGCGCCTGAGCGAGACGAAATACGCGATCGCTGTTAAAAGGACA
ATTACAAACAGGAATCGAATGCAACCGGCGCAGGAACACTGCCAGCGCATCAACAATATTTTCACCTG
AATCAGGATATTCTTCTAATACCTGGAATGCTGTTTTCCCGGGGATCGCAGTGGTGAGTAACCATGCAT
CATCAGGAGTACGGATAAAATGCTTGATGGTCGGAAGAGGCATAAATTCCGTCAGCCAGTTTAGTCTG
ACCATCTCATCTGTAACATCATTGGCAACGCTACCTTTGCCATGTTTCAGAAACAACTCTGGCGCATCG
GGCTTCCCATACAATCGATAGATTGTCGCACCTGATTGCCCGACATTATCGCGAGCCCATTTATACCCA
TATAAATCAGCATCCATGTTGGAATTTAATCGCGGCCTAGAGCAAGACGTTTCCCGTTGAATATGGCTC
ATAACACCCCTTGTATTACTGTTTATGTAAGCAGACAGTTTTATTGTTCATGACCAAAATCCCTTAACG
TGAGTTTTCGTTCCACTGAGCGTCAGACCCCGTAGAAAAGATCAAAGGATCTTCTTGAGATCCTTTTTT
TCTGCGCGTAATCTGCTGCTTGCAAACAAAAAAACCACCGCTACCAGCGGTGGTTTGTTTGCCGGATC
AAGAGCTACCAACTCTTTTTCCGAAGGTAACTGGCTTCAGCAGAGCGCAGATACCAAATACTGTCCTT
CTAGTGTAGCCGTAGTTAGGCCACCACTTCAAGAACTCTGTAGCACCGCCTACATACCTCGCTCTGCTA
ATCCTGTTACCAGTGGCTGCTGCCAGTGGCGATAAGTCGTGTCTTACCGGGTTGGACTCAAGACGATA
GTTACCGGATAAGGCGCAGCGGTCGGGCTGAACGGGGGGTTCGTGCACACAGCCCAGCTTGGAGCGA
ACGACCTACACCGAACTGAGATACCTACAGCGTGAGCTATGAGAAAGCGCCACGCTTCCCGAAGGGA
GAAAGGCGGACAGGTATCCGGTAAGCGGCAGGGTCGGAACAGGAGAGCGCACGAGGGAGCTTCCAG
GGGGAAACGCCTGGTATCTTTATAGTCCTGTCGGGTTTCGCCACCTCTGACTTGAGCGTCGATTTTTGT
GATGCTCGTCAGGGGGGCGGAGCCTATGGAAAAACGCCAGCAACGCGGCCTTTTTACGGTTCCTGGCC
TTTTGCTGGCCTTTTGCTCACATGTTCTTTCCTGCGTTATCCCCTGATTCTGTGGATAACCGTATTACCG
CCTTTGAGTGAGCTGATACCGCTCGCCGCAGCCGAACGACCGAGCGCAGCGAGTCAGTGAGCGAGGA
AGCGGAAGAGCGCCTGATGCGGTATTTTCTCCTTACGCATCTGTGCGGTATTTCACACCGCATATATGG
TGCACTCTCAGTACAATCTGCTCTGATGCCGCATAGTTAAGCCAGTATACACTCCGCTATCGCTACGTG
ACTGGGTCATGGCTGCGCCCCGACACCCGCCAACACCCGCTGACGCGCCCTGACGGGCTTGTCTGCTC
CCGGCATCCGCTTACAGACAAGCTGTGACCGTCTCCGGGAGCTGCATGTGTCAGAGGTTTTCACCGTC
ATCACCGAAACGCGCGAGGCAGCTGCGGTAAAGCTCATCAGCGTGGTCGTGAAGCGATTCACAGATG
TCTGCCTGTTCATCCGCGTCCAGCTCGTTGAGTTTCTCCAGAAGCGTTAATGTCTGGCTTCTGATAAAG
CGGGCCATGTTAAGGGCGGTTTTTTCCTGTTTGGTCACTGATGCCTCCGTGTAAGGGGGATTTCTGTTC
ATGGGGGTAATGATACCGATGAAACGAGAGAGGATGCTCACGATACGGGTTACTGATGATGAACATG
CCCGGTTACTGGAACGTTGTGAGGGTAAACAACTGGCGGTATGGATGCGGCGGGACCAGAGAAAAAT
CACTCAGGGTCAATGCCAGCGCTTCGTTAATACAGATGTAGGTGTTCCACAGGGTAGCCAGCAGCATC
CTGCGATGCAGATCCGGAACATAATGGTGCAGGGCGCTGACTTCCGCGTTTCCAGACTTTACGAAACA

CGGAAACCGAAGACCATTCATGTTGTTGCTCAGGTCGCAGACGTTTTGCAGCAGCAGTCGCTTCACGT
TCGCTCGCGTATCGGTGATTCATTCTGCTAACCAGTAAGGCAACCCCGCCAGCCTAGCCGGGTCCTCA
ACGACAGGAGCACGATCATGCGCACCCGTGGGGCCGCCATGCCGGCGATAATGGCCTGCTTCTCGCCG
AAACGTTTGGTGGCGGGACCAGTGACGAAGGCTTGAGCGAGGGCGTGCAAGATTCCGAATACCGCAA
GCGACAGGCCGATCATCGTCGCGCTCCAGCGAAAGCGGTCCTCGCCGAAAATGACCCAGAGCGCTGC
CGGCACCTGTCCTACGAGTTGCATGATAAAGAAGACAGTCATAAGTGCGGCGACGATAGTCATGCCCC
GCGCCCACCGGAAGGAGCTGACTGGGTTGAAGGCTCTCAAGGGCATCGGTCGAGATCCCGGTGCCTA
ATGAGTGAGCTAACTTACATTAATTGCGTTGCGCTCACTGCCCGCTTTCCAGTCGGGAAACCTGTCGTG
CCAGCTGCATTAATGAATCGGCCAACGCGCGGGGAGAGGCGGTTTGCGTATTGGGCGCCAGGGTGGTT
TTTCTTTTCACCAGTGAGACGGGCAACAGCTGATTGCCCTTCACCGCCTGGCCCTGAGAGAGTTGCAGC
AAGCGGTCCACGCTGGTTTGCCCCAGCAGGCGAAAATCCTGTTTGATGGTGGTTAACGGCGGGATATA
ACATGAGCTGTCTTCGGTATCGTCGTATCCCACTACCGAGATATCCGCACCAACGCGCAGCCCGGACT
CGGTAATGGCGCGCATTGCGCCCAGCGCCATCTGATCGTTGGCAACCAGCATCGCAGTGGGAACGATG
CCCTCATTCAGCATTTGCATGGTTTGTTGAAAACCGGACATGGCACTCCAGTCGCCTTCCCGTTCCGCT
ATCGGCTGAATTTGATTGCGAGTGAGATATTTATGCCAGCCAGCCAGACGCAGACGCGCCGAGACAGA
ACTTAATGGGCCCGCTAACAGCGCGATTTGCTGGTGACCCAATGCGACCAGATGCTCCACGCCCAGTC
GCGTACCGTCTTCATGGGAGAAAATAATACTGTTGATGGGTGTCTGGTCAGAGACATCAAGAAATAAC
GCCGGAACATTAGTGCAGGCAGCTTCCACAGCAATGGCATCCTGGTCATCCAGCGGATAGTTAATGAT
CAGCCCACTGACGCGTTGCGCGAGAAGATTGTGCACCGCCGCTTTACAGGCTTCGACGCCGCTTCGTT
CTACCATCGACACCACCACGCTGGCACCCAGTTGATCGGCGCGAGATTTAATCGCCGCGACAATTTGC
GACGGCGCGTGCAGGGCCAGACTGGAGGTGGCAACGCCAATCAGCAACGACTGTTTGCCCGCCAGTT
GTTGTGCCACGCGGTTGGGAATGTAATTCAGCTCCGCCATCGCCGCTTCCACTTTTTCCCGCGTTTTCG
CAGAAACGTGGCTGGCCTGGTTCACCACGCGGGAAACGGTCTGATAAGAGACACCGGCATACTCTGC
GACATCGTATAACGTTACTGGTTTCACATTCACCACCCTGAATTGACTCTCTTCCGGGCGCTATCATGC
CATACCGCGAAAGGTTTTGCGCCATTCGATGGTGTCCGGGATCTCGACGCTCTCCCTTATGCGACTCCT
GCATTAGGAAGCAGCCCAGTAGTAGGTTGAGGCCGTTGAGCACCGCCGCCGCAAGGAATGGTGCATG
CAAGGAGATGGCGCCCAACAGTCCCCCGGCCACGGGGCCTGCCACCATACCCACGCCGAAACAAGCG
CTCATGAGCCCGAAGTGGCGAGCCCGATCTTCCCCATCGGTGATGTCGGCGATATAGGCGCCAGCAAC
CGCACCTGTGGCGCCGGTGATGCCGGCCACGATGCGTCCGGCGTAGAGGATCGAGATCTCGATCCCGC
GAAATTAATACGACTCACTATAGGGGAATTGTGAGCGGATAACAATTCCCCTCTAGAAATAATTTTGT
TTAACTTTAAGAAGGAGATATACCATGGGCAGCAGCCATCATCATCATCACCACAGCCTGGAAGTTCT
GTTCCAGGGGCCCGGATCCCGTGATAGCAGCGATGATTGGGAGATTCCGGATGGACAGATTACCGTGG
GCCAGCGTATTGGCAGCGGGAGCTTCGGCACCGTGTATAAAGGCAAATGGCACGGCGATGTGGCAGT
GAAAATGCTGAACGTGACCGCCCCTACCCCGCAACAGCTGCAGGCGTTTAAGAATGAAGTGGGCGTG
CTGCGTAAAACCCGTCATGTGAATATCTTGCTGTTTATGGGCTATTCGACCAAACCGCAGCTTGCGATT
GTGACCCAGTGGTGCGAGGGCAGCAGTTTGTACCATCATTTGCATGCGAGCGAAACCAAGTTTGAGAT
GAAAAAACTGATTGATATTGCGCGTCAGACTGCGCGTGGCATGGACTATCTGCACGCGAAGTCAATTA

TTCACCGTGACCTGAAGAGCAACAACATCTTTCTGCATGAAGACAATACCGTGAAGATCGGCGACTTC
GGCCTGGCGACCGAAAAAAGCCGTTGGAGCGGATCGCATCAATTTGAACAACTGTCAGGATCGATTCT
GTGGATGGCACCCGAGGTAATTCGTATGCAGGATAGCAATCCGTATAGCTTTCAGAGCGATGTATATG
CGTTTGGCATTGTGCTTTATGAACTGATGACCGGCCAACTGCCGTATTCCAACATTAACAATCGTGATC
AGATTATCGAAATGGTTGGTCGTGGCAGCCTGAGCCCGGATCTGAGCAAAGTACGTAGCAATTGTCCT
AAACGTATGAAACGCTTGATGGCTGAATGCCTGAAAAAGAAACGTGATGAACGTCCGAGCTTTCCGCG
TATTTTGGCGGAAATTGAAGAACTGGCTCGCGAATTGAGCGGCTAACTCGAGCACCACCACCACCACC
ACTGAGATCCGGCTGCTAACAAAGCCCGAAAGGAAGCTGAGTTGGCTGCTGCCACCGCTGAGCAATA
ACTAGCATAACCCCTTGGGGCCTCTAAACGGGTCTTGAGGGGTTTTTTGCTGAAAGGAGGAACTATAT
CCGGAT

Hsp90B

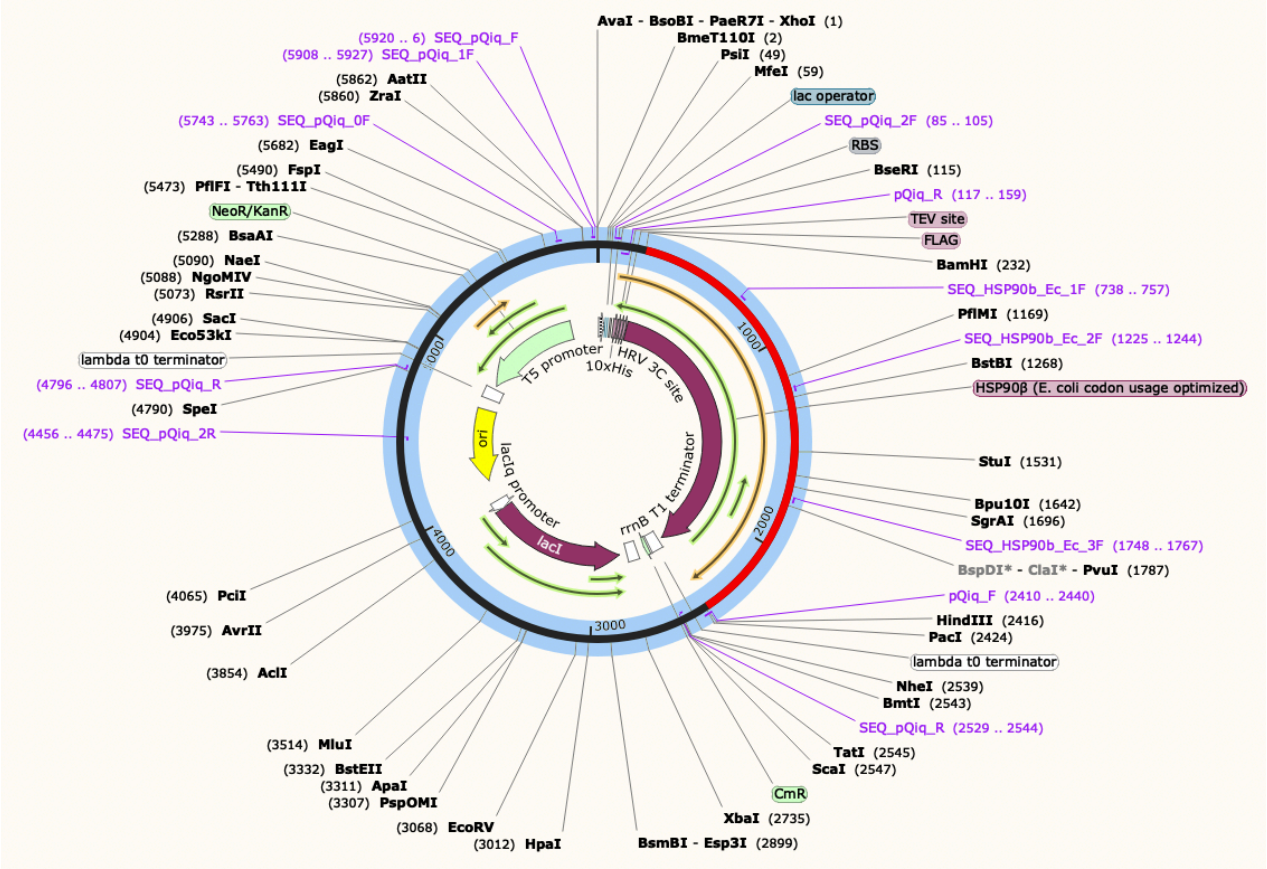

CTCGAGAAATCATAAAAAATTTATTTGCTTTGTGAGCGGATAACAATTATAATAGATTCAATTGTGAG
CGGATAACAATTTCACACAGAATTCATTAAAGAGGAGAAATTAACTatgagaggatcgcatcatcaccaccatcaccatcat
catcacggcgaaaatctgtattttcagggtagcgattacaaggatgatgatgataaactggaagtgctgtttcagggtccgggatccATGCCTGAAGAAGTT
CATCACGGCGAAGAAGAAGTTGAAACCTTTGCATTTCAGGCAGAAATTGCACAGCTGATGAGCCTGAT
TATCAACACCTTTTATAGCAATAAAGAAATTTTCCTGCGCGAACTGATTAGCAATGCATCTGATGCCCT
GGATAAAATTCGTTATGAGAGCCTGACCGATCCGAGCAAACTGGATAGCGGTAAAGAGCTGAAAATT
GATATTATTCCGAATCCGCAGGAACGTACCCTGACCCTGGTTGATACCGGTATTGGTATGACCAAAGC
CGATCTGATTAATAATCTGGGCACCATTGCAAAAAGCGGCACCAAAGCATTTATGGAAGCACTGCAGG
CAGGCGCAGATATTAGCATGATTGGTCAGTTTGGTGTGGGTTTTTATAGCGCATATCTGGTTGCCGAAA
AAGTTGTGGTCATCACCAAACACAATGATGATGAACAGTATGCATGGGAAAGCAGCGCAGGCGGTAG
CTTTACCGTTCGTGCAGATCATGGTGAACCGATTGGTCGTGGCACCAAAGTTATTCTGCACCTGAAAG
AAGATCAGACCGAATATCTGGAAGAACGTCGTGTTAAAGAAGTGGTGAAAAAACACAGCCAGTTTAT
TGGTTATCCGATCACCCTGTATCTGGAAAAAGAACGCGAAAAAGAAATCTCTGATGATGAAGCCGAA
GAAGAAAAAGGCGAAAAAGAAGAAGAGGATAAAGACGACGAAGAGAAACCGAAAATTGAAGATGT
GGGCTCCGATGAAGAAGATGATAGCGGCAAAGATAAAAAGAAAAAGACTAAGAAGATCAAAGAGAA

ATACATTGATCAGGAAGAACTGAACAAAACCAAACCGATTTGGACCCGTAATCCGGATGATATTACCC
AGGAAGAATACGGCGAATTCTATAAAAGCCTGACCAACGATTGGGAAGATCATCTGGCCGTTAAACA
TTTTAGCGTTGAAGGCCAGCTGGAATTTCGTGCACTGCTGTTTATTCCGCGTCGTGCACCGTTTGACCT
GTTCGAAAACAAGAAGAAGAAAAACAATATTAAACTGTATGTGCGTCGCGTGTTTATTATGGATAGCT
GCGACGAACTGATCCCGGAATATCTGAATTTTATTCGCGGTGTTGTGGATAGCGAAGATCTGCCGCTG
AATATTAGCCGTGAAATGCTGCAGCAGAGCAAAATTCTGAAAGTGATTCGCAAAAATATTGTGAAAA
AATGCCTGGAACTGTTTAGCGAACTGGCCGAAGATAAAGAAAATTACAAAAAATTCTATGAGGCCTTT
AGCAAAAATCTGAAACTGGGCATCCATGAAGATAGCACCAATCGTCGTCGTCTGAGCGAACTGCTGCG
TTATCATACCAGCCAGAGCGGTGATGAAATGACCAGCCTGAGCGAATATGTTAGCCGTATGAAAGAA
ACCCAGAAAAGCATCTATTATATCACCGGTGAATCGAAAGAACAGGTTGCAAATAGCGCATTTGTTGA
ACGTGTTCGCAAACGTGGTTTTGAAGTGGTGTATATGACCGAACCGATCGATGAATATTGTGTGCAGC
AGCTGAAAGAATTTGATGGTAAAAGCCTGGTTAGCGTTACCAAAGAAGGTCTGGAACTGCCGGAAGA
TGAAGAAGAGAAAAAAAAAAATGGAAGAAAGCAAAGCCAAATTTGAAAATCTGTGCAAACTGATGAA
AGAGATTCTGGATAAAAAAGTGGAAAAAGTGACCATTAGCAATCGTCTGGTTAGCAGCCCGTGTTGTA
TTGTTACCAGCACCTATGGTTGGACCGCAAATATGGAACGTATTATGAAAGCACAGGCCCTGCGTGAT
AATAGCACCATGGGTTACATGATGGCCAAAAAACACCTGGAAATCAATCCGGATCATCCGATTGTTGA
AACCCTGCGTCAGAAAGCAGAAGCAGATAAAAACGATAAAGCCGTGAAAGATCTGGTTGTTCTGCTG
TTTGAAACCGCACTGCTGTCTAGCGGTTTTAGCCTGGAAGATCCGCAGACCCATAGCAATCGTATTTAT
CGCATGATTAAACTGGGTCTGGGCATTGATGAAGATGAAGTTGCAGCAGAAGAACCGAACGCAGCAG
TTCCGGATGAAATTCCGCCTCTGGAAGGTGATGAAGATGCAAGCCGTATGGAAGAAGTGGATtaatgaaag
cttaattaatgaCTGAGCTTGGACTCCTGTTGATAGATCCAGTAATGACCTCAGAACTCCATCTGGATTTGTTC
AGAACGCTCGGTTGCCGCCGGGCGTTTTTTATTGGTGAGAATCCAAGCTAGCAGTACTGCGATGAGTG
GCAGGGCGGGGCGTAATTTTTTTAAGGCAGTTATTGGTGCCCTTAAACGCCTGGGGTAATGACTCTCTA
GTTTGAGGCATCAAATAAAACGAAAGGCTCAGTCGAAAGACTGGGCCTTTCGTTTTATCTGTTGTTTGT
CGGTGAACGCTCTCCTGAGTAGGACAAATCCGCCGCTCTAGAGATTTCCCTCGACAATTCGCGCTAAC
TTACATTAATTGCGTTGCGCTCACTGCCCGCTTTCCAGTCGGGAAACCTGTCGTGCCAGCTGCATTAAT
GAATCGGCCAACGCGCGGGGAGAGGCGGTTTGCGTATTGGGCGCCAGGGTGGTTTTTCTTTTCACCAG
TGAGACGGGCAACAGCTGATTGCCCTTCACCGCCTGGCCCTGAGAGAGTTGCAGCAAGCGGTCCACGC
TGGTTTGCCCCAGCAGGCGAAAATCCTGTTTGATGGTGGTTAACGGCGGGATATAACATGAGCTGTCT
TCGGTATCGTCGTATCCCACTACCGAGATATCCGCACCAACGCGCAGCCCGGACTCGGTAATGGCGCG
CATTGCGCCCAGCGCCATCTGATCGTTGGCAACCAGCATCGCAGTGGGAACGATGCCCTCATTCAGCA
TTTGCATGGTTTGTTGAAAACCGGACATGGCACTCCAGTCGCCTTCCCGTTCCGCTATCGGCTGAATTT
GATTGCGAGTGAGATATTTATGCCAGCCAGCCAGACGCAGACGCGCCGAGACAGAACTTAATGGGCC
CGCTAACAGCGCGATTTGCTGGTGACCCAATGCGACCAGATGCTCCACGCCCAGTCGCGTACCGTCTT
CATGGGAGAAAATAATACTGTTGATGGGTGTCTGGTCAGAGACATCAAGAAATAACGCCGGAACATT
AGTGCAGGCAGCTTCCACAGCAATGGCATCCTGGTCATCCAGCGGATAGTTAATGATCAGCCCACTGA
CGCGTTGCGCGAGAAGATTGTGCACCGCCGCTTTACAGGCTTCGACGCCGCTTCGTTCTACCATCGACA

CCACCACGCTGGCACCCAGTTGATCGGCGCGAGATTTAATCGCCGCGACAATTTGCGACGGCGCGTGC
AGGGCCAGACTGGAGGTGGCAACGCCAATCAGCAACGACTGTTTGCCCGCCAGTTGTTGTGCCACGCG
GTTGGGAATGTAATTCAGCTCCGCCATCGCCGCTTCCACTTTTTCCCGCGTTTTCGCAGAAACGTGGCT
GGCCTGGTTCACCACGCGGGAAACGGTCTGATAAGAGACACCGGCATACTCTGCGACATCGTATAACG
TTACTGGTTTCACATTCACCACCCTGAATTGACTCTCTTCCGGGCGCTATCATGCCATACCGCGAAAGG
TTTTGCACCTTTCGATGGTGTCAACGTAAATGCATGCCGCTTCGCCTTCCCTAGGGCGTTCGGCTGCGG
CGAGCGGTATCAGCTCACTCAAAGGCGGTAATACGGTTATCCACAGAATCAGGGGATAACGCAGGAA
AGAACATGTGAGCAAAAGGCCAGCAAAAGGCCAGGAACCGTAAAAAGGCCGCGTTGCTGGCGTTTTT
CCATAGGCTCCGCCCCCCTGACGAGCATCACAAAAATCGACGCTCAAGTCAGAGGTGGCGAAACCCG
ACAGGACTATAAAGATACCAGGCGTTTCCCCCTGGAAGCTCCCTCGTGCGCTCTCCTGTTCCGACCCTG
CCGCTTACCGGATACCTGTCCGCCTTTCTCCCTTCGGGAAGCGTGGCGCTTTCTCATAGCTCACGCTGT
AGGTATCTCAGTTCGGTGTAGGTCGTTCGCTCCAAGCTGGGCTGTGTGCACGAACCCCCCGTTCAGCCC
GACCGCTGCGCCTTATCCGGTAACTATCGTCTTGAGTCCAACCCGGTAAGACACGACTTATCGCCACTG
GCAGCAGCCACTGGTAACAGGATTAGCAGAGCGAGGTATGTAGGCGGTGCTACAGAGTTCTTGAAGT
GGTGGCCTAACTACGGCTACACTAGAAGGACAGTATTTGGTATCTGCGCTCTGCTGAAGCCAGTTACC
TTCGGAAAAAGAGTTGGTAGCTCTTGATCCGGCAAACAAACCACCGCTGGTAGCGGTGGTTTTTTTGTT
TGCAAGCAGCAGATTACGCGCAGAAAAAAAGGATCTCAAGAAGATCCTTTGATCTTTTCTACGGGGTC
TGACGCTCAGTGGAACGAAAACTCACGTTAAGGGATTTTGGTCATGACTAGTGCTTGGATTCTCACCA
ATAAAAAACGCCCGGCGGCAACCGAGCGTTCTGAACAAATCCAGATGGAGTTCTGAGGTCATTACTGG
ATCTATCAACAGGAGTCCAAGCGAGCTCTCGAACCCCAGAGTCCCGCTCAGAAGAACTCGTCAAGAA
GGCGATAGAAGGCGATGCGCTGCGAATCGGGAGCGGCGATACCGTAAAGCACGAGGAAGCGGTCAGC
CCATTCGCCGCCAAGCTCTTCAGCAATATCACGGGTAGCCAACGCTATGTCCTGATAGCGGTCCGCCA
CACCCAGCCGGCCACAGTCGATGAATCCAGAAAAGCGGCCATTTTCCACCATGATATTCGGCAAGCAG
GCATCGCCATGGGTCACGACGAGATCCTCGCCGTCGGGCATGCGCGCCTTGAGCCTGGCGAACAGTTC
GGCTGGCGCGAGCCCCTGATGCTCTTCGTCCAGATCATCCTGATCGACAAGACCGGCTTCCATCCGAG
TACGTGCTCGCTCGATGCGATGTTTCGCTTGGTGGTCGAATGGGCAGGTAGCCGGATCAAGCGTATGC
AGCCGCCGCATTGCATCAGCCATGATGGATACTTTCTCGGCAGGAGCAAGGTGAGATGACAGGAGATC
CTGCCCCGGCACTTCGCCCAATAGCAGCCAGTCCCTTCCCGCTTCAGTGACAACGTCGAGCACAGCTG
CGCAAGGAACGCCCGTCGTGGCCAGCCACGATAGCCGCGCTGCCTCGTCCTGCAGTTCATTCAGGGCA
CCGGACAGGTCGGTCTTGACAAAAAGAACCGGGCGCCCCTGCGCTGACAGCCGGAACACGGCGGCAT
CAGAGCAGCCGATTGTCTGTTGTGCCCAGTCATAGCCGAATAGCCTCTCCACCCAAGCGGCCGGAGAA
CCTGCGTGCAATCCATCTTGTTCAATCATGCGAAACGATCCTCATCCTGTCTCTTGATCAGATCTTGAT
CCCCTGCGCCATCAGATCCTTGTCGGCAAGAAAGCCATCCAGTTTACTTTGCAGGGCTTCCCAACCTTA
CCAGAGGGCGCCCCAGCTGGCAATTCCGACGTCTAAGAAACCATTATTATCATGACATTAACCTATAA
AAATAGGCGTATCACGAGGCCCTTTCGTCTTCAC

Protein Phosphatase 5

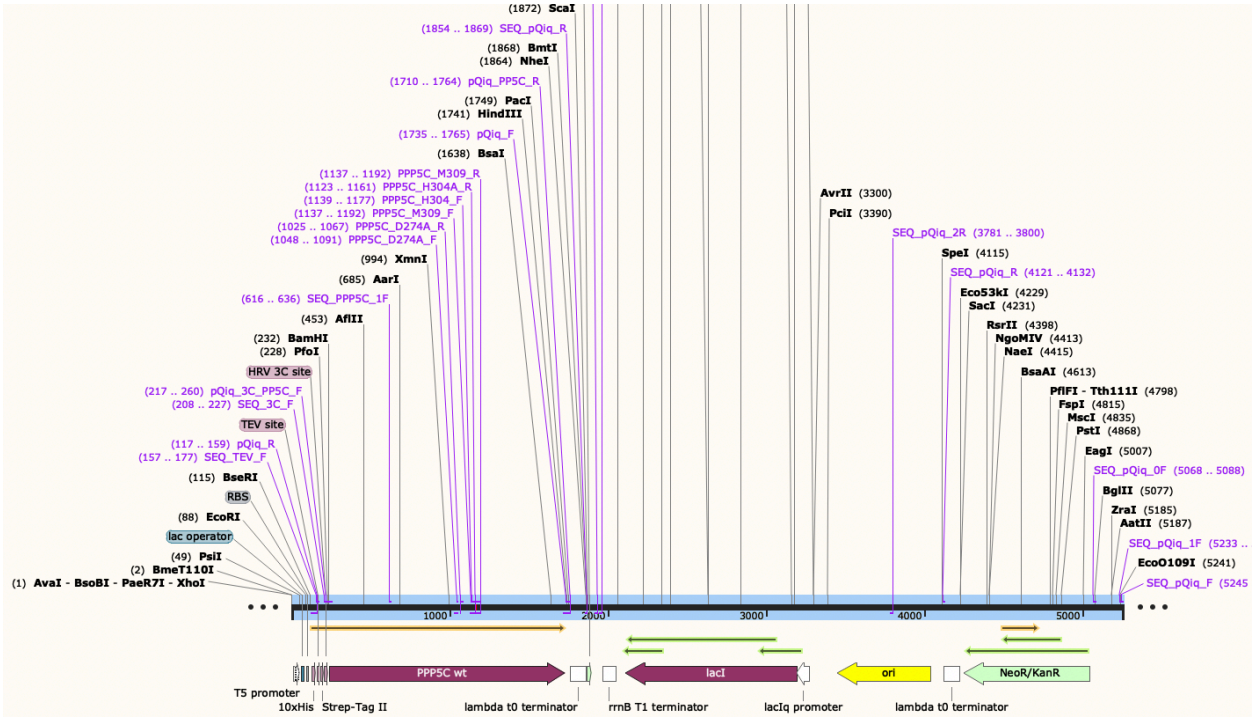

CTCGAGAAATCATAAAAAATTTATTTGCTTTGTGAGCGGATAACAATTATAATAGATTCAATTGTGAG
CGGATAACAATTTCACACAGAATTCATTAAAGAGGAGAAATTAACTatgagaggatcgcatcatcaccaccatcaccatcat
catcacggcgaaaatctgtattttcagggtagctggagccatccgcagtttgaaaaactggaagtgctgtttcagggtccgggatccATGGCTATGGCAGAA
GGTGAAAGAACTGAATGTGCAGAACCACCAAGAGATGAACCACCAGCTGATGGTGCATTAAAGAGAG
CTGAAGAATTGAAGACACAAGCTAATGATTATTTTAAAGCAAAGGATTACGAAAACGCTATTAAATTC
TATTCTCAAGCAATCGAATTAAACCCATCAAACGCTATCTATTACGGTAATAGATCATTGGCTTACTTA
AGAACTGAATGTTATGGTTACGCTTTAGGTGACGCTACAAGAGCAATTGAATTGGATAAGAAATACAT
CAAGGGTTACTACAGAAGAGCTGCATCAAATATGGCTTTGGGTAAATTCAGAGCTGCATTGAGAGATT
ACGAAACTGTTGTTAAGGTTAAGCCACATGATAAGGATGCAAAGATGAAGTACCAAGAATGTAATAA
GATCGTTAAGCAAAAAGCATTTGAAAGAGCTATTGCAGGTGACGAACATAAGAGATCAGTTGTTGATT
CATTAGATATTGAATCTATGACTATTGAAGATGAATACTCAGGTCCAAAATTAGAAGATGGTAAAGTT
ACAATTTCTTTTATGAAAGAATTGATGCAATGGTACAAGGATCAAAAGAAATTGCATAGAAAGTGTGC
TTACCAAATTTTGGTTCAAGTTAAGGAAGTTTTGTCTAAATTATCAACTTTGGTTGAAACTACATTGAA
GGAAACTGAAAAGATTACAGTTTGTGGTGACACACATGGTCAATTCTACGATTTGTTGAACATCTTCG
AATTAAATGGTTTGCCATCAGAAACTAATCCATACATTTTCAATGGTGACTTTGTTGATAGAGGTTCTT
TTTCAGTTGAAGTTATTTTGACATTGTTCGGTTTTAAATTGTTATATCCAGATCATTTCCATTTGTTGAG
AGGTAACCATGAAACTGATAACATGAACCAAATATATGGTTTCGAAGGTGAAGTTAAGGCTAAGTAC
ACAGCACAAATGTACGAATTATTTTCTGAAGTTTTTGAATGGTTGCCATTAGCTCAATGTATCAACGGT

AAAGTTTTGATCATGCATGGTGGTTTGTTTTCAGAAGATGGTGTTACATTGGATGATATTAGAAAGATC
GAAAGAAATAGACAACCACCAGATTCTGGTCCAATGTGTGATTTGTTATGGTCAGATCCACAACCACA
AAACGGTAGATCAATTTCTAAGAGAGGTGTTTCTTGTCAATTTGGTCCAGATGTTACTAAAGCATTTTT
AGAAGAAAACAATTTGGATTACATTATTAGATCACATGAAGTTAAAGCAGAAGGTTACGAAGTTGCTC
ATGGTGGTAGATGCGTTACAGTTTTCTCTGCACCAAACTACTGTGATCAAATGGGTAATAAGGCTTCTT
ACATTCATTTGCAAGGTTCAGATTTGAGACCACAATTTCATCAATTCACTGCTGTTCCACATCCAAATG
TTAAACCAATGGCTTACGCAAACACATTGTTACAATTGGGTATGATGtaatgaaagcttaattaatgaCTGAGCTTG
GACTCCTGTTGATAGATCCAGTAATGACCTCAGAACTCCATCTGGATTTGTTCAGAACGCTCGGTTGCC
GCCGGGCGTTTTTTATTGGTGAGAATCCAAGCTAGCAGTACTGCGATGAGTGGCAGGGCGGGGCGTAA
TTTTTTTAAGGCAGTTATTGGTGCCCTTAAACGCCTGGGGTAATGACTCTCTAGTTTGAGGCATCAAAT
AAAACGAAAGGCTCAGTCGAAAGACTGGGCCTTTCGTTTTATCTGTTGTTTGTCGGTGAACGCTCTCCT
GAGTAGGACAAATCCGCCGCTCTAGAGATTTCCCTCGACAATTCGCGCTAACTTACATTAATTGCGTTG
CGCTCACTGCCCGCTTTCCAGTCGGGAAACCTGTCGTGCCAGCTGCATTAATGAATCGGCCAACGCGC
GGGGAGAGGCGGTTTGCGTATTGGGCGCCAGGGTGGTTTTTCTTTTCACCAGTGAGACGGGCAACAGC
TGATTGCCCTTCACCGCCTGGCCCTGAGAGAGTTGCAGCAAGCGGTCCACGCTGGTTTGCCCCAGCAG
GCGAAAATCCTGTTTGATGGTGGTTAACGGCGGGATATAACATGAGCTGTCTTCGGTATCGTCGTATCC
CACTACCGAGATATCCGCACCAACGCGCAGCCCGGACTCGGTAATGGCGCGCATTGCGCCCAGCGCCA
TCTGATCGTTGGCAACCAGCATCGCAGTGGGAACGATGCCCTCATTCAGCATTTGCATGGTTTGTTGAA
AACCGGACATGGCACTCCAGTCGCCTTCCCGTTCCGCTATCGGCTGAATTTGATTGCGAGTGAGATATT
TATGCCAGCCAGCCAGACGCAGACGCGCCGAGACAGAACTTAATGGGCCCGCTAACAGCGCGATTTG
CTGGTGACCCAATGCGACCAGATGCTCCACGCCCAGTCGCGTACCGTCTTCATGGGAGAAAATAATAC
TGTTGATGGGTGTCTGGTCAGAGACATCAAGAAATAACGCCGGAACATTAGTGCAGGCAGCTTCCACA
GCAATGGCATCCTGGTCATCCAGCGGATAGTTAATGATCAGCCCACTGACGCGTTGCGCGAGAAGATT
GTGCACCGCCGCTTTACAGGCTTCGACGCCGCTTCGTTCTACCATCGACACCACCACGCTGGCACCCAG
TTGATCGGCGCGAGATTTAATCGCCGCGACAATTTGCGACGGCGCGTGCAGGGCCAGACTGGAGGTGG
CAACGCCAATCAGCAACGACTGTTTGCCCGCCAGTTGTTGTGCCACGCGGTTGGGAATGTAATTCAGC
TCCGCCATCGCCGCTTCCACTTTTTCCCGCGTTTTCGCAGAAACGTGGCTGGCCTGGTTCACCACGCGG
GAAACGGTCTGATAAGAGACACCGGCATACTCTGCGACATCGTATAACGTTACTGGTTTCACATTCAC
CACCCTGAATTGACTCTCTTCCGGGCGCTATCATGCCATACCGCGAAAGGTTTTGCACCTTTCGATGGT
GTCAACGTAAATGCATGCCGCTTCGCCTTCCCTAGGGCGTTCGGCTGCGGCGAGCGGTATCAGCTCAC
TCAAAGGCGGTAATACGGTTATCCACAGAATCAGGGGATAACGCAGGAAAGAACATGTGAGCAAAAG
GCCAGCAAAAGGCCAGGAACCGTAAAAAGGCCGCGTTGCTGGCGTTTTTCCATAGGCTCCGCCCCCCT
GACGAGCATCACAAAAATCGACGCTCAAGTCAGAGGTGGCGAAACCCGACAGGACTATAAAGATACC
AGGCGTTTCCCCCTGGAAGCTCCCTCGTGCGCTCTCCTGTTCCGACCCTGCCGCTTACCGGATACCTGT
CCGCCTTTCTCCCTTCGGGAAGCGTGGCGCTTTCTCATAGCTCACGCTGTAGGTATCTCAGTTCGGTGT
AGGTCGTTCGCTCCAAGCTGGGCTGTGTGCACGAACCCCCCGTTCAGCCCGACCGCTGCGCCTTATCCG
GTAACTATCGTCTTGAGTCCAACCCGGTAAGACACGACTTATCGCCACTGGCAGCAGCCACTGGTAAC

AGGATTAGCAGAGCGAGGTATGTAGGCGGTGCTACAGAGTTCTTGAAGTGGTGGCCTAACTACGGCTA
CACTAGAAGGACAGTATTTGGTATCTGCGCTCTGCTGAAGCCAGTTACCTTCGGAAAAAGAGTTGGTA
GCTCTTGATCCGGCAAACAAACCACCGCTGGTAGCGGTGGTTTTTTTGTTTGCAAGCAGCAGATTACGC
GCAGAAAAAAAGGATCTCAAGAAGATCCTTTGATCTTTTCTACGGGGTCTGACGCTCAGTGGAACGAA
AACTCACGTTAAGGGATTTTGGTCATGACTAGTGCTTGGATTCTCACCAATAAAAAACGCCCGGCGGC
AACCGAGCGTTCTGAACAAATCCAGATGGAGTTCTGAGGTCATTACTGGATCTATCAACAGGAGTCCA
AGCGAGCTCTCGAACCCCAGAGTCCCGCTCAGAAGAACTCGTCAAGAAGGCGATAGAAGGCGATGCG
CTGCGAATCGGGAGCGGCGATACCGTAAAGCACGAGGAAGCGGTCAGCCCATTCGCCGCCAAGCTCT
TCAGCAATATCACGGGTAGCCAACGCTATGTCCTGATAGCGGTCCGCCACACCCAGCCGGCCACAGTC
GATGAATCCAGAAAAGCGGCCATTTTCCACCATGATATTCGGCAAGCAGGCATCGCCATGGGTCACGA
CGAGATCCTCGCCGTCGGGCATGCGCGCCTTGAGCCTGGCGAACAGTTCGGCTGGCGCGAGCCCCTGA
TGCTCTTCGTCCAGATCATCCTGATCGACAAGACCGGCTTCCATCCGAGTACGTGCTCGCTCGATGCGA
TGTTTCGCTTGGTGGTCGAATGGGCAGGTAGCCGGATCAAGCGTATGCAGCCGCCGCATTGCATCAGC
CATGATGGATACTTTCTCGGCAGGAGCAAGGTGAGATGACAGGAGATCCTGCCCCGGCACTTCGCCCA
ATAGCAGCCAGTCCCTTCCCGCTTCAGTGACAACGTCGAGCACAGCTGCGCAAGGAACGCCCGTCGTG
GCCAGCCACGATAGCCGCGCTGCCTCGTCCTGCAGTTCATTCAGGGCACCGGACAGGTCGGTCTTGAC
AAAAAGAACCGGGCGCCCCTGCGCTGACAGCCGGAACACGGCGGCATCAGAGCAGCCGATTGTCTGT
TGTGCCCAGTCATAGCCGAATAGCCTCTCCACCCAAGCGGCCGGAGAACCTGCGTGCAATCCATCTTG
TTCAATCATGCGAAACGATCCTCATCCTGTCTCTTGATCAGATCTTGATCCCCTGCGCCATCAGATCCT
TGTCGGCAAGAAAGCCATCCAGTTTACTTTGCAGGGCTTCCCAACCTTACCAGAGGGCGCCCCAGCTG
GCAATTCCGACGTCTAAGAAACCATTATTATCATGACATTAACCTATAAAAATAGGCGTATCACGAGG
CCCTTTCGTCTTCAC

Hsp90:Cdc37:CRaf$^{336\text{-}618}$ – yeast expressed

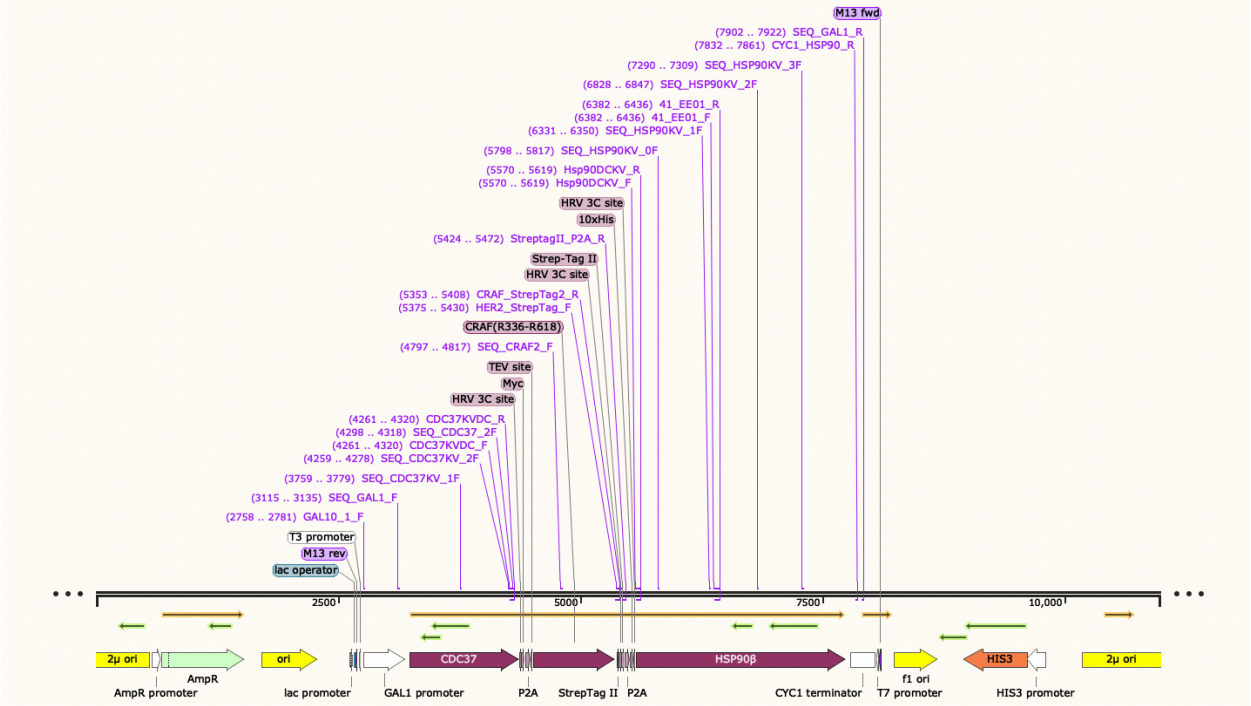

ATCCACATCGGTATAGAATATAATCGGGGATGCCTTTATCTTGAAAAAATGCACCCGCAGCTTCGCTA
GTAATCAGTAAACGCGGGAAGTGGAGTCAGGCTTTTTTTATGGAAGAGAAAATAGACACCAAAGTAG
CCTTCTTCTAACCTTAACGGACCTACAGTGCAAAAAGTTATCAAGAGACTGCATTATAGAGCGCACAA
AGGAGAAAAAAAGTAATCTAAGATGCTTTGTTAGAAAAATAGCGCTCTCGGGATGCATTTTTGTAGAA
CAAAAAAGAAGTATAGATTCTTTGTTGGTAAAATAGCGCTCTCGCGTTGCATTTCTGTTCTGTAAAAAT
GCAGCTCAGATTCTTTGTTTGAAAAATTAGCGCTCTCGCGTTGCATTTTTGTTTTACAAAAATGAAGCA
CAGATTCTTCGTTGGTAAAATAGCGCTTTCGCGTTGCATTTCTGTTCTGTAAAAATGCAGCTCAGATTC
TTTGTTTGAAAAATTAGCGCTCTCGCGTTGCATTTTTGTTCTACAAAATGAAGCACAGATGCTTCGTTC
AGGTGGCACTTTTCGGGGAAATGTGCGCGGAACCCCTATTTGTTTATTTTTCTAAATACATTCAAATAT
GTATCCGCTCATGAGACAATAACCCTGATAAATGCTTCAATAATATTGAAAAAGGAAGAGTATGAGTA
TTCAACATTTCCGTGTCGCCCTTATTCCCTTTTTTGCGGCATTTTGCCTTCCTGTTTTTGCTCACCCAGAA
ACGCTGGTGAAAGTAAAAGATGCTGAAGATCAGTTGGGTGCACGAGTGGGTTACATCGAACTGGATCT
CAACAGCGGTAAGATCCTTGAGAGTTTTCGCCCCGAAGAACGTTTTCCAATGATGAGCACTTTTAAAG
TTCTGCTATGTGGCGCGGTATTATCCCGTATTGACGCCGGGCAAGAGCAACTCGGTCGCCGCATACAC
TATTCTCAGAATGACTTGGTTGAGTACTCACCAGTCACAGAAAAGCATCTTACGGATGGCATGACAGT
AAGAGAATTATGCAGTGCTGCCATAACCATGAGTGATAACACTGCGGCCAACTTACTTCTGACAACGA
TCGGAGGACCGAAGGAGCTAACCGCTTTTTTGCACAACATGGGGGATCATGTAACTCGCCTTGATCGT

TGGGAACCGGAGCTGAATGAAGCCATACCAAACGACGAGCGTGACACCACGATGCCTGTAGCAATGG
CAACAACGTTGCGCAAACTATTAACTGGCGAACTACTTACTCTAGCTTCCCGGCAACAATTAATAGAC
TGGATGGAGGCGGATAAAGTTGCAGGACCACTTCTGCGCTCGGCCCTTCCGGCTGGCTGGTTTATTGCT
GATAAATCTGGAGCCGGTGAGCGTGGGTCTCGCGGTATCATTGCAGCACTGGGGCCAGATGGTAAGCC
CTCCCGTATCGTAGTTATCTACACGACGGGGAGTCAGGCAACTATGGATGAACGAAATAGACAGATCG
CTGAGATAGGTGCCTCACTGATTAAGCATTGGTAACTGTCAGACCAAGTTTACTCATATATACTTTAGA
TTGATTTAAAACTTCATTTTTAATTTAAAAGGATCTAGGTGAAGATCCTTTTTGATAATCTCATGACCA
AAATCCCTTAACGTGAGTTTTCGTTCCACTGAGCGTCAGACCCCGTAGAAAAGATCAAAGGATCTTCTT
GAGATCCTTTTTTTCTGCGCGTAATCTGCTGCTTGCAAACAAAAAAACCACCGCTACCAGCGGTGGTTT
GTTTGCCGGATCAAGAGCTACCAACTCTTTTTCCGAAGGTAACTGGCTTCAGCAGAGCGCAGATACCA
AATACTGTCCTTCTAGTGTAGCCGTAGTTAGGCCACCACTTCAAGAACTCTGTAGCACCGCCTACATAC
CTCGCTCTGCTAATCCTGTTACCAGTGGCTGCTGCCAGTGGCGATAAGTCGTGTCTTACCGGGTTGGAC
TCAAGACGATAGTTACCGGATAAGGCGCAGCGGTCGGGCTGAACGGGGGGTTCGTGCACACAGCCCA
GCTTGGAGCGAACGACCTACACCGAACTGAGATACCTACAGCGTGAGCTATGAGAAAGCGCCACGCT
TCCCGAAGGGAGAAAGGCGGACAGGTATCCGGTAAGCGGCAGGGTCGGAACAGGAGAGCGCACGAG
GGAGCTTCCAGGGGGAAACGCCTGGTATCTTTATAGTCCTGTCGGGTTTCGCCACCTCTGACTTGAGCG
TCGATTTTTGTGATGCTCGTCAGGGGGGCGGAGCCTATGGAAAAACGCCAGCAACGCGGCCTTTTTAC
GGTTCCTGGCCTTTTGCTGGCCTTTTGCTCACATGTTCTTTCCTGCGTTATCCCCTGATTCTGTGGATAA
CCGTATTACCGCCTTTGAGTGAGCTGATACCGCTCGCCGCAGCCGAACGACCGAGCGCAGCGAGTCAG
TGAGCGAGGAAGCGGAAGAGCGCCCAATACGCAAACCGCCTCTCCCCGCGCGTTGGCCGATTCATTAA
TGCAGCTGGCACGACAGGTTTCCCGACTGGAAAGCGGGCAGTGAGCGCAACGCAATTAATGTGAGTT
ACCTCACTCATTAGGCACCCCAGGCTTTACACTTTATGCTTCCGGCTCCTATGTTGTGTGGAATTGTGA
GCGGATAACAATTTCACACAGGAAACAGCTATGACCATGATTACGCCAAGCGCGCAATTAACCCTCAC
TAAAGGGAACAAAAGCTGGAGCTCTAGTACGGATTAGAAGCCGCCGAGCGGGTGACAGCCCTCCGAA
GGAAGACTCTCCTCCGTGCGTCCTCGTCTTCACCGGTCGCGTTCCTGAAACGCAGATGTGCCTCGCGCC
GCACTGCTCCGAACAATAAAGATTCTACAATACTAGCTTTTATGGTTATGAAGAGGAAAAATTGGCAG
TAACCTGGCCCCACAAACCTTCAAATGAACGAATCAAATTAACAACCATAGGATGATAATGCGATTAG
TTTTTTAGCCTTATTTCTGGGGTAATTAATCAGCGAAGCGATGATTTTTGATCTATTAACAGATATATA
AATGCAAAAACTGCATAACCACTTTAACTAATACTTTCAACATTTTCGGTTTGTATTACTTCTTATTCAA
ATGTAATAAAAGTATCAACAAAAAATTGTTAATATACCTCTATACTTTAACGTCAAGGAGAAAAAACC
CCGGATTCTAGAACTAGTGGATCCATGGTTGATTACTCTGTTTGGGATCATATCGAAGTTTCCGATGAT
GAAGATGAAACCCACCCAAATATTGATACCGCTTCTTTGTTTAGATGGAGACATCAAGCTAGAGTTGA
AAGAATGGAACAATTCCAAAAAGAAAAAGAAGAATTGGACAGAGGTTGCAGAGAATGCAAAAGAAA
AGTTGCTGAATGTCAAAGAAAATTGAAAGAATTAGAAGTCGCCGAAGGTGGTAAAGCTGAATTGGAA
AGATTGCAAGCTGAAGCCCAACAATTGAGAAAAGAAGAAAGATCCTGGGAACAAAAGTTGGAAGAA
ATGAGAAAGAAAGAAAAATCCATGCCATGGAACGTTGACACCTTGTCTAAAGATGGTTTCTCCAAGTC
TATGGTTAACACCAAACCAGAAAAGACCGAAGAAGATTCCGAAGAAGTCAGAGAACAAAAGCACAA

GACTTTCGTCGAAAAGTACGAAAAGCAAATCAAGCACTTCGGTATGTTGAGAAGATGGGATGATTCTC
AAAAGTACTTGTCCGATAACGTTCACTTGGTTTGTGAAGAAACTGCCAACTACTTGGTTATTTGGTGCA
TCGATTTGGAAGTCGAAGAAAAATGTGCCTTGATGGAACAAGTTGCTCATCAAACTATCGTCATGCAA
TTCATCTTGGAATTGGCCAAGTCTTTGAAGGTTGATCCAAGAGCTTGTTTCAGACAATTCTTCACCAAG
ATTAAGACCGCCGACAGACAATATATGGAAGGTTTTAATGACGAATTGGAAGCTTTCAAAGAAAGAG
TTAGAGGTAGAGCCAAGTTGAGAATTGAAAAGGCTATGAAGGAATACGAAGAAGAAGAAAGAAAAA
AAAGATTGGGTCCAGGTGGTTTGGATCCAGTTGAAGTTTATGAATCTTTGCCTGAAGAATTACAAAAG
TGCTTCGATGTTAAGGACGTTCAAATGTTGCAAGATGCCATCTCTAAAATGGATCCAACTGATGCTAA
GTACCACATGCAAAGATGTATTGATTCAGGTTTGTGGGTCCCAAATTCTAAAGCTTCTGAAGCTAAAG
AAGGTGAAGAAGCTGGTCCAGGTGACCCATTGTTAGAAGCAGTTCCAAAAACTGGTGACGAAAAGGA
TGTTTCTGTTTTGGAAGTTTTGTTTCAAGGTCCAgaacaaaaattgatttctgaagaagatttgGGTTCTGGTGCTACAAA
CTTCTCATTGTTGAAGCAAGCAGGTGACGTTGAAGAAAATCCAGGTCCAGAAAATTTGTACTTCCAAG
GTGGTAGAGATTCAAGCTATTATTGGGAAATAGAAGCCAGTGAAGTGATGCTGTCCACTCGGATTGGG
TCAGGCTCTTTTGGAACTGTTTATAAGGGTAAATGGCACGGAGATGTTGCAGTAAAGATCCTAAAGGT
TGTCGACCCAACCCCAGAGCAATTCCAGGCCTTCAGGAATGAGGTGGCTGTTCTGCGCAAAACACGGC
ATGTGAACATTCTGCTTTTCATGGGGTACATGACAAAGGACAACCTGGCAATTGTGACCCAGTGGTGC
GAGGGCAGCAGCCTCTACAAACACCTGCATGTCCAGGAGACCAAGTTTCAGATGTTCCAGCTAATTGA
CATTGCCCGGCAGACGGCTCAGGGAATGGACTATTTGCATGCAAAGAACATCATCCATAGAGACATGA
AATCCAACAATATATTTCTCCATGAAGGCTTAACAGTGAAAATTGGAGATTTTGGTTTGGCAACAGTA
AAGTCACGCTGGAGTGGTTCTCAGCAGGTTGAACAACCTACTGGCTCTGTCCTCTGGATGGCCCCAGA
GGTGATCCGAATGCAGGATAACAACCCATTCAGTTTCCAGTCGGATGTCTACTCCTATGGCATCGTATT
GTATGAACTGATGACGGGGGAGCTTCCTTATTCTCACATCAACAACCGAGATCAGATCATCTTCATGG
TGGGCCGAGGATATGCCTCCCCAGATCTTAGTAAGCTATATAAGAACTGCCCCAAAGCAATGAAGAGG
CTGGTAGCTGACTGTGTGAAGAAAGTAAAGGAAGAGAGGCCTCTTTTTCCCCAGATCCTGTCTTCCATT
GAGCTGCTCCAACACTCTCTACCGAAGATCAACCGGTTGCCAGAATCTGGTTGGTCCCATCCACAATTT
GAAAAGTTAGAAGTCTTATTTCAAGGTCCATGGTCACATCCACAATTTGAAAAAGGTTCTGGTGCAAC
AAACTTCTCATTGTTGAAGCAAGCTGGTGACGTTGAAGAAAATCCAGGTCCACATCACCACCATCACC
ACCATCATCATCATTTGGAAGTCTTATTTCAAGGTCCAGGTATGCCAGAAGAAGTTCATCATGGTGAA
GAAGAAGTTGAAACTTTTGCTTTCCAAGCCGAAATTGCCCAATTGATGTCCTTGATTATTAACACCTTC
TACTCTAACAAAGAAATCTTCTTGAGAGAATTGATCTCCAACGCTTCTGATGCCTTGGATAAGATTAGA
TACGAATCTTTGACCGACCCATCCAAATTGGATTCTGGTAAAGAATTGAAGATCGACATCATCCCAAA
CCCACAAGAAAGAACTTTGACTTTGGTTGATACTGGTATCGGTATGACTAAGGCCGATTTGATTAACA
ACTTGGGTACTATTGCTAAGTCCGGTACTAAGGCTTTTATGGAAGCCTTACAAGCTGGTGCTGATATTT
CTATGATTGGTCAATTTGGTGTCGGTTTCTACTCTGCTTACTTGGTTGCTGAAAAGGTTGTTGTTATTAC
CAAGCACAACGACGATGAACAATATGCTTGGGAATCTTCAGCTGGTGGTTCTTTTACTGTTAGAGCTG
ATCATGGTGAACCTATTGGTAGAGGTACAAAGGTTATCTTGCACTTGAAAGAAGATCAAACCGAATAC
TTGGAAGAAAGAAGAGTCAAAGAAGTCGTCAAGAAGCACTCTCAATTCATTGGTTATCCAATCACCTT

GTATTTGGAAAAAGAAAGAGAAAAAGAAATCTCCGACGACGAAGCTGAAGAAGAAAAAGGTGAAAA
AGAAGAAGAAGATAAGGACGACGAAGAAAAGCCAAAGATTGAAGATGTTGGTTCCGACGAAGAAGA
TGATTCAGGTAAAGACAAGAAAAAGAAAACTAAGAAAATCAAAGAAAAGTACATCGATCAAGAAGA
ATTGAACAAGACCAAGCCAATCTGGACTAGAAACCCAGATGATATTACCCAAGAAGAATACGGTGAA
TTCTACAAGTCCTTGACTAACGATTGGGAAGATCATTTGGCTGTCAAGCACTTTTCTGTAGAAGGTCAA
TTGGAATTCAGAGCCTTGTTGTTCATTCCAAGAAGAGCACCATTTGACTTGTTCGAAAACAAAAAGAA
GAAGAACAACATCAAGTTGTACGTTAGAAGAGTTTTCATCATGGACTCTTGCGACGAATTGATTCCAG
AATACTTGAACTTCATCAGAGGTGTTGTTGATTCTGAAGATTTGCCATTGAACATTTCCAGAGAAATGT
TACAACAATCCAAGATTTTGAAGGTCATCAGAAAGAACATCGTCAAGAAGTGCTTGGAATTATTCTCC
GAATTGGCCGAAGATAAGGAAAACTACAAGAAGTTCTACGAAGCCTTCTCCAAGAACTTGAAGTTGG
GTATTCATGAAGATTCCACCAACAGAAGAAGATTGTCCGAATTATTGAGATACCACACCTCTCAATCT
GGTGACGAAATGACTTCTTTGTCTGAATACGTCAGTAGAATGAAGGAAACCCAAAAGTCCATCTACTA
CATTACCGGTGAATCCAAAGAACAAGTTGCTAACTCTGCTTTCGTTGAAAGAGTTAGAAAGAGAGGTT
TCGAAGTTGTCTACATGACCGAACCTATTGATGAATACTGCGTTCAACAATTGAAAGAATTCGATGGT
AAATCCTTGGTTTCCGTCACAAAAGAAGGTTTGGAATTGCCAGAAGATGAAGAAGAAAAGAAAAAGA
TGGAAGAATCCAAGGCCAAGTTTGAAAACTTGTGCAAGTTGATGAAGGAAATTTTGGACAAGAAGGT
CGAAAAGGTCACCATCTCTAATAGATTGGTTTCTTCTCCATGTTGCATCGTTACTTCTACTTATGGTTGG
ACTGCTAATATGGAAAGAATCATGAAGGCTCAAGCCTTGAGAGATAATTCTACTATGGGTTACATGAT
GGCCAAGAAGCACTTGGAAATCAATCCAGATCATCCAATCGTTGAAACCTTGAGACAAAAAGCTGAA
GCTGATAAGAATGATAAGGCCGTTAAGGATTTGGTCGTTTTGTTGTTTGAAACCGCCTTGTTATCTTCC
GGTTTCTCATTGGAAGATCCACAAACACATTCCAACAGAATCTACAGAATGATCAAGTTGGGTTTGGG
TATCGACGAAGATGAAGTTGCTGCTGAAGAACCTAATGCTGCTGTTCCAGACGAAATTCCACCATTGG
AAGGTGATGAAGATGCTTCTAGAATGGAAGAAGTTGACTGATAAGAATTCGATATCAAGCTTATCGAT
ACCGTCGACCTCGAGTCATGTAATTAGTTATGTCACGCTTACATTCACGCCCTCCCCCCACATCCGCTC
TAACCGAAAAGGAAGGAGTTAGACAACCTGAAGTCTAGGTCCCTATTTATTTTTTTATAGTTATGTTAG
TATTAAGAACGTTATTTATATTTCAAATTTTTCTTTTTTTTCTGTACAGACGCGTGTACGCATGTAACAT
TATACTGAAAACCTTGCTTGAGAAGGTTTTGGGACGCTCGAAGGCTTTAATTTGCGGCCGGTACCCAA
TTCGCCCTATAGTGAGTCGTATTACGCGCGCTCACTGGCCGTCGTTTTACAACGTCGTGACTGGGAAAA
CCCTGGCGTTACCCAACTTAATCGCCTTGCAGCACATCCCCCTTTCGCCAGCTGGCGTAATAGCGAAGA
GGCCCGCACCGATCGCCCTTCCCAACAGTTGCGCAGCCTGAATGGCGAATGGACGCGCCCTGTAGCGG
CGCATTAAGCGCGGCGGGTGTGGTGGTTACGCGCAGCGTGACCGCTACACTTGCCAGCGCCCTAGCGC
CCGCTCCTTTCGCTTTCTTCCCTTCCTTTCTCGCCACGTTCGCCGGCTTTCCCCGTCAAGCTCTAAATCG
GGGGCTCCCTTTAGGGTTCCGATTTAGTGCTTTACGGCACCTCGACCCCAAAAAACTTGATTAGGGTGA
TGGTTCACGTAGTGGGCCATCGCCCTGATAGACGGTTTTTCGCCCTTTGACGTTGGAGTCCACGTTCTT
TAATAGTGGACTCTTGTTCCAAACTGGAACAACACTCAACCCTATCTCGGTCTATTCTTTTGATTTATA
AGGGATTTTGCCGATTTCGGCCTATTGGTTAAAAAATGAGCTGATTTAACAAAAATTTAACGCGAATTT
TAACAAAATATTAACGTTTACAATTTCCTGATGCGGTATTTTCTCCTTACGCATCTGTGCGGTATTTCAC

ACCGCATAGATCCGTCGAGTTCAAGAGAAAAAAAAAGAAAAAGCAAAAAGAAAAAAGGAAAGCGCG
CCTCGTTCAGAATGACACGTATAGAATGATGCATTACCTTGTCATCTTCAGTATCATACTGTTCGTATA
CATACTTACTGACATTCATAGGTATACATATATACACATGTATATATATCGTATGCTGCAGCTTTAAAT
AATCGGTGTCACTACATAAGAACACCTTTGGTGGAGGGAACATCGTTGGTACCATTGGGCGAGGTGGC
TTCTCTTATGGCAACCGCAAGAGCCTTGAACGCACTCTCACTACGGTGATGATCATTCTTGCCTCGCAG
ACAATCAACGTGGAGGGTAATTCTGCTAGCCTCTGCAAAGCTTTCAAGAAAATGCGGGATCATCTCGC
AAGAGAGATCTCCTACTTTCTCCCTTTGCAAACCAAGTTCGACAACTGCGTACGGCCTGTTCGAAAGAT
CTACCACCGCTCTGGAAAGTGCCTCATCCAAAGGCGCAAATCCTGATCCAAACCTTTTTACTCCACGCG
CCAGTAGGGCCTCTTTAAAAGCTTGACCGAGAGCAATCCCGCAGTCTTCAGTGGTGTGATGGTCGTCT
ATGTGTAAGTCACCAATGCACTCAACGATTAGCGACCAGCCGGAATGCTTGGCCAGAGCATGTATCAT
ATGGTCCAGAAACCCTATACCTGTGTGGACGTTAATCACTTGCGATTGTGTGGCCTGTTCTGCTACTGC
TTCTGCCTCTTTTTCTGGGAAGATCGAGTGCTCTATCGCTAGGGGACCACCCTTTAAAGAGATCGCAAT
CTGAATCTTGGTTTCATTTGTAATACGCTTTACTAGGGCTTTCTGCTCTGTCATCTTTGCCTTCGTTTATC
TTGCCTGCTCATTTTTTAGTATATTCTTCGAAGAAATCACATTACTTTATATAATGTATAATTCATTATG
TGATAATGCCAATCGCTAAGAAAAAAAAAGAGTCATCCGCTAGGGGAAAAAAAAAAATGAAAATCAT
TACCGAGGCATAAAAAAATATAGAGTGTACTAGAGGAGGCCAAGAGTAATAGAAAAAGAAAATTGCG
GGAAAGGACTGTGTTATGACTTCCCTGACTAATGCCGTGTTCAAACGATACCTGGCAGTGACTCCTAG
CGCTCACCAAGCTCTTAAAACGGGAATTTATGGTGCACTCTCAGTACAATCTGCTCTGATGCCGCATAG
TTAAGCCAGCCCCGACACCCGCCAACACCCGCTGACGCGCCCTGACGGGCTTGTCTGCTCCCGGCATC
CGCTTACAGACAAGCTGTGACCGTCTCCGGGAGCTGCATGTGTCAGAGGTTTTCACCGTCATCACCGA
AACGCGCGAGACGAAAGGGCCTCGTGATACGCCTATTTTTATAGGTTAATGTCATGATAATAATGGTT
TCTTAGATGATCCAATATCAAAGGAAATGATAGCATTGAAGGATGAGACTAATCCAATTGAGGAGTGG
CAGCATATAGAACAGCTAAAGGGTAGTGCTGAAGGAAGCATACGATACCCCGCATGGAATGGGATAA
TATCACAGGAGGTACTAGACTACCTTTCATCCTACATAAATAGACGCATATAAGTACGCATTTAAGCA
TAAACACGCACTATGCCGTTCTTCTCATGTATATATATATACAGGCAACACGCAGATATAGGTGCGAC
GTGAACAGTGAGCTGTATGTGCGCAGCTCGCGTTGCATTTTCGGAAGCGCTCGTTTTCGGAAACGCTTT
GAAGTTCCTATTCCGAAGTTCCTATTCTCTAGAAAGTATAGGAACTTCAGAGCGCTTTTGAAAACCAA
AAGCGCTCTGAAGACGCACTTTCAAAAAACCAAAAAACGCACCGGACTGTAACGAGCTACTAAAATAT
TGCGAATACCGCTTCCACAAACATTGCTCAAAAGTATCTCTTTGCTATATATCTCTGTGCTATATCCCT
ATATAACCTACCCATCCACCTTTCGCTCCTTGAACTTGCATCTAAACTCGACCTCTACATTTTTTATGTT
TATCTCTAGTATTACTCTTTAGACAAAAAAATTGTAGTAAGAACTATTCATAGAGTGAATCGAAAACA
ATACGAAAATGTAAACATTTCCTATACGTAGTATATAGAGACAAAATAGAAGAAACCGTTCATAATTT
TCTGACCAATGAAGAATCATCAACGCTATCACTTTCTGTTCACAAAGTATGCGCA

Hsp90:Cdc37:CRaf – mammalian cell expressed

Extended domain CRaf cleaved: residues 304-648

Kinase domain CRaf cleaved: residues 336-648

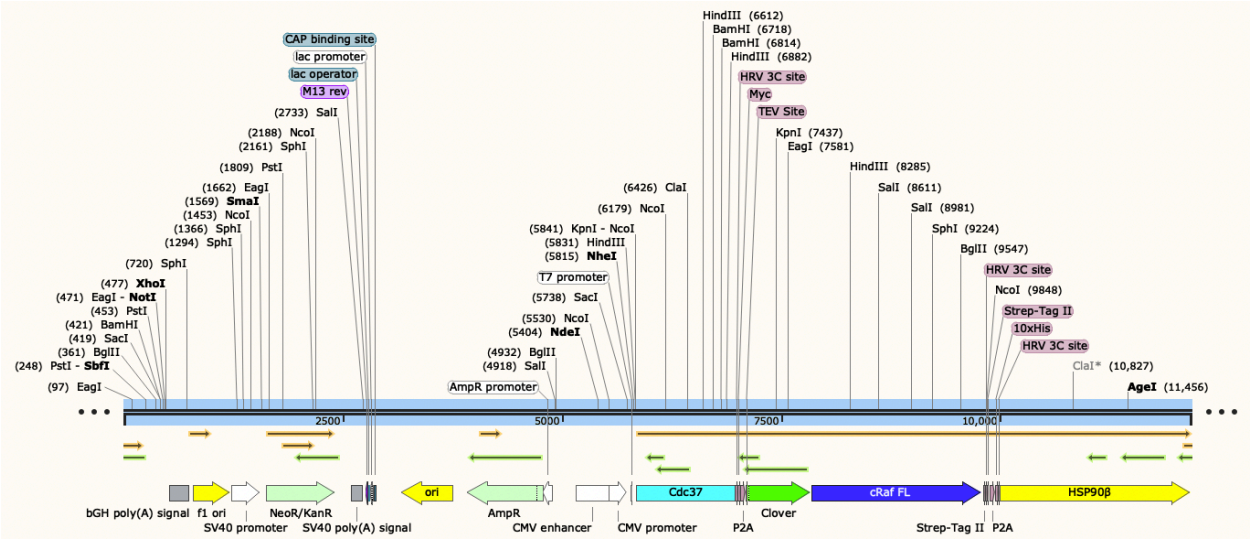

CCCCGGAGGAGCTGGGCCAGCCGCCCACCCCCACCCCCAGTGCAGGGCTGGTCTTGGGGAGGCAGGG
CAGCCTCGCGGTCTTGGGCACTGGTGGGTCGGCCGCCATAGCCCCAGTAGGACAAACGGGCTCGGGTC
TGGGCAGCACCTCTGGTCAGGAGGGTCACCCTGGCCTGCCAGTCTGCCTTCCCCCAACCCCGTGTCCTG
TGGTTTGGTTGGGGCTTCACAGCCACACCTGGACTGACCCTGCAGGTTGTTCATAGTCAGAATTGTATT
TTGGATTTTTACACAACTGTCCCGTTCCCCGCTCCACAGAGATACACAGATATATACACACAGTGGATG
GACGGACAAGACAGGCAGAGATCTATAAACAGACAGGCTCTATGCTATGGCAAAAAAAAAAAAAAAA
AAATAGGAGCTCGGATCCACTAGTCCAGTGTGGTGGAATTCTGCAGATATCCAGCACAGTGGCGGCCG
CTCGAGTCTAGAGGGCCCGTTTAAACCCGCTGATCAGCCTCGACTGTGCCTTCTAGTTGCCAGCCATCT
GTTGTTTGCCCCTCCCCCGTGCCTTCCTTGACCCTGGAAGGTGCCACTCCCACTGTCCTTTCCTAATAAA
ATGAGGAAATTGCATCGCATTGTCTGAGTAGGTGTCATTCTATTCTGGGGGGTGGGGTGGGGCAGGAC
AGCAAGGGGGAGGATTGGGAAGACAATAGCAGGCATGCTGGGGATGCGGTGGGCTCTATGGCTTCTG
AGGCGGAAAGAACCAGCTGGGGCTCTAGGGGGTATCCCCACGCGCCCTGTAGCGGCGCATTAAGCGC
GGCGGGTGTGGTGGTTACGCGCAGCGTGACCGCTACACTTGCCAGCGCCCTAGCGCCCGCTCCTTTCG
CTTTCTTCCCTTCCTTTCTCGCCACGTTCGCCGGCTTTCCCCGTCAAGCTCTAAATCGGGGGCTCCCTTT
AGGGTTCCGATTTAGTGCTTTACGGCACCTCGACCCCAAAAAACTTGATTAGGGTGATGGTTCACGTA
GTGGGCCATCGCCCTGATAGACGGTTTTTCGCCCTTTGACGTTGGAGTCCACGTTCTTTAATAGTGGAC
TCTTGTTCCAAACTGGAACAACACTCAACCCTATCTCGGTCTATTCTTTTGATTTATAAGGGATTTTGCC
GATTTCGGCCTATTGGTTAAAAAATGAGCTGATTTAACAAAAATTTAACGCGAATTAATTCTGTGGAA
TGTGTGTCAGTTAGGGTGTGGAAAGTCCCCAGGCTCCCCAGCAGGCAGAAGTATGCAAAGCATGCATC
TCAATTAGTCAGCAACCAGGTGTGGAAAGTCCCCAGGCTCCCCAGCAGGCAGAAGTATGCAAAGCAT
GCATCTCAATTAGTCAGCAACCATAGTCCCGCCCCTAACTCCGCCCATCCCGCCCCTAACTCCGCCCAG
TTCCGCCCATTCTCCGCCCCATGGCTGACTAATTTTTTTTATTTATGCAGAGGCCGAGGCCGCCTCTGCC
TCTGAGCTATTCCAGAAGTAGTGAGGAGGCTTTTTTGGAGGCCTAGGCTTTTGCAAAAAGCTCCCGGG
AGCTTGTATATCCATTTTCGGATCTGATCAAGAGACAGGATGAGGATCGTTTCGCATGATTGAACAAG
ATGGATTGCACGCAGGTTCTCCGGCCGCTTGGGTGGAGAGGCTATTCGGCTATGACTGGGCACAACAG

ACAATCGGCTGCTCTGATGCCGCCGTGTTCCGGCTGTCAGCGCAGGGGCGCCCGGTTCTTTTTGTCAAG
ACCGACCTGTCCGGTGCCCTGAATGAACTGCAGGACGAGGCAGCGCGGCTATCGTGGCTGGCCACGAC
GGGCGTTCCTTGCGCAGCTGTGCTCGACGTTGTCACTGAAGCGGGAAGGGACTGGCTGCTATTGGGCG
AAGTGCCGGGGCAGGATCTCCTGTCATCTCACCTTGCTCCTGCCGAGAAAGTATCCATCATGGCTGAT
GCAATGCGGCGGCTGCATACGCTTGATCCGGCTACCTGCCCATTCGACCACCAAGCGAAACATCGCAT
CGAGCGAGCACGTACTCGGATGGAAGCCGGTCTTGTCGATCAGGATGATCTGGACGAAGAGCATCAG
GGGCTCGCGCCAGCCGAACTGTTCGCCAGGCTCAAGGCGCGCATGCCCGACGGCGAGGATCTCGTCGT
GACCCATGGCGATGCCTGCTTGCCGAATATCATGGTGGAAAATGGCCGCTTTTCTGGATTCATCGACTG
TGGCCGGCTGGGTGTGGCGGACCGCTATCAGGACATAGCGTTGGCTACCCGTGATATTGCTGAAGAGC
TTGGCGGCGAATGGGCTGACCGCTTCCTCGTGCTTTACGGTATCGCCGCTCCCGATTCGCAGCGCATCG
CCTTCTATCGCCTTCTTGACGAGTTCTTCTGAGCGGGACTCTGGGGTTCGAAATGACCGACCAAGCGAC
GCCCAACCTGCCATCACGAGATTTCGATTCCACCGCCGCCTTCTATGAAAGGTTGGGCTTCGGAATCGT
TTTCCGGGACGCCGGCTGGATGATCCTCCAGCGCGGGGATCTCATGCTGGAGTTCTTCGCCCACCCCA
ACTTGTTTATTGCAGCTTATAATGGTTACAAATAAAGCAATAGCATCACAAATTTCACAAATAAAGCA
TTTTTTTCACTGCATTCTAGTTGTGGTTTGTCCAAACTCATCAATGTATCTTATCATGTCTGTATACCGT
CGACCTCTAGCTAGAGCTTGGCGTAATCATGGTCATAGCTGTTTCCTGTGTGAAATTGTTATCCGCTCA
CAATTCCACACAACATACGAGCCGGAAGCATAAAGTGTAAAGCCTGGGGTGCCTAATGAGTGAGCTA
ACTCACATTAATTGCGTTGCGCTCACTGCCCGCTTTCCAGTCGGGAAACCTGTCGTGCCAGCTGCATTA
ATGAATCGGCCAACGCGCGGGGAGAGGCGGTTTGCGTATTGGGCGCTCTTCCGCTTCCTCGCTCACTG
ACTCGCTGCGCTCGGTCGTTCGGCTGCGGCGAGCGGTATCAGCTCACTCAAAGGCGGTAATACGGTTA
TCCACAGAATCAGGGGATAACGCAGGAAAGAACATGTGAGCAAAAGGCCAGCAAAAGGCCAGGAAC
CGTAAAAAGGCCGCGTTGCTGGCGTTTTTCCATAGGCTCCGCCCCCCTGACGAGCATCACAAAAATCG
ACGCTCAAGTCAGAGGTGGCGAAACCCGACAGGACTATAAAGATACCAGGCGTTTCCCCCTGGAAGC
TCCCTCGTGCGCTCTCCTGTTCCGACCCTGCCGCTTACCGGATACCTGTCCGCCTTTCTCCCTTCGGGAA
GCGTGGCGCTTTCTCATAGCTCACGCTGTAGGTATCTCAGTTCGGTGTAGGTCGTTCGCTCCAAGCTGG
GCTGTGTGCACGAACCCCCCGTTCAGCCCGACCGCTGCGCCTTATCCGGTAACTATCGTCTTGAGTCCA
ACCCGGTAAGACACGACTTATCGCCACTGGCAGCAGCCACTGGTAACAGGATTAGCAGAGCGAGGTA
TGTAGGCGGTGCTACAGAGTTCTTGAAGTGGTGGCCTAACTACGGCTACACTAGAAGAACAGTATTTG
GTATCTGCGCTCTGCTGAAGCCAGTTACCTTCGGAAAAAGAGTTGGTAGCTCTTGATCCGGCAAACAA
ACCACCGCTGGTAGCGGTTTTTTTGTTTGCAAGCAGCAGATTACGCGCAGAAAAAAAGGATCTCAAGA
AGATCCTTTGATCTTTTCTACGGGGTCTGACGCTCAGTGGAACGAAAACTCACGTTAAGGGATTTTGGT
CATGAGATTATCAAAAAGGATCTTCACCTAGATCCTTTTAAATTAAAAATGAAGTTTTAAATCAATCTA
AAGTATATATGAGTAAACTTGGTCTGACAGTTACCAATGCTTAATCAGTGAGGCACCTATCTCAGCGA
TCTGTCTATTTCGTTCATCCATAGTTGCCTGACTCCCCGTCGTGTAGATAACTACGATACGGGAGGGCT
TACCATCTGGCCCCAGTGCTGCAATGATACCGCGAGACCCACGCTCACCGGCTCCAGATTTATCAGCA
ATAAACCAGCCAGCCGGAAGGGCCGAGCGCAGAAGTGGTCCTGCAACTTTATCCGCCTCCATCCAGTC
TATTAATTGTTGCCGGGAAGCTAGAGTAAGTAGTTCGCCAGTTAATAGTTTGCGCAACGTTGTTGCCAT
TGCTACAGGCATCGTGGTGTCACGCTCGTCGTTTGGTATGGCTTCATTCAGCTCCGGTTCCCAACGATC
AAGGCGAGTTACATGATCCCCCATGTTGTGCAAAAAAGCGGTTAGCTCCTTCGGTCCTCCGATCGTTGT
CAGAAGTAAGTTGGCCGCAGTGTTATCACTCATGGTTATGGCAGCACTGCATAATTCTCTTACTGTCAT
GCCATCCGTAAGATGCTTTTCTGTGACTGGTGAGTACTCAACCAAGTCATTCTGAGAATAGTGTATGCG
GCGACCGAGTTGCTCTTGCCCGGCGTCAATACGGGATAATACCGCGCCACATAGCAGAACTTTAAAAG
TGCTCATCATTGGAAAACGTTCTTCGGGGCGAAAACTCTCAAGGATCTTACCGCTGTTGAGATCCAGTT
CGATGTAACCCACTCGTGCACCCAACTGATCTTCAGCATCTTTTACTTTCACCAGCGTTTCTGGGTGAG
CAAAAACAGGAAGGCAAAATGCCGCAAAAAAGGGAATAAGGGCGACACGGAAATGTTGAATACTCA
TACTCTTCCTTTTTCAATATTATTGAAGCATTTATCAGGGTTATTGTCTCATGAGCGGATACATATTTGA
ATGTATTTAGAAAAATAAACAAATAGGGGTTCCGCGCACATTTCCCCGAAAAGTGCCACCTGACGTCG
ACGGATCGGGAGATCTCCCGATCCCCTATGGTGCACTCTCAGTACAATCTGCTCTGATGCCGCATAGTT
AAGCCAGTATCTGCTCCCTGCTTGTGTGTTGGAGGTCGCTGAGTAGTGCGCGAGCAAAATTTAAGCTA

CAACAAGGCAAGGCTTGACCGACAATTGCATGAAGAATCTGCTTAGGGTTAGGCGTTTTGCGCTGCTT
CGCGATGTACGGGCCAGATATACGCGTTGACATTGATTATTGACTAGTTATTAATAGTAATCAATTACG
GGGTCATTAGTTCATAGCCCATATATGGAGTTCCGCGTTACATAACTTACGGTAAATGGCCCGCCTGGC
TGACCGCCCAACGACCCCCGCCCATTGACGTCAATAATGACGTATGTTCCCATAGTAACGCCAATAGG
GACTTTCCATTGACGTCAATGGGTGGAGTATTTACGGTAAACTGCCCACTTGGCAGTACATCAAGTGT
ATCATATGCCAAGTACGCCCCCTATTGACGTCAATGACGGTAAATGGCCCGCCTGGCATTATGCCCAG
TACATGACCTTATGGGACTTTCCTACTTGGCAGTACATCTACGTATTAGTCATCGCTATTACCATGGTG
ATGCGGTTTTGGCAGTACATCAATGGGCGTGGATAGCGGTTTGACTCACGGGGATTTCCAAGTCTCCA
CCCCATTGACGTCAATGGGAGTTTGTTTTGGCACCAAAATCAACGGGACTTTCCAAAATGTCGTAACA
ACTCCGCCCCATTGACGCAAATGGGCGGTAGGCGTGTACGGTGGGAGGTCTATATAAGCAGAGCTCTC
TGGCTAACTAGAGAACCCACTGCTTACTGGCTTATCGAAATTAATACGACTCACTATAGGGAGACCCA
AGCTGGCTAGCGTTTAAACTTAAGCTTGGTACCATGGTTGATTACTCTGTTTGGGATCATATCGAAGTT
TCCGATGATGAAGATGAAACCCACCCAAATATTGATACCGCTTCTTTGTTTAGATGGAGACATCAAGC
TAGAGTTGAAAGAATGGAACAATTCCAAAAAGAAAAAGAAGAATTGGACAGAGGTTGCAGAGAATG
CAAAAGAAAAGTTGCTGAATGTCAAAGAAAATTGAAAGAATTAGAAGTCGCCGAAGGTGGTAAAGCT
GAATTGGAAAGATTGCAAGCTGAAGCCCAACAATTGAGAAAAGAAGAAAGATCCTGGGAACAAAAGT
TGGAAGAAATGAGAAAGAAAGAAAAATCCATGCCATGGAACGTTGACACCTTGTCTAAAGATGGTTT
CTCCAAGTCTATGGTTAACACCAAACCAGAAAAGACCGAAGAAGATTCCGAAGAAGTCAGAGAACAA
AAGCACAAGACTTTCGTCGAAAAGTACGAAAAGCAAATCAAGCACTTCGGTATGTTGAGAAGATGGG
ATGATTCTCAAAAGTACTTGTCCGATAACGTTCACTTGGTTTGTGAAGAAACTGCCAACTACTTGGTTA
TTTGGTGCATCGATTTGGAAGTCGAAGAAAAATGTGCCTTGATGGAACAAGTTGCTCATCAAACTATC
GTCATGCAATTCATCTTGGAATTGGCCAAGTCTTTGAAGGTTGATCCAAGAGCTTGTTTCAGACAATTC
TTCACCAAGATTAAGACCGCCGACAGACAATATATGGAAGGTTTTAATGACGAATTGGAAGCTTTCAA
AGAAAGAGTTAGAGGTAGAGCCAAGTTGAGAATTGAAAAGGCTATGAAGGAATACGAAGAAGAAGA
AAGAAAAAAAAAGATTGGGTCCAGGTGGTTTGGATCCAGTTGAAGTTTATGAATCTTTGCCTGAAGAAT
TACAAAAGTGCTTCGATGTTAAGGACGTTCAAATGTTGCAAGATGCCATCTCTAAAATGGATCCAACT
GATGCTAAGTACCACATGCAAAGATGTATTGATTCAGGTTTGTGGGTCCCAAATTCTAAAGCTTCTGA
AGCTAAAGAAGGTGAAGAAGCTGGTCCAGGTGACCCATTGTTAGAAGCAGTTCCAAAAACTGGTGAC
GAAAAGGATGTTTCTGTTTTGGAAGTTTTGTTTCAAGGTCCAGAACAAAAATTGATTTCTGAAGAAGA
TTTGGGTTCTGGTGCTACAAACTTCTCATTGTTGAAGCAAGCAGGTGACGTTGAAGAAAATCCAGGTC
CAGAAAATTTGTACTTCCAAGGTGGTATGGTGAGCAAGGGCGAGGAGCTGTTCACCGGGGTGGTGCCC
ATCCTGGTCGAGCTGGACGGCGACGTAAACGGCCACAAGTTCAGCGTCCGCGGCGAGGGCGAGGGCG
ATGCCACCAACGGCAAGCTGACCCTGAAGTTCATCTGCACCACCGGCAAGCTGCCCGTGCCCTGGCCC
ACCCTCGTGACCACCTTCGGCTACGGCGTGGCCTGCTTCAGCCGCTACCCCGACCACATGAAGCAGCA
CGACTTCTTCAAGTCCGCCATGCCCGAAGGCTACGTCCAGGAGCGCACCATCTCTTTCAAGGACGACG
GTACCTACAAGACCCGCGCCGAGGTGAAGTTCGAGGGCGACACCCTGGTGAACCGCATCGAGCTGAA
GGGCATCGACTTCAAGGAGGACGGCAACATCCTGGGGCACAAGCTGGAGTACAACTTCAACAGCCAC
TACGTCTATATCACGGCCGACAAGCAGAAGAACAGCATCAAGGCTAACTTCAAGATCCGCCACAACGT
TGAGGACGGCAGCGTGCAGCTCGCCGACCACTACCAGCAGAACACCCCCATCGGCGACGGCCCCGTG
CTGCTGCCCGACAACCACTACCTGAGCCATCAGTCCGCCCTGAGCAAAGACCCCAACGAGAAGCGCG
ATCACATGGTCCTGCTGGAGTTCGTGACCGCCGCCGGGATTACACATGGCATGGACGAGCTGTACAAG
GGCTCAATGGAGCACATACAGGGAGCTTGGAAGACGATCAGCAATGGTTTTGGATTCAAAGATGCCGT
GTTTGATGGCTCCAGCTGCATCTCTCCTACAATAGTTCAGCAGTTTGGCTATCAGCGCCGGGCATCAGA
TGATGGCAAACTCACAGATCCTTCTAAGACAAGCAACACTATCCGTGTTTTCTTGCCGAACAAGCAAA
GAACAGTGGTCAATGTGCGAAATGGAATGAGCTTGCATGACTGCCTTATGAAAGCACTCAAGGTGAG
GGGCCTGCAACCAGAGTGCTGTGCAGTGTTCAGACTTCTCCACGAACACAAAGGTAAAAAAGCACGCT
TAGATTGGAATACTGATGCTGCGTCTTTGATTGGAGAAGAACTTCAAGTAGATTTCCTGGATCATGTTC
CCCTCACAACACACAACTTTGCTCGGAAGACGTTCCTGAAGCTTGCCTTCTGTGACATCTGTCAGAAAT
TCCTGCTCAATGGATTTCGATGTCAGACTTGTGGCTACAAATTTCATGAGCACTGTAGCACCAAAGTAC

CTACTATGTGTGTGGACTGGAGTAACATCAGACAACTCTTATTGTTTCCAAATTCCACTATTGGTGATA
GTGGAGTCCCAGCACTACCTTCTTTGACTATGCGTCGTATGCGAGAGTCTGTTTCCAGGATGCCTGTTA
GTTCTCAGCACAGATATTCTACACCTCACGCCTTCACCTTTAACACCTCCAGTCCCTCATCTGAAGGTT
CCCTCTCCCAGAGGCAGAGGTCGACATCCACACCTAATGTCCACATGGTCAGCACCACCCTGCCTGTG
GACAGCAGGATGATTGAGGATGCAATTCGAAGTCACAGCGAATCAGCCTCACCTTCAGCCCTGTCCAG
TAGCCCCAACAATCTGAGCCCAACAGGCTGGTCACAGCCGAAAACCCCCGTGCCAGCACAAAGAGAG
CGGGCACCAGTATCTGGGACCCAGGAGAAAAACAAAATTAGGCCTCGTGGACAGAGAGATTCAAGCT
ATTATTGGGAAATAGAAGCCAGTGAAGTGATGCTGTCCACTCGGATTGGGTCAGGCTCTTTTGGAACT
GTTTATAAGGGTAAATGGCACGGAGATGTTGCAGTAAAGATCCTAAAGGTTGTCGACCCAACCCCAGA
GCAATTCCAGGCCTTCAGGAATGAGGTGGCTGTTCTGCGCAAAACACGGCATGTGAACATTCTGCTTT
TCATGGGGTACATGACAAAGGACAACCTGGCAATTGTGACCCAGTGGTGCGAGGGCAGCAGCCTCTA
CAAACACCTGCATGTCCAGGAGACCAAGTTTCAGATGTTCCAGCTAATTGACATTGCCCGGCAGACGG
CTCAGGGAATGGACTATTTGCATGCAAAGAACATCATCCATAGAGACATGAAATCCAACAATATATTT
CTCCATGAAGGCTTAACAGTGAAAATTGGAGATTTTGGTTTGGCAACAGTAAAGTCACGCTGGAGTGG
TTCTCAGCAGGTTGAACAACCTACTGGCTCTGTCCTCTGGATGGCCCCAGAGGTGATCCGAATGCAGG
ATAACAACCCATTCAGTTTCCAGTCGGATGTCTACTCCTATGGCATCGTATTGTATGAACTGATGACGG
GGGAGCTTCCTTATTCTCACATCAACAACCGAGATCAGATCATCTTCATGGTGGGCCGAGGATATGCC
TCCCCAGATCTTAGTAAGCTATATAAGAACTGCCCCAAAGCAATGAAGAGGCTGGTAGCTGACTGTGT
GAAGAAAGTAAAGGAAGAGAGGCCTCTTTTTCCCCAGATCCTGTCTTCCATTGAGCTGCTCCAACACT
CTCTACCGAAGATCAACCGGAGCGCTTCCGAGCCATCCTTGCATCGGGCAGCCCACACTGAGGATATC
AATGCTTGCACGCTGACCACGTCCCCGAGGCTGCCTGTCTTCTTGCCAGAATCTGGTTGGTCCCATCCA
CAATTTGAAAAGTTAGAAGTCTTATTTCAAGGTCCATGGTCACATCCACAATTTGAAAAAGGTTCTGGT
GCAACAAACTTCTCATTGTTGAAGCAAGCTGGTGACGTTGAAGAAAATCCAGGTCCACATCACCACCA
TCACCACCATCATCATCATTTGGAAGTCTTATTTCAAGGTCCAGGTATGCCAGAAGAAGTTCATCATGG
TGAAGAAGAAGTTGAAACTTTTGCTTTCCAAGCCGAAATTGCCCAATTGATGTCCTTGATTATTAACAC
CTTCTACTCTAACAAAGAAATCTTCTTGAGAGAATTGATCTCCAACGCTTCTGATGCCTTGGATAAGAT
TAGATACGAATCTTTGACCGACCCATCCAAATTGGATTCTGGTAAAGAATTGAAGATCGACATCATCC
CAAACCCACAAGAAAGAACTTTGACTTTGGTTGATACTGGTATCGGTATGACTAAGGCCGATTTGATT
AACAACTTGGGTACTATTGCTAAGTCCGGTACTAAGGCTTTTATGGAAGCCTTACAAGCTGGTGCTGAT
ATTTCTATGATTGGTCAATTTGGTGTCGGTTTCTACTCTGCTTACTTGGTTGCTGAAAAGGTTGTTGTTA
TTACCAAGCACAACGACGATGAACAATATGCTTGGGAATCTTCAGCTGGTGGTTCTTTTACTGTTAGAG
CTGATCATGGTGAACCTATTGGTAGAGGTACAAAGGTTATCTTGCACTTGAAAGAAGATCAAACCGAA
TACTTGGAAGAAAGAAGAGTCAAAGAAGTCGTCAAGAAGCACTCTCAATTCATTGGTTATCCAATCAC
CTTGTATTTGGAAAAAGAAAGAGAAAAAGAAATCTCCGACGACGAAGCTGAAGAAGAAAAAGGTGA
AAAAGAAGAAGAAGATAAGGACGACGAAGAAAAGCCAAAGATTGAAGATGTTGGTTCCGACGAAGA
AGATGATTCAGGTAAAGACAAGAAAAAGAAAACTAAGAAAATCAAAGAAAAGTACATCGATCAAGA
AGAATTGAACAAGACCAAGCCAATCTGGACTAGAAACCCAGATGATATTACCCAAGAAGAATACGGT
GAATTCTACAAGTCCTTGACTAACGATTGGGAAGATCATTTGGCTGTCAAGCACTTTTCTGTAGAAGGT
CAATTGGAATTCAGAGCCTTGTTGTTCATTCCAAGAAGAGCACCATTTGACTTGTTCGAAAACAAAAA
GAAGAAGAACAACATCAAGTTGTACGTTAGAAGAGTTTTCATCATGGACTCTTGCGACGAATTGATTC
CAGAATACTTGAACTTCATCAGAGGTGTTGTTGATTCTGAAGATTTGCCATTGAACATTTCCAGAGAAA
TGTTACAACAATCCAAGATTTTGAAGGTCATCAGAAAGAACATCGTCAAGAAGTGCTTGGAATTATTC
TCCGAATTGGCCGAAGATAAGGAAAACTACAAGAAGTTCTACGAAGCCTTCTCCAAGAACTTGAAGTT
GGGTATTCATGAAGATTCCACCAACAGAAGAAGATTGTCCGAATTATTGAGATACCACACCTCTCAAT
CTGGTGACGAAATGACTTCTTTGTCTGAATACGTCAGTAGAATGAAGGAAACCCAAAAGTCCATCTAC
TACATTACCGGTGAATCCAAAGAACAAGTTGCTAACTCTGCTTTCGTTGAAAGAGTTAGAAAGAGAGG
TTTCGAAGTTGTCTACATGACCGAACCTATTGATGAATACTGCGTTCAACAATTGAAAGAATTCGATG
GTAAATCCTTGGTTTCCGTCACAAAAGAAGGTTTGGAATTGCCAGAAGATGAAGAAGAAAAGAAAAA
GATGGAAGAATCCAAGGCCAAGTTTGAAAACTTGTGCAAGTTGATGAAGGAAATTTTGGACAAGAAG

GTCGAAAAGGTCACCATCTCTAATAGATTGGTTTCTTCTCCATGTTGCATCGTTACTTCTACTTATGGTT
GGACTGCTAATATGGAAAGAATCATGAAGGCTCAAGCCTTGAGAGATAATTCTACTATGGGTTACATG
ATGGCCAAGAAGCACTTGGAAATCAATCCAGATCATCCAATCGTTGAAACCTTGAGACAAAAAGCTG
AAGCTGATAAGAATGATAAGGCCGTTAAGGATTTGGTCGTTTTGTTGTTTGAAACCGCCTTGTTATCTT
CCGGTTTCTCATTGGAAGATCCACAAACACATTCCAACAGAATCTACAGAATGATCAAGTTGGGTTTG
GGTATCGACGAAGATGAAGTTGCTGCTGAAGAACCTAATGCTGCTGTTCCAGACGAAATTCCACCATT
GGAAGGTGATGAAGATGCTTCTAGAATGGAAGAAGTTGACTGA

Publishing Agreement

It is the policy of the University to encourage open access and broad distribution of all theses, dissertations, and manuscripts. The Graduate Division will facilitate the distribution of UCSF theses, dissertations, and manuscripts to the UCSF Library for open access and distribution. UCSF will make such theses, dissertations, and manuscripts accessible to the public and will take reasonable steps to preserve these works in perpetuity.

I hereby grant the non-exclusive, perpetual right to The Regents of the University of California to reproduce, publicly display, distribute, preserve, and publish copies of my thesis, dissertation, or manuscript in any form or media, now existing or later derived, including access online for teaching, research, and public service purposes.

DocuSigned by:
Maria Jaime Garza
1E3FAA58258043C...
Author Signature

5/29/2023
Date